

MATHEMATICAL MODELLING OF
CONVECTIVE FLOW OVER A HORIZONTAL
CIRCULAR CYLINDER WITH CONVECTIVE
BOUNDARY CONDITIONS IN VISCOUS,
MICROPOLAR AND NANOFUID

NORHAFIZAH BINTI MD SARIF

UMP

DOCTOR OF PHILOSOPHY
UNIVERSITI MALAYSIA PAHANG

UNIVERSITI MALAYSIA PAHANG

DECLARATION OF THESIS AND COPYRIGHT

Author's full name : NORHAFIZAH BINTI MD SARIF

Date of birth : 08.10.1983

Title : MATHEMATICAL MODELLING OF CONVECTIVE
FLOW OVER A HORIZONTAL CIRCULAR CYLINDER
WITH CONVECTIVE BOUNDARY CONDITIONS IN
VISCOUS, MICROPOLAR AND NANOFLUID

Academic Session : SEM I 2018/2019

I declare that this thesis is classified as:

- CONFIDENTIAL (Contains confidential information under the Official Secret Act 1972)
- RESTRICTED (Contains restricted information as specified by the organization where research was done)
- OPEN ACCESS I agree that my thesis to be published as online open access (Full text)

I acknowledge that the Universiti Malaysia Pahang reserve the right as follows:

1. The Thesis is the Property of Universiti Malaysia Pahang.
2. The Library of Universiti Malaysia Pahang has the right to make copies for the purpose of research only.
3. The Library has the right to make copies of the thesis for academic exchange.

Certified by:

(Student's Signature)

831008-06-5130

New IC / Passport Number

Date: 15.12.2018

(Signature of Supervisor)

ASSOC. PROF. DR. MOHD ZUKI BIN SALLEH

Name of Supervisor

Date: 15.12.2018

SUPERVISOR'S DECLARATION

I hereby declare that I have checked this thesis and in my opinion, this thesis is adequate in terms of scope and quality for the award of the degree of Doctor of Philosophy.

(Supervisor's Signature)

Full Name : DR. MOHD ZUKI BIN SALLEH
Position : ASSOCIATE PROFESSOR
Date : DECEMBER 2018



UMP

STUDENT'S DECLARATION

I hereby declare that the work in this thesis is based on my original work except for quotations and citation which have been duly acknowledged. I also declare that it has not been previously or concurrently submitted for any other degree at Universiti Malaysia Pahang or any other institutions.

(Author's Signature)

Full Name : NORHAFIZAH BINTI MD SARIF
ID Number : PSE12001
Date : DECEMBER 2018



UMP

MATHEMATICAL MODELLING OF CONVECTIVE FLOW OVER A HORIZONTAL
CIRCULAR CYLINDER WITH CONVECTIVE BOUNDARY CONDITIONS IN
VISCOUS, MICROPOLAR AND NANOFLUID

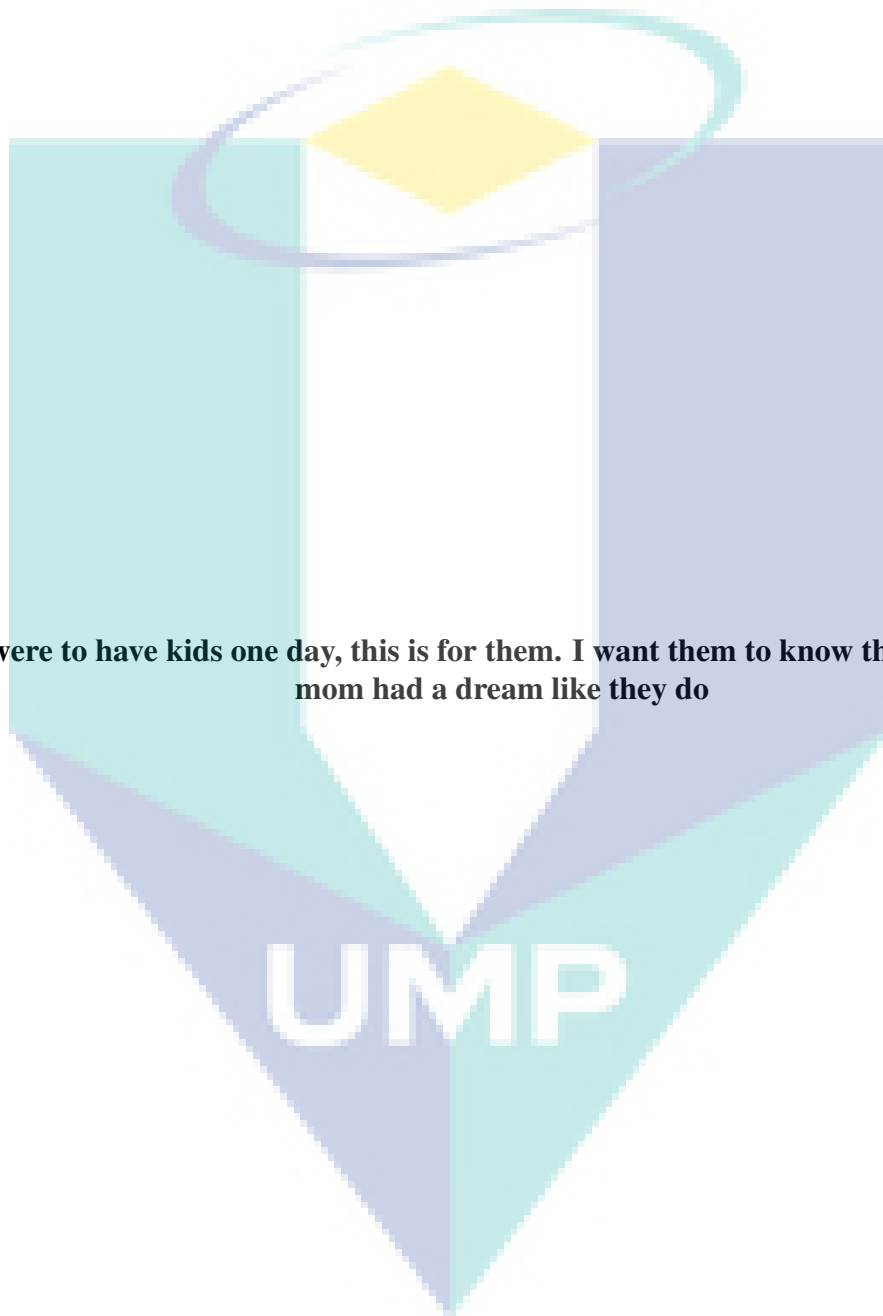
The logo of the University of Malaysia Pahang (UMP) is a shield-shaped emblem. It features a central white vertical band with a yellow diamond at the top. The shield is divided into four quadrants by this central band and a horizontal line. The top-left and bottom-right quadrants are light blue, while the top-right and bottom-left quadrants are a darker blue. A stylized, swirling graphic in shades of blue and yellow is positioned above the central white band.

NORHAFIZAH BINTI MD SARIF

This thesis submitted in fulfilment of the requirements
for the award of the degree of
Doctor of Philosophy

UMP
Faculty of Industrial Sciences & Technology
UNIVERSITI MALAYSIA PAHANG

DECEMBER 2018



If I were to have kids one day, this is for them. I want them to know that once, their mom had a dream like they do

ACKNOWLEDGEMENTS

In the name of Allah, the Most Gracious, the Most Merciful

Alhamdulillah, all praise belongs to Allah for His guidance and for giving me the strength to finish this arduous study. The journey to complete the study is not always smooth as laminar flow. Unpredictable things occur just like a turbulence flow and making life extra complicated to handle. But I believe, the more turbulent your journey, the sweeter your reward. Therefore, I am grateful to Him for all tests and trials befall upon me, and I am sure that without His help, this thesis would not have been possible.

The entire output of this thesis are not my work alone. There are exceptional individuals around me that have made it easier for me to finish my writing. First and foremost, I would like to take this opportunity to express my immeasurable appreciation to my supervisor Assoc. Prof. Dr. Mohd Zuki Bin Salleh for his assistance, continuous support and encouragement throughout this period of my study. I am genuinely moved by his understanding and tolerance of my silly mistakes. Besides him, my external supervisor Prof. Dr. Roslinda Binti Mohd Nazar also played a vital role throughout completion of this thesis. I wish to extend my gratitude to her for the helpful suggestions and for spending time checking my work and monitoring my progress despite her busy schedule.

I wish to express my love to my mother Pn. Saadiah Binti Any who had never ceased to provide emotional support and motivational words for me. She is always there whenever needed support. Her unconditional love and patience is my pillar of strength. Special thanks go to my siblings for always believing in me and for keep reminding me that 'there is always a light at the end of the tunnel'.

I gratefully acknowledge the funding source of my PhD from Universiti Malaysia Pahang and the Ministry of Higher Education which approved my study leave and awarding SLAI scholarship to me. Finally, I would like to thanks, everyone who has been involved directly or indirectly in the preparation of this thesis.

ABSTRAK

Aliran bendalir dan pemindahan haba merupakan faktor penting dalam proses industri, pembuatan dan aplikasi kejuruteraan. Oleh sebab itu, adalah sangat perlu untuk memodelkan sistem bagi meningkatkan proses aliran bendalir dan pemindahan haba di mana kualiti akhir bagi sesuatu produk adalah bergantung kepada aliran kinematik serta pemanasan dan penyejukan secara serentak. Walau bagaimanapun, permasalahan matematik untuk aliran bendalir dan pemindahan haba terutamanya bagi geometri berbentuk silinder bulat mengufuk adalah sangat rumit untuk diselesaikan disebabkan wujudnya persamaan tak linear berpasangan. Bagi mendapatkan persamaan tepat, ia memerlukan masa yang lama dan usaha yang banyak manakala untuk menyediakan alat eksperimen pula memerlukan kos yang tinggi. Dalam kes ini, teknik berangka membuka jalan dalam mendapatkan penyelesaian terbaik untuk menyelesaikan masalah. Oleh itu, persamaan menakluk bagi aliran bendalir dan pemindahan haba beserta dengan syarat sempadan diselesaikan secara berangka. Kebiasaannya apabila model aliran olakan dilaksanakan, kebanyakan penyelidik menggunakan suhu dinding malar atau fluks haba malar sebagai syarat sempadan. Walau bagaimanapun, syarat sempadan ini tidak cukup lengkap untuk menggambarkan keadaan proses pemanasan bagi sesetengah keadaan dalam industri. Terdapat satu lagi jenis syarat sempadan yang telah diperkenalkan di mana permukaan bawah silinder dipanaskan dengan olakan dan ini dikenali sebagai syarat sempadan olakan. Dimotivasikan oleh syarat sempadan yang baharu ini, skema berangka yang dibangunkan dalam kajian ini diharap dapat dijadikan sebagai teori rujukan kepada penyelesaian tepat atau kepada kerja makmal di masa hadapan. Oleh itu, lima masalah berbeza bagi aliran bendalir dan pemindahan haba telah dipertimbangkan dalam kajian ini dengan mengambil kira syarat sempadan olakan sebagai pemanasan haba. Semua model matematik ini kemudiannya diterbitkan bagi kes aliran olakan paksaan, bebas dan juga campuran di atas silinder bulat mengufuk di dalam tiga jenis bendalir berbeza iaitu likat, mikrokutub dan juga nanobendalir. Persamaan menakluk pembezaan separa parabola yang menerangkan tentang aliran kemudiannya ditukar kepada penjelmaan ketakserupaan, dan kemudiannya diselesaikan secara berangka menggunakan kaedah teknik pembezaan terhingga yang stabil tanpa syarat dikenali sebagai kaedah kotak-Keller. Kod berangka dalam bentuk atur cara komputer dibina menggunakan perisian MATLAB. Penyelesaian berangka terdiri daripada profil halaju, suhu, isipadu pecahan nanozarah, geseran permukaan, dan perubahan haba bagi nilai parameter yang berbeza untuk keadaan fizikal bagi parameter olakan, olakan campuran, nombor Lewis, parameter poros dan juga nombor Prandtl. Didapati, bagi kes semua masalah yang dipertimbangkan, profil halaju dan suhu meningkat bagi peningkatan syarat sempadan olakan. Bagi kes nanobendalir, profil isipadu pecahan nanozarah turut meningkat jika syarat sempadan olakan meningkat. Begitu juga bagi setiap kenaikan parameter olakan, pekali geseran permukaan juga meningkat kecuali bagi kes nanobendalir, di mana jika parameter olakan menurun, ia menunjukkan penurunan bagi kedua-dua kes; Tiwari dan Das serta Buongiorno. Manakala, bagi pekali perubahan haba dan Nusselt number, dapat diperhatikan bahawa kesan parameter olakan meningkat secara signifikan. Kesimpulannya, dengan menggunakan syarat sempadan olakan terhadap silinder bulat mengufuk, didapati bahawa trend yang diperolehi bagi kes sempadan olakan adalah menyerupai kes suhu permukaan malar apabila nilai parameter sempadan olakan $\gamma \rightarrow \infty$.

ABSTRACT

Fluid flow and heat transfer play a significant factor in industrial processes, manufacturing and engineering applications. Therefore, a model is needed to enhance the process of fluid flow and heat transfer, as the final products are heavily reliant upon the kinematics of the flow and the simultaneous heating or cooling. However, the mathematical description of fluid flow and heat transfer specifically in geometry of horizontal circular cylinder are quite difficult to solve due to the nonlinearity existence and coupled equations. Indeed, obtaining an analytical solution requires additional effort and time meanwhile to setup an experiment is costly. In such a case, numerical methods provide means to solve the problem. Therefore, the governing equation of fluid flow and heat transfer together with the boundary conditions are solved numerically. Normally when modelling convection flow, many researchers applied constant wall temperature or constant heat flux in the boundary conditions. Nevertheless, these types of boundary conditions appear insufficient to adequately describe the heating process for some cases. Another type of boundary condition; where convection heats the bottom surface of the cylinder are applied in this study. This type of heating process is called convective boundary condition. Motivated by this newly type of boundary condition, the numerical scheme derived in this research is anticipated to provide a theoretical reference to other analytical solution or for future experimental work. Five different problems of fluid flow and heat transfer have been considered by incorporating convective boundary conditions as thermal heating. Accordingly, these mathematical models are then derived for steady laminar forced, free, and mixed convection boundary layer flows over a horizontal circular cylinder immersed in three types of fluid namely viscous, micropolar fluid and nanofluid. The governing parabolic partial differential equations describing the flow are transformed using non-similar transformation, which is then solved numerically using the unconditionally stable implicit finite difference scheme known as the Keller-box method. The numerical codes in the form of computer programmes are developed using MATLAB software. The numerical results obtained consists of velocity, temperature, nanoparticle volume fraction profiles, skin friction and heat transfer for various parameters of physical conditions such as convective, mixed convection, Lewis number, porosity parameters, as well as Prandtl number. It was observed that in all considered problems, the profiles of velocity and temperature profiles increase for increased values of convective boundary conditions. In the case of nanofluids, the values of nanoparticle volume fraction profile increases with with the increment on the values of convective boundary condition. Correspondingly, as the value of convective parameter increases, the skin friction coefficient increase as well except for nanofluid where the convective parameter decreased in both cases; Tiwari and Das, and Buongiorno. However for heat transfer coefficient and Nusselt number, it was observed that the effects of convective parameter has increased significantly. In conclusion, by applying the convective boundary condition over a horizontal circular cylinder, it is found that the trend of the solutions obtained for the convective boundary condition case is similar to the constant wall temperature case, especially when convective parameter $\gamma \rightarrow \infty$.

TABLE OF CONTENT

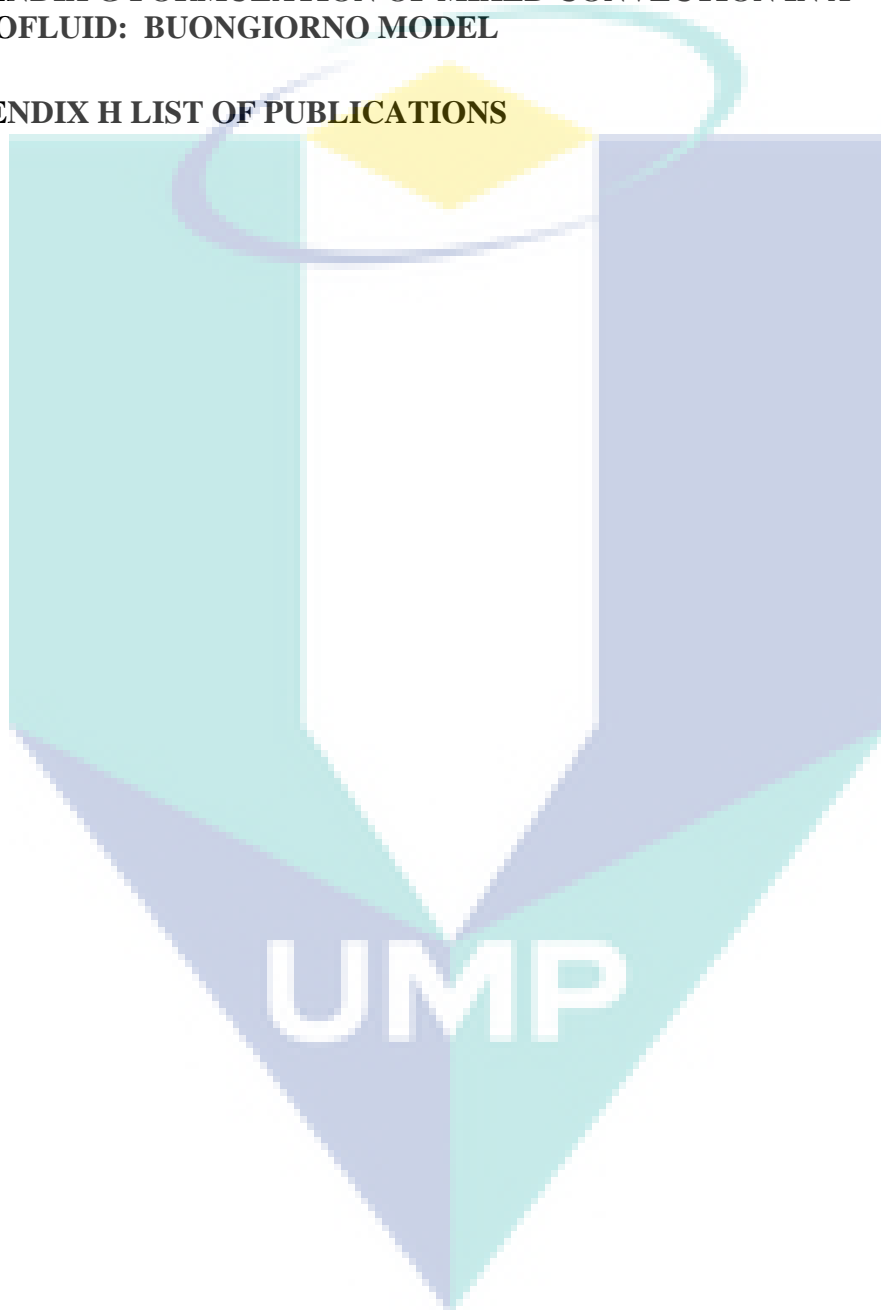
DECLARATION	
TITLE PAGE	i
ACKNOWLEDGEMENTS	ii
ABSTRAK	iii
ABSTRACT	iv
TABLE OF CONTENT	v
LIST OF TABLES	x
LIST OF FIGURES	xi
LIST OF SYMBOLS	xvi
LIST OF ABBREVIATIONS	xix
CHAPTER 1 INTRODUCTION	1
1.1 Research Background	1
1.2 Problem Statement	4
1.3 Research Objectives	5
1.4 Research Scope	6
1.5 Significance of Research	6
1.6 Overview of the Thesis	7
CHAPTER 2 LITERATURE REVIEW	8
2.1 Introduction	8
2.2 Basic Concept of Flow and Heat Transfer	8
2.2.1 Convective Heat Transfer	9

2.2.2	Boundary Layer Theory	10
2.2.3	Type of Fluids	12
2.2.4	Convective Boundary Conditions	15
2.3	Keller-box Method	16
2.4	Forced Convection Viscous Fluid	17
2.5	Free Convection Micropolar Fluid	20
2.6	Mixed Convection Viscous Fluid	22
2.7	Mixed Convection Nanofluid : Tiwari and Das Model	24
2.8	Mixed Convection Nanofluid : Buongiorno Model	26
CHAPTER 3 PROBLEM FORMULATIONS AND NUMERICAL METHOD		34
3.1	Introduction	34
3.2	Problem Formulations	35
3.2.1	Conservation of Mass	35
3.2.2	Conservation of Momentum	37
3.2.3	Conservation of Energy	41
3.2.4	Conservation of Nanoparticle	47
3.2.5	Governing Equations	48
3.2.6	Boundary Conditions	49
3.2.7	Boundary Layer Approximation	50
3.2.8	Non-Dimensional Variables	54
3.2.9	Non-Similar Transformation	55
3.3	Keller-box Scheme	56
3.3.1	First Order System	57
3.3.2	Finite Difference Method	58
3.3.3	Newton's Method	62

3.3.4	Block Elimination Technique	68
3.4	Initial Conditions	77
3.5	Initial Profile	78
CHAPTER 4 FORCED CONVECTION BOUNDARY LAYER FLOW OVER A HORIZONTAL CIRCULAR CYLINDER IN A VISCOUS FLUID		82
4.1	Introduction	82
4.2	Mathematical Formulation	83
4.3	Results and Discussion	86
4.4	Conclusions	93
CHAPTER 5 FREE CONVECTION BOUNDARY LAYER FLOW OVER A HORIZONTAL CIRCULAR CYLINDER IN A MICROPOLAR FLUID		94
5.1	Introduction	94
5.2	Mathematical Formulation	95
5.3	Results and Discussion	99
5.4	Conclusions	108
CHAPTER 6 MIXED CONVECTION BOUNDARY LAYER FLOW OVER A HORIZONTAL CIRCULAR CYLINDER IN A VISCOUS FLUID		110
6.1	Introduction	110
6.2	Mathematical Formulation	111
6.3	Results and Discussion	114
6.4	Conclusions	121

CHAPTER 7 MIXED CONVECTION BOUNDARY LAYER FLOW OVER A HORIZONTAL CIRCULAR CYLINDER IN A NANOFLUID : TIWARI AND DAS MODEL	123
7.1 Introduction	123
7.2 Mathematical Formulation	124
7.3 Results and Discussion	128
7.4 Conclusions	138
CHAPTER 8 MIXED CONVECTION BOUNDARY LAYER FLOW OVER A HORIZONTAL CIRCULAR CYLINDER IN A NANOFLUID : BUONGIORNO MODEL	139
8.1 Introduction	139
8.2 Mathematical Formulation	140
8.3 Results and Discussion	142
8.4 Conclusions	154
CHAPTER 9 CONCLUSION	156
9.1 Summary of Research	156
9.2 Suggestion for Future Research	159
REFERENCES	161
APPENDIX A LIST OF SYMBOLS IN MATLAB PROGRAM	173
APPENDIX B MATLAB PROGRAM	174
APPENDIX C FORMULATION OF FORCED CONVECTION IN VISCOUS FLUID	184
APPENDIX D FORMULATION OF FREE CONVECTION IN MICROPOLAR FLUID	188

APPENDIX E FORMULATION OF MIXED CONVECTION IN VISCOUS FLUIDS	193
APPENDIX F FORMULATION OF MIXED CONVECTION IN A NANOFLUID: TIWARI AND DAS MODEL	197
APPENDIX G FORMULATION OF MIXED CONVECTION IN A NANOFLUID: BUONGIORNO MODEL	201
APPENDIX H LIST OF PUBLICATIONS	206



LIST OF TABLES

Table 2.1	Development of forced convection in viscous fluid	29
Table 2.2	Development of free convection in micropolar fluid	30
Table 2.3	Development of mixed convection in viscous fluid	31
Table 2.4	Development of mixed convection : Tiwari and Das model	32
Table 2.5	Development of mixed convection : Buongiorno model	33
Table 3.1	Analysis order of magnitude for momentum equation Buongiorno model of nanofluids	51
Table 3.2	Analysis order of magnitude for energy equation Buongiorno model of nanofluids	52
Table 3.3	Analysis order of magnitude for nanoparticle volume fraction equation Buongiorno model of nanofluids	53
Table 4.1	Values of the reduced skin friction coefficient at some positions x when $\gamma = 1.0$	87
Table 4.2	Values of heat transfer coefficient Q_w when $Pr = 1.0$	87
Table 5.1	Comparison for the local Nusselt number Nu for the Newtonian case when $\gamma \rightarrow \infty$ (CWT)	99
Table 6.1	Comparison results for the heat transfer coefficient with $Pr = 1.0$, $\lambda = -1, 0, 1$ and $\gamma \rightarrow \infty$	114
Table 7.1	Thermophysical properties of fluid and nanoparticles	128
Table 7.2	Values of the the local Nusselt number $Re_x^{-1/2} Nu$ for $\phi = 0$ $Pr = 1.0$, $\gamma \rightarrow \infty$ and various values of λ	129
Table 8.1	Values of heat transfer coefficient $-\theta'(0)$ in viscous fluid	143
Table 8.2	Values of the dimensionless skin friction, heat flux and mass flux for various values of λ	144

LIST OF FIGURES

Figure 2.1	Boundary layer region	10
Figure 2.2	Separation of boundary layer	12
Figure 2.3	Physical model of nanofluids	14
Figure 3.1	Net rectangle for difference approximation	58
Figure 3.2	Flow diagram for Keller-box method	80
Figure 3.3	Flow chart of solution procedure	81
Figure 4.1	Physical model and coordinate system	83
Figure 4.2	Variation of the local skin friction coefficient $C_f(x, 0)$	88
Figure 4.3	Variation of the local heat transfer coefficient for various values of Pr	89
Figure 4.4	Variation of the local heat transfer coefficient for various values of γ	89
Figure 4.5	Velocity profiles $f'(y)$ near the lower stagnation point of the cylinder, $x \approx 0$	90
Figure 4.6	Temperature profiles $\theta(y)$ near the lower stagnation point of the cylinder, $x \approx 0$ when $\gamma = 1.0$	90
Figure 4.7	Temperature profiles $\theta(y)$ near the lower stagnation point of the cylinder, $x \approx 0$ when Pr = 1.0	91
Figure 4.8	Variation of the wall temperature $\theta(x, 0)$ at the lower stagnation point of the cylinder $x \approx 0$ with Prandtl number when $\gamma = 0.5$ and 1.0	91
Figure 4.9	Variation of the wall temperature $\theta(x, 0)$ at the lower stagnation point of the cylinder $x \approx 0$ with convective parameter γ when Pr = 0.72, 1.0 and 7.0	92
Figure 5.1	Physical model and coordinate system	95
Figure 5.2	Variation of the skin friction coefficient C_f for Pr = 7.0, $K = 1$ and various values of γ	100
Figure 5.3	Variation of the heat transfer coefficient Q_w for Pr = 7.0, $K = 1$ and various values of γ	100
Figure 5.4	Variation of the skin friction coefficient C_f for Pr = 7.0, $\gamma = 0.1$ and various values of material parameter K	102
Figure 5.5	Variation of the heat transfer coefficient Q_w for Pr = 7.0, $\gamma = 0.1$ and various values of material parameter K	102

Figure 5.6	Variation of the skin friction coefficient C_f for $K = 1$, $\gamma = 0.1$ and various values of material parameter Pr	103
Figure 5.7	Variation of the heat transfer coefficient Q_w for $K = 1$, $\gamma = 0.1$ and various values of material parameter Pr	103
Figure 5.8	Velocity profile $f'(y)$ for various values of K when $Pr = 7.0$, and $\gamma = 0.1$	104
Figure 5.9	Temperature profiles $\theta(y)$ for various values of K when $Pr = 7.0$ and $\gamma = 0.1$	104
Figure 5.10	Angular velocity profiles $G(y)$ for various values of K when $Pr = 7.0$ and $\gamma = 0.1$	105
Figure 5.11	Velocity profiles $f'(y)$ for various values of Pr when $\gamma = 0.1$ and $K = 1$	105
Figure 5.12	Temperature profiles $\theta(y)$ for various values of Pr when $\gamma = 0.1$ and $K = 1$	106
Figure 5.13	Angular velocity profiles $G(y)$ for various values of Pr when $\gamma = 0.1$ and $K = 1$	106
Figure 5.14	Velocity profiles $f'(y)$ for various values of γ when $Pr = 7.0$ and $K = 1$	107
Figure 5.15	Temperature profiles $\theta(y)$ for various values of γ when $Pr = 7.0$ and $K = 1$	107
Figure 5.16	Angular velocity profiles $G(y)$ for various values of γ when $Pr = 7.0$ and $K = 1$	108
Figure 6.1	Variation of the skin friction coefficient C_f for $\lambda = 1$, $\gamma = 0.1$ and various value of Pr	115
Figure 6.2	Variation of the heat transfer coefficient Q_w for $\lambda = 1$, $\gamma = 0.1$ and various values of Pr	116
Figure 6.3	Variation of the skin friction coefficient C_f for $\lambda = 1$, $Pr = 7.0$ and various value of γ	116
Figure 6.4	Variation of the heat transfer coefficient Q_w for $\lambda = 1$, $Pr = 7.0$ and various values of γ	117
Figure 6.5	Variation of the skin friction coefficient C_f for $Pr = 7.0$, $\gamma = 0.1$ and various value of λ	117
Figure 6.6	Variation of the heat transfer coefficient Q_w for $Pr = 7.0$, $\gamma = 0.1$ and various values of λ	118
Figure 6.7	Velocity profiles $f'(y)$ for various values of γ when $Pr = 7.0$, and $\lambda = 1$	118

Figure 6.8	Temperature profiles $\theta(y)$ for various values of γ when $Pr = 7.0$ and $\lambda = 1$	119
Figure 6.9	Velocity profiles $f'(y)$ for various values of Pr when $\gamma = 0.1$ and $\lambda = 1$	119
Figure 6.10	Temperature profiles $\theta(y)$ for various values of Pr when $\gamma = 0.1$ and $\lambda = 1$	120
Figure 6.11	Velocity profiles $f'(y)$ for various values of λ when $Pr = 7.0$ and $\gamma = 0.1$	120
Figure 6.12	Temperature profiles $\theta(y)$ for various values of λ when $Pr = 7.0$ and $\gamma = 0.1$	121
Figure 7.1	Comparison of the skin friction coefficient $Re_x^{1/2} C_f$ using Cu nanoparticles with $\phi = 0, 0.1, 0.2$, $\gamma = 0.1$, $Pr = 6.2$ and various values of λ	129
Figure 7.2	Comparison of the skin friction coefficient $Re_x^{1/2} C_f$ using Al_2O_3 nanoparticles with $\phi = 0, 0.1, 0.2$, $\gamma = 0.1$, $Pr = 6.2$ and various values of λ	130
Figure 7.3	Comparison of the skin friction coefficient $Re_x^{1/2} C_f$ using TiO_2 nanoparticles with $\phi = 0, 0.1, 0.2$, $\gamma = 0.1$, $Pr = 6.2$ and various values of λ	131
Figure 7.4	Comparison of the local Nusselt number $Re_x^{1/2} Nu$ using Cu nanoparticles with $\phi = 0, 0.1, 0.2$, $\gamma = 0.1$, $Pr = 6.2$ and various values of λ	131
Figure 7.5	Comparison of the local Nusselt number $Re_x^{1/2} Nu$ using Al_2O_3 nanoparticles with $\phi = 0, 0.1, 0.2$, $\gamma = 0.1$, $Pr = 6.2$ and various values of λ	132
Figure 7.6	Comparison of the local Nusselt number $Re_x^{1/2} Nu$ using TiO_2 nanoparticles with $\phi = 0, 0.1, 0.2$, $\gamma = 0.1$, $Pr = 6.2$ and various values of λ	132
Figure 7.7	Velocity profiles $f'(y)$ using Cu nanoparticles with $\gamma = 0.1$, $Pr = 6.2$, $\phi = 0, 0.1, 0.2$ and various values of λ	133
Figure 7.8	Velocity profiles $f'(y)$ using Al_2O_3 nanoparticles with $\gamma = 0.1$, $Pr = 6.2$, $\phi = 0, 0.1, 0.2$ and various values of λ	133
Figure 7.9	Velocity profiles $f'(y)$ using TiO_2 nanoparticles with $\gamma = 0.1$, $Pr = 6.2$, $\phi = 0, 0.1, 0.2$ and various values of λ	134
Figure 7.10	Temperature profiles $\theta(y)$ using Cu nanoparticles with $\gamma = 0.1$, $Pr = 6.2$, $\phi = 0, 0.1, 0.2$ and various values of λ	134

Figure 7.11	Temperature profiles $\theta(y)$ using Al_2O_3 nanoparticles with $\gamma = 0.1$, $\text{Pr} = 6.2$, $\phi = 0, 0.1, 0.2$ and various values of λ	135
Figure 7.12	Temperature profiles $\theta(y)$ using TiO_2 nanoparticles with $\gamma = 0.1$, $\text{Pr} = 6.2$, $\phi = 0, 0.1, 0.2$ and various values of λ	135
Figure 7.13	Comparison of the skin friction coefficient $\text{Re}_x^{1/2} C_f$ with $\phi = 0.1$, $\lambda = 1$, $\text{Pr} = 6.2$ and various values of γ	136
Figure 7.14	Comparison of the local Nusselt number $\text{Re}_x^{1/2} Nu$ with $\phi = 0.1$, $\gamma = 0.1$, $\text{Pr} = 6.2$ and various values of γ	136
Figure 7.15	Velocity profiles $f'(y)$ using various nanoparticles with $\text{Pr} = 6.2$, $\phi = 0.1$, $\lambda = 1$ and various values of γ	137
Figure 7.16	Temperature profiles $\theta(y)$ using various nanoparticles with $\text{Pr} = 6.2$, $\phi = 0.1$, $\lambda = 1$ and various values of γ	137
Figure 8.1	Physical model and coordinate system	140
Figure 8.2	Variation of the dimensionless skin friction coefficient $(\text{Pe}^{1/2}/\text{Pr})C_f$ for $Le = 2$, $\gamma = 0.05, 0.1, 0.2$, $Nb = 0.5$, $Nr = 0.5$, $Nt = 0.5$ and $\lambda = 1$	145
Figure 8.3	Variation of the dimensionless heat flux coefficient $\text{Pe}^{1/2} Nu$ for $Le = 2$, $\gamma = 0.05, 0.1, 0.2$, $Nb = 0.5$, $Nr = 0.5$, $Nt = 0.5$ and $\lambda = 1$	145
Figure 8.4	Variation of the dimensionless mass flux coefficient $\text{Pe}^{1/2} Sh$ for $Le = 2$, $\gamma = 0.05, 0.1, 0.2$, $Nb = 0.5$, $Nr = 0.5$, $Nt = 0.5$ and $\lambda = 1$	146
Figure 8.5	Velocity profiles $f'(y)$ for various values of γ for $Nb = 0.5$, $Nr = 0.5$, $Nt = 0.5$ and $\lambda = 1$	146
Figure 8.6	Temperature profiles $\theta(y)$ for various values of γ for $Le = 2$, $Nb = 0.5$, $Nr = 0.5$, $Nt = 0.5$ and $\lambda = 1$	147
Figure 8.7	Nanoparticles volume fraction profiles $\phi(y)$ for various values of γ for $Le = 2$, $Nb = 0.5$, $Nr = 0.5$, $Nt = 0.5$ and $\lambda = 1$	147
Figure 8.8	Variation of the dimensionless skin friction coefficient $(\text{Pe}^{1/2}/\text{Pr})C_f$ for $\lambda = 1$, $Le = 2, 6, 10$, $Nb = 0.5$, $Nr = 0.5$, $Nt = 0.5$ and $\gamma = 0.1$	148
Figure 8.9	Variation of the dimensionless heat flux coefficient $\text{Pe}^{1/2} Nu$ for $\lambda = 1$, $Le = 2, 6, 10$, $Nb = 0.5$, $Nr = 0.5$, $Nt = 0.5$ and $\gamma = 0.1$	148
Figure 8.10	Variation of the dimensionless mass flux coefficient $\text{Pe}^{1/2} Sh$ for $\lambda = 1$, $Le = 2, 6, 10$, $Nb = 0.5$, $Nr = 0.5$, $Nt = 0.5$ and $\gamma = 0.1$	149
Figure 8.11	Velocity profiles $f'(y)$ for various values of Le for $Nb = 0.5$, $Nr = 0.5$, $Nt = 0.5$, $\lambda = 1$ and $\gamma = 0.1$	149

Figure 8.12	Temperature profiles $\theta(y)$ for various values of Le for $Nb = 0.5, Nr = 0.5, Nt = 0.5, \lambda = 1$ and $\gamma = 0.1$	150
Figure 8.13	Nanoparticles volume fraction profiles $\phi(y)$ for various values of Le for $Nb = 0.5, Nr = 0.5, Nt = 0.5, \lambda = 1$ and $\gamma = 0.1$	150
Figure 8.14	Variation of the skin friction coefficient $(Pe^{1/2}/Pr)C_f$ for $Le = 2, Nb = 0.1, 0.3, 0.5, Nr = 0.5, Nt = 0.1, 0.3, 0.5, \lambda = 1$ and $\gamma = 0.1$	151
Figure 8.15	Variation of the heat flux coefficient $Pe^{1/2}Nu$ for $Le = 2, Nb = 0.1, 0.3, 0.5, Nr = 0.5, Nt = 0.1, 0.3, 0.5, \lambda = 1$ and $\gamma = 0.1$	151
Figure 8.16	Variation of the mass flux coefficient $Pe^{1/2}Sh$ for $Le = 2, Nb = 0.1, 0.3, 0.5, Nr = 0.5, Nt = 0.1, 0.3, 0.5, \lambda = 1$ and $\gamma = 0.1$	152
Figure 8.17	Velocity profiles $f'(y)$ for various values of Nb and Nt for $Nr = 0.5, Le = 2, \lambda = 1$ and $\gamma = 0.1$	152
Figure 8.18	Temperature profiles $\theta(y)$ for various values of Nb and Nt for $Nr = 0.5, Le = 2, \lambda = 1$ and $\gamma = 0.1$	153

UMP

LIST OF SYMBOLS

a	Radius of cylinder
A	Area of the object
A_1	Rivlin-Ericksen tensor
A_m	Acceleration
C	Nanoparticle volume fraction
Cu	Copper/Cuprum
C_f	Skin friction coefficient
C_p	Specific heat
D_B	Brownian motion
D_T	Thermophoretic diffusion
e_t	Total energy
e_{int}	Kinetic energy
F_s	Surface forces
F_b	Body forces
f	Dimensionless stream function
Gr	Grashof number
G	Angular velocity
g	Gravity vector
h	Heat transfer coefficient
I	Identity tensor
h_f	Heat transfer coefficient
J	Microinertia per unit mass
K_1	Micropolar parameter
K_2	Permeability of the porous medium
k	Thermal conductivity
k_{nf}	Thermal conductivity of the nanofluids
k_s	Thermal conductivity of the solid
L	Length of the cylinder
Le	Lewis number
Nu	Nusselt number
N_b	Brownian motion parameter

N_r	Buoyancy ratio parameter
N_t	Thermophoresis parameter
Pe	Peclet number
p	Pressure
Pr	Prandtl number
Pr_c	Critical value of Prandtl number
q	Heat transfer per unit time
q_m	Mass flux
q_w	Heat flux
Ra	Rayleigh number
Re	Reynolds number
$S(t)$	Control surface
Sh	Sherwood number
T	Temperature
T_f	Temperature of the hot fluid
T_w	Local temperature
T_∞	Fluid temperature
U_∞	Free stream velocity
u, v	Velocity component in x, y direction
u_e	Free stream velocity
V	Fluid filtration velocity
$V(t)$	Control volume

Greek Symbol

α	Thermal diffusivity
α_{nf}	Thermal diffusivity of nanofluids
α_m	Effective thermal diffusivity
β	Thermal expansion coefficient
β_f	Thermal expansion coefficient of the fluid
β_s	Thermal expansion coefficient of the solid

δ	Boundary layer thickness
ε	Porosity of the porous medium
γ	Convective parameter
γ_c	Critical value of convective parameter
κ	Vortex viscosity
λ	Mixed convection parameter
μ	Viscosity
μ_f	Viscosity of the fluid fraction
ν	Kinematic viscosity
ϕ	Nanoparticle volume fraction
ψ	Stream function
ρ	Fluid density
ρ_p	Density of particle
ρ_{nf}	Density of nanofluid
ρ_{cm}	Effective heat capacity
$\rho_{f\infty}$	Density of the base fluid
τ	Shear stress
τ_w	Skin friction coefficient
θ	Nondimensional temperature
σ	Shear stress
ξ	Rate of shear

Subscripts

c	Critical value
f	Fluid
w	Surface condition
∞	Ambient condition
nf	Nanofluid
p	Particle

LIST OF ABBREVIATIONS

BVP	Boundary value problem
CBC	Convective boundary conditions
CHF	Constant heat flux
CWT	Constant wall temperature
CWFEM	Control volume finite element method
HAM	Homotopy analysis method
KBM	Keller-box method
MHD	Magnetohydrodynamic
NH	Newtonian heating
ODE	Ordinary differential equations
PDE	Partial differential equations
FDM	Finite difference method
FEM	Finite element method
FVM	Finite volume method
RKF	Runge-Kutta Fehlberg



UMP

CHAPTER 1

INTRODUCTION

1.1 Research Background

The modelling of convection flow phenomena has been investigated over past decades resulting from the increased demand in industrial and manufacturing processes such as cooling of an infinite metallic plate in a cooling bath, paper production and glass blowing. The output and quality of the final product produced depend on the heat transfer rate at the surface (Ishak, 2010). To achieve the desired outcome, it is essential to understand the convection process, which can be performed by experimental work, adopting a theoretical approach and by modelling the system mathematically. This study focusses on the latter approach and mathematical model of the convection process requires specification of the dependent variables of interest (velocity, temperature and pressure), the governing equation of the problem, the initial and boundary conditions, the geometry of the surfaces, the type of the fluids and the solution method of the resulting system of equations. In considering these specifications, the desirable results will be achieved (Botte et al., 2000).

Convection by definition is the transfer of heat from one place to another by the movement of fluids. Mathematically, the Navier-Stokes equations are the perfect equations that can conceptualise the mathematical description of the fluid movement. The solution of the Navier-Stokes equations is a flow velocity. Once the velocity has been determined, the other variables of interest such as temperature, pressure and skin friction can be found. Although the Navier-Stokes equations could adequately describe the motion of flow mathematically, the equation itself is very complex and challenging to solve as it is elliptic. The inability to solve the Navier-Stokes equations for flow problems has continue to hinder researchers in calculating friction within a fluid. However, the breakthrough that provides a solution for the previous problem was when the boundary layer theory concept was introduced many years ago by Prandtl. The boundary layer equations simplifies the full Navier-Stokes equations by dividing the flow into two regions. Indeed, this dramatically

simplifies the equation without changing the physical sense and still acceptable to describe the flow characteristics (Kasim, 2014). Details of this concept will be explained further in Section 2.2.2.

Once the simplification process has been completed, the boundary layer equations then need to be solved. Accordingly, there are two methods available: analytical and numerical methods. Analytical method produces an exact solution, is continuous in the independent variables and provide further insight into a system. Unfortunately however, the focus of this study is on the geometry surface of a horizontal circular cylinder and involving complex equations, which is where the numerical method is applied. Numerical methods albeit very general, are appropriate for most models. Importantly, the accuracy of the technique depends upon the system, complexity of the boundary conditions, and so forth. The most common techniques used for modelling convection flow are the finite difference method (FDM) and the finite element method (FEM). The numerical method used in this study is the implicit finite difference method namely the Keller-box method. This method has been found to be suitable for dealing with convective boundary layer flow problems (Shu and Wilks, 1995). Another advantage of the Keller-box method is that the method is unconditionally stable, and can solve problems in any order (Na, 1979; Mohamed, 2013). Furthermore, the vast number of published papers on various flow problems has successfully applied the Keller-box method in solving many flow problems. Also, many books describing the Keller-box method can be found in publications by Na (1979) and by Cebeci and Bradshaw (1988).

The primary focus of early research in convection flow has been concentrated primarily on Newtonian fluid. Most low molecular weight substances such as inorganic salt, water, ethyl alcohol, exhibit Newtonian flow characteristic i.e. constant temperature and pressure, shear stress σ proportional to the rate of shear ξ . However many substances especially of multi-phase nature (foams, emulsions and slurries) and polymeric melts do not conform to the Newtonian postulate of linear relationship between σ and ξ in a simple linear. Accordingly, these fluids are variously known as non-Newtonian, non-linear and complex fluids. Therefore, another non-Newtonian fluid that shall be considered along with viscous fluids in this study are micropolar fluids. Likewise, recent demand for small size equipment has prompted researchers to develop fluids with high thermal conductivity. Notably, research exploration leads to the discovery of the nanofluids; fluids that could enhance thermal conductivity and improve heat transfer efficiency. The study on nanofluid is also considered in this study.

Even though there have been many numerical studies and theoretical work undertaken previously on the flow and heat transfer process, it seems that majority of these

studies are limited in the case constant wall temperature (CWT) and constant heat flux (CHF). Furthermore, the Newtonian heating (NH) condition initially used by Merkin (1994) and later Aziz (2009) has incorporated another type of boundary condition known as convective boundary conditions (CBC). The convective boundary condition can be described as a situation where convection heats the bottom surface of the cylinder from a hot fluid. Unlike constant wall temperature and constant heat flux, convective boundary condition is more realistic to apply to the real situation since the heat coefficient value changes as the wall temperature changing.

To date, there have been relatively limited number of published works on convective heat transfer from heated bodies of higher complexity, such as horizontal circular cylinders. Indeed, the geometrical shape of the cylinder creates non-uniformity in heat transfer around the cylinder surface. With a better understanding and insight of the flow behaviour around the cylinder, it is then possible to devise a method for heat transfer enhancement (Eiyad et al., 2008). The horizontal circular cylinder was selected as an example for studying the effect of the parameters especially the convective boundary condition due to the significant variation in heat transfer rates around the cylinder surface in the tangential direction.

Therefore, this study proposes to formulate a mathematical model of the convection flow and investigate if there is a significant effect of convective boundary conditions in five different flow problems: forced, free and mixed convection flow over horizontal circular cylinder in viscous, micropolar and nanofluids, respectively. Besides the convective parameter, the influence of other governing parameters on the flow and heat transfer characteristics is also considered including the physical quantity of interest. Throughout the five problems, the effect of all parameters and physical quantities of interest in each chapters are discussed. Physical quantities of interest such as heat transfer coefficient and skin friction play a significant role in any practical situations. For instance, heat transfer coefficients provide information regarding the rate of heat transfer from the body to fluid and the type of material used in order to avoid body being exposed to high temperature. Otherwise skin friction coefficient is also important for practical problems as it determines the heating of the body due to the shear stress on the body and heat loss by friction. Therefore, the nature of the flow and its separation from the body surface can be determined as well by skin friction coefficients (Nazar, 2003). The flow becomes unstable and rotational when it separates from the body. This phenomenon of separation is very crucial for designing and building a plane.

It is worth mentioning at this point that a mathematical model of the five problems has been derived for the case of convective boundary conditions. The simulated results of a mathematical model are illustrated and the analysed data are given in the five different

chapters corresponding to the five different problems . The contribution of this study will serve as a reference for future research in experimental work and used as a comparison with analytical results or theories.

1.2 Problem Statement

As mentioned earlier in the *previous* section, most of the published results in the open literature are incorporated with constant wall temperature and constant heat flux as a heating process at their boundary conditions. However, there are a relatively limited number of published solutions that have been attempted for the convective boundary conditions especially in the horizontal circular cylinder. Moreover the topics of convective boundary conditions have not clearly developed yet. Accordingly, the present work is prepared as an attempt to continue in developing the heating process of CBC, so that the research gap between CWT, CHF and CBC can be narrowed.

Among the references, it is quite noticeable that minimal progress has been made in CBC, but instead, attention on CBC is focussed more on simpler geometry such as stretching sheet and vertical plate. Until now, there is not much investigation of CBC in the horizontal circular cylinder to facilitate the effect of convective parameter of profile. Notwithstanding, most researchers have focused more on CWT and CHF as it is easier to solve. However, the effect of the CBC case cannot be ignored as many natural phenomena involve the changing process of wall temperatures. Therefore, is it natural to ask the question, "Is it possible for us to extend the pioneering work of convection flow to investigate the effect of convective on the velocity and temperature of the cylinder?"

The involvement of convective boundary condition as a heating process leads to the complexity of creating the initial profile in MATLAB programming that can satisfy the boundary condition asymptotically. The wall temperature or heat flux is no longer constant, and therefore this factor contributes to the difficulties of the problem. Choosing the appropriate initial profile is a challenging task yet is interesting to obtain the most accurate result for the analysis.

Cylindrical shape bodies exhibit boundary layer separation. Boundary layer separation occur when the flow is unstable and transition from laminar to turbulence flow. Up to a certain point, singularities are encountered. The questions then start to arise, "At what point separation occur?". By modifying the boundary conditions, it will influence the separation point, convection process as well as the flow of the fluid. Hence, this study aims to explore the following research questions:

- i) How are the mathematical models of viscous, micropolar and nanofluid problems with the convective boundary conditions formulated?
- ii) What are the effects of the convective boundary conditions parameter on the flow and heat transfer characteristics over a horizontal circular cylinder, along with other parameters?
- iii) Will the convective boundary conditions delay the separation process?

Question 1 is covered in Chapter 3, whereas Chapter 4 to Chapter 8 provides the answers to Question 2. Discussion and explanation for Question 3 are given at the end of the Chapter 4 to Chapter 9.

1.3 Research Objectives

Based on the research questions posed before, the objectives of the present study are to:

- i) derive mathematical models for the proposed problems of boundary layer flows
- ii) carry out mathematical formulation and analyses
- iii) develop numerical algorithm and programming for computations in generating numerical solutions
- iv) analyse the effect of the convective parameter and other parameters on the heat transfer characterisation

Five problems that are considered in this study are listed as the following:

- i) Forced convection boundary layer flow over a horizontal circular cylinder in a viscous fluid
- ii) Free convection boundary layer flow over a horizontal circular cylinder in a micropolar fluid
- iii) Mixed convection boundary layer flow over a horizontal circular cylinder in a viscous fluid
- iv) Mixed convection boundary layer flow over a horizontal circular cylinder in a nanofluid: Tiwari and Das Model

- v) Mixed convection boundary layer flow over a horizontal circular cylinder in a nanofluid: Buongiorno Model.

1.4 Research Scope

The scope of this study is limited to a problem involving steady two-dimensional forced, free and mixed convection boundary layer flows where the geometry of the surface considered in this study is a horizontal circular cylinder, immersed in viscous, micropolar and nanofluid with convective boundary conditions. Notably, this study examines the effect of convective boundary conditions and other parameters on the flow and heat transfer. The governing equations of the problems are then formulated using non-similar transformation and solved numerically using the Keller-box method.

1.5 Significance of Research

The demand in many fields of applications such as engineering, physics and biology contributes to an accelerating interest in the development of convection flow and heat transfer. Earlier investigations have focused on the constant temperature, and only recently, the case of convective boundary conditions has been highlighted. As a result, research on boundary flow by incorporating convective boundary conditions is required as work in this area is far less advanced. With the convective boundary conditions, the model is presumed to obtain a realistic solution to practical problems.

On the other hand, the heat transfer characteristics improved by suspending the nanoparticle. Thus, the study of nanofluid is important because nanofluid are widely used in the heat exchanger, microchannel heat sink and many more. Compared to conventional fluid, nanofluid has high specific area and more heat transfer surface between the particle and fluids. Therefore, there is substantial need to investigate and identify other unique applications for these fields.

Undoubtedly, the result or output from the numerical methods of the modelling of convection flow is hoped to enhance the understanding of the fluid flow phenomenon and to improve the development of related industries, for example in the manufacturing industries. Besides that, the results obtained can be used for validation purposes in the future. Furthermore, it is hoped that this study will facilitate researchers, engineers or other people related to this specific field to explore this area more broadly.

1.6 Overview of the Thesis

This thesis consists of nine chapters, including the introduction in Chapter 1, presenting the problem statement, objectives, scope and research significance. Chapter 2 discusses on the literature review for the proposed problems. The literature review is divided into several sections which discusses on the flow on a forced, free, mixed in viscous, micropolar and nanofluids, respectively. In addition, brief introduction to the research are included here.

In Chapter 3, the problem formulations and numerical method are presented and discussed. A full discussion and details of the numerical method are also explained for the case of mixed convection boundary flow in nanofluids using Buongiorno Model. The procedure of the prescribed solution for the Keller-box method is given here. The entire MATLAB program of the problem discussed in Chapter 3 is presented in Appendix A and B.

The main body of the thesis is given in Chapter 4 to Chapter 8. In Chapter 4, 5 and 6 we discussed on the problem in forced convection in viscous fluid, free convection in micropolar fluid, mixed convection in viscous fluid respectively. Chapters 7 and 8 prescribe the problem on mixed convection boundary layer flow of a nanofluid fluid past a horizontal circular cylinder considering two nanofluid models namely the Tiwari and Das and Buongiorno. The full derivation of governing equations of Chapter 8 are presented in Chapter 3.

Finally, Chapter 9 provides the overarching conclusions for the entire content and work performed in the thesis. Additionally, some recommendations for future study based on present solution also highlighted in this chapter. Further, the list of symbols used in MATLAB system is provided in Appendix A and the solution procedures are given in Appendix B. Appendix C to G provide detailed formulation of the five problems discussed in the thesis and list of publications are shown in Appendix H.

CHAPTER 2

LITERATURE REVIEW

2.1 Introduction

The purpose of this chapter is to elaborate the literature review used in this study. The literature review are divided into several sections which addresses basic concepts to understand the theoretical framework for the method and also contains information from previous studies, earliest investigations including the finding on the respective topic. The basic concept of the research including the convective heat transfer; boundary layer theory; type of fluids; and convective boundary conditions, as well as the numerical method namely Keller-box method. As there are numerous papers devoted to the research on fluid flow, we are going to present only a few of them, a cursory discussion of the quintessential contribution of which is going to justify the re-examination of the subject in the present research as well as the chosen framework.

2.2 Basic Concept of Flow and Heat Transfer

The effort to obtain a mathematical formulation of a fluid flow took shape during the century following the publications of research by well known mathematicians. The next subsection reviews the background materials required in this study. It provides an introduction from the beginning of the mathematical formulation especially about flow and heat transfer. It commences with heat transfer characteristics, the backbone of mathematical modelling in a convection flow as given in the Subsection 2.2.1. The boundary layer part is provided in Subsection 2.2.2 followed by a brief review of fluids.

2.2.1 Convective Heat Transfer

Convection is the transfer of heat by the movement of fluid. The fluid movement enhances heat transfer. Movement of fluids is very complex, making convection a difficult subject. An everyday example of convection is the radiator, oceanic circulation, heat exchangers, air conditioning and many more (Cebeci and Bradshaw, 1988).

Convection can be divided into two distinct types, free convection and forced convection. Free convection occurs when fluid motion is caused by buoyancy forces that resulted from density variation due to the difference in temperature in the fluid and in the presence of body force such as gravity. When a less dense fluid is heated, the density change causes the heated fluid to rise and replaced by cooler (dense) fluid without external induced flow arising. Conversely, if the motion of the fluid arises from an external agent, for instance, a fan, a blower, the wind, or the motion of a heated object itself, which imparts the pressure to drive the flow, the process is termed forced convection. In any forced convection situation, free convection is also present under the pressure of gravitational body forces. The main difference between free and forced convection lies in the mechanism by which the flow is generated.

In addition, there is another type of convection that exists when free convection and forced convection mechanism act together to heat transfer. The process is called mixed convection flow. The effect is noticeable in a situation where the forced fluid velocity is low and the temperature difference is significant.

Internal and external flow can also be classified convection. The internal flow describes a case when fluid is enclosed by a solid boundary such as pipes and channel. Meanwhile, external flow occurs when a fluid extends without encountering a solid surface such as a flat plate, cylinder and sphere. Therefore, this research focuses on the convection that takes place at horizontal circular cylinder, the case of external flow.

The type of the flow also influences the convection process. A flow can be described as laminar, turbulent or transitional in nature. Smooth flow with a particle of fluid moving steadily in a smooth line parallel to the surface is called laminar flow. The velocity of the laminar fluid is constant at any point. The opposite trend is observed for turbulence flow. Turbulence flow is characterised by a chaotic flow with particles moving unsteadily in an unpredictable path. Turbulence flow occurs when the Reynolds number is high while laminar flow is when the Reynolds number is low. The process of laminar becoming turbulent is known as transitional flow.

Apart from the flow type, other criteria that mainly contribute to convection is determined by the thermal heating conditions, fluid properties, the roughness of surface i.e. geometry and orientation. The first key to understanding heat transfer by convection is the boundary layer.

2.2.2 Boundary Layer Theory

Boundary layer theory was first proposed by Ludwig Prandtl in 1904. Prandtl's idea describes a concept that would revolutionise the understanding and analysis of fluid dynamics. The idea behind the concept is in the effect of friction which causes the fluid immediately adjacent to the surface to stick to the surface i.e. no slip condition at the surface and frictional effects are experienced only in a boundary layer, a thin region near the surface (Anderson, 2005). Outside the boundary layer, the flow is essentially the inviscid flow.

Referring to Figure 2.1, the velocity changes enormously over a very short distance normal to the surface of a body immersed in a flow. This means that the boundary layer is a region of a very large velocity gradient. According to Newton's shear stress law which states the shear stress is proportional to the velocity gradient, the local shear stress can be very large within the boundary layer. This results in the skin friction drag force exerted on the body is negligible, contrary to what some previous investigators believed.

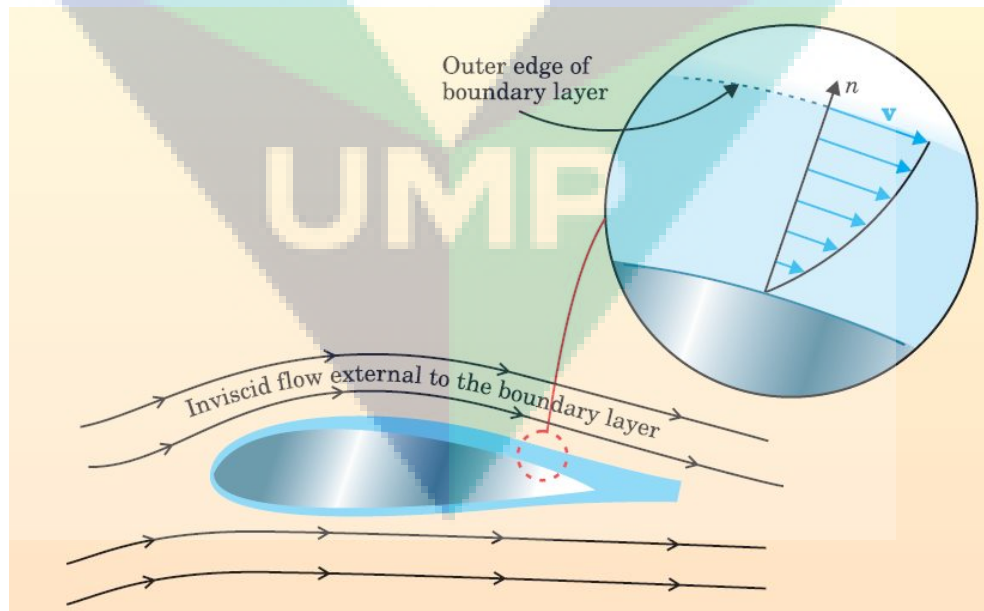


Figure 2.1. Boundary layer region. Source: Acheson (1990)

Prandtl simplifies the equations of fluid flow by dividing the flow field into two regions which are stated as follows:

- i) outer layer where it is far from any solid surface and the viscosity can be neglected, and considered to be inviscid
- ii) thin layer adjacent to a solid surface dominated by viscosity and creating the majority of drag experienced by the boundary body. This thin layer where the friction effect cannot be neglected is called the boundary layer

With the advent of Prandtl's boundary layer concept, it soon became possible for the simplification of the Navier Stokes equation. As a result, the boundary layer equations are likened to Navier Stokes in that each system consists of coupled, nonlinear partial differential equations. The major mathematical discovery however is that the boundary layer equations exhibit an entirely different mathematical behaviour than the Navier-Stokes equations. The Navier Stokes equations possessed elliptic behaviour where the complete flow field must be solved simultaneously, in accord with the specific boundary conditions defined along the entire boundary of the flow. On the contrary, the boundary layer equations have parabolic behaviour, which affords tremendous analytical and computational simplifications. The boundary layer equations can be solved in a few stages by marching downstream from where the flow encounters a body, subject to specified inflow condition at the encounter and specified boundary conditions at the outer edge of the boundary layer. With these step by step solutions, the prediction can be made on skin friction, the location of the flow separation and many more.

Prandtl's idea allows closed form solution in both areas, significant simplification of the full Navier-Stokes equations. The majority of the heat transfer to and from a body take place within the boundary layer again allowing the equations to be simplified in the flow field outside the boundary layer. Prandtl simplifying the equation by estimating the order of magnitude of the various of terms in the conservation equations, and then derived the so-called the boundary layer equations. The boundary layer approximation and analysis order of magnitude by Prandtl can be seen in Chapter 3 Section 3.2.7.

Another astonishing result by Prandtl is flow separation. Flow separation is a case when the boundary layer separates from the surface and trails downstream. A separated flow region with some low energy flow forms in the wake behind the body, but essentially the region is dead air. At the separation point, the fluid elements deep inside the boundary layer have already had substantial portions of the kinetic energies dissipated by friction and so

cannot work their way uphill in a region where the pressure is increasing. Hence the velocity profile depleted near the surface. Beyond the separation point, the boundary layer simply lifts off the surface. There are some case in this study that involved separation flow. The phenomenon described above is shown in Figure 2.2.

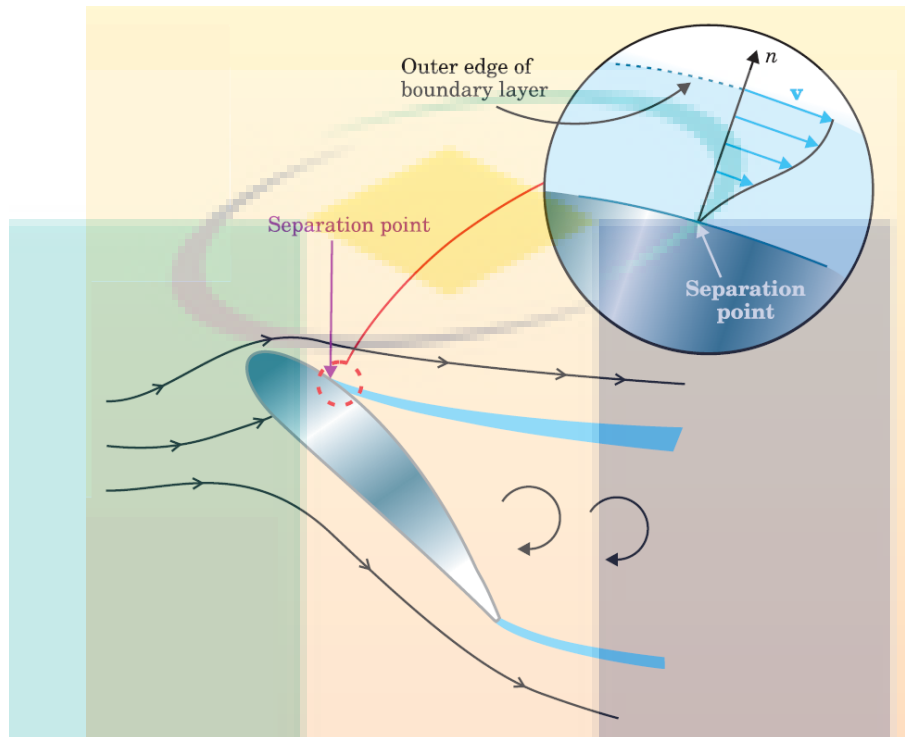


Figure 2.2. Separation of boundary layer. Source : Acheson (1990)

2.2.3 Type of Fluids

As discussed in Section 2.2.1, the convective heat transfer coefficient depends on some fluid properties such as thermal conductivity, specific heat capacity, velocity, viscosity and other flow and temperature dependent properties. Besides that, surface geometry and flow conditions also play a significant role in determining the convection coefficient. Thus, the type of fluid influences the process of heat transfer. In the next subsection, the details of Newtonian, non-Newtonian and nanofluid are provided.

2.2.3.1 Newtonian Fluid

A fluid that behaves accordingly to Newton's law, which viscosity μ is independent of the stress, is said to be Newtonian or known as viscous fluids. Air, water, oil, and electrolyte

can be considered Newtonian. Due to this reason, extensive research has been devoted to heat transfer in Newtonian (viscous) fluids.

Viscous fluids can be described as one which resists movement of an object through the fluid. All fluids, liquid, gas or plasma have some measure of viscosity which can be compared using mathematical formulas or direct measurement or movement. The type of matter a fluid is made of is the main determiner of how viscous it is. In general, liquid will become less viscous as their temperature rises, while gases become more viscous with an increase in temperature. (Mohamed, 2013). Study of the viscous fluid is presented in Chapter 4 and Chapter 6.

2.2.3.2 Non-Newtonian Fluid

In contrast, non-Newtonian fluid properties differ in many ways from those of Newtonian. Most commonly, the viscosity of the non-Newtonian fluid is dependent on the shear rate. Although the concept of viscosity is often used in fluid mechanics to characterise the shear properties of the fluid, it can be inadequate to describe non-Newtonian fluids. The development of the processing industry whose behaviour in shear cannot be characterised by Newtonian relationship has made the research in non-Newtonian increasing. A number of industrially important fluids exhibit a non-Newtonian fluid behaviour. Because of the growing use of these non-Newtonian fluids, considerable efforts have been directed towards understanding their friction and heat transfer characteristics. Amongst the various non-Newtonian fluid models, micropolar is considered in Chapter 5 respectively.

The inadequacy of the classical Navier Stokes to describe rheologically complex fluids such as liquid crystal, animal blood had led Na (1979) to study the boundary layer flow of a micropolar fluid due to a stretching wall. Micropolar fluids are fluids with microstructure. Theory of micropolar fluid was proposed by Eringen (1972). The theory of micropolar fluids can be used to analyse the behaviour to exotic lubricant, liquid crystal, colloidal suspensions or polymeric fluids, and animal blood. Physically, micropolar fluid display the effects of rotary inertia and couple stress. As the fluids consist of randomly oriented molecules, and as each volume element of the fluid has a translation as well as rotation, the analysis of the physical problems in these fluids has revealed several interesting phenomena, which are not found in the Newtonian fluid. Correspondingly, the theory of micropolar fluids requires that one must add a transport equation representing the principle of conservation of mass and momentum, and additional local constitutive parameters are introduced. A detailed survey of microcontinuum fluid mechanics with several applications in physiological fluid flows has been presented by Ariman et al. (1973).

Interesting aspects of theory and applications of micropolar fluids are dealt in the books by Eringen (1966) and Birkhauser (1999).

2.2.3.3 Nanofluid

In the fast growing technology industry globally, many high-tech industries like microelectronics, manufacturing and transportation are facing a problems associated with limiting the cooling efficiency of heat transfer fluids like water, ethylene glycol, lubricants and oil. On the other hand, rapid cooling is also an essential requirement in food science and technology. Hence, the enhancement of thermal properties of conventional fluids can be improved by taking a dilute suspension of nanoparticles into conventional fluids. This suspension which is called nanofluid is a relatively new class of fluids which consist of a base fluid with nano-sized particles.

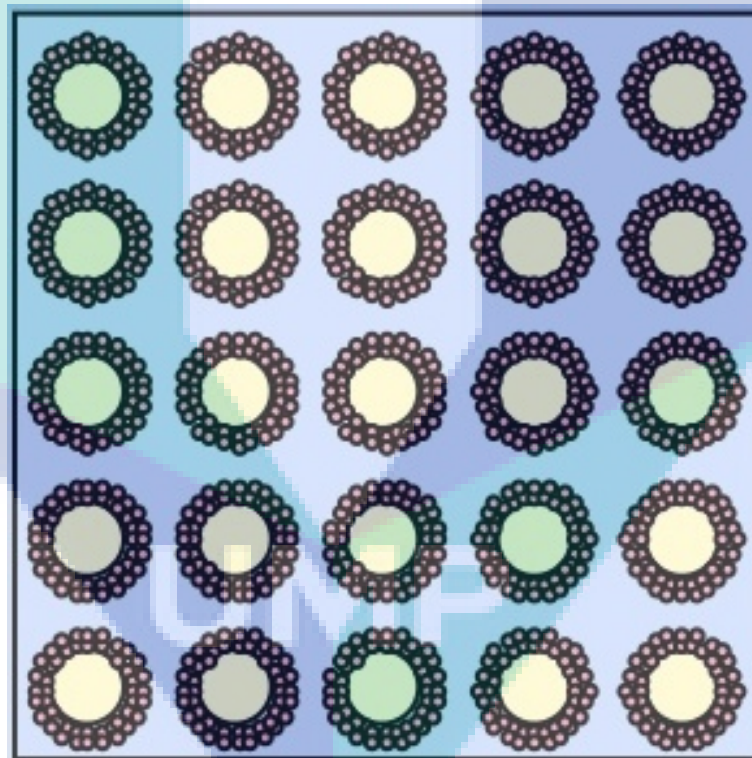


Figure 2.3. Physical model of nanofluids

The term of nanofluids was first introduced by Choi (1995). The nanofluid possesses a significantly higher thermal conductivity and single phase heat transfer coefficients than respective base fluids. In conventional case, the suspended particles are of micrometre or even millimetre dimensions. This large dimension causes severe problems such as abrasion and clogging. Hence, suspended large particles in fluids are hindering the thermal

conductivities in fluid. Therefore, the discovery of nanofluid has boosted the work in improving thermal conductivity. Other major advantages of nanofluids are that the size of nanoparticle is nanometre-sized, and can easily flow smoothly through the microchannel (Khanafar et al., 2003), and therefore, improve thermal conductivity. Reducing and enhancing the heat transfer capabilities will make nanofluid a smart fluid. Besides that nanofluid is very stable due to the tiny size of the nanoelement with no additional problems. The enhanced thermal behaviour of nanofluids could provide a basis for an enormous innovation for heat transfer intensification, which is of major importance to many industrial sectors including transportation, chemical and metallurgical sectors, power generation, micro-manufacturing, thermal therapy for cancer treatment, as well as heating, cooling and air-conditioning. Indeed, nanofluids are also important for the production of nanostructured materials, for the engineering of complex fluids, as well as for cleaning oil from surfaces due to their excellent wetting and spreading behaviour (Ding et al., 2007). However, the thermal conductivity of the nanofluid is strongly dependent on the volume fraction dimension, properties of the solid particle, shape and also the size of the particle (Eastman et al., 1997; Xuan, 2000). Study on nanofluid is presented in Chapter 7 and 8.

2.2.4 Convective Boundary Conditions

Determining the boundary conditions at a surface exposed to a flowing fluid is one of the major concerns for convection. Early studies revealed that in flow problems incorporated either constant or prescribed wall temperature; or constant or prescribed surface heat flux. However, more recent developments of the convection flow have identified that another two heating processes have been used to specifying the wall-to-ambient temperature distributions, namely Newtonian heating and the convective boundary conditions.

Correspondingly, Newtonian heating is a case where the heat transfer rate from the bounding surface with a finite heat capacity is proportional to the local surface temperature usually termed conjugate convective flow. In contrast conjugate conditions are where heat is supplied through a bounding surface of finite thickness and finite heat capacity. In this case, the interface temperature is not known beforehand, but depends on the intrinsic properties of the system, namely the thermal conductivity of the fluid and solid (Salleh et al., 2010a). In other words, a situation where convection heats the bottom surface of the plate from a hot fluid. It is well known in that in convection along a surface with a convective temperature boundary condition the temperature will change along the surface.

In many actual cases the heat transfer from the surface is proportional to the local surface temperature (Hayat et al., 2017). In the boundary layer flow and heat transfer analysis, constant wall temperature and constant heat flux are widely used. However there are instances where the heat transfer is occurring at the surface relies on the wall temperature, resulting mostly in heat exchangers. In this case, the convective boundary condition is used to replace the condition prescribed by the wall temperature or heat flux (Mansur and Ishak, 2013).

Heat transfer problems for flow regarding the convective boundary condition were investigated by Aziz (2009), where a similarity solution for the laminar thermal boundary layer over a flat plate was studied. Furthermore, Aziz in his study, demonstrated that a similarity solution is possible if the convective heat transfer of the plate is proportional to $x^{-1/2}$. The appearance of the paper simulated a large number of subsequent studies concerning different boundary layer problems with convective boundary conditions. See for example, Magyari (2011), Aziz and Khan (2012), Makinde and Aziz (2011), Alsaedi et al. (2012), Ishak et al. (2011) and Mohamed (2013).

Notwithstanding, constant wall temperature and heat flux may be easy to formulate, but it seems unrealistic to apply to real life applications. On the other hand, incorporating the convective boundary condition in the governing system may add further difficulties and challenging equations as the stabilities and inconsistency occurrences persist, but the results obtained may be worth to the industrial applications, and likewise to bridge the thermal heating process gap. An excellent review of the topics covering convective heat transfer problems can be found in the books by Martynenko and Khramtsov (2005) and Bejan (2013).

It is worth mentioning at this juncture, the convective boundary condition changes into constant wall temperature when the value of convective parameter is substantial. Since the study of the convective boundary condition is still at its early stage, comparison against available literature is limited, if existing at all. Therefore by choosing a big value of convective parameters, a comparison can be undertaken with the existing and relevant published research works.

2.3 Keller-box Method

The box scheme for the numerical solution of parabolic differential equations was originally proposed by Keller (1970), namely Keller-box method. Keller-box method is an efficient and accurate implicit numerical scheme devised specially for case of parabolic differential equations. The method has few desirable characteristics that make it suitable

and fit for the solution of all parabolic partial differential equations (Cebeci and Bradshaw, 1988). There are other desirable features which are not so apparent. Being implicit, the method will be unconditionally stable.

The procedure of fourth - order accurate extension of Keller-box method is capable of treating laminar or turbulent boundary layers up to separation point and includes transverse curvature effects. The analysis has been coded and has been shown to provide solutions comparable in accuracy to similar second order schemes but with fewer grid points and with less computer time (Cimbala, 1979).

This method has been applied widely and it seems to be the most flexible of the common methods. It has been tested extensively on laminar boundary layer flows and turbulent boundary layer flow (Keller, 1970). It has also been shown by Keller and Cebeci (1972) and Mucoglu and Chen (1988) that Keller-box method is to be much faster, easier to program, more efficient and flexible to use.

The scheme is also applicable to various type of boundary flow problems, which are the free and mixed convection flow. Na (1979) discussed the isothermal free convection over a vertical plate using the Keller-box method. Kumari et al. (1987) considered the mixed convection boundary flow over a sphere embedded in a saturated porous medium using this numerical method. Next, Kumari et al. (1996) extended this method to solve the unsteady free convection flow over a continuous moving vertical surface.

The procedure includes an implicit finite difference scheme in conjunction with Newton's method for linearisation. Implementation of the box scheme will entail the solution of linear systems of algebraic equations. We shall use the method of factorization of block tridiagonal matrices recommended by Keller (1970) in the five problems considered in this study.

2.4 Forced Convection Viscous Fluid

The first solution of the steady forced convection momentum was described initially by Blasius (1908) who determined the flow from the stagnation point by using series-expansion. In 1940, Frössling (1940) then solved the thermal equation of this problem for the case when the surface temperature of the cylinder is subjected to a constant temperature (Schlichting, 1968). Apart from series expansion method, Merkin and Pop (1988) proposed a numerical solution for the case when there is constant heat flux from the cylinder. The numerical solutions obtained were then used to compare with the series expansion where

it was determined that the Blasius expansion was better in estimating temperature profile, whereas the Gortler-type expansion was better at estimating the velocity profile.

Nonetheless, research on forced convection has been extended where the flow and thermal equations are solved simultaneously using various numerical methods. (Bharti et al., 2007) presented in their paper two types of thermal conditions which are constant temperature and uniform heat flux on the surface of the cylinder. Furthermore, they investigated numerically the momentum and thermal energy equations using the finite volume method. Indeed, they stated that uniform heat flux always shows the higher value of the heat transfer coefficient than the constant wall temperature at the surface of the cylinder. Next, Sumaily et al. (2012) in a separate study, applied high-order finite-element in solving forced convection embedded in the porous medium. The study analyses forced convection heat transfer from a circular cylinder by applying constant wall temperature as the thermal boundary condition. Further, Soares et al. (2005) studied flow and heat transfer behaviour of non-Newtonian fluids by incorporating the iterative Gauss-Seidel relaxation method. They reported that kinematic condition is a major factor that influenced the power law index and less by the type of thermal conditions. In a recent study on forced convection, Durgam et al. (2017) and Sheikholeslami and Bhatti (2017) demonstrated the optimal distribution of the heat source array under forced convection and nanofluid forced in the presence of a magnetic field respectively. The numerical solution was executed using COMSOL as in the former paper and the control volume based finite element method was used in the latter.

Equally important in the numerical approach, the analytical solution on forced convection also available in the literature. Magyari and Keller (2001) provided the solution for the problem of forced convection flow over plane or axisymmetric bodies of arbitrary shapes and power-law surface temperature distribution analytically in porous medium. Meanwhile, Mirgolbabaei et al. (2010) solved forced convection over a flat plate and applying the Adomian Decomposition Method (ADM) with the series solution of the nonlinear differential equations governing on the problem thereby developed. The ADM combined with the Pade approximant to provide efficient alternative tools for solving nonlinear models.

However, the literature on forced convection on the experimental work has not been studied as extensively compared to the numerical methods. Some of the studies on the mechanism behind the forced convection flow using experimental techniques may be found in several papers by Sanitjai and Goldstein (2004), Mohammed and Salman (2007) and Mahgoub (2013). The latter researcher investigated forced convection heat transfer over a flat plate in a porous medium with air as the working fluid. The experiments have been carried out for the Reynolds numbers ranging from 10^5 to 10^6 based on the test plate length

under the condition of constant heat flux. Accordingly, it was found that higher heat transfer coefficients were obtained with larger particle size and higher particle thermal conductivity.

On the other hand, Salleh et al. (2011) conducted a study on forced convection over a horizontal circular cylinder with Newtonian heating boundary conditions. It was shown that the flow problem is unaffected by the heat transfer due to the decoupling equations and there are critical values in the parameters to achieve an acceptable solution for the temperature profiles. The Newtonian heating conditions were introduced by Merkin (1994), and the condition has also been used in many studies by investigators such as in Chaudhary and Jain (2006), Salleh et al. (2009, 2011) and many more.

In addition, another type of boundary conditions which is convective boundary condition has been investigated over a flat surface by Merkin and Pop (2011). The result was obtained numerically based on the Crank-Nicolson method and the Newton-Raphson iteration to finite difference equations that arise at each step space. Before that, Bharti et al. (2007) had already solved the forced convection problem numerically using the finite volume method. These researchers considered viscous fluids in their studies. However in more recent research, Mohd Rohni et al. (2013) expanded the work and focused towards nanofluid as this fluid gave promising results in increasing the thermal conductivities. These authors incorporated constant wall temperature in their studies concluding that by increasing the nanoparticles thereby leads to the increase in thermal conductivity. Moreover, a most recent paper by Mabood et al. (2016) studied nanofluid in the forced convection numerically considering convective boundary conditions as the thermal conditions. Also, the experimental investigation by Vimala et al. (2016) in the forced convection considered nanofluids as a base fluid as well.

Therefore, the above literature review demonstrates that even though a significant work has been performed in the area of forced convection, the effect of the convective parameter on heat transfer has not been investigated in detail. Accordingly, this research aims to is examine the steady forced convection flow over a horizontal circular cylinder with convective boundary conditions. Motivated by the studies of Merkin and Pop (2011) and Salleh et al. (2011), problem in Chapter 4 follows closely the formulation of that proposed by the latter. Next subtopic discussed the development of free convection in micropolar fluids.

2.5 Free Convection Micropolar Fluid

Several of the earlier studies on free convection can be found in the articles written by Willson (1969) and Peddieson and McNitt (1970). Indeed, Willson introduced the concept of the boundary layer in the theory of micropolar fluids meanwhile Peddieson and McNitt applied the micropolar theory to the problem of steady stagnation point flow, steady flow over a semi infinite plate and impulsive flow past an infinite plate. Balaram and Sastri (1973) and Maiti (1975) further studied convective heat transfer in a micropolar fluid through a vertical channel and horizontal flat plate respectively. In the following year, Sastry and Maity (1976) collaborated together on the problem of forced and free convection in a micropolar fluid in an annulus of two vertical pipes. Notably, in the previous three studies mentioned, the boundary layer concepts in convective flow are not considered.

Elliott (1970) investigated and pioneered work on free convection flow on a two dimensional or axisymmetric body. However, it appears that Merkin (1976) was the first to present the complete solution of this classical (Newtonian) fluid using the Blasius and Gortler series expansion method along with the integral and finite difference scheme. Nonetheless, over the years, many numerical techniques have been applied to solve the free convection problem. Some of the methods include the Runge Kutta integration scheme with the Newton Raphson shooting method by Hassanien (1997), McCormick's technique Rebhi et al. (2007), Runge-Kutta Fehlberg Yacob et al. (2011), and the finite element method using the variational Ritz model by Takhar et al. (1998). Also, Elgazery and Elazem (2009) studied the effect of thermal radiation and variable viscosity and thermal conductivity of micropolar fluids using the Chebyshev finite difference method. The method proposed by Elgazery and Elazem (2009) demonstrated that the variable viscosity and thermal conductivity in the presence of thermal radiation had significant influences on the velocity, the angular velocity and temperature profiles, shear stress, couple shear stress and the Nusselt numbers.

Recently, Borrelli et al. (2013) solved MHD flow in micropolar fluids by using numerical method. The numerical solutions are obtained using the MATLAB routine BVP4C. Most recently, Abdallaoui et al. (2015) studied this numerically using the lattice Boltzmann method where heating is maintained at a constant wall temperature. One remarkable finding in their research is that fluid flow and heat transfer are profoundly affected by the heating cylinder position. Later, Zhang et al. (2016) investigated numerically a natural convection elliptic cylinder using the variational multiscale element free Galerkin method.

On the other hand, Kim and Lee (2003) performed several analytical studies on the MHD oscillatory flow of a micropolar fluid over a vertical porous plate, and the effects of non-zero values of micro-rotation vector on the velocity and temperature fields across the boundary layer. Moreover, this was studied using small perturbation approximation. Furthermore, the Homotopy Analysis method is noted to be among the most popular analytical methods in solving flow problems and is frequently applied to obtain the expression for velocity and microrotation profiles Sajid et al. (2009). Meanwhile, Deka et al. (2017) studied one dimensional unsteady free convection past an vertical cylinder under constant heat flux at the surface. The closed form solution obtains the Bessel function & modified Bessel functions by Laplace transformation. Also, Abou-Ziyan et al. (2017) investigated a short horizontal cylinder experimentally with a large Pr number under constant heat flux for both Newtonian and non-Newtonian fluids where the results indicated that the Newtonian fluid achieves a higher free convection heat transfer coefficient than the non-Newtonian fluid.

The effect of the micropolar parameter in the unsteady mixed convection was investigated by Gorla (1995). The findings by Bhargava and Takhar (2000), Mathur et al. (1978) on the boundary flow immersed in micropolar fluid demonstrated that temperature increases inside the boundary layer compared to the Newtonian flows. Likewise, Mansour et al. (2000) studied the effects of heat and mass transfer on the magnetohydrodynamic flow of micropolar fluid on a circular cylinder with uniform heat and mass flux. The results indicated that micropolar fluids display a reduction in drag as well as heat transfer when compared with Newtonian fluids. Accordingly, Kelson and Desseaux (2001) set self-similar solutions for the boundary layer flow of micropolar fluids driven by a stretching sheet with uniform suction or blowing through the surface. In a separate study, Ibrahim and Hassanien (2001) obtained local similarity solutions for mixed convection boundary layer flow of a micropolar fluid on horizontal flat plates with variable surface temperature. More recently, Gibanov et al. (2016) studied convection in a trapezoidal cavity filled with a micropolar fluid and (Hussanan et al., 2017) extended the convection flow in micropolar nanofluids with oxide nanoparticles in water, kerosene and engine oil.

Research on free convection over flat plates in micropolar fluid has been carried out by Jena and Mathur (1981). The authors studied free convection in the boundary layer flow of a micropolar fluid past a non-isothermal vertical flat plate. Undoubtedly the study of the free convection boundary layer over horizontal circular cylinder is not as extensive as the boundary layer flow over a flat plate. Among the early investigations over a horizontal circular or elliptic cross section are given by Bhattacharyya and Pop (1996) where they studied free convection in a micropolar fluid. This work is an extension of the problem

studied by Merkin (1977) in a viscous fluid. Hassanien and Gorla (1990) examined combined forced and free convection in micropolar fluid over a horizontal cylinder. Next, Amin and Riley (1990) analysed the problem over a heated horizontal plane and Merkin (1976) considered free convection on the isothermal horizontal cylinder in a viscous fluid. Free convection over a horizontal circular cylinder was likewise studied by Merkin and Pop (1988) by incorporating constant heat flux in a viscous fluid. Notably, Nazar et al. (2002b) extended the work of Merkin (1976) of the problem in a micropolar fluid with constant wall temperature. Nazar et al. (2002a) then revisited the same problem applying the constant wall heat flux. Recently, Salleh and Nazar (2010) investigated Newtonian heating in the boundary condition, in this problem to study the effect of the convective parameter and Mahfouz (2013) examined free convection within an eccentric annulus filled with micropolar fluid and was solved using the spectral method and applied CWT.

Motivated by the studies conducted by Salleh and Nazar (2010), and Nazar et al. (2002a,b), the present study in Chapter 5 consider the laminar free convection boundary layer flow over a horizontal circular cylinder in a micropolar fluid.

2.6 Mixed Convection Viscous Fluid

Acrivos (1966) was first to theoretically proposed the problem of mixed convection flow from general bodies in the existence of a boundary layer. Joshi and Sukhatme (1971) solved the boundary layer of this problem using the series method in which the cases of assisting and opposing flow considered by using the technique of Gill Runge-Kutta integration technique along with the Shooting method. Conversely, Nakai and Okazaki (1975) studied the mixed convection problem of a circular cylinder for the cases of both small Grashof and Reynolds numbers.

Further, Sparrow and Lee (1976) studied mixed convection of a horizontal circular cylinder subjected to constant wall temperature. However, these authors only considered the opposing flow in their research studies. Then, Merkin (1977) extended the problem discussed by latter, where a numerical solution to the boundary layer equations with $Pr = 1$ is obtained, and solved it based on the Crank - Nicolson method, using Newton - Raphson method coupled with the Choleski decomposition technique. The solution was restricted to the region preceding the point of boundary layer separation since boundary layer are not valid beyond that point.

The study on mixed convection boundary layer flow over a stretching cylinder in a porous medium was conducted by Mukhopadhyay (2012). The results were numerically

obtained using Shooting method, where the skin-friction coefficient increased with an increasing mixed convection parameter. Notably, the research on mixed convection in the horizontal circular cylinder is not only limited to the case when fluid viscosity is constant, but is also found in the case where there is variation in viscosity. For instance, Ahmad et al. (2009) considered the problem of mixed convection with temperature dependent viscosity and the obtained results indicated that the flow and thermal characteristics are significantly influenced by the effect of temperature-dependent viscosity especially when the viscosity of a fluid is sensitive to temperature variations. More recently, Malik et al. (2016) extended the problem carried out by Ahmad et al. (2009) by investigating temperature dependent viscosity and thermal conductivity. The authors have also indicated that the effect of viscous dissipation is considered in the energy equation.

On the other hand, Roca and Pop (2013) performed stability analysis for the problem of mixed convection flow past a vertical flat plate in the case of heat flux where they obtained a dual solution to establish which of the solutions was stable; the stability analysis was therefore required in this case. Other studies covering practical applications in engineering heat transfer on this topic are those by Chin et al. (2007), Merkin and Pop (2002), Chen (2000) and recently Danai et al. (2016). The more recent reference is given by Seshadri and Munjam (2016) and Elsherbiny et al. (2017) where they designed a study to observe convection across a horizontal square isothermal cylinder.

This problem has also been expanded to different geometries and extended in several cases in viscoelastic, micropolar and the more recent development in nanofluids. The problem of mixed convection flow of a micropolar fluid over a stretching sheet has been solved by Takhar et al. (1998). Anwar et al. (2008) has also analysed the mixed convection boundary layer flows in the viscoelastic fluid over a horizontal cylinder with a constant temperature while Ishak et al. (2009) considered mixed convection in a micropolar fluid and found that dual solutions exist in assisting flow. On the other hand, Ahmad et al. (2012) reported that for the case of mixed convection in laminar film flow of a micropolar fluids, a dual solution exists for the case of assisting flow and with no dual solutions for the case of opposing flow. Recently, Tham et al. (2014) considered mixed convection flow from a horizontal circular cylinder embedded in a porous medium and nanofluid using the model proposed by Buongiorno. The authors discussed the influence of several parameters of nanofluids and concluding that the parameters affected the flow and heat transfer characteristics.

Various numerical techniques and methods have been adopted to solve the mixed boundary flow problem. Mukhopadhyay and Mandal (2015) reported the effect of velocity slip and thermal slip on magnetohydrodynamic by applying the Shooting method. On the

other hand, Bhowmick et al. (2014) solved numerically non-Newtonian mixed problem by applying the marching order implicit finite difference method with the double sweep technique. For an analytical solution, the Homotopy analysis method has been widely used. See for example Abbasi et al. (2016) and Waqas et al. (2016). Recently Samyuktha and Ravindran (2015) examined the thermal radiation effect on mixed convection flow over a vertical stretching sheet using CWT. More recently, Abbasi et al. (2016) and Altunkaya et al. (2017) investigated the vertical parallel plate by using the perturbation series method and CHF respectively.

Furthermore, Nazar et al. (2003, 2004) investigated the problem of mixed convection in the horizontal circular cylinder for both heating conditions namely, constant wall temperature and constant heat flux. In their papers, they explained how the governing parameters affected the flow and heat transfer characteristics as well as the position of the boundary layer separation. Following Nazar's work, Salleh et al. (2010b) solved the same problem by incorporating Newtonian heating in boundary conditions. Therefore, in the present study in Chapter 6, the problem of mixed convection boundary layer flow over a horizontal circular cylinder is considered by extending the work of Salleh et al. (2010b) by changing the thermal heating from Newtonian to convective boundary conditions.

2.7 Mixed Convection Nanofluid : Tiwari and Das Model

Early investigation on nanofluid using the Tiwari and Das model in the horizontal circular cylinder is presented by Eiyad et al. (2008) using the second order finite volume scheme. Thanks to the advancement of numerical methods, most problems are solved via the numerical approach and modelled by the nonlinear ordinary or partial differential equations. In particular, Soleimani et al. (2012) conducted a numerical investigation on the natural convection inside the semi-annulus cavity filled with a nanofluid using the Control Volume based Finite Element Method (CVFEM). Moreover, Seyyedi et al. (2015) applied the finite volume method numerically to analyse the natural convective heat transfer in an annulus filled with a Cu/water nanofluid. Through finite volume as well, Nayak et al. (2015) concluded that the heat transfer rate increases remarkably by the addition of nanoparticles.

Besides the finite volume and finite elements, some researchers have employed the Lattice Boltzmann in solving the nanofluid Tiwari and Das problem. Among the investigators using this method are Ashorynejad et al. (2013) and Rahmati et al. (2016). These authors studied numerically the effect of magnetic field on natural convection in a

horizontal cylindrical annulus and mixed convection in a double lid-driven cavity respectively. Sheremet et al. (2015) conducted a similar study in the cavity

Interestingly, Dinarvand and Pop (2017) combined both methods; analytical and numerical in solving the convection flow problem for a rotating down-pointing cone. A general analytical method known as the Homotopy Analysis Method is proposed together with the Keller-box method in this study. Before that, Hassani et al. (2011) previously applied HAM in their research and found that their result in nanofluid over a stretching sheet for the Nusselt number are contradicted with the result obtained by Khan and Pop (2010).

The studies of nanofluid in the horizontal cylinder are less than those studies associated with the stretching sheet. Indeed, major attention is given to the problem caused by a stretching surface because of its immense potential as a technological tool in many engineering applications. The effect of the parameters namely the Soret effect, the inclination angle and the thermal radiation effect in nanofluids have recently been investigated by RamReddy et al. (2013), Abu-Nada and Oztop (2009) and Das et al. (2015), respectively. In addition, Bachok et al. (2012) studied the stagnation point flow over a permeable stretching/shrinking sheet. Subsequently, these authors focused on Copper nanoparticles diluted in a water based fluid. Furthermore, they concluded in their study that the inclusion of nanoparticles into the base fluid produced an increase in the skin friction coefficient and the local Nusselt number.

Also, Mabood et al. (2017) and Tham et al. (2012) investigated the effect of viscous dissipation on unsteady mixed convection and steady mixed convection for a horizontal cylinder using the Tiwari and Das model by considering the constant wall temperature, respectively. Notwithstanding, constant heat flux has also been used in mixed convection in the lid-driven square cavity with Cu-water nanofluid by Ismael et al. (2016).

The pioneering work of Aziz (2009) on convective boundary conditions stimulated a vast number of subsequent papers concerning different boundary layer problems. See for example, Yacob et al. (2011) who investigated the problem of stretching shrinking in nanofluid numerically using the Runge-Kutta-Felbergh method with shooting techniques by incorporating convective boundary conditions. Further, Hajmohammadi et al. (2015) analysed nanofluid flow and heat transfer over a permeable flat plate using convective boundary condition. More recently, Khan et al. (2016) investigated the rotating flow of nanofluid induced by a convectively heated deformable surface using a combination of the shooting approach with the fifth order Runge-Kutta method determining the velocity and temperature distributions above the sheet.

Although there are great number of studies conducted on different variations of geometry, temperature and heat flux, limited work has been undertaken (perhaps only a few) to investigate nanofluid using the Tiwari and Das model of a circular cylinder using convective boundary conditions. Therefore, problem in Chapter 7 concentrates on employing the convective boundary condition whereby three different nanoparticles namely Cu, Al₂O₃ and TiO₂ are diluted in water-based fluid to form a nanofluid. Indeed, particular efforts is concentrated on the effects of the skin friction coefficient, the local Nusselt number, flow field, temperature distribution, mixed convection and convective parameters. To the author's knowledge, little focus has been undertaken in studies highlighting the boundary layer flow of nanofluid over a surface with convective boundary conditions.

2.8 Mixed Convection Nanofluid : Buongiorno Model

The other popular nanofluid model besides Tiwari and Das is Buongiorno. Based on Buongiorno's exploration on nanofluid, the study on the flow in porous medium filled with nanofluid has garnered considerable interest and attention. Nield and Kuznetsov (2009) pioneered the study of porous medium saturated in nanofluid by presenting the influence of nanoparticle on natural convection past a vertical plate, using model in which Brownian motion and thermophoresis are accounted for. This problem is initially extends from the classical problem of porous medium studied by Cheng and Minkowycz (1977) while Nield and Kuznetsov (2009, 2011) extended the Cheng-Minkowycz problem for natural convective boundary layer flow in a porous medium saturated by a nanofluid. Moreover, Nield and Kuznetsov (2009) analysed free convection boundary layer flow along a vertical flat plate embedded in a porous medium and Nield and Kuznetsov (2011) investigated the problem of thermal instability in a porous medium layer saturated by a nanofluid. In this model, the Brownian motion and thermophoresis enter to produce their effects directly into the equations expressing the conservation of energy and nanoparticles. Notably, this is so the temperature and the particle density is coupled in a certain way, and that the results in the thermal and concentration buoyancy effects being coupled in the same way.

In a series of papers, Kuznetsov and Nield (2010, 2011) further presented the natural convective boundary layer flow of a porous medium filled by a nanofluid past a vertical plate. The boundary layer flow over a moving semi-infinite plate in a flowing fluid is investigated by Bachok et al. (2010). Khan and Aziz (2011) examined the double-diffusion natural convection from a vertical plate embedded in a porous medium saturated with a nanofluid. Recently, Tham et al. (2014) studied the steady mixed convection boundary layer

flow of a circular cylinder in a nanofluid with a constant wall temperature. It is also worth mentioning that in this chapter, the work of Tham et al. (2014) has been carefully examined.

Convection in fluid-saturated porous media has a remarkable impact upon some of the applications in industry, such as heat removal from nuclear fuel debris, underground disposal of radioactive waste material, storage of foodstuffs and exothermic and/or endothermic chemical reactions and dissociating fluids in packed-bed reactors (Mukhopadhyay, 2012). Since nanofluids are being used as coolants for the future, it is therefore useful to conduct further studies involving nanofluid in porous media. A recently published paper by Sakai et al. (2014), reviewed a macroscopic set of governing equations for describing the heat transfer in nanofluid saturated porous media. Moreover, the equations were derived using a volume averaging theory, and a numerical method for a solution to the boundary value problem for the partial differential equations. At the same time it is possible to transform these equations to Ordinary Differential Equations (ODE) and to solve them using semi-analytical methods (Sheremet and Pop, 2015).

Most of the work in Buongiorno nanofluid were solved numerically due to the ramification of governing equations in a nanofluid. However, several problems being solved via analytical solutions. For instance, Hassani et al. (2011) investigated analytically convection flow past a stretching sheet using HAM. The comparison has been made with the numerical method presented earlier by Khan and Pop (2010) and the result is found to be in excellent agreement. The extended HAM known as the Optimal Homotopy Analysis Method (OHAM) has been applied recently by Nadeem et al. (2014) in the study which deals with the Casson nanofluid in the presence of convective boundary conditions.

On the more recent development by Dhanai et al. (2016), they investigated numerically mixed convection slip flow and heat transfer of uniformly conducting nanofluid past an inclined cylinder under the influence of Brownian motion, thermophoresis and viscous dissipation via the fourth order Runge Kutta Fehlberg (RKF) method with shooting method. Meanwhile, Kefayati (2017) extended mixed convection non-Newtonian nanofluids using the Buongiorno's mathematical model in a cavity analysed by finite difference Lattice Boltzmann method. Numerical simulation applying the finite volume method using Buongiorno's model has also been discussed by Garoosi et al. (2015).

Further studies on nanofluid are observed on a stretching sheet by Mansur and Ishak (2013), Das et al. (2015) and Othman et al. (2017). The first two papers applied the convective boundary condition and the latter incorporating constant wall temperature. In a further study, Othman et al. (2017) and Moshizi et al. (2017) used CWT to investigate mixed convection magnetohydrodynamic nanofluid inside microtubes. The authors were

specifically interested in the effect of nanoparticle migration on fluid flow and heat transfer characteristics, and examining the figure of merit of thermal performance. In contrast, Ramzan et al. (2016) applied convective boundary conditions in investigating radiative flow of second grade nanofluid.

Heat transfer under convective boundary conditions plays a vital role in the process. Despite the considerable research previously undertaken and the enhancement efforts on the development of heat transfer, only a few papers have highlighted convective boundary conditions. A significant portion of the literature has focused on other geometries such as flat plate and stretching sheet. Indeed, this form of thermal heating in complex geometry is very important in processes involving high temperatures and in many engineering applications. Therefore, assuming that the nanoparticles being suspended in a nanofluid, the convection flow by implementing the convective boundary condition as thermal condition is further studied in this thesis, extending the research by Tham et al. (2014) by applying convective boundary conditions.

As a summary, the development of research in five different flow problems are listed in the Table 2.1 to Table 2.5.



UMP

Table 2.1. Development of forced convection in viscous fluid

Author	Year	Contribution
Blasius	1908	Solved the steady forced convection momentum at the stagnation point using series-expansion
Frossling	1940	Solved the thermal equation for the case of when surface temperature is subjected to constant wall temperature
Merkin and Pop	1988	Proposed numerical solution for the case when constant heat flux is applied
Magyari and Keller	2001	Provide analytical solution for flow over axisymmetric bodies of arbitrary shape
Sanitjai and Goldstein	2004	Obtain experimental result for the forced convection of the horizontal cylinder
Soares et al	2005	Study flow and heat transfer behaviour of non-Newtonian fluids using iterative Gauss Seidal relaxation method
Bharti et al.	2007	Investigated momentum and thermal equation of forced convection using finite volume method for case constant temperature and uniform heat flux
Mirgolbabaei et al.	2010	Apply analytical method namely Adomian Decomposition method with the series solution on forced convection over flat plate
Salleh et al.	2011	Derive a numerical study on forced convection with Newtonian heating are applied as the thermal boundary condition over horizontal circular cylinder with Keller-box method
Merkin and Pop	2012	Construct numerical study based on Crank-Nicolson method and Newton-Rhapson iteration with convective boundary condition
Sumaily et al.	2012	Study high order finite element method in solving forced convection in porous medium with constant wall temperature
Mabood et al.	2016	Extend the research in forced convection by using nanofluids Tiwari and Das model with convective boundary condition
Durgam et al.	2017	Demonstrate the optimal distribution of heat source under forced convection where the numerical solutions are obtained via COMSOL

Table 2.2. Development of free convection in micropolar fluid

Author	Year	Contribution
Eringen	1966	Proposed the theory of micropolar fluid
Willson	1969	Introduced the concept of boundary layer in the theory of micropolar fluids
Peddieson and McNitt	1970	Apply the micropolar theory to the problem of steady flow past an infinite plate
Elliot	1970	Pioneered in free convection flow on a two-dimensional or or axisymmetric body
Merkin	1976	Present the complete solution of the Newtonian fluid using the Blasius and Gortler series expansion over horizontal circular cylinder with constant wall temperature
Merkin	1988	Study the same problem as in 1976, but using constant heat flux as thermal heating
Bhattacharyya and Pop	1996	Extend the work of Merkin(1976) by considering micropolar fluid instead of Newtonian
Nazar et al.	2002	Revisit Merkin's (1988) work of steady free convection by considering micropolar fluid
Rebhi et al.	2007	Investigate the unsteady free convection in micropolar with constant heat flux numerically using McCormick's technique
Sajid et al.	2009	Perform analytical study to obtain the expression for velocity and microrotation profile using Homotopy Analysis method
Salleh and Nazar	2010	Construct a study on free convection micropolar fluid by considering Newtonian heating at the boundary conditions via numerical approach using Keller-box method
Abdallaoui et al	2015	Provide numerical study of free convection using lattice Boltzmann method where heating is maintained at constant temperature
Abou-Ziyan et al	2017	Set up experiment under constant heat flux for free convection micropolar for Newtonian and non-Newtonian fluid

Table 2.3. Development of mixed convection in viscous fluid

Author	Year	Contribution
Acrivos	1966	Proposed the problem of mixed convection from general bodies in the existence of a boundary layer.
Joshi and Sukhatme	1971	Solve mixed convection using Gill Runge-Kutta with shooting method
Nakai and Okazaki	1975	Study mixed convection using both small Grashof and Reynolds number.
Sparrow and Lee	1976	Considered constant wall temperature for the problem of mixed convection of horizontal circular cylinder and only focus on opposing flow
Merkin	1977	Extend the work of Sparrow and Lee (1976) and solve based on Crank-Nicolson using Newton-Raphson coupled with the Choleski decomposition technique
Nazar et al.	2003 2004	Investigate mixed convection in the horizontal circular cylinder for both heating conditions namely, constant wall temperature and constant heat flux.
Anwar et al.	2008	Present the mixed convection problem with viscoelastic fluid with constant temperature
Ishak et al.	2009	Formulate the mixed convection problem with micropolar fluid with constant temperature
Ahmad et al	2009	Construct derivation of mixed convection with temperature dependent viscosity
Salleh et al.	2010	Revisit Merkin's (1988) work of steady free convection by considering Newtonian heating
Roca and Pop	2013	Perform stability analysis and obtained dual solution which can determine the stableness of the solution
Abbasi et al.	2016	Investigate the mixed convection over vertical plate by using pertubation series method with constant heat flux
Malik et al.	2016	Extend the problem carried out by Ahmad et al. (2009) by adding the effect of viscous dissipation in the energy equation

Table 2.4. Development of mixed convection: Tiwari and Das model

Author	Year	Contribution
Tiwari and Das	2007	Proposed the concept of heat transfer enhancement via the solid volume fraction of different nanoparticle at the base fluid.
Daungthongsuk	2007	Provide review on the convective transport in nanofluids
Eiyad et al.	2008	Pioneer researcher of mixed convection nanofluid and solved numerically using the second order finite volume scheme
Yacob et al.	2011	Study problem of mixed in nanofluid past stretching sheet and solution obtained via numerical approach namely Runge Kutta Felbergh with shooting method
Hassani et al.	2011	Obtain an analytical solution via Homotopy analysis method for case boundary layer flow filled with nanofluid
Bachok et al.	2012	Derive the unsteady case of flow and heat transfer problem over a permeable stretching and shrinking sheet
Soleimani et al.	2012	Conducted numerical investigation inside semi annulus cavity in nanofluid using control volume based finite element
Tham et al.	2012	Present output of mixed convection over circular cylinder applying Tiwari and Das model by considering constant wall temperature
Ashorynejad et al.	2013	Perform analysis using Lattice Boltzmann method to check the effect of magnetic field over a horizontal circular cylinder
Hajmohammadi et al.	2015	Analysed nanofluid flow and heat transfer over permeable flat plate using convective boundary conditions
Khan et al.	2016	Study the rotating flow of nanofluids using numerical approach via 5th order runge Kutta and shooting using convective boundary conditions
Dinarvand and Pop	2017	Combined analytical and numerical approach in solving problem rotating down pointing cone. Homotopy analysis together with Keller-box is proposed in this study
Mabood et al.	2017	Investigate the effect of viscous dissipation on unsteady mixed convection in nanofluid using Tiwari and Das model

Table 2.5. Development of mixed convection: Buongiorno model

Author	Year	Contribution
Buongiorno	2006	Conducted extensive study on convective transport focusing on heat transfer enhancement observed during convective situation.
Nield and Kuznetsov	2009	Pionereed the study of porous medium immersed in nanofluid and present the effect of nanoparticle on free convection problem past a vertical plate
Nield and Kuznetsov	2011	Extend the previous problem by investigating the thermal instability in a porous medium
Khan and Aziz	2011	Examined double diffusion from vertical plate embedded in porous medium immersed in nanofluid Kutta Felbergh with shooting method
Mansur et al.	2013	Analysed flow and heat transfer nanofluid past stretching & shrinking sheet with convective boundary conditions
Tham et al.	2014	Studied the steady mixed convection embedded in porous medium by applying constant wall temperature as thermal heating
Nadeem et al.	2014	Extended HAM known as Optimal homotopy analysis is applied in oblique flow of Casson fluid with convective boundary conditions
Garoosi et al.	2015	Applied finite volume method in convection flow problem using Buongiorno's nanofluids model
Sheremet and Pop	2015	Investigate the convection problem in a porous horizontal cylinder annulus with nanofluids and solve the governing equations using semi-analytical method
Dhanai et al.	2016	Perform the numerical analysis on mixed convection slip flow on uniformly conducting nanofluids past an inclined cylinder via the fourth order Runge Kutta Felhbergh due to velocity and thermal slip effects
Kefayati	2017	Extend non-Newtonian nanofluids in cavity by using finite difference method namely lattice Boltzmann.
Othman et al.	2017	Investigate the effect of constant wall temperature in the problem of mixed convection past a vertical stretching surface in nanofluids

CHAPTER 3

PROBLEM FORMULATIONS AND NUMERICAL METHODS

3.1 Introduction

The purpose of this chapter is to provide description of mathematical model used in this study. Two essential elements in the mathematical model are the governing equation and the numerical method. The derivation and formulation of governing equations from basic fluid mechanic principles that consist of the continuity equation, momentum equation, energy equation and nanoparticle volume fraction are discussed for a case of mixed convection boundary layer flow in a nanofluid using Buongiorno's model, where the finding of the results and discussion can be found in Chapter 8. A detailed explanation of the equations and process that governs the flow such as the non-dimensional equation, approximations and transformation are highlighted in the Section 3.2.

Section 3.3 elaborates on the numerical method used which is the Keller-box method. This method has been used extensively in solving boundary layer problems due to the desirable features that thereby makes it appropriate for the solution of the parabolic differential equation. The full procedures of the Keller-box method are presented in Subsection 3.3.1 to 3.3.4. These procedures are required later in solving another four convection flow problems presented in Chapters 4 to 8.

A further crucial element in modelling the convection flow are the boundary conditions and initial profile. Therefore in Sections 3.4 and 3.5, the description of the boundary condition and initial profile are provided.

3.2 Problem Formulations

This section provides thorough derivation of the governing equations of the problem that is presented in Chapter 8 starting from the conservation of mass, momentum, energy and nanoparticle equation derived based on the principle of conservation law. Initially, the governing equations are in elliptical form which consists of field equation embody the conservation of the total mass, momentum, thermal energy and nanoparticles that given in the following section (Buongiorno, 2006). The governing equation are then simplified into a parabolic form by the analysis of the magnitude, non-dimensional variables and non-similarity transformation as given in Section 3.2.7, 3.2.8 and 3.2.9, respectively.

3.2.1 Conservation of Mass

Generally, mass can be added or removed and can be changed into different types of particles. However mass can neither be created or destroyed. In an isolated system, a volume fixed or moving in a frame through which gas or liquid can flow is called control volume $V(t)$ and enclosing surface to control volume is known as control surface, $S(t)$. The conservation of mass can be written as follows (Darus, 1994)

$$\frac{DM_t}{Dt} = 0$$

where $M_t = \int_{V(t)} \rho dV$ is a total mass and ρ is the nanofluid density. Applying Reynolds transport theorem on total mass, then

$$\frac{DM_t}{Dt} = \int_{V(t)} \frac{\partial \rho}{\partial t} dV + \int_{S(a)} \rho \bar{\mathbf{V}} \cdot d\mathbf{S} \quad 3.1$$

Assume that there is no sources or sinks of mass within dV . Then $DM_t/Dt =$ the rate at which mass enters or leaves through the surface dS . For nanofluid, $\rho \bar{\mathbf{V}}$ is considered as $\rho \bar{\mathbf{V}} + \mathbf{j}_p$ (Anwar, 2013). Equation (3.1) then becomes,

$$\int_{V(t)} \frac{\partial \rho}{\partial t} dV + \int_{S(a)} (\rho \bar{\mathbf{V}} + \mathbf{j}_p) \cdot d\mathbf{S} = 0 \quad 3.2$$

Note that \mathbf{j}_p is the nanoparticle mass flux defined as

$$\mathbf{j}_p = \mathbf{j}_{p,B} + \mathbf{j}_{p,T} = -\rho_p \left(D_B \nabla \bar{C} - D_T \frac{\nabla T}{T_\infty} \right) \quad 3.3$$

where $\mathbf{j}_{p,B}$ and $\mathbf{j}_{p,T}$ are the mass fluxes due to Brownian and thermophoresis diffusion respectively. Equation 3.2 shows that summation rate of change for mass in control volume with net mass flow rate from the control surface is zero and Equation 3.2 is a continuity equation in an integral form. The continuity equation in differential form can be derived by transforming the surface integral which is the second term in Equation 3.2 to a volume integral. By applying the Gauss divergence theorem, Equation 3.2 becomes

$$\int_{V(a)} \frac{\partial \rho}{\partial t} dV + \int_{V(a)} \nabla \cdot (\rho \bar{\mathbf{V}} + \mathbf{j}_p) \cdot dV = 0 \quad 3.4$$

This expression must hold for every arbitrarily shaped volume, the only way that it can be satisfied is if the integrand vanishes identically, or

$$\frac{\partial \rho}{\partial t} + \nabla \cdot (\rho \bar{\mathbf{V}} + \mathbf{j}_p) = 0 \quad 3.5$$

According to Buongiorno (2006), the nanofluid density ρ can be written as

$$\rho = C\rho_p + (1 - \bar{C})\rho_{bf} \quad 3.6$$

where ρ_{bf} is the density for the base fluid. Therefore,

$$\frac{\partial [C\rho_p + (1 - \bar{C})\rho_{bf}]}{\partial t} + \nabla \cdot ([C\rho_p + (1 - \bar{C})\rho_{bf}]\bar{\mathbf{V}} + \mathbf{j}_p) = 0 \quad 3.7$$

Equation 3.7 can be split into base fluid and nanoparticles term as follows:

$$\frac{\partial (1 - \bar{C})\rho_{bf}}{\partial t} + \nabla \cdot (1 - \bar{C})\rho_{bf}\bar{\mathbf{V}} = 0 \quad 3.8$$

and

$$\frac{\partial \bar{C}\rho_p}{\partial t} + \nabla \cdot (C\rho_p\bar{\mathbf{V}} + \mathbf{j}_p) = 0 \quad 3.9$$

Equations 3.8 and 3.9 are the continuity equations for base fluid and nanoparticles, respectively. In Equation 3.8, since the volume fraction nanoparticles is infinitely small, then $(1 - \bar{C})\rho_{bf} \approx \rho$, therefore Equation 3.8 reduces to

$$\frac{\partial \rho}{\partial t} + \nabla \cdot \rho \bar{\mathbf{V}} = 0 \quad 3.10$$

For a steady incompressible flow, ρ is constant and flow is independent on time t , hence

$$\nabla \cdot \bar{\mathbf{V}} = 0 \quad 3.11$$

Equation 3.11 is the **continuity equation** where $\bar{\mathbf{V}}$ is the nanofluid velocity.

3.2.2 Conservation of Momentum

Fundamental physical principle namely Newton's second law of motion is the conservation of momentum with a total force $\mathbf{F}_t = M_t \mathbf{A}_m$ where \mathbf{F}_t is the combination of surface forces \mathbf{F}_s and body forces \mathbf{F}_b while $\mathbf{A}_m = \frac{d\mathbf{V}}{dt}$ is the acceleration. Based on the definitions, two relations are obtained:

$$\mathbf{F}_t = \frac{D(M_t \mathbf{V})}{Dt} \quad 3.12$$

and

$$\mathbf{F}_t = \int_{S(a)} \mathbf{F}_s d\mathbf{S} + \int_{V(a)} \mathbf{F}_b dV \quad 3.13$$

Equation 3.12 can be written in integral form as

$$\mathbf{F}_t = \frac{D}{Dt} \int_{V(t)} \rho \bar{\mathbf{V}} dV$$

Comparing Equations 3.12 and 3.13 and by applying the Reynolds transport theorem, the following equation is obtained

$$\frac{\partial}{\partial t} \int_{V(a)} \rho \bar{\mathbf{V}} dV + \int_{S(a)} \bar{\mathbf{V}} \rho \bar{\mathbf{V}} \cdot d\mathbf{S} = \int_{S(a)} \mathbf{F}_s d\mathbf{S} + \int_{V(a)} \mathbf{F}_b dV \quad 3.14$$

The surface forces \mathbf{F}_s are the forces acting on the surface of the control volume, It is a combination of shear stress and normal stress. According to Darus (1994), \mathbf{F}_s is ordinarily denotes as Cauchy stress tensor $\bar{\tau}$ and defined by

$$\bar{\tau} = \begin{bmatrix} \sigma_{xx} & \tau_{xy} & \tau_{xz} \\ \tau_{yx} & \sigma_{yy} & \tau_{yz} \\ \tau_{zx} & \tau_{zy} & \sigma_{zz} \end{bmatrix}$$

Therefore, the total surface forces can be written as

$$\int_{S(a)} \mathbf{F}_s d\mathbf{S} = \int_{S(a)} \bar{\tau} d\mathbf{S} \quad 3.15$$

Substituting Equation 3.15 into Equation 3.14, then applying the Gauss divergence theorem, Equation 3.15 becomes

$$\frac{\partial}{\partial t} \int_{V(a)} \rho \bar{\mathbf{V}} dV + \int_{V(a)} \nabla \cdot \rho \bar{\mathbf{V}} \bar{\mathbf{V}} dV = \int_{V(a)} \nabla \cdot \bar{\tau} dV + \int_{V(a)} \mathbf{F}_b dV \quad 3.16$$

Equation 3.16 is written in differential form as

$$\frac{\partial \rho \bar{\mathbf{V}}}{\partial t} + \nabla \cdot \rho \bar{\mathbf{V}} \bar{\mathbf{V}} = \nabla \cdot \bar{\tau} + \mathbf{F}_b \quad 3.17$$

Expanding $\nabla \cdot \rho \bar{\mathbf{V}} \bar{\mathbf{V}} = \rho \bar{\mathbf{V}} \cdot \nabla \bar{\mathbf{V}} + \bar{\mathbf{V}} \nabla \cdot \rho \bar{\mathbf{V}}$ and substitute into Equation 3.17, we obtained

$$\rho \frac{\partial \bar{\mathbf{V}}}{\partial t} + \rho \bar{\mathbf{V}} \cdot \nabla \bar{\mathbf{V}} + \bar{\mathbf{V}} (\nabla \cdot \rho \bar{\mathbf{V}}) = \nabla \cdot \bar{\tau} + \mathbf{F}_b \quad 3.18$$

Eliminate the first bracket which is continuity equation, the Equation 3.18 is reduced to

$$\rho \frac{\partial \bar{\mathbf{V}}}{\partial t} + \rho \bar{\mathbf{V}} \cdot \nabla \bar{\mathbf{V}} = \nabla \cdot \bar{\tau} + \mathbf{F}_b \quad 3.19$$

Referring to Anwar (2013), $\bar{\tau}$ is defined as

$$\bar{\tau} = -\bar{p}\mathbf{I} + \mu \mathbf{A}_1 \quad 3.20$$

where \bar{p} is the pressure, \mathbf{I} is the identity tensor, μ is dynamic viscosity and \mathbf{A}_1 is the first order Rivlin-Ericksen tensor which is given as

$$\mathbf{A}_1 = \nabla \bar{\mathbf{V}} + (\nabla \bar{\mathbf{V}})^T \quad 3.21$$

$\nabla \bar{\mathbf{V}}$ and $(\nabla \bar{\mathbf{V}})^T$ are the velocity gradient and its transpose, respectively which is defined in matrices form as:

$$\nabla \bar{\mathbf{V}} = \begin{bmatrix} \frac{\partial \bar{u}}{\partial \bar{x}} & \frac{\partial \bar{u}}{\partial \bar{y}} & \frac{\partial \bar{u}}{\partial \bar{z}} \\ \frac{\partial \bar{v}}{\partial \bar{x}} & \frac{\partial \bar{v}}{\partial \bar{y}} & \frac{\partial \bar{v}}{\partial \bar{z}} \\ \frac{\partial \bar{w}}{\partial \bar{x}} & \frac{\partial \bar{w}}{\partial \bar{y}} & \frac{\partial \bar{w}}{\partial \bar{z}} \end{bmatrix} \quad 3.22$$

Equation 3.19 is rewritten by substituting Equations 3.20 and 3.21

$$\rho \frac{\partial \bar{\mathbf{V}}}{\partial t} + \rho \bar{\mathbf{V}} \cdot \nabla \bar{\mathbf{V}} = -\nabla \bar{p} + \mu \nabla \cdot [\nabla \bar{\mathbf{V}} + (\nabla \bar{\mathbf{V}})^T] + \mathbf{F}_b \quad 3.23$$

Equation 3.23 shows a vector form equation for momentum. By deleting several terms, the momentum equation of a steady form in x , y , and z can be written as

$$\rho \left(\bar{u} \frac{\partial \bar{u}}{\partial \bar{x}} + \bar{v} \frac{\partial \bar{u}}{\partial \bar{y}} + \bar{w} \frac{\partial \bar{u}}{\partial \bar{z}} \right) = -\frac{\partial \bar{p}}{\partial \bar{x}} + \mu \left(\frac{\partial^2 \bar{u}}{\partial \bar{x}^2} + \frac{\partial^2 \bar{u}}{\partial \bar{y}^2} + \frac{\partial^2 \bar{u}}{\partial \bar{z}^2} \right) + F_{bx} \quad 3.24$$

$$\rho \left(\bar{u} \frac{\partial \bar{v}}{\partial \bar{x}} + \bar{v} \frac{\partial \bar{v}}{\partial \bar{y}} + \bar{w} \frac{\partial \bar{v}}{\partial \bar{z}} \right) = -\frac{\partial \bar{p}}{\partial \bar{x}} + \mu \left(\frac{\partial^2 \bar{v}}{\partial \bar{x}^2} + \frac{\partial^2 \bar{v}}{\partial \bar{y}^2} + \frac{\partial^2 \bar{v}}{\partial \bar{z}^2} \right) + F_{by} \quad 3.25$$

$$\rho \left(\bar{u} \frac{\partial \bar{w}}{\partial \bar{x}} + \bar{v} \frac{\partial \bar{w}}{\partial \bar{y}} + \bar{w} \frac{\partial \bar{w}}{\partial \bar{z}} \right) = -\frac{\partial \bar{p}}{\partial \bar{x}} + \mu \left(\frac{\partial^2 \bar{w}}{\partial \bar{x}^2} + \frac{\partial^2 \bar{w}}{\partial \bar{y}^2} + \frac{\partial^2 \bar{w}}{\partial \bar{z}^2} \right) + F_{bz} \quad 3.26$$

where F_{bx} , F_{by} and F_{bz} are the body forces or external forces in a direction of x , y and z , respectively. In addition, based from the Equations 3.24 to 3.26, the vector of Equation 3.23 can be simplified as stated by Bejan (2013) for case porous medium saturated by a nanofluid given by

$$\rho \frac{\partial \bar{\mathbf{V}}}{\partial t} + \rho \bar{\mathbf{V}} \cdot \nabla \bar{\mathbf{V}} = -\nabla \bar{p} + \mu \nabla^2 \bar{\mathbf{V}} + \frac{\mu}{K} \bar{\mathbf{V}} + \rho \mathbf{g} \quad 3.27$$

Then, we assume that the variation in density is neglected everywhere except in the buoyancy term. Hence, the Boussinesq approximation is adopted in the buoyancy term and is approximated by

$$\rho \mathbf{g} \cong [\bar{C}\rho_p + (1 - \bar{C}) \{\rho_f[(1 - \beta(\bar{T} - \bar{T}_\infty))]\}] \mathbf{g} \quad 3.28$$

The nanofluid density ρ can be approximated by the base-fluid density ρ_f when \bar{C} is small and Darcy velocity is related to $\bar{\mathbf{V}}/\varepsilon$. Substituting Equation 3.28 into 3.27 yields

$$\frac{\rho_f}{\varepsilon} \frac{\partial \bar{\mathbf{V}}}{\partial t} + \frac{\mu}{K} \bar{\mathbf{V}} = -\nabla \bar{p} + [\bar{C}\rho_p + (1 - \bar{C}) \{\rho_f[(1 - \beta(\bar{T} - \bar{T}_\infty))]\}] \mathbf{g} \quad 3.29$$

Unlike Boussinesq in which the density difference are being ignored, Oberbeck-Boussinesq approximation assumed that fluid have a uniform density; density differences are recognised only in those terms which drive the motion. In keeping with the Oberbeck-Boussinesq approximation and an assumption that the nanoparticle concentration is dilute, and with a suitable choice for the reference pressure, momentum Equation 3.29 can be linearized and written as

$$\frac{\rho_f}{\varepsilon} \frac{\partial \bar{\mathbf{V}}}{\partial t} + \frac{\partial \bar{p}}{\partial x} + \frac{\mu}{K} \bar{\mathbf{V}} = [(\rho_p - \rho_{f_\infty})(\bar{C} - \bar{C}_\infty) + (1 - \bar{C}_\infty)\rho_{f_\infty}\beta(T - T_\infty)] \mathbf{g} \quad 3.30$$

Elimination of p can be done from Equations 3.30 by cross-differentiation.

$$\frac{\rho_f}{\varepsilon} \frac{\partial}{\partial y} \frac{\partial \bar{\mathbf{V}}}{\partial t} + \frac{\partial}{\partial y} \left(\frac{\partial \bar{p}}{\partial x} \right) + \frac{\partial}{\partial y} \left(\frac{\mu}{K} \bar{\mathbf{V}} \right) = \frac{\partial}{\partial y} \left([(\rho_p - \rho_{f_\infty})(\bar{C} - \bar{C}_\infty) + (1 - \bar{C}_\infty)\rho_{f_\infty}\beta(T - T_\infty)] \mathbf{g} \right) \quad 3.31$$

$$\frac{\rho_f}{\varepsilon} \frac{\partial}{\partial y} \frac{\partial \bar{\mathbf{V}}}{\partial t} + \frac{\partial}{\partial x} \left(\frac{\partial \bar{p}}{\partial y} \right) + \frac{\mu}{K} \left(\frac{\partial \bar{u}}{\partial x} + \frac{\partial \bar{v}}{\partial y} \right) = \left[(1 - \bar{C}_\infty)\beta\rho_{f_\infty} \frac{\partial \bar{T}}{\partial \bar{y}} + (\rho_p - \rho_{f_\infty}) \frac{\partial \bar{C}}{\partial \bar{y}} \right] \mathbf{g} \quad 3.32$$

where $\partial p/\partial y$ and g are given as follows (Nield and Kuznetsov, 2011),

$$\frac{\partial p}{\partial y} = 0 \quad \text{and} \quad \mathbf{g} = g \sin \left(\frac{\bar{x}}{a} \right)$$

Equation 3.32 reduces to

$$\frac{\rho_f}{\varepsilon} \frac{\partial}{\partial y} \frac{\partial \bar{V}}{\partial t} + \frac{\mu}{K} \left(\frac{\partial \bar{u}}{\partial x} + \frac{\partial \bar{v}}{\partial y} \right) = \left[(1 - \bar{C}_\infty) \beta \rho_{f\infty} \frac{\partial \bar{T}}{\partial \bar{y}} + (\rho_p - \rho_{f\infty}) \frac{\partial \bar{C}}{\partial \bar{y}} \right] g \sin \left(\frac{\bar{x}}{a} \right) \quad 3.33$$

where $\rho_{f\infty}$ is the density of the base fluid, μ and β are the viscosity and volume expansion coefficient of the fluid, ρ_p is the density of the particles, ρ_f is the density, K is the permeability of the porous medium and \mathbf{g} is the vector gravity.

3.2.3 Conservation of Energy

Conservation of energy derived based on the first law of thermodynamics. According to the first law of thermodynamics

$$\frac{DE_s}{Dt} = \frac{DQ_s}{Dt} + \frac{DW_s}{Dt} \quad 3.34$$

where $\frac{DE_s}{Dt}$ is rate of change in energy inside fluid, $\frac{DQ_s}{Dt}$ is the heat flux into element and $\frac{DW_s}{Dt}$ is the rate of work done on element due to body and surface forces element (Kasim, 2014). From Equation 3.34,

$$\frac{DE_s}{Dt} = \frac{D}{Dt} \int_{V(t)} \rho e_t dV \quad 3.35$$

where ρ is the fluid density, e_t is total energy defined as the combination of internal energy due to random molecular motion e_{int} and the kinetic energy due to translational motion of the fluid element $\frac{V^2}{2}$

$$e_t = e_{int} + \frac{V^2}{2} \quad 3.36$$

Next, $\frac{DQ_s}{Dt} = - \int_{S(a)} \mathbf{q} \cdot d\mathbf{S} + \int_{S(a)} h_p \mathbf{j}_p \cdot d\mathbf{S}$ where

$$\mathbf{q} = -k_m \nabla T + h_p \mathbf{j}_p \quad 3.37$$

Further, $\frac{DW_s}{Dt} = \frac{D}{Dt}(\mathbf{F}_s + \mathbf{F}_b)$ where $\frac{D\mathbf{F}_b}{Dt} = \int_{V(a)} \mathbf{F}_b dV$ and $\frac{D\mathbf{F}_s}{Dt} = \int_{S(a)} \bar{\boldsymbol{\tau}} \cdot d\mathbf{S}$. Using definition stated above, the energy equation for ordinary viscous fluid can be defined as

$$\frac{D}{Dt} \int_{V(t)} \rho e_t dV = - \int_{S(s)} \mathbf{q} \cdot d\mathbf{S} + \int_{S(a)} h_p \mathbf{j}_p \cdot d\mathbf{S} + \int_{S(a)} \bar{\boldsymbol{\tau}} \cdot d\mathbf{S} + \int_{V(a)} \mathbf{F}_b dV \quad 3.38$$

Applying Reynolds transport theorem on the left hand side Equation 3.38 and obtained

$$\frac{\partial}{\partial t} \int_{V(a)} \rho e_t dV + \int_{S(a)} \rho e_t d\mathbf{S} = - \int_{S(a)} \mathbf{q} \cdot d\mathbf{S} + \int_{S(a)} h_p \mathbf{j}_p \cdot d\mathbf{S} + \int_{S(a)} \bar{\boldsymbol{\tau}} \cdot d\mathbf{S} + \int_{V(a)} \mathbf{F}_b dV \quad 3.39$$

According to Gauss divergence theorem, Equation 3.39 can be written in a convenient way as

$$\begin{aligned} \int_{V(a)} \frac{\partial(\rho e_t)}{\partial t} dV + \int_{V(a)} \nabla \cdot \rho e_t \bar{\mathbf{V}} dV = \\ - \int_{V(a)} \nabla \cdot \mathbf{q} dV + \int_{V(a)} h_p \nabla \cdot \mathbf{j}_p dV + \int_{V(a)} \nabla \cdot \bar{\boldsymbol{\tau}} dV + \int_{V(a)} \mathbf{F}_b dV \end{aligned} \quad 3.40$$

Since the integral is consistence in right and left, the integral function can be eliminated in Equation 3.40 and simplified in differential form as

$$\frac{\partial(\rho e_t)}{\partial t} + \nabla \cdot \rho e_t \bar{\mathbf{V}} = -\nabla \cdot \mathbf{q} + h_p \nabla \cdot \mathbf{j}_p + (\nabla \cdot \bar{\boldsymbol{\tau}} + \mathbf{F}_b) \quad 3.41$$

Noticed that $\nabla \cdot \rho e_t \bar{\mathbf{V}} = e_t \nabla \cdot \rho \bar{\mathbf{V}} + \rho \bar{\mathbf{V}} \cdot \nabla e_t$. Continuity expression can be eliminated and Equation 3.41 is written as follow

$$\rho \frac{\partial e_t}{\partial t} + \rho \bar{\mathbf{V}} \cdot \nabla e_t = -\nabla \cdot \mathbf{q} + h_p \nabla \cdot \mathbf{j}_p + (\nabla \cdot \bar{\boldsymbol{\tau}} + \mathbf{F}_b) \quad 3.42$$

The definition $\frac{De_t}{Dt} = \frac{\partial e_t}{\partial t} + \bar{\mathbf{V}} \cdot \nabla e_t$ is applied in order to make this analysis easier to be understood. Equation 3.42 is simplified as

$$\rho \frac{De_t}{Dt} = -\nabla \cdot \mathbf{q} + h_p \nabla \cdot \mathbf{j}_p + (\nabla \cdot \bar{\boldsymbol{\tau}} + \mathbf{F}_b) \quad 3.43$$

Substituted the definition of \mathbf{q} from Equation 3.37, then Equation 3.43 becomes

$$\rho \frac{De_t}{Dt} = -\nabla \cdot (-k_m \nabla \bar{T} + h_p \mathbf{j}_p) + h_p \nabla \cdot \mathbf{j}_p + (\nabla \cdot \bar{\boldsymbol{\tau}} + \mathbf{F}_b) \quad 3.44$$

Notice that $\nabla \cdot (h_p \mathbf{j}_p) = h_p \nabla \cdot \mathbf{j}_p + \mathbf{j}_p \cdot \nabla h_p$. Equation 3.44 is simplified as

$$\rho \frac{De_t}{Dt} = \nabla \cdot k_m \nabla \bar{T} - \mathbf{j}_p \cdot \nabla h_p + (\nabla \cdot \bar{\boldsymbol{\tau}} + \mathbf{F}_b) \quad 3.45$$

The term ∇h_p is set equal to $C_p \nabla T$ where C_p is the specific heat of nanoparticles, then using Equation 3.3, Equation 3.45 becomes

$$\rho \frac{De_t}{Dt} = \nabla \cdot k_m \nabla \bar{T} + \varepsilon(\rho c)_p [D_B \nabla \bar{T} \cdot \nabla \bar{C} + \frac{D_T}{T_\infty} \nabla \bar{T} \cdot \nabla \bar{T}] + (\nabla \cdot \bar{\boldsymbol{\tau}} + \mathbf{F}_b) \quad 3.46$$

Term on the right hand side of Equation 3.46 is written in the form as follow

$$\nabla \cdot k_m \nabla \bar{T} = k_m \left[\frac{\partial}{\partial \bar{x}} \left(\frac{\partial \bar{T}}{\partial \bar{x}} \right) + \frac{\partial}{\partial \bar{y}} \left(\frac{\partial \bar{T}}{\partial \bar{y}} \right) + \frac{\partial}{\partial \bar{z}} \left(\frac{\partial \bar{T}}{\partial \bar{z}} \right) \right] \quad 3.47$$

Second term are define as

$$\begin{aligned} \varepsilon(\rho c)_p [D_B \nabla \bar{T} \cdot \nabla \bar{C} + \frac{D_T}{T_\infty} \nabla \bar{T} \cdot \nabla \bar{T}] &= \varepsilon(\rho c)_p \\ &\left[D_B \left(\frac{\partial \bar{C}}{\partial \bar{x}} \frac{\partial \bar{T}}{\partial \bar{x}} + \frac{\partial \bar{C}}{\partial \bar{y}} \frac{\partial \bar{T}}{\partial \bar{y}} + \frac{\partial \bar{C}}{\partial \bar{z}} \frac{\partial \bar{T}}{\partial \bar{z}} \right) + \frac{D_T}{T_\infty} \left(\frac{\partial \bar{T}}{\partial \bar{x}} \frac{\partial \bar{T}}{\partial \bar{x}} + \frac{\partial \bar{T}}{\partial \bar{y}} \frac{\partial \bar{T}}{\partial \bar{y}} + \frac{\partial \bar{T}}{\partial \bar{z}} \frac{\partial \bar{T}}{\partial \bar{z}} \right) \right] \end{aligned} \quad 3.48$$

Total work done on the moving fluid due to the surface and body forces are as follow

$$\begin{aligned} (\nabla \cdot \bar{\boldsymbol{\tau}} + \mathbf{F}_b) &= -\frac{\partial \bar{u} \bar{p}}{\partial \bar{x}} + \mu \left[\frac{\bar{u} \sigma_{xx}}{\partial \bar{x}} + \frac{\bar{u} \tau_{yx}}{\partial \bar{y}} + \frac{\bar{u} \tau_{zx}}{\partial \bar{z}} \right] - \frac{\partial \bar{v} \bar{p}}{\partial \bar{y}} + \mu \left[\frac{\bar{v} \tau_{xy}}{\partial \bar{x}} + \frac{\bar{v} \sigma_{yy}}{\partial \bar{y}} + \frac{\bar{v} \tau_{zy}}{\partial \bar{z}} \right] \\ &- \frac{\partial \bar{w} \bar{p}}{\partial \bar{z}} + \mu \left[\frac{\bar{w} \tau_{xz}}{\partial \bar{x}} + \frac{\bar{w} \sigma_{yz}}{\partial \bar{y}} + \frac{\bar{w} \sigma_{zz}}{\partial \bar{z}} \right] + (F_{bx} + F_{by} + F_{bz}) \end{aligned} \quad 3.49$$

Next the term on the left hand side is expanded by Equation 3.36 and becomes

$$\rho \frac{De_t}{Dt} = \rho_m \frac{De_{int}}{Dt} + \rho_f \frac{D}{Dt} \left(\frac{V^2}{2} \right) \quad 3.50$$

According to Incropera et al. (2006) and Bejan (2013), in order to express the energy equation in terms of temperature, it is tempting to replace the internal energy e_{int} with the product of specific heat at constant pressure of fluid c_m and temperature T that is

$$\frac{De_{int}}{Dt} = c_m \frac{\partial T}{\partial t} \quad 3.51$$

Substitute Equation 3.51 into Equation 3.50 yields

$$\begin{aligned} \rho \frac{De_t}{Dt} = & \rho C_p \left(\frac{\partial \bar{T}}{\partial t} + \bar{u} \frac{\partial \bar{T}}{\partial \bar{x}} + \bar{v} \frac{\partial \bar{T}}{\partial \bar{y}} + \bar{w} \frac{\partial \bar{T}}{\partial \bar{z}} \right) + \rho \bar{u} \left(\bar{u} \frac{\partial \bar{u}}{\partial \bar{x}} + \bar{v} \frac{\partial \bar{u}}{\partial \bar{y}} + \bar{w} \frac{\partial \bar{u}}{\partial \bar{z}} \right) \\ & + \rho \bar{v} \left(\bar{u} \frac{\partial \bar{v}}{\partial \bar{x}} + \bar{v} \frac{\partial \bar{v}}{\partial \bar{y}} + \bar{w} \frac{\partial \bar{v}}{\partial \bar{z}} \right) + \rho \bar{w} \left(\bar{u} \frac{\partial \bar{w}}{\partial \bar{x}} + \bar{v} \frac{\partial \bar{w}}{\partial \bar{y}} + \bar{w} \frac{\partial \bar{w}}{\partial \bar{z}} \right) \end{aligned} \quad 3.52$$

Combine term that represent left and right

$$\begin{aligned} & \rho C_p \left(\frac{\partial \bar{T}}{\partial t} + \bar{u} \frac{\partial \bar{T}}{\partial \bar{x}} + \bar{v} \frac{\partial \bar{T}}{\partial \bar{y}} + \bar{w} \frac{\partial \bar{T}}{\partial \bar{z}} \right) + \rho \bar{u} \left(\bar{u} \frac{\partial \bar{u}}{\partial \bar{x}} + \bar{v} \frac{\partial \bar{u}}{\partial \bar{y}} + \bar{w} \frac{\partial \bar{u}}{\partial \bar{z}} \right) \\ & + \rho \bar{v} \left(\bar{u} \frac{\partial \bar{v}}{\partial \bar{x}} + \bar{v} \frac{\partial \bar{v}}{\partial \bar{y}} + \bar{w} \frac{\partial \bar{v}}{\partial \bar{z}} \right) + \rho \bar{w} \left(\bar{u} \frac{\partial \bar{w}}{\partial \bar{x}} + \bar{v} \frac{\partial \bar{w}}{\partial \bar{y}} + \bar{w} \frac{\partial \bar{w}}{\partial \bar{z}} \right) = \\ & k_m \left[\frac{\partial}{\partial \bar{x}} \left(\frac{\partial \bar{T}}{\partial \bar{x}} \right) + \frac{\partial}{\partial \bar{y}} \left(\frac{\partial \bar{T}}{\partial \bar{y}} \right) + \frac{\partial}{\partial \bar{z}} \left(\frac{\partial \bar{T}}{\partial \bar{z}} \right) \right] + \varepsilon (\rho c)_p \\ & \left[D_B \left(\frac{\partial \bar{C}}{\partial \bar{x}} \frac{\partial \bar{T}}{\partial \bar{x}} + \frac{\partial \bar{C}}{\partial \bar{y}} \frac{\partial \bar{T}}{\partial \bar{y}} + \frac{\partial \bar{C}}{\partial \bar{z}} \frac{\partial \bar{T}}{\partial \bar{z}} \right) + \frac{D_T}{T_\infty} \left(\frac{\partial \bar{T}}{\partial \bar{x}} \frac{\partial \bar{T}}{\partial \bar{x}} + \frac{\partial \bar{T}}{\partial \bar{y}} \frac{\partial \bar{T}}{\partial \bar{y}} + \frac{\partial \bar{T}}{\partial \bar{z}} \frac{\partial \bar{T}}{\partial \bar{z}} \right) \right] \\ & - \frac{\partial \bar{u} \bar{p}}{\partial \bar{x}} + \mu \left[\frac{\bar{u} \sigma_{xx}}{\partial \bar{x}} + \frac{\bar{u} \tau_{yx}}{\partial \bar{y}} + \frac{\bar{u} \tau_{zx}}{\partial \bar{z}} \right] - \frac{\partial \bar{v} \bar{p}}{\partial \bar{y}} + \mu \left[\frac{\bar{v} \tau_{xy}}{\partial \bar{x}} + \frac{\bar{v} \sigma_{yy}}{\partial \bar{y}} + \frac{\bar{v} \tau_{zy}}{\partial \bar{z}} \right] \\ & - \frac{\partial \bar{w} \bar{p}}{\partial \bar{z}} + \mu \left[\frac{\bar{w} \tau_{xz}}{\partial \bar{x}} + \frac{\bar{w} \sigma_{yz}}{\partial \bar{y}} + \frac{\bar{w} \sigma_{zz}}{\partial \bar{z}} \right] + (F_{bx} + F_{by} + F_{bz}) \end{aligned} \quad 3.53$$

Equation 3.53 can be expanded by using chain rule

$$\begin{aligned}
& \rho C_p \left(\frac{\partial \bar{T}}{\partial t} + \bar{u} \frac{\partial \bar{T}}{\partial \bar{x}} + \bar{v} \frac{\partial \bar{T}}{\partial \bar{y}} + \bar{w} \frac{\partial \bar{T}}{\partial \bar{z}} \right) + \rho \bar{u} \left(\bar{u} \frac{\partial \bar{u}}{\partial \bar{x}} + \bar{v} \frac{\partial \bar{u}}{\partial \bar{y}} + \bar{w} \frac{\partial \bar{u}}{\partial \bar{z}} \right) \\
& + \rho \bar{v} \left(\bar{u} \frac{\partial \bar{v}}{\partial \bar{x}} + \bar{v} \frac{\partial \bar{v}}{\partial \bar{y}} + \bar{w} \frac{\partial \bar{v}}{\partial \bar{z}} \right) + \rho \bar{w} \left(\bar{u} \frac{\partial \bar{w}}{\partial \bar{x}} + \bar{v} \frac{\partial \bar{w}}{\partial \bar{y}} + \bar{w} \frac{\partial \bar{w}}{\partial \bar{z}} \right) = \\
& k_m \frac{\partial^2 \bar{T}}{\partial \bar{x}^2} + k \frac{\partial^2 \bar{T}}{\partial \bar{y}^2} + k \frac{\partial^2 \bar{T}}{\partial \bar{z}^2} + \varepsilon(\rho c)_p \\
& \left[D_B \left(\frac{\partial \bar{C}}{\partial \bar{x}} \frac{\partial \bar{T}}{\partial \bar{x}} + \frac{\partial \bar{C}}{\partial \bar{y}} \frac{\partial \bar{T}}{\partial \bar{y}} + \frac{\partial \bar{C}}{\partial \bar{z}} \frac{\partial \bar{T}}{\partial \bar{z}} \right) + \frac{D_T}{T_\infty} \left(\left(\frac{\partial \bar{T}}{\partial \bar{x}} \right)^2 + \left(\frac{\partial \bar{T}}{\partial \bar{y}} \right)^2 + \left(\frac{\partial \bar{T}}{\partial \bar{z}} \right)^2 \right) \right] \\
& - \bar{u} \frac{\partial \bar{p}}{\partial \bar{x}} - \bar{p} \frac{\partial \bar{u}}{\partial \bar{x}} + \mu \left[\bar{u} \frac{\partial \sigma_{xx}}{\partial \bar{x}} + \sigma_{xx} \frac{\partial \bar{u}}{\partial \bar{x}} + u \frac{\partial \tau_{yx}}{\partial \bar{y}} + \tau_{yx} \frac{\partial \bar{u}}{\partial \bar{y}} + \bar{u} \frac{\partial \tau_{zx}}{\partial \bar{z}} + \tau_{zx} \frac{\partial \bar{u}}{\partial \bar{z}} \right] + F_{bx} \\
& - \bar{v} \frac{\partial \bar{p}}{\partial \bar{y}} - \bar{p} \frac{\partial \bar{v}}{\partial \bar{y}} + \mu \left[\bar{v} \frac{\partial \tau_{xy}}{\partial \bar{x}} + \tau_{xy} \frac{\partial \bar{v}}{\partial \bar{x}} + v \frac{\partial \sigma_{yy}}{\partial \bar{y}} + \sigma_{yy} \frac{\partial \bar{v}}{\partial \bar{y}} + \bar{v} \frac{\partial \tau_{zy}}{\partial \bar{z}} + \tau_{zy} \frac{\partial \bar{v}}{\partial \bar{z}} \right] + F_{by} \\
& - \bar{w} \frac{\partial \bar{p}}{\partial \bar{z}} - \bar{p} \frac{\partial \bar{w}}{\partial \bar{z}} + \mu \left[\bar{w} \frac{\partial \tau_{xz}}{\partial \bar{x}} + \tau_{xz} \frac{\partial \bar{w}}{\partial \bar{x}} + w \frac{\partial \tau_{yz}}{\partial \bar{y}} + \tau_{yz} \frac{\partial \bar{w}}{\partial \bar{y}} + \bar{w} \frac{\partial \sigma_{zz}}{\partial \bar{z}} + \sigma_{zz} \frac{\partial \bar{w}}{\partial \bar{z}} \right] + F_{bz}
\end{aligned} \tag{3.54}$$

Equation 3.54 is rearranged as follow

$$\begin{aligned}
& \rho C_p \left(\frac{\partial \bar{T}}{\partial t} + \bar{u} \frac{\partial \bar{T}}{\partial \bar{x}} + \bar{v} \frac{\partial \bar{T}}{\partial \bar{y}} + \bar{w} \frac{\partial \bar{T}}{\partial \bar{z}} \right) + \rho \bar{u} \left(\bar{u} \frac{\partial \bar{u}}{\partial \bar{x}} + \bar{v} \frac{\partial \bar{u}}{\partial \bar{y}} + \bar{w} \frac{\partial \bar{u}}{\partial \bar{z}} \right) \\
& + \rho \bar{v} \left(\bar{u} \frac{\partial \bar{v}}{\partial \bar{x}} + \bar{v} \frac{\partial \bar{v}}{\partial \bar{y}} + \bar{w} \frac{\partial \bar{v}}{\partial \bar{z}} \right) + \rho \bar{w} \left(\bar{u} \frac{\partial \bar{w}}{\partial \bar{x}} + \bar{v} \frac{\partial \bar{w}}{\partial \bar{y}} + \bar{w} \frac{\partial \bar{w}}{\partial \bar{z}} \right) = \\
& k_m \frac{\partial^2 \bar{T}}{\partial \bar{x}^2} + k \frac{\partial^2 \bar{T}}{\partial \bar{y}^2} + k \frac{\partial^2 \bar{T}}{\partial \bar{z}^2} - \bar{p} \frac{\partial \bar{u}}{\partial \bar{x}} + \\
& \varepsilon(\rho c)_p \left[D_B \left(\frac{\partial \bar{C}}{\partial \bar{x}} \frac{\partial \bar{T}}{\partial \bar{x}} + \frac{\partial \bar{C}}{\partial \bar{y}} \frac{\partial \bar{T}}{\partial \bar{y}} + \frac{\partial \bar{C}}{\partial \bar{z}} \frac{\partial \bar{T}}{\partial \bar{z}} \right) + \frac{D_T}{T_\infty} \left(\left(\frac{\partial \bar{T}}{\partial \bar{x}} \right)^2 + \left(\frac{\partial \bar{T}}{\partial \bar{y}} \right)^2 + \left(\frac{\partial \bar{T}}{\partial \bar{z}} \right)^2 \right) \right] \\
& - \bar{u} \frac{\partial \bar{p}}{\partial \bar{x}} + \mu \left[\bar{u} \left(\frac{\partial \sigma_{xx}}{\partial \bar{x}} + \frac{\partial \tau_{yx}}{\partial \bar{y}} + \frac{\tau_{zx}}{\partial \bar{z}} \right) + \sigma_{xx} \frac{\partial \bar{u}}{\partial \bar{x}} + \tau_{yx} \frac{\partial \bar{u}}{\partial \bar{y}} + \tau_{zx} \frac{\partial \bar{u}}{\partial \bar{z}} \right] + F_{bx} \\
& - \bar{v} \frac{\partial \bar{p}}{\partial \bar{y}} + \mu \left[\bar{v} \left(\frac{\partial \tau_{xy}}{\partial \bar{x}} + \frac{\partial \sigma_{yy}}{\partial \bar{y}} + \frac{\partial \tau_{zy}}{\partial \bar{z}} \right) + \tau_{xy} \frac{\partial \bar{v}}{\partial \bar{x}} + \sigma_{yy} \frac{\partial \bar{v}}{\partial \bar{y}} + \tau_{zy} \frac{\partial \bar{v}}{\partial \bar{z}} \right] + F_{by} \\
& - \bar{w} \frac{\partial \bar{p}}{\partial \bar{z}} + \mu \left[\bar{w} \left(\frac{\partial \tau_{xz}}{\partial \bar{x}} + \frac{\partial \tau_{yz}}{\partial \bar{y}} + \frac{\sigma_{zz}}{\partial \bar{z}} \right) + \tau_{yz} \frac{\partial \bar{w}}{\partial \bar{x}} + \tau_{yz} \frac{\partial \bar{w}}{\partial \bar{y}} + \sigma_{zz} \frac{\partial \bar{w}}{\partial \bar{z}} \right] + F_{bz}
\end{aligned} \tag{3.55}$$

The terms $\frac{\partial u}{\partial x} + \frac{\partial v}{\partial y} + \frac{\partial w}{\partial z} = 0$ are continuity equation. Further, Equation 3.55 is a combination of momentum and energy. Eliminating momentum, the energy equation is expressed in

$$\begin{aligned} \rho C_p \left(\frac{\partial \bar{T}}{\partial t} + \bar{u} \frac{\partial \bar{T}}{\partial \bar{x}} + \bar{v} \frac{\partial \bar{T}}{\partial \bar{y}} + \bar{w} \frac{\partial \bar{T}}{\partial \bar{z}} \right) &= k_m \frac{\partial^2 \bar{T}}{\partial \bar{x}^2} + k_m \frac{\partial^2 \bar{T}}{\partial \bar{y}^2} + k_m \frac{\partial^2 \bar{T}}{\partial \bar{z}^2} \\ &+ \varepsilon(\rho c)_p \left[D_B \left(\frac{\partial \bar{C}}{\partial \bar{x}} \frac{\partial \bar{T}}{\partial \bar{x}} + \frac{\partial \bar{C}}{\partial \bar{y}} \frac{\partial \bar{T}}{\partial \bar{y}} + \frac{\partial \bar{C}}{\partial \bar{z}} \frac{\partial \bar{T}}{\partial \bar{z}} \right) + \frac{D_T}{T_\infty} \left(\left(\frac{\partial \bar{T}}{\partial \bar{x}} \right)^2 + \left(\frac{\partial \bar{T}}{\partial \bar{y}} \right)^2 + \left(\frac{\partial \bar{T}}{\partial \bar{z}} \right)^2 \right) \right] \\ &+ \mu \left[\sigma_{xx} \frac{\partial \bar{u}}{\partial \bar{x}} + \tau_{yx} \frac{\partial \bar{u}}{\partial \bar{y}} + \tau_{zx} \frac{\partial \bar{u}}{\partial \bar{z}} + \tau_{xy} \frac{\partial \bar{v}}{\partial \bar{x}} + \sigma_{yy} \frac{\partial \bar{v}}{\partial \bar{y}} + \tau_{zy} \frac{\partial \bar{v}}{\partial \bar{z}} + \tau_{xz} \frac{\partial \bar{w}}{\partial \bar{x}} + \tau_{yz} \frac{\partial \bar{w}}{\partial \bar{y}} + \sigma_{zz} \frac{\partial \bar{w}}{\partial \bar{z}} \right] \end{aligned} \quad 3.56$$

By referring to Rivlin-Ericksen tensor, $\tau_{xy} = \tau_{yx}$, $\tau_{xz} = \tau_{zx}$, $\tau_{zy} = \tau_{yz}$. Equation 3.56 can be factorised as follow

$$\begin{aligned} \rho C_p \left(\frac{\partial \bar{T}}{\partial t} + \bar{u} \frac{\partial \bar{T}}{\partial \bar{x}} + \bar{v} \frac{\partial \bar{T}}{\partial \bar{y}} + \bar{w} \frac{\partial \bar{T}}{\partial \bar{z}} \right) &= k_m \frac{\partial^2 \bar{T}}{\partial \bar{x}^2} + k_m \frac{\partial^2 \bar{T}}{\partial \bar{y}^2} + k_m \frac{\partial^2 \bar{T}}{\partial \bar{z}^2} \\ &+ \varepsilon(\rho c)_p \left[D_B \left(\frac{\partial \bar{C}}{\partial \bar{x}} \frac{\partial \bar{T}}{\partial \bar{x}} + \frac{\partial \bar{C}}{\partial \bar{y}} \frac{\partial \bar{T}}{\partial \bar{y}} + \frac{\partial \bar{C}}{\partial \bar{z}} \frac{\partial \bar{T}}{\partial \bar{z}} \right) + \frac{D_T}{T_\infty} \left(\left(\frac{\partial \bar{T}}{\partial \bar{x}} \right)^2 + \left(\frac{\partial \bar{T}}{\partial \bar{y}} \right)^2 + \left(\frac{\partial \bar{T}}{\partial \bar{z}} \right)^2 \right) \right] \\ &+ \mu \left[\sigma_{xx} \frac{\partial \bar{u}}{\partial \bar{x}} + \sigma_{yy} \frac{\partial \bar{v}}{\partial \bar{y}} + \sigma_{zz} \frac{\partial \bar{w}}{\partial \bar{z}} + \tau_{yx} \left(\frac{\partial \bar{u}}{\partial \bar{y}} + \frac{\partial \bar{v}}{\partial \bar{x}} \right) + \tau_{zx} \left(\frac{\partial \bar{u}}{\partial \bar{z}} + \tau_{xz} \frac{\partial \bar{w}}{\partial \bar{x}} \right) + \tau_{zy} \left(\frac{\partial \bar{v}}{\partial \bar{z}} + \frac{\partial \bar{w}}{\partial \bar{y}} \right) \right] \end{aligned} \quad 3.57$$

The vector form of energy equation for nanofluid can be expressed as (Buongiorno (2006))

$$(\rho c)_m \frac{\partial \bar{T}}{\partial t} + (\rho c)_f \bar{\mathbf{V}} \cdot \nabla \bar{T} = k_m \nabla^2 \bar{T} + \varepsilon(\rho c)_p [D_B \nabla \bar{T} \cdot \nabla \bar{C} + \frac{D_T}{T_\infty} \nabla \bar{T} \cdot \nabla \bar{T}] + \mu \omega \quad 3.58$$

where

$$\begin{aligned} (\rho c)_m \frac{\partial \bar{T}}{\partial t} + (\rho c)_f \left(\bar{u} \frac{\partial \bar{T}}{\partial \bar{x}} + \bar{v} \frac{\partial \bar{T}}{\partial \bar{y}} \right) &= k_m \left(\frac{\partial^2 \bar{T}}{\partial \bar{x}^2} + \frac{\partial^2 \bar{T}}{\partial \bar{y}^2} \right) + \\ \varepsilon(\rho c)_p \left[D_B \left(\frac{\partial \bar{T}}{\partial \bar{x}} + \frac{\partial \bar{T}}{\partial \bar{y}} \right) \left(\frac{\partial \bar{C}}{\partial \bar{x}} + \frac{\partial \bar{C}}{\partial \bar{y}} \right) + \frac{D_T}{T_\infty} \left(\left(\frac{\partial \bar{T}}{\partial \bar{x}} \right)^2 + \left(\frac{\partial \bar{T}}{\partial \bar{y}} \right)^2 \right) \right] \end{aligned} \quad 3.59$$

Rearrange 3.59, we obtained

$$\begin{aligned} \frac{(\rho c)_m}{(\rho c)_f} \frac{\partial \bar{T}}{\partial t} + \bar{u} \frac{\partial \bar{T}}{\partial \bar{x}} + \bar{v} \frac{\partial \bar{T}}{\partial \bar{y}} = \alpha_m \left(\frac{\partial^2 \bar{T}}{\partial \bar{x}^2} + \frac{\partial^2 \bar{T}}{\partial \bar{y}^2} \right) + \\ \tau \left[D_B \left(\frac{\partial \bar{T}}{\partial \bar{x}} \frac{\partial \bar{C}}{\partial \bar{x}} + \frac{\partial \bar{T}}{\partial \bar{y}} \frac{\partial \bar{C}}{\partial \bar{y}} \right) + \left(\frac{D_T}{T_\infty} \right) \left(\left(\frac{\partial \bar{T}}{\partial \bar{x}} \right)^2 + \left(\frac{\partial \bar{T}}{\partial \bar{y}} \right)^2 \right) \right] \end{aligned} \quad 3.60$$

in which

$$\alpha_m = \frac{k_m}{(\rho c)_f}, \quad \tau = \frac{\varepsilon(\rho c)_p}{(\rho c)_f}$$

where α_m is the effective thermal diffusivity of the porous medium and $\tau = (\rho c)_p/(\rho c)_f$ with $(\rho c)_p$ is the effective heat capacity of the nanoparticle material, $(\rho c)_m$ is the effective heat capacity, k_m is the effective thermal conductivity and $(\rho c)_f$ is the heat capacity of the fluid.

3.2.4 Conservation of Nanoparticles

The conservation equation for nanoparticle volume fraction will be treated as a two-component mixture base fluid and nanoparticles with several assumptions: incompressible flow, no chemical reactions, negligible viscous dissipation, negligible radiative heat transfer and negligible external forces is

$$\frac{\partial \bar{C}}{\partial t} + \bar{\mathbf{V}} \cdot \nabla \bar{C} = -\frac{1}{\rho_p} \nabla \cdot \mathbf{j}_p \quad 3.61$$

Substitute \mathbf{j}_p from Equation 3.3 into Equation 3.61 yields

$$\rho_p \frac{\partial \bar{C}}{\partial t} + \frac{\rho_p}{\varepsilon} (\mathbf{V} \nabla \cdot \bar{C} + \bar{C} \nabla \cdot \mathbf{V}) = \rho_p \nabla \cdot \left[D_B \nabla \bar{C} + \frac{D_T \nabla \bar{T}}{T_\infty} \right] \quad 3.62$$

Notice that continuity equation is $\nabla \cdot \mathbf{V} = 0$ and $\nabla \cdot \nabla = \nabla^2$, therefore the Equation 3.63 is simplified to

$$\frac{\partial \bar{C}}{\partial t} + \frac{\mathbf{V}}{\varepsilon} \nabla \cdot \bar{C} = D_B \nabla^2 \bar{C} + \frac{D_T \nabla^2 \bar{T}}{T_\infty} \quad 3.63$$

Substituting Equation 3.3 in Equation 3.61, we get

$$\frac{\partial \bar{C}}{\partial t} + \frac{\bar{\mathbf{V}}}{\varepsilon} \cdot \nabla \bar{C} = \nabla \cdot \left[D_B \nabla \bar{C} + D_T \frac{\nabla \bar{T}}{T_\infty} \right] \quad 3.64$$

In the case of porous medium, the nanoparticles equation is also known as the concentration equation. The conservation equation in the vector form is given as follow

$$\frac{\partial \bar{C}}{\partial t} + \frac{1}{\varepsilon} \bar{\mathbf{V}} \cdot \nabla \bar{C} = D_B \nabla^2 \bar{C} + \frac{D_T}{T_\infty} \nabla^2 \bar{T} \quad 3.65$$

Therefore,

$$\frac{\partial \bar{C}}{\partial t} + \frac{1}{\varepsilon} \left(\bar{u} \frac{\partial \bar{C}}{\partial \bar{x}} + \bar{v} \frac{\partial \bar{C}}{\partial \bar{y}} \right) = D_B \left(\frac{\partial^2 \bar{C}}{\partial \bar{x}^2} + \frac{\partial^2 \bar{C}}{\partial \bar{y}^2} \right) + \left(\frac{D_T}{T_\infty} \right) \left[\frac{\partial^2 \bar{T}}{\partial \bar{x}^2} + \frac{\partial^2 \bar{T}}{\partial \bar{y}^2} \right] \quad 3.66$$

where $\bar{\mathbf{V}}$ is the fluid filtration velocity, \bar{T} is the temperature, \bar{C} is nanoparticle volume fraction, \bar{p} is the pressure, ε is the porosity of the porous medium, D_B is the Brownian diffusion coefficient, D_T is the thermophoretic diffusion coefficient of the nanoparticle volume fraction, and ∇^2 is the Laplacian operator.

3.2.5 Governing Equations

A steady state flow is considered which defines the behaviour of the system unchanging with time, meaning that the partial derivative with respect to time is zero. Therefore, the steady state of two-dimensional governing dimensional Equations 3.11, 3.33, 3.60 and 3.66 can be written in the two dimensional Cartesian coordinate system as follows:

$$\frac{\partial \bar{u}}{\partial \bar{x}} + \frac{\partial \bar{v}}{\partial \bar{y}} = 0 \quad 3.67$$

$$\frac{\mu}{K} \left(\frac{\partial \bar{u}}{\partial \bar{x}} + \frac{\partial \bar{v}}{\partial \bar{y}} \right) = \left[(1 - \bar{C}_\infty) \beta \rho_{f\infty} \frac{\partial \bar{T}}{\partial \bar{y}} + (\rho_p - \rho_{f\infty}) \frac{\partial \bar{C}}{\partial \bar{y}} \right] g \sin \left(\frac{\bar{x}}{a} \right) \quad 3.68$$

$$\bar{u} \frac{\partial \bar{T}}{\partial \bar{x}} + \bar{v} \frac{\partial \bar{T}}{\partial \bar{y}} = \alpha_m \left(\frac{\partial^2 \bar{T}}{\partial \bar{x}^2} + \frac{\partial^2 \bar{T}}{\partial \bar{y}^2} \right) + \tau \left[D_B \left(\frac{\partial \bar{T}}{\partial \bar{x}} \frac{\partial \bar{C}}{\partial \bar{x}} + \frac{\partial \bar{T}}{\partial \bar{y}} \frac{\partial \bar{C}}{\partial \bar{y}} \right) + \left(\frac{D_T}{T_\infty} \right) \left(\left(\frac{\partial \bar{T}}{\partial \bar{x}} \right)^2 + \left(\frac{\partial \bar{T}}{\partial \bar{y}} \right)^2 \right) \right] \quad 3.69$$

$$\frac{1}{\varepsilon} \left(\bar{u} \frac{\partial \bar{C}}{\partial \bar{x}} + \bar{v} \frac{\partial \bar{C}}{\partial \bar{y}} \right) = D_B \left(\frac{\partial^2 \bar{C}}{\partial \bar{x}^2} + \frac{\partial^2 \bar{C}}{\partial \bar{y}^2} \right) + \left(\frac{D_T}{T_\infty} \right) \left[\frac{\partial^2 \bar{T}}{\partial \bar{x}^2} + \frac{\partial^2 \bar{T}}{\partial \bar{y}^2} \right] \quad 3.70$$

3.2.6 Boundary Conditions

In order to solve the above equation, we need to specify boundary conditions. The boundary conditions will either specify pressures or flow rates at two positions of the system. The boundary condition on the velocity depend on the nature of the fluid flow and geometry of the boundary wall. The mathematical form of the velocity boundary conditions can be expressed as follow

$$\begin{aligned} \bar{v}(\bar{x}, \bar{y}) &= 0, \quad \text{at } \bar{y} = 0, \quad 0 \leq \bar{x} \leq \pi \\ \bar{u}(\bar{x}, \bar{y}) &\rightarrow \bar{u}_e(\bar{x}), \quad \text{as } \bar{y} \rightarrow \infty, \quad 0 \leq \bar{x} \leq \pi \end{aligned}$$

Convective boundary condition corresponds to the existence of convection heating at the surface and is obtained from the surface energy balance. Therefore, we assume the bottom surface of the cylinder is heated by convection from a hot fluid at temperature T_f which provides a heat transfer coefficient h_f . The heating conditions at the cylinder surface and far into the hot fluid may be written as

$$\begin{aligned} -k \frac{\partial \bar{T}}{\partial \bar{y}} &= h_f (T_f - \bar{T}), \quad \text{at } \bar{y} = 0, \quad 0 \leq \bar{x} \leq \pi \\ \bar{T}(\bar{x}, \bar{y}) &\rightarrow \bar{T}_\infty \quad \text{as } \bar{y} \rightarrow \infty, \quad 0 \leq \bar{x} \leq \pi \end{aligned}$$

The relevant concentration boundary conditions associated with the physical problem under discussion are

$$\begin{aligned} \bar{C}(\bar{x}, \bar{y}) &= \bar{C}_w \quad \text{at } \bar{y} = 0, \quad 0 \leq \bar{x} \leq \pi \\ \bar{C}(\bar{x}, \bar{y}) &\rightarrow \bar{C}_\infty \quad \text{as } \bar{y} \rightarrow \infty, \quad 0 \leq \bar{x} \leq \pi \end{aligned}$$

By combining the boundary condition for velocity, temperature and concentration, we obtain

$$\begin{aligned} \bar{v}(\bar{x}, \bar{y}) = 0, \quad -k \frac{\partial \bar{T}}{\partial \bar{y}} = h_f(T_f - \bar{T}), \quad \bar{C}(\bar{x}, \bar{y}) = \bar{C}_w \quad \text{at } \bar{y} = 0, \quad 0 \leq \bar{x} \leq \pi \\ \bar{u}(\bar{x}, \bar{y}) \rightarrow \bar{u}_e(\bar{x}), \quad \bar{T}(\bar{x}, \bar{y}) \rightarrow \bar{T}_\infty, \quad \bar{C}(\bar{x}, \bar{y}) \rightarrow \bar{C}_\infty \quad \text{as } \bar{y} \rightarrow \infty, \quad 0 \leq \bar{x} \leq \pi \end{aligned} \quad 3.71$$

3.2.7 Boundary Layer Approximation

The dimensionless Equations 3.67 to 3.70 are also nonlinear partial differential equations in an elliptic system. Therefore, by applying the boundary layer approximation, the number of governing equations can be converted from elliptic to the parabolic system. The parabolic partial differential equations can be solved much easier (Nazar, 2003). The following assumptions are made to derive the boundary layer equations (Schlichting, 1968):

- i) All the viscosity effect of flow field is restricted to the boundary layer, which is closed to the surface. The viscosity effect is not important for the outer boundary layer, so that flow can be determined by inviscid solution such as potential flow or Euler's equations
- ii) The boundary layer is assumed to be much less than the length of the surface. If δ is the boundary layer thickness and L is the length of the surface, then $\delta/L \ll 1$, $x = O(L)$ and $y = O(\delta)$
- iii) The fluid has no slip condition at the surface when the velocity is zero (Acheson, 1990) and the free flow conditions outside of the boundary layer given by $u(x, 0) = 0, v(x, 0) = 0, u(x, \infty) = U_\infty, v(x, \infty) = 0$, where u and v are the velocity components along x - and y -axes, respectively and U_∞ is the free stream velocity.
- iv) At the boundary layer, $u = O(U_\infty)$

By referring to the assumption above, we write

$$\bar{x} \sim L, \quad \bar{y} \sim \delta, \quad \bar{u} \sim U_\infty, \quad \bar{T} \sim t, \quad \bar{C} \sim c \quad 3.72$$

where L is the length of the cylinder, δ is the boundary layer thickness, U_∞ is free stream velocity, c is the fractional nanoparticles and t is the temperature of fluid. The process of analysis order of magnitude will be done for each of the conservation equation. For

continuity Equation 3.67,

$$\frac{\partial \bar{u}}{\partial \bar{x}} + \frac{\partial \bar{v}}{\partial \bar{y}} = 0$$

By using analysis of magnitude, $\partial \bar{u} / \partial \bar{x}$ and $\partial \bar{v} / \partial \bar{y}$ is defined as U_∞ / L and \bar{v} / δ . Note that $\partial \bar{v} / \partial \bar{y}$ should be in the same order with $\partial u / \partial x$ or in other word $\left(\frac{\partial \bar{u}}{\partial \bar{x}} \neq 0 \right)$. Therefore, \bar{v} is given by

$$\bar{v} \sim \frac{U_\infty \delta}{L}$$

From the boundary layer approximation, second assumption stated that $\delta \ll L$ where δ is very small compared to characteristic length $L \left(\frac{\delta}{L} \ll 1 \right)$ and velocity component in the direction of fluid flow u is greater than the velocity component normal to the fluid flow ($u \gg v$). Order of analysis magnitude coupled with the boundary layer approximation produced a powerful tool for the simplification of equations where some negligible small terms may be neglected from the full equation without affecting the accuracy of the solution.

Table 3.1. Analysis order of magnitude for momentum equation Buongiorno model of nanofluids

Terms of equation	Used Equations	Simplified	Magnitude Order	$\delta \leq L$
	3.68		$\times \frac{\delta}{U_\infty}$	
$\frac{\partial \bar{u}}{\partial \bar{x}}$	$\frac{U_\infty}{L}$	-	$\frac{\delta}{L} \ll 1$	$\frac{\partial \bar{u}}{\partial \bar{x}}$ can be negligible
$\frac{\partial \bar{u}}{\partial \bar{y}}$	$\frac{U_\infty}{\delta}$	-	O(1)	remain unchanged
$\frac{\partial \bar{T}}{\partial \bar{y}}$	$\frac{t}{\delta}$		$\frac{t}{U_\infty}$	remain unchanged
$\frac{\partial \bar{C}}{\partial \bar{y}}$	$\frac{c}{\delta}$		$\frac{c}{U_\infty}$	remain unchanged

Table 3.1 illustrated the analysis order for momentum equation. Comparing the first two terms, we see that the force in the x direction is negligible when compared to that in the y direction. Therefore, the first term is neglected whereas the other three terms remained unchanged

$$\frac{\mu}{K} \frac{\partial \bar{u}}{\partial \bar{y}} = \left[(1 - \bar{C}_\infty) \beta \rho_{f\infty} \frac{\partial \bar{T}}{\partial \bar{y}} - (\rho_p - \rho_{f\infty}) \frac{\partial \bar{C}}{\partial \bar{y}} \right] g \sin \left(\frac{\bar{x}}{a} \right) \quad 3.73$$

The analysis order of magnitude for energy equations are shown in Table 3.2. Several terms have been ignored due to size of magnitude order which is much smaller when paired with another. Therefore, the following terms will be neglected.

$$\frac{\partial^2 \bar{T}}{\partial x^2}, \quad \frac{\partial \bar{C} \partial \bar{T}}{\partial \bar{x} \partial \bar{x}}, \quad \left(\frac{\partial \bar{T}}{\partial \bar{x}} \right)^2$$

Table 3.2. Analysis order of magnitude for energy equation Buongiorno model of nanofluids

Terms of equation	Used Equation 3.69	Simplified	Magnitude Order $\times \frac{L}{U_\infty t}$	$\delta \leq L$
$\bar{u} \frac{\partial \bar{T}}{\partial \bar{x}}$	$U_\infty \frac{t}{L}$		O(1)	remain unchanged
$\bar{v} \frac{\partial \bar{T}}{\partial \bar{y}}$	$\frac{U_\infty \delta t}{L \delta}$	$\frac{U_\infty t}{L}$	O(1)	remain unchanged
$\alpha_m \frac{\partial^2 \bar{T}}{\partial y^2}$	$\alpha_m \frac{t}{\delta^2}$		$\alpha_m \frac{L}{\delta^2 U_\infty}$	$\frac{\partial^2 \bar{T}}{\partial y^2} \gg \frac{\partial^2 \bar{T}}{\partial x^2}$
$\alpha_m \frac{\partial^2 \bar{T}}{\partial x^2}$	$\alpha_m \frac{t}{L^2}$		$\alpha_m \frac{1}{L U_\infty}$	$\frac{\partial^2 \bar{T}}{\partial x^2}$ can be negligible
$\tau D_B \frac{\partial \bar{C} \partial \bar{T}}{\partial \bar{x} \partial \bar{x}}$	$\tau D_B \frac{c t}{L L}$		$\tau D_B \frac{c}{L U_\infty}$	$\frac{\partial \bar{C} \partial \bar{T}}{\partial \bar{x} \partial \bar{x}}$ can be negligible
$\tau D_B \frac{\partial \bar{C} \partial \bar{T}}{\partial \bar{y} \partial \bar{y}}$	$\tau D_B \frac{c t}{\delta \delta}$		$\tau D_B \frac{c L}{\delta^2 U}$	$\frac{\partial \bar{C} \partial \bar{T}}{\partial \bar{y} \partial \bar{y}} \gg \frac{\partial \bar{C} \partial \bar{T}}{\partial \bar{x} \partial \bar{x}}$
$\frac{D_T}{T_\infty} \left(\frac{\partial \bar{T}}{\partial \bar{x}} \right)^2$	$\frac{D_T}{T_\infty} \left(\frac{t}{L} \right)^2$		$\frac{D_T}{T_\infty} \frac{t}{L U_\infty}$	$\left(\frac{\partial \bar{T}}{\partial \bar{x}} \right)^2$ can be negligible
$\frac{D_T}{T_\infty} \left(\frac{\partial \bar{T}}{\partial \bar{y}} \right)^2$	$\frac{D_T}{T_\infty} \left(\frac{t}{\delta} \right)^2$		$\frac{D_T}{T_\infty} \frac{t L}{\delta^2 U_\infty}$	$\left(\frac{\partial \bar{T}}{\partial \bar{y}} \right)^2 \gg \left(\frac{\partial \bar{T}}{\partial \bar{x}} \right)^2$

Thus energy Equation 3.70 becomes

$$\bar{u} \frac{\partial \bar{T}}{\partial \bar{x}} + \bar{v} \frac{\partial \bar{T}}{\partial \bar{y}} = \alpha_m \frac{\partial^2 \bar{T}}{\partial \bar{y}^2} + \tau D_B \frac{\partial \bar{T}}{\partial \bar{y}} \frac{\partial \bar{C}}{\partial \bar{y}} + \left(\frac{D_T}{T_\infty} \right) \left(\frac{\partial \bar{T}}{\partial \bar{y}} \right)^2 \quad 3.74$$

Table 3.3. Analysis order of magnitude for nanoparticle volume fraction equation Buongiorno model of nanofluids

Terms of equation	Used Equation	Simplified	Magnitude Order	$\delta \ll L$
	3.70		$\times \frac{L}{cU_\infty}$	
$\bar{u} \frac{\partial \bar{C}}{\partial \bar{x}}$	$U_\infty \frac{c}{L}$		O(1)	remain unchanged
$\bar{v} \frac{\partial \bar{C}}{\partial \bar{y}}$	$\frac{U_\infty \delta c}{L \delta}$	$\frac{U_\infty c}{L}$	O(1)	remain unchanged
$D_B \frac{\partial^2 \bar{C}}{\partial \bar{x}^2}$	$D_B \frac{c}{L^2}$		$D_B \frac{1}{LU_\infty}$	$D_B \frac{\partial^2 \bar{C}}{\partial \bar{x}^2}$ can be negligible
$D_B \frac{\partial^2 \bar{C}}{\partial \bar{y}^2}$	$D_B \frac{c}{\delta^2}$		$D_B \frac{L}{\delta^2 U_\infty}$	$\frac{\partial^2 \bar{C}}{\partial \bar{y}^2} \gg \frac{\partial^2 \bar{C}}{\partial \bar{x}^2}$
$\frac{D_T}{T_\infty} \frac{\partial^2 \bar{T}}{\partial \bar{x}^2}$	$\frac{D_T t}{T_\infty L^2}$		$\frac{D_T t}{T_\infty LU_\infty c}$	$\frac{\partial^2 \bar{T}}{\partial \bar{x}^2}$ can be negligible
$\frac{D_T}{T_\infty} \frac{\partial^2 \bar{T}}{\partial \bar{y}^2}$	$\frac{D_T t}{T_\infty \delta^2}$		$\frac{D_T Lt}{T_\infty \delta^2 U_\infty c}$	$\frac{\partial^2 \bar{T}}{\partial \bar{y}^2} \gg \frac{\partial^2 \bar{T}}{\partial \bar{x}^2}$

Further, an analysis order of magnitude for nanoparticle volume fraction equations is shown in Table 3.3. Similar as energy equation, some of the terms in nanoparticle volume

fraction is negligible such as $D_B \frac{\partial^2 \bar{C}}{\partial \bar{x}^2}$ and $\frac{D_T}{T_\infty} \frac{\partial^2 \bar{T}}{\partial \bar{x}^2}$ where

$$\frac{\partial^2 \bar{C}}{\partial \bar{y}^2} / \frac{\partial^2 \bar{C}}{\partial \bar{x}^2} = O\left(\frac{L}{\delta}\right)^2 \geq 1$$

Therefore new nanoparticle Equation 3.70 is given by

$$\frac{1}{\varepsilon} \left(\bar{u} \frac{\partial \bar{C}}{\partial \bar{x}} + \bar{v} \frac{\partial \bar{C}}{\partial \bar{y}} \right) = D_B \frac{\partial^2 \bar{C}}{\partial \bar{y}^2} + \left(\frac{D_T}{T_\infty} \right) \frac{\partial^2 \bar{T}}{\partial \bar{y}^2} \quad 3.75$$

3.2.8 Non-Dimensional Variables

Equations 3.73, 3.74 to 3.75 are in dimensional form. Notably, the dimensional form involves a wide number of variables and different physical quantities thereby causing difficulties when needing to solve the problem numerically. Although by introducing the non-dimensional variables, the equations can be further simplified by reducing the number of variables used therefore making the problem much easier to solve. Also, non-dimensional variables can rescale the parameters so that all the quantities are of the same order and the effects of numerical error are minimised when calculating the residual. Therefore, the following non-dimensional variables are introduced:

$$\begin{aligned} x &= \frac{\bar{x}}{a}, & y &= \frac{Pe^{1/2}\bar{y}}{a}, & u &= \frac{\bar{u}}{U_\infty}, & v &= \frac{Pe^{1/2}\bar{v}}{U_\infty}, \\ \theta &= \frac{\bar{T} - T_\infty}{T_f - T_\infty}, & \phi &= \frac{\bar{C} - C_\infty}{C_w - C_\infty} \end{aligned} \quad 3.76$$

where $Pe = U_\infty a / \alpha_m$ is the Peclet number. By using the expression in Equation 3.76 into Equations 3.73, 3.74 to 3.75, we obtain

$$\frac{\partial u}{\partial x} + \frac{\partial v}{\partial y} = 0 \quad 3.77$$

$$\frac{\partial u}{\partial y} = \left(\frac{\partial \theta}{\partial y} - Nr \frac{\partial \phi}{\partial y} \right) \lambda \sin x \quad 3.78$$

$$u \frac{\partial \theta}{\partial x} + v \frac{\partial \theta}{\partial y} = \frac{\partial^2 \theta}{\partial y^2} + Nb \frac{\partial \theta}{\partial y} \frac{\partial \phi}{\partial y} + Nt \left(\frac{\partial \theta}{\partial y} \right)^2 \quad 3.79$$

$$Le \left(u \frac{\partial \phi}{\partial x} + v \frac{\partial \phi}{\partial y} \right) = \frac{\partial^2 \phi}{\partial y^2} + \left(\frac{Nt}{Nb} \right) \frac{\partial^2 \theta}{\partial y^2} \quad 3.80$$

where $u_e(x) = \sin x$. Here λ is the constant mixed convection parameter, Le is the Lewis number, Nr is the buoyancy ratio parameter, Nb is the Brownian motion parameter and Nt is the thermophoresis parameter which are defined as

$$\lambda = \frac{Ra}{Pe}, \quad Le = \frac{\alpha_m}{\varepsilon D_b}, \quad Nr = \frac{(\rho_p - \rho_{f\infty})(C_w - C_\infty)}{\beta \rho_{f\infty} (1 - C_\infty)(T_f - T_\infty)} \quad 3.81$$

$$Nb = \frac{\tau D_B (C_w - C_\infty)}{\alpha_m}, \quad Nt = \frac{\tau D_T (T_f - T_\infty)}{\alpha_m T_\infty}$$

The modified Rayleigh number for porous medium filled by nanofluid is $Ra = (1 - C_\infty)gK\rho_{f\infty}\beta(T_f - T_\infty)/(\mu\alpha_m)$ (Tham et al., 2014).

For case of boundary condition, the conditions for this problem is assumed to be

- i) The velocity of external flow (inviscid flow) is $u_e(x)$, where x is the coordinate measured along the surface of cylinder starting from the lower stagnation point and y is the coordinate measured in the direction normal to the surface of the cylinder.
- ii) The uniform temperature and the uniform nanoparticle volume fraction of the surface of the cylinder are T_f and C_w while the ambient values are T_∞ and C_∞ where $T_f > T_\infty$.
- iii) The nanofluid particle on the boundary is passively rather the actively controlled. The fractional nanoparticles in the boundary layer approach to free stream fractional nanoparticles $C \rightarrow C_\infty$.

Therefore, by substituting the non-dimensional variable into boundary conditions, Equation 3.71 becomes

$$\begin{aligned} v(x,y) = 0, \quad \theta'(x,y) = -\gamma(1 - \theta(x,y)), \quad \phi(x,y) = 1 \quad \text{at} \quad y = 0, \quad 0 \leq x \leq \pi \\ u(x,y) \rightarrow u_e(x), \quad \theta(x,y) \rightarrow 0, \quad \phi(x,y) \rightarrow 0 \quad \text{as} \quad y \rightarrow \infty, \quad 0 \leq x \leq \pi \end{aligned} \quad 3.82$$

It is worth mentioning here that Equations 3.77 to 3.80 are now the non-dimension equations.

3.2.9 Non-Similar Transformation

In this section, non-similar transformation variables are used to reduce the parabolic nonlinear partial differential equation to an ordinary differential equation. This method reduces several independent variables to single variable. The dimensionless variable as proposed by Merkin (1977) is given as follows:

$$\psi = xf(x,y), \quad \theta = \theta(x,y), \quad \phi = \phi(x,y) \quad 3.83$$

where ψ is the stream function defined as $u = \partial\psi/\partial y$ and $v = -\partial\psi/\partial x$. Substituting these variables into Equations 3.78, 3.79 and 3.80, the following boundary layer equations for the problem under consideration in dimensionless form are obtained:

$$\frac{\partial f}{\partial y} = [1 + (\theta - Nr\phi)\lambda] \frac{\sin x}{x} \quad 3.84$$

$$\frac{\partial^2 \theta}{\partial y^2} + f \frac{\partial \theta}{\partial y} + Nb \frac{\partial \theta}{\partial y} \frac{\partial \phi}{\partial y} + Nt \left(\frac{\partial \theta}{\partial y} \right)^2 = x \left(\frac{\partial f}{\partial y} \frac{\partial \theta}{\partial x} - \frac{\partial f}{\partial x} \frac{\partial \theta}{\partial y} \right) \quad 3.85$$

$$\frac{\partial^2 \phi}{\partial y^2} + Le f \frac{\partial \phi}{\partial y} + \frac{Nb}{Nt} \frac{\partial^2 \theta}{\partial y^2} = x Le \left(\frac{\partial f}{\partial y} \frac{\partial \phi}{\partial x} - \frac{\partial f}{\partial x} \frac{\partial \phi}{\partial y} \right) \quad 3.86$$

with the boundary conditions

$$\begin{aligned} f(x,y) = 0, \quad \theta'(x,y) = -\gamma(1 - \theta(x,y)), \quad \phi(x,y) = 1 \quad \text{at } y = 0, \quad 0 \leq x \leq \pi \\ \theta(x,y) \rightarrow 0, \quad \phi(x,y) \rightarrow 0 \quad \text{as } y \rightarrow \infty, \quad 0 \leq x \leq \pi \end{aligned} \quad 3.87$$

Since most of the nanofluids examined to date have focused on constant wall temperature and constant heat flux, interest at this moment is mainly in the effect of convective boundary conditions. Also we are interested in the case where it is heat transfer (rather than mass transfer) that is driving the flow.

The boundary layer equations described in Equations 3.84 to 3.86 subject to boundary conditions 3.87 are solved numerically using the implicit finite difference method known as the Keller-box method. The following section provides insight regarding the numerical procedure in solving these nonlinear partial differential equations, while the complete result is discussed further in Chapter 8.

3.3 Keller-box Scheme

All the flow problems presented in this thesis are solved numerically using the Keller-box method. Keller (1970) first proposed this method and it is found to be efficient and most suitable to solve convective boundary layer problems. The Keller-box method described in

this study is explained clearly by Na (1979) and Cebeci and Bradshaw (1988). Indeed the Keller-box method is implicit finite different method.

Generally, there are four steps in Keller-box method which will be explained in detail in the next subsection. Firstly, the equations are reduced to first order equation. Then, equation are written into finite difference forms. These equations are nonlinear. Newton's method is proposed to linearized the nonlinear equations and finally, the solutions are obtained using the block elimination techniques, by employing a block tridiagonal factorization scheme on the coefficient matrix of the finite difference equations for all y at given x .

3.3.1 First Order System

The first procedure of Keller-box method for problem presented in Chapter 8 are written here as a system of first order equations. For this reason, new dependent variables are introduced,

$$f' = u, \quad u' = v, \quad s' = t, \quad p' = q \quad 3.88$$

where prime denote differentiation with respect to y . Applying above equations into Equations 3.84 to 3.86, first order equation is obtained as given below:

$$f' = [1 + (s - Nr \cdot p)\lambda] \frac{\sin x}{x} \quad 3.89$$

$$t' + ft + Nb \cdot tq + Nt \cdot (t)^2 = x \left(u \frac{\partial s}{\partial x} - t \frac{\partial f}{\partial x} \right) \quad 3.90$$

$$q' + Lefq + \frac{Nt}{Nb} t' = xLe \left(u \frac{\partial p}{\partial x} - q \frac{\partial f}{\partial x} \right) \quad 3.91$$

the boundary conditions 3.87 becomes

$$\begin{aligned} f(x,y) = 0, \quad t(x,y) = -\gamma(1 - s(x,y)), \quad p(x,y) = 1 \quad \text{at } y = 0, \quad 0 \leq x \leq \pi \\ s(x,y) \rightarrow 0, \quad p(x,y) \rightarrow 0 \quad \text{as } y \rightarrow \infty, \quad 0 \leq x \leq \pi \end{aligned} \quad 3.92$$

3.3.2 Finite Difference Method

Once the equations has been transform to first order system, the following procedure is discretization. Discretization concerns the process of transferring continous function into discrete counterparts, making it suitable for numerical evaluation. For the discretization of Equations 3.89 to 3.91, and 3.92, a finite difference method was employed. The net rectangle considered in the $x - y$ plane is shown in Figure 3.1, and the net points are denoted by

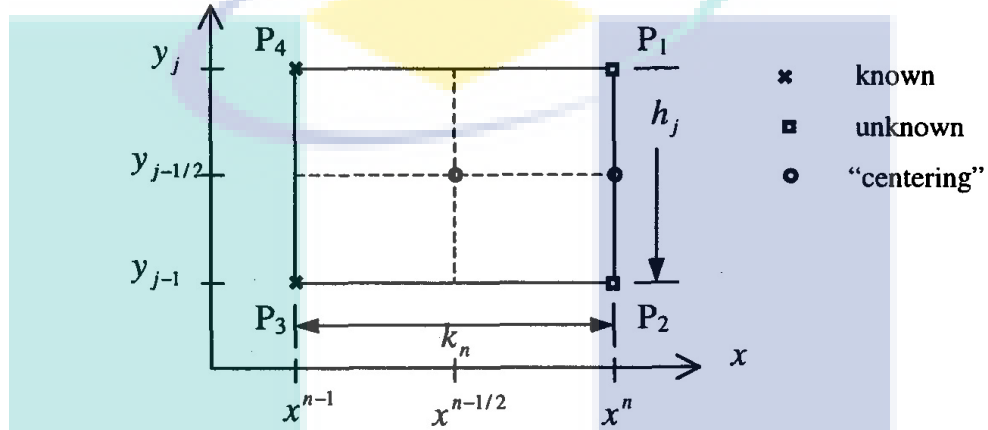


Figure 3.1. Net rectangle for difference approximation

$$x^0 = 0, \quad x^n = x^{n-1} + k_n, \quad n = 1, 2, \dots, N$$

$$y^0 = 0, \quad y^j = y_{j-1} + h_j, \quad n = 1, 2, \dots, J \quad y_J \equiv y_\infty$$

where k_n is the ∇x - spacing and h_j is the ∇y - spacing. Here n and j are the sequence numbers that indicate the coordinate location. The notation $()_j^n$ for points and quantities midway between net points and for any net function are given by

$$()_{j-1/2}^n = \frac{1}{2} [()_j^n + ()_{j-1}^n], \quad ()_j^{n-1/2} = \frac{1}{2} [()_j^n + ()_j^{n-1}] \quad 3.93$$

The derivatives in the x - and y - direction are replaced by finite difference. Generally we have

$$\frac{\partial ()}{\partial x} = \frac{()^n - ()^{n-1}}{k_n}, \quad \frac{\partial ()}{\partial y} = \frac{()_j - ()_{j-1}}{h_j} \quad 3.94$$

by using central differences. Hence, the following are obtained

$$\frac{f_j^n - f_{j-1}^n}{h_j} = \frac{u_j^n + u_{j-1}^n}{2} = u_{j-1/2}^n \quad 3.95$$

$$\frac{u_j^n - u_{j-1}^n}{h_j} = \frac{v_j^n + v_{j-1}^n}{2} = v_{j-1/2}^n \quad 3.96$$

$$\frac{s_j^n - s_{j-1}^n}{h_j} = \frac{t_j^n + t_{j-1}^n}{2} = t_{j-1/2}^n \quad 3.97$$

$$\frac{p_j^n - p_{j-1}^n}{h_j} = \frac{q_j^n + q_{j-1}^n}{2} = q_{j-1/2}^n \quad 3.98$$

Following $P_1P_2P_3P_4$, we obtain the following equations

$$\frac{1}{2}(L_1^n + L_1^{n-1}) = 0 \quad 3.99$$

$$\frac{1}{2}(L_2^n + L_2^{n-1}) = x^{n-\frac{1}{2}} \left(u^{n-\frac{1}{2}} \frac{s^n - s^{n-1}}{k_n} - t^{n-\frac{1}{2}} \frac{f^n - f^{n-1}}{k_n} \right) \quad 3.100$$

$$\frac{1}{2}(L_3^n + L_3^{n-1}) = Le \cdot x^{n-\frac{1}{2}} \left(u^{n-\frac{1}{2}} \frac{p^n - p^{n-1}}{k_n} - q^{n-\frac{1}{2}} \frac{f^n - f^{n-1}}{k_n} \right) \quad 3.101$$

Rearranging these equations

$$(f')^n - [1 + (s^n - Nr \cdot p^n)\lambda] \beta = -L_1^{n-1} \quad 3.102$$

$$(t')^n + (ft)^n + Nb \cdot (tq)^n + (t^2)^n \cdot Nt - \alpha(us)^n - \alpha u^{n-1} s^n + \alpha s^{n-1} u^n + \alpha(ft)^n + \alpha t^{n-1} f^n - \alpha f^{n-1} t^n = \left[-L_2 - \alpha(us) + \alpha(ft) \right]^{n-1} \quad 3.103$$

$$(q')^n + Le(fq)^n + \frac{Nt}{Nb}(t')^n - \sigma(up)^n + \sigma p^{n-1} u^n - \sigma u^{n-1} p^n + \sigma(fq)^n + \sigma q^{n-1} f^n - \sigma f^{n-1} q^n = \left[-L_3 - \sigma(up) + \sigma(fq) \right]^{n-1} \quad 3.104$$

where the abbreviation is

$$\alpha = \frac{x^{n-1/2}}{k_n} \quad 3.105$$

$$\beta = \frac{\sin(x^{n-1/2})}{x^{n-1/2}} \quad 3.106$$

$$\sigma = Le \frac{\sin(x^{n-1/2})}{x^{n-1/2}} \quad 3.107$$

$$L_1^{n-1} = (f')^{n-1} - \beta [1 + (s - Nr \cdot p)\lambda]^{n-1} \quad 3.108$$

$$L_2^{n-1} = [(t') + (ft) + (tq)Nb + Nt \cdot (t^2)]^{n-1} \quad 3.109$$

$$L_3^{n-1} = [(q') + Le(fq) + \frac{Nt}{Nb}(t')]^{n-1} \quad 3.110$$

Next, we center Equations 3.102 to 3.104 at the point $(x^{n-1/2}, y_{j-1/2})$ by using

$$\frac{f_j^n - f_{j-1}^n}{h_j} - [1 + (s_{j-1/2}^n - Nr \cdot p_{j-1/2}^n)\lambda] \beta = -L_1^{n-1} \quad 3.111$$

$$\begin{aligned} & \frac{t_j^n - t_{j-1}^n}{h_j} + f_{j-1/2}^n t_{j-1/2}^n + Nb \cdot t_{j-1/2}^n q_{j-1/2}^n + (t^2)_{j-1/2}^n \cdot Nt - \alpha u_{j-1/2}^n s_{j-1/2}^n \\ & - \alpha u_{j-1/2}^{n-1} s_{j-1/2}^n + \alpha s_{j-1/2}^{n-1} u_{j-1/2}^n + \alpha f_{j-1/2}^n t_{j-1/2}^n + \alpha t_{j-1/2}^{n-1} f_{j-1/2}^n \\ & - \alpha f_{j-1/2}^{n-1} t_{j-1/2}^n = \left[-L_2 - \alpha u_{j-1/2} s_{j-1/2} + \alpha f_{j-1/2} t_{j-1/2} \right]^{n-1} \end{aligned} \quad 3.112$$

$$\begin{aligned} & \frac{q_j^n - q_{j-1}^n}{h_j} + L e f_{j-1/2}^n q_{j-1/2}^n + \frac{Nt}{Nb} \frac{t_j^n - t_{j-1}^n}{h_j} - \sigma u_{j-1/2}^n p_{j-1/2}^n + \sigma p_{j-1/2}^{n-1} u_{j-1/2}^n \\ & - \sigma u_{j-1/2}^{n-1} p_{j-1/2}^n + \sigma f_{j-1/2}^n q_{j-1/2}^n + \sigma q_{j-1/2}^{n-1} f_{j-1/2}^n - \sigma f_{j-1/2}^{n-1} q_{j-1/2}^n \\ & = \left[-L_3 - \sigma u_{j-1/2} p_{j-1/2} + \sigma f_{j-1/2} q_{j-1/2} \right]^{n-1} \end{aligned} \quad 3.113$$

where

$$(L_1)_{j-1/2}^{n-1} = \left(\frac{f_j - f_{j-1}}{h_j} \right)^{n-1} - \beta [1 + (s_{j-1/2} - Nr \cdot p_{j-1/2})\lambda]^{n-1} \quad 3.114$$

$$(L_2)_{j-1/2}^{n-1} = \left[\frac{t_j - t_{j-1}}{h_j} + f_{j-1/2} t_{j-1/2} + t_{j-1/2} q_{j-1/2} Nb + Nt \cdot (t^2)_{j-1/2} \right]^{n-1} \quad 3.115$$

$$(L_3)_{j-1/2}^{n-1} = \left[\frac{q_j - q_{j-1}}{h_j} + L e f_{j-1/2} q_{j-1/2} + \frac{Nt}{Nb} \frac{t_j - t_{j-1}}{h_j} \right]^{n-1} \quad 3.116$$

At $x = x^n$, the boundary conditions (3.92) become

$$f_0^n = 0, \quad t_0^n = -\gamma(1 - s_0^n), \quad p_0^n = 1, \quad s_j^n = 0, \quad p_j^n = 0 \quad 3.117$$

3.3.3 Newton's Method

Equations 3.111 to 3.113 are nonlinear equations, Newton's method is proposed to linearize the nonlinear equations. Suppose $f_j^{n-1}, u_j^{n-1}, v_j^{n-1}, s_j^{n-1}, t_j^{n-1}, p_j^{n-1}, q_j^{n-1}$ are known for $0 \leq j \leq J$ then Equations 3.111 to 3.113 form a system of equations for the solution of the unknown variables $(f_j^n, u_j^n, v_j^n, s_j^n, t_j^n, p_j^n, q_j^n)$, $j = 0, 1, \dots, J$. For simplification the unknown variable $(f_j^n, u_j^n, v_j^n, s_j^n, t_j^n, p_j^n, q_j^n)$ is written as $(f_j, u_j, v_j, s_j, t_j, p_j, q_j)$. By using

$$f_j - f_{j-1} - \frac{h_j}{2}(u_j + u_{j-1}) = 0 \quad 3.118$$

$$u_j - u_{j-1} - \frac{h_j}{2}(v_j + v_{j-1}) = 0 \quad 3.119$$

$$s_j - s_{j-1} - \frac{h_j}{2}(t_j + t_{j-1}) = 0 \quad 3.120$$

$$p_j - p_{j-1} - \frac{h_j}{2}(q_j + q_{j-1}) = 0 \quad 3.121$$

$$f_j - f_{j-1} - h_j \left[1 + \left(\frac{s_j + s_{j-1}}{2} \right) - Nr \cdot \left(\frac{p_j + p_{j-1}}{2} \right) \lambda \right] \beta = (R_1)_{j-1/2}^{n-1} \quad 3.122$$

$$\begin{aligned} & t_j - t_{j-1} + \frac{h_j}{4}(f_j + f_{j-1})(t_j + t_{j-1}) + \frac{h_j}{4}Nb \cdot (t_j + t_{j-1})(q_j + q_{j-1}) \\ & + \frac{h_j}{4}(t_j + t_{j-1})^2 \cdot Nt - \frac{h_j}{4}\alpha(u_j + u_{j-1})(s_j + s_{j-1}) - \frac{h_j}{2}\alpha u_{j-1/2}^{n-1}(s_j + s_{j-1}) \\ & + \frac{h_j}{2}\alpha s_{j-1/2}^{n-1}(u_j + u_{j-1}) + \frac{h_j}{4}\alpha(f_j + f_{j-1})(t_j + t_{j-1}) + \frac{h_j}{2}\alpha t_{j-1/2}^{n-1}(f_j + f_{j-1}) \\ & - \frac{h_j}{2}\alpha f_{j-1/2}^{n-1}(t_j + t_{j-1}) = (R_2)_{j-1/2}^{n-1} \end{aligned} \quad 3.123$$

$$\begin{aligned}
& q_j - q_{j-1} + \frac{h_j}{4} Le(f_j + f_{j-1})(q_j + q_{j-1}) + \frac{Nt}{Nb}(t_j - t_{j-1}) - \frac{h_j}{4} \sigma(u_j + u_{j-1})(p_j + p_{j-1}) \\
& + \frac{h_j}{2} \sigma p_{j-1/2}^{n-1}(u_j + u_{j-1}) - \frac{h_j}{2} \sigma u_{j-1/2}^{n-1}(p_j + p_{j-1}) + \frac{h_j}{4} \sigma(f_j + f_{j-1})(q_j + q_{j-1}) \\
& + \frac{h_j}{2} \sigma q_{j-1/2}^{n-1}(f_j + f_{j-1}) - \frac{h_j}{2} \sigma f_{j-1/2}^{n-1}(q_j + q_{j-1}) = (R_3)_{j-1/2}^{n-1}
\end{aligned} \tag{3.124}$$

where

$$(R_1)_{j-1/2}^{n-1} = -h_j \left\{ \frac{f_j + f_{j-1}}{h_j} - \beta [1 + (s_{j-1/2} - Nr \cdot p_{j-1/2}) \lambda] \right\}^{n-1} \tag{3.125}$$

$$(R_2)_{j-1/2}^{n-1} = -h_j \left[\frac{t_j + t_{j-1}}{h_j} + f_{j-1/2} t_{j-1/2} + Nbt_{j-1/2} q_{j-1/2} + (t^2)_{j-1/2} Nt \right]^{n-1} \tag{3.126}$$

$$(R_3)_{j-1/2}^{n-1} = -h_j \left[\frac{q_j + q_{j-1}}{h_j} + Le f_{j-1/2} q_{j-1/2} + \frac{Nt}{Nb} \left(\frac{t_j + t_{j-1}}{h_j} \right) \right]^{n-1} \tag{3.127}$$

$(R_1)_{j-1/2}^{n-1}$, $(R_2)_{j-1/2}^{n-1}$ and $(R_3)_{j-1/2}^{n-1}$ involve known quantities if we assume that the solution is known on $x = x^{n-1}$. To solve the nonlinear Equations 3.122 to 3.124 by using Newton's method, we introduces

$$\begin{aligned}
f_j^{(i+1)} &= f_j^{(i)} + \delta f_j^{(i)}, & u_j^{(i+1)} &= u_j^{(i)} + \delta u_j^{(i)} \\
s_j^{(i+1)} &= s_j^{(i)} + \delta s_j^{(i)}, & t_j^{(i+1)} &= t_j^{(i)} + \delta t_j^{(i)} \\
p_j^{(i+1)} &= p_j^{(i)} + \delta p_j^{(i)}, & q_j^{(i+1)} &= q_j^{(i)} + \delta q_j^{(i)}
\end{aligned} \tag{3.128}$$

The iteration is substitute into Equations 3.118 to 3.124

$$(f_j^{(i)} + \delta f_j^{(i)}) - (f_{j-1}^{(i)} + \delta f_{j-1}^{(i)}) - \frac{h_j}{2} (u_j^{(i)} + \delta u_j^{(i)} + u_{j-1}^{(i)} + \delta u_{j-1}^{(i)}) = 0 \tag{3.129}$$

$$(u_j^{(i)} + \delta u_j^{(i)}) - (u_{j-1}^{(i)} + \delta u_{j-1}^{(i)}) - \frac{h_j}{2} (v_j^{(i)} + \delta v_j^{(i)} + v_{j-1}^{(i)} + \delta v_{j-1}^{(i)}) = 0 \tag{3.130}$$

$$(s_j^{(i)} + \delta s_j^{(i)}) - (s_{j-1}^{(i)} + \delta s_{j-1}^{(i)}) - \frac{h_j}{2}(t_j^{(i)} + \delta t_j^{(i)} + t_{j-1}^{(i)} + \delta t_{j-1}^{(i)}) = 0 \quad 3.131$$

$$(p_j^{(i)} + \delta p_j^{(i)}) - (p_{j-1}^{(i)} + \delta p_{j-1}^{(i)}) - \frac{h_j}{2}(q_j^{(i)} + \delta q_j^{(i)} + q_{j-1}^{(i)} + \delta q_{j-1}^{(i)}) = 0 \quad 3.132$$

$$(f_j^{(i)} + \delta f_j^{(i)}) - (f_{j-1}^{(i)} + \delta f_{j-1}^{(i)}) - h_j \left[1 + \frac{1}{2} \{ (s_j^{(i)} + \delta s_j^{(i)}) + (s_{j-1}^{(i)} + \delta s_{j-1}^{(i)}) \} \right. \\ \left. - Nr \cdot \frac{1}{2} \{ (p_j^{(i)} + \delta p_j^{(i)}) + (p_{j-1}^{(i)} + \delta p_{j-1}^{(i)}) \} \right] \lambda \beta = (R_1)_{j-1/2}^{n-1} \quad 3.133$$

$$(t_j^{(i)} + \delta t_j^{(i)}) - (t_{j-1}^{(i)} + \delta t_{j-1}^{(i)}) + \frac{h_j}{4} [(f_j^{(i)} + \delta f_j^{(i)}) + (f_{j-1}^{(i)} + \delta f_{j-1}^{(i)})] [(t_j^{(i)} + \delta t_j^{(i)}) \\ + (t_{j-1}^{(i)} + \delta t_{j-1}^{(i)})] + \frac{h_j}{4} Nb \cdot [(t_j^{(i)} + \delta t_j^{(i)}) + (t_{j-1}^{(i)} + \delta t_{j-1}^{(i)})] [(q_j^{(i)} + \delta q_j^{(i)}) + (q_{j-1}^{(i)} + \delta q_{j-1}^{(i)})] \\ + \frac{h_j}{4} [(t_j^{(i)} + \delta t_j^{(i)}) + (t_{j-1}^{(i)} + \delta t_{j-1}^{(i)})]^2 \cdot Nt - \frac{h_j}{4} \alpha [(u_j^{(i)} + \delta u_j^{(i)}) + (u_{j-1}^{(i)} + \delta u_{j-1}^{(i)})] \\ [(s_j^{(i)} + \delta s_j^{(i)}) + (s_{j-1}^{(i)} + \delta s_{j-1}^{(i)})] - \frac{h_j}{2} \alpha u_{j-1/2}^{n-1} [(s_j^{(i)} + \delta s_j^{(i)}) + (s_{j-1}^{(i)} + \delta s_{j-1}^{(i)})] \\ + \frac{h_j}{2} \alpha s_{j-1/2}^{n-1} [(u_j^{(i)} + \delta u_j^{(i)}) + (u_{j-1}^{(i)} + \delta u_{j-1}^{(i)})] + \frac{h_j}{4} \alpha [(f_j^{(i)} + \delta f_j^{(i)}) + (f_{j-1}^{(i)} + \delta f_{j-1}^{(i)})] \\ [(t_j^{(i)} + \delta t_j^{(i)}) + (t_{j-1}^{(i)} + \delta t_{j-1}^{(i)})] + \frac{h_j}{2} \alpha t_{j-1/2}^{n-1} [(f_j^{(i)} + \delta f_j^{(i)}) + (f_{j-1}^{(i)} + \delta f_{j-1}^{(i)})] \\ - \frac{h_j}{2} \alpha f_{j-1/2}^{n-1} [(t_j^{(i)} + \delta t_j^{(i)}) + (t_{j-1}^{(i)} + \delta t_{j-1}^{(i)})] = (R_2)_{j-1/2}^{n-1} \quad 3.134$$

$$\begin{aligned}
& (q_j^{(i)} + \delta q_j^{(i)}) - (q_{j-1}^{(i)} + \delta q_{j-1}^{(i)}) + \frac{h_j}{4} Le [(f_j^{(i)} + \delta f_j^{(i)}) - (f_{j-1}^{(i)} + \delta f_{j-1}^{(i)})] [(q_j^{(i)} + \delta q_j^{(i)}) \\
& - (q_{j-1}^{(i)} + \delta q_{j-1}^{(i)})] + \frac{Nt}{Nb} [(t_j^{(i)} + \delta t_j^{(i)}) - (t_{j-1}^{(i)} - \delta t_{j-1}^{(i)})] - \frac{h_j}{4} \sigma [(u_j^{(i)} + \delta u_j^{(i)}) - (u_{j-1}^{(i)} \\
& + \delta u_{j-1}^{(i)})] [(p_j^{(i)} + \delta p_j^{(i)}) - (p_{j-1}^{(i)} + \delta p_{j-1}^{(i)})] + \frac{h_j}{2} \sigma p_{j-1/2}^{n-1} [(u_j^{(i)} + \delta u_j^{(i)}) - (u_{j-1}^{(i)} \\
& + \delta u_{j-1}^{(i)})] - \frac{h_j}{2} \sigma u_{j-1/2}^{n-1} [(p_j^{(i)} + \delta p_j^{(i)}) - (p_{j-1}^{(i)} + \delta p_{j-1}^{(i)})] + \frac{h_j}{4} \sigma [(f_j^{(i)} \\
& + \delta f_j^{(i)}) - (f_{j-1}^{(i)} + \delta f_{j-1}^{(i)})] [(q_j^{(i)} + \delta q_j^{(i)}) - (q_{j-1}^{(i)} + \delta q_{j-1}^{(i)})] + \frac{h_j}{2} \sigma q_{j-1/2}^{n-1} \\
& [(f_j^{(i)} + \delta f_j^{(i)}) - (f_{j-1}^{(i)} + \delta f_{j-1}^{(i)})] - \frac{h_j}{2} \sigma f_{j-1/2}^{n-1} [(q_j^{(i)} + \delta q_j^{(i)}) - (q_{j-1}^{(i)} \\
& + \delta q_{j-1}^{(i)})] = (R_3)_{j-1/2}^{n-1}
\end{aligned} \tag{3.135}$$

For simplicity, the superscript i are neglected. After a few steps of algebraic operation and ignoring the higher order terms for $\delta f_j^i, \delta u_j^i, \delta v_j^i, \delta s_j^i, \delta t_j^i, \delta p_j^i, \delta q_j^i$ the system of the equations can be written as below

$$\delta f_j - \delta f_{j-1} - \frac{1}{2} h_j (\delta u_j + \delta u_{j-1}) = (r_1)_{j-1/2} \tag{3.136}$$

$$\delta s_j - \delta s_{j-1} - \frac{1}{2} h_j (\delta t_j + \delta t_{j-1}) = (r_2)_{j-1/2} \tag{3.137}$$

$$\delta p_j - \delta p_{j-1} - \frac{1}{2} h_j (\delta q_j + \delta q_{j-1}) = (r_3)_{j-1/2} \tag{3.138}$$

$$\begin{aligned}
& (a_1)_j \delta f_j + (a_2)_j \delta f_{j-1} + (a_3)_s \delta s_j + (a_4)_j \delta s_{j-1} \\
& + (a_5)_j \delta p_j + (a_6)_j \delta p_{j-1} = (r_4)_{j-1/2}
\end{aligned} \tag{3.139}$$

$$\begin{aligned}
& (b_1)_j \delta t_j + (b_2)_j \delta t_{j-1} + (b_3)_j \delta f_j + (b_4)_j \delta f_{j-1} + \\
& (b_5)_j \delta q_j + (b_6)_j \delta q_{j-1} + (b_7)_j \delta u_j + \\
& (b_8)_j \delta u_{j-1} + (b_9)_j \delta s_j + (b_{10})_j \delta s_{j-1} = (r_5)_{j-1/2}
\end{aligned} \tag{3.140}$$

$$\begin{aligned}
& (c_1)_j \delta q_j + (c_2)_j \delta q_{j-1} + (c_3)_j \delta f_j + (c_4)_j \delta f_{j-1} + \\
& (c_5)_j \delta t_j + (c_6)_j \delta t_{j-1} + (c_7)_j \delta u_j + (c_8)_j \delta u_{j-1} \\
& + (c_9)_j \delta p_j + (c_{10})_j \delta p_{j-1} = (r_6)_{j-1/2}
\end{aligned} \tag{3.141}$$

where the coefficient for Equation 3.139 is

$$\begin{aligned}
& (a_1)_j = 1 \\
& (a_2)_j = -1 \\
& (a_3)_j = -\frac{1}{2} h_j \beta \lambda \\
& (a_4)_j = (a_3)_j \\
& (a_5)_j = \frac{1}{2} h_j N r \beta \lambda \\
& (a_6)_j = (a_5)_j
\end{aligned} \tag{3.142}$$

meanwhile the coefficient for Equation 3.140 is

$$\begin{aligned}
& (b_1)_j = 1 + \frac{h_j}{2} ((1 + \alpha) f_{j-1/2} + N b q_{j-1/2} + (t_{j-1/2})^2 N t - \alpha f_{j-1/2}^{n-1}) \\
& (b_2)_j = (b_1)_j - 2 \\
& (b_3)_j = \frac{h_j}{2} ((1 + \alpha) t_{j-1/2} + \alpha t_{j-1/2}^{n-1}) \\
& (b_4)_j = (b_3)_j \\
& (b_5)_j = \frac{h_j}{2} (N b t_{j-1/2}) \\
& (b_6)_j = (b_5)_j \\
& (b_7)_j = \frac{h_j}{2} (-\alpha s_{j-1/2} + \alpha s_{j-1/2}^{n-1}) \\
& (b_8)_j = (b_7)_j \\
& (b_9)_j = \frac{h_j}{2} (-\alpha u_{j-1/2} - \alpha u_{j-1/2}^{n-1}) \\
& (b_{10})_j = (b_9)_j
\end{aligned} \tag{3.143}$$

whereas the coefficient for Equation 3.141 is

$$(c_1)_j = 1 + \frac{h_j}{2} Le((1 + \alpha)f_{j-1/2} - \alpha f_{j-1/2}^{n-1})$$

$$(c_2)_j = (c_1)_j - 2$$

$$(c_3)_j = \frac{h_j}{2} Le((1 + \alpha)q_{j-1/2} + \alpha q_{j-1/2}^{n-1})$$

$$(c_4)_j = (c_3)_j$$

$$(c_5)_j = \frac{Nt}{Nb}$$

$$(c_6)_j = -\frac{Nt}{Nb}$$

$$(c_7)_j = \frac{h_j}{2} Le(-p_{j-1/2} + \alpha p_{j-1/2}^{n-1})$$

$$(c_8)_j = (c_7)_j$$

$$(c_9)_j = \frac{h_j}{2} Le(-\alpha u_{j-1/2} - \alpha u_{j-1/2}^{n-1})$$

$$(c_{10})_j = (c_9)_j$$

3.144

Expressions of r_j

$$(r_1)_{j-1/2} = f_{j-1} - f_j + h_j u_{j-1/2}$$

$$(r_2)_{j-1/2} = s_{j-1} - s_j + h_j t_{j-1/2}$$

$$(r_3)_{j-1/2} = p_{j-1} - p_j + h_j q_{j-1/2}$$

$$(r_4)_{j-1/2} = R1_{j-1/2}^{n-1} + f_{j-1} - f_j + h_j \beta + h_j \beta \lambda s_{j-1/2} - h_j N r \beta \lambda p_{j-1/2}$$

$$(r_5)_{j-1/2} = R2_{j-1/2}^{n-1} + t_{j-1} - t_j - h_j [(1 + \alpha)f_{j-1/2} t_{j-1/2} - Nb q_{j-1/2} t_{j-1/2}$$

$$- Nt(t_{j-1/2})^2 + \alpha u_{j-1/2} s_{j-1/2} - \alpha s_{j-1/2}^{n-1} u_{j-1/2}$$

$$+ \alpha u_{j-1/2}^{n-1} s_{j-1/2} + \alpha (f_{j-1/2}^{n-1} t_{j-1/2}) - \alpha t_{j-1/2}^{n-1} f_{j-1/2}]$$

3.145

$$(r_6)_{j-1/2} = R3_{j-1/2}^{n-1} + q_{j-1} - q_j - h_j Le[(1 + \alpha)f_{j-1/2} q_{j-1/2} + \frac{Nt}{Nb}(t_j - t_{j-1})$$

$$\alpha(u_{j-1/2} p_{j-1/2} - \alpha p_{j-1/2}^{n-1} u_{j-1/2} + \alpha u_{j-1/2}^{n-1} p_{j-1/2}$$

$$+ \alpha f_{j-1/2}^{n-1} q_{j-1/2} - \alpha q_{j-1/2}^{n-1} f_{j-1/2}]$$

The system of 3.136 to 3.141 is completed with the boundary conditions 3.117. According to Cebeci and Bradshaw (1988), Equation 3.117 can be satisfied exactly with no iteration. Therefore, to maintain these correct values, we take

$$\delta f_0 = 0, \quad \delta t_0 = 0, \quad \delta p_0 = 0, \quad \delta s_J = 0, \quad \delta p_J = 0. \quad 3.146$$

3.3.4 Block Elimination Technique

The linearised difference equation can be solved by using block elimination techniques (Na, 1979). It is because of the system consists of three diagonal block structure.

Normally, the three diagonal block structure consists of variable or constants. However for Keller-box method, the approach is different because it consists of block matrices. In order to solve the linearised difference Equations 3.136 to 3.141 by using the block elimination technique, the elements of block matrices from Equations 3.142 to 3.144 must be defined by considering three different cases which is when $j = 1$, $j = 2, \dots, j = J - 1$ and $j = J$.

When $j = 1$ the linearised difference Equations 3.136 to 3.141 become

$$\delta f_1 - \delta f_0 - \frac{1}{2}h_1(\delta u_1 + \delta u_0) = (r_1)_{1-(1/2)}$$

$$\delta s_1 - \delta s_0 - \frac{1}{2}h_1(\delta t_1 + \delta t_0) = (r_2)_{1-(1/2)}$$

$$\delta p_1 - \delta p_0 - \frac{1}{2}h_1(\delta q_1 + \delta q_0) = (r_3)_{1-(1/2)}$$

$$(a_1)_1 \delta f_1 + (a_2)_1 \delta f_0 + (a_3)_1 \delta s_1 + (a_4)_1 \delta s_0 \\ + (a_5)_1 \delta p_1 + (a_6)_1 \delta p_0 = (r_4)_{1-(1/2)}$$

$$(b_1)_1 \delta t_1 + (b_2)_1 \delta t_0 + (b_3)_1 \delta f_1 + (b_4)_1 \delta f_0 \\ + (b_5)_1 \delta q_1 + (b_6)_1 \delta q_0 + (b_7)_1 \delta u_1 + (b_8)_1 \delta u_0 \\ + (b_9)_1 \delta s_1 + (b_{10})_1 \delta s_0 = (r_5)_{1-(1/2)}$$

$$\begin{aligned}
& (c_1)_1 \delta q_1 + (c_2)_1 \delta q_0 + (c_3)_1 \delta f_1 + (c_4)_1 \delta f_0 \\
& + (c_5)_1 \delta t_1 + (c_6)_1 \delta t_0 + (c_7)_1 \delta u_1 + (c_8)_1 \delta u_0 \\
& + (c_9)_1 \delta p_1 + (c_{10})_1 \delta p_0 = (r_6)_{1-(1/2)}
\end{aligned}$$

The corresponding matrix form is

$$\begin{aligned}
& \begin{bmatrix} -\frac{h_j}{2} & 0 & 0 & 1 & 0 & 0 \\ 0 & -1 & 0 & 0 & -\frac{h_j}{2} & 0 \\ 0 & 0 & -\frac{h_j}{2} & 0 & 0 & -\frac{h_j}{2} \\ 0 & (a_4) & 0 & (a_1) & 0 & 0 \\ (b_8) & (b_{10}) & (b_6) & (b_3) & (b_1) & (b_5) \\ (c_8) & 0 & (c_2) & (c_3) & (c_5) & (c_1) \end{bmatrix} \begin{bmatrix} \delta u_0 \\ \delta s_0 \\ \delta q_0 \\ \delta f_1 \\ \delta t_1 \\ \delta q_1 \end{bmatrix} \\
& + \begin{bmatrix} -\frac{h_j}{2} & 0 & 0 & 0 & 0 & 0 \\ 0 & 1 & 0 & 0 & 0 & 0 \\ 0 & 0 & 1 & 0 & 0 & 0 \\ 0 & (a_3) & (a_5) & 0 & 0 & 0 \\ (b_7) & (b_9) & 0 & 0 & 0 & 0 \\ (c_7) & 0 & (c_9) & 0 & 0 & 0 \end{bmatrix} \begin{bmatrix} \delta u_1 \\ \delta s_1 \\ \delta p_1 \\ \delta f_2 \\ \delta t_2 \\ \delta q_2 \end{bmatrix} = \begin{bmatrix} (r_1)_{1-1/2} \\ (r_2)_{1-1/2} \\ (r_3)_{1-1/2} \\ (r_4)_{1-1/2} \\ (r_5)_{1-1/2} \\ (r_6)_{1-1/2} \end{bmatrix}
\end{aligned}$$

For the value of $j = 1$, we have $[A_1][\delta_1] + [C_1][\delta_2] = [r_1]$.

When $j = 2, \dots, j = J$, the linearised difference equations become

$$\delta f_{j-1} - \delta f_{j-2} - \frac{1}{2} h_{j-1} (\delta u_{j-1} + \delta u_{j-2}) = (r_1)_{(j-1)-1/2}$$

$$\delta s_{j-1} - \delta s_{j-2} - \frac{1}{2} h_{j-1} (\delta t_{j-1} + \delta t_{j-2}) = (r_2)_{(j-1)-1/2}$$

$$\delta p_{j-1} - \delta p_{j-2} - \frac{1}{2} h_{j-1} (\delta q_{j-1} + \delta q_{j-2}) = (r_3)_{(j-1)-1/2}$$

$$\begin{aligned}
& (a_1)_{j-1} \delta f_{j-1} + (a_2)_{j-1} \delta s_{j-2} + (a_3)_{j-1} \delta f_{j-1} + (a_4)_{j-1} \delta s_{j-2} \\
& + (a_5)_{j-1} \delta p_{j-1} + (a_6)_{j-1} \delta p_{j-2} = (r_4)_{(j-1)-1/2}
\end{aligned}$$

$$\begin{aligned}
& (b_1)_{J-1} \delta t_{J-1} + (b_2)_{J-1} \delta t_{J-2} + (b_3)_{J-1} \delta f_{J-1} + (b_4)_{J-1} \delta f_{J-2} + (b_5)_{J-1} \delta q_{J-1} \\
& + (b_6)_{J-1} \delta q_{J-2} + (b_7)_{J-1} \delta u_{J-1} + (b_8)_{J-1} \delta u_{J-2} \\
& + (b_9)_{J-1} \delta s_{J-1} + (b_{10})_{J-1} \delta s_{J-2} = (r_5)_{(J-1)-1/2}
\end{aligned}$$

$$\begin{aligned}
& (c_1)_{J-1} \delta q_{J-1} + (c_2)_{J-1} \delta q_{J-2} + (c_3)_{J-1} \delta f_{J-1} + (c_4)_{J-1} \delta f_{J-2} + (c_5)_{J-1} \delta t_{J-1} \\
& + (c_6)_{J-1} \delta t_{J-2} + (c_7)_{J-1} \delta u_{J-1} + (c_8)_{J-1} \delta u_{J-2} \\
& + (c_9)_{J-1} \delta p_{J-1} + (c_{10})_{J-1} \delta p_{J-2} = (r_6)_{(J-1)-1/2}
\end{aligned}$$

The corresponding matrix form is

$$\begin{aligned}
& \begin{bmatrix} 0 & 0 & 0 & -1 & 0 & 0 \\ 0 & 0 & 0 & 0 & -\frac{h_j}{2} & 0 \\ 0 & 0 & 0 & 0 & 0 & -\frac{h_j}{2} \\ 0 & 0 & 0 & (a_2) & 0 & 0 \\ 0 & 0 & 0 & (b_4) & (b_2) & (b_6) \\ 0 & 0 & 0 & (c_4) & (c_6) & (c_2) \end{bmatrix} \begin{bmatrix} \delta u_{J-3} \\ \delta s_{J-3} \\ \delta p_{J-3} \\ \delta f_{J-2} \\ \delta t_{J-2} \\ \delta q_{J-2} \end{bmatrix} \\
& + \begin{bmatrix} -\frac{h_j}{2} & 0 & 0 & 1 & 0 & 0 \\ 0 & -1 & 0 & 0 & -\frac{h_j}{2} & 0 \\ 0 & 0 & -1 & 0 & 0 & -\frac{h_j}{2} \\ 0 & (a_4) & (a_6) & (a_1) & 0 & 0 \\ (b_8) & (b_{10}) & 0 & (b_3) & (b_1) & (b_5) \\ (c_8) & 0 & (c_{10}) & (c_3) & (c_5) & (c_1) \end{bmatrix} \begin{bmatrix} \delta u_{J-2} \\ \delta s_{J-2} \\ \delta p_{J-2} \\ \delta f_{J-1} \\ \delta t_{J-1} \\ \delta q_{J-1} \end{bmatrix} \\
& + \begin{bmatrix} -\frac{h_j}{2} & 0 & 0 & 0 & 0 & 0 \\ 0 & 1 & 0 & 0 & 0 & 0 \\ 0 & 0 & 1 & 0 & 0 & 0 \\ 0 & (a_3) & (a_5) & 0 & 0 & 0 \\ (b_7) & (b_9) & 0 & 0 & 0 & 0 \\ (c_7) & 0 & (c_9) & 0 & 0 & 0 \end{bmatrix} \begin{bmatrix} \delta u_{J-1} \\ \delta s_{J-1} \\ \delta p_{J-1} \\ \delta f_J \\ \delta t_J \\ \delta q_J \end{bmatrix} = \begin{bmatrix} (r_1)_{(J-1)-1/2} \\ (r_2)_{(J-1)-1/2} \\ (r_3)_{(J-1)-1/2} \\ (r_4)_{(J-1)-1/2} \\ (r_5)_{(J-1)-1/2} \\ (r_6)_{(J-1)-1/2} \end{bmatrix}
\end{aligned}$$

Hence for $j = 2, \dots, j = J$, we can written as

$$[B_j][\delta_{j-1}] + [A_j][\delta_{j-1}] + [C_j][\delta_{j+1}] = [r_j]$$

Finally when $j = J$, the linear system becomes

$$\delta f_J - \delta f_{J-1} - \frac{1}{2}h_J(\delta u_J + \delta u_{J-1}) = (r_1)_{J-1/2}$$

$$\delta s_J - \delta s_{J-1} - \frac{1}{2}h_J(\delta t_J + \delta t_{J-1}) = (r_2)_{J-1/2}$$

$$\delta p_J - \delta p_{J-1} - \frac{1}{2}h_J(\delta q_J + \delta q_{J-1}) = (r_3)_{J-1/2}$$

$$(a_1)_J \delta f_J + (a_2)_J \delta f_{J-1} + (a_3)_J \delta s_J + (a_4)_J \delta s_{J-1} \\ + (a_5)_J \delta q_J + (a_6)_J \delta q_{J-1} = (r_4)_{J-1/2}$$

$$(b_1)_J \delta t_J + (b_2)_J \delta t_{J-1} + (b_3)_J \delta f_J + (b_4)_J \delta f_{J-1} + (b_5)_J \delta q_J \\ + (b_6)_J \delta q_{J-1} + (b_7)_J \delta u_J + (b_8)_J \delta u_{J-1} \\ + (b_9)_J \delta s_J + (b_{10})_J \delta s_{J-1} = (r_5)_{J-1/2}$$

$$(c_1)_J \delta q_J + (c_2)_J \delta q_{J-1} + (c_3)_J \delta f_J + (c_4)_J \delta f_{J-1} + (c_5)_J \delta t_J \\ + (c_6)_J \delta t_{J-1} + (c_7)_J \delta u_J + (c_8)_J \delta u_{J-1} \\ + (c_9)_J \delta p_J + (c_{10})_J \delta p_{J-1} = (r_6)_{J-1/2}$$

Subjected to the boundary conditions Equation 3.117, the suitable matrices can be form as

$$\begin{bmatrix} 0 & 0 & 0 & -1 & 0 & 0 \\ 0 & 0 & 0 & 0 & -\frac{h_j}{2} & 0 \\ 0 & 0 & 0 & 0 & 0 & -\frac{h_j}{2} \\ 0 & 0 & 0 & (a_2) & 0 & 0 \\ 0 & 0 & 0 & (b_4) & (b_2) & (b_6) \\ 0 & 0 & 0 & (c_4) & (c_6) & (c_2) \end{bmatrix} \begin{bmatrix} \delta u_{J-2} \\ \delta s_{J-2} \\ \delta p_{J-2} \\ \delta f_{J-1} \\ \delta t_{J-1} \\ \delta q_{J-1} \end{bmatrix}$$

$$+ \begin{bmatrix} -\frac{h_j}{2} & 0 & 0 & 1 & 0 & 0 \\ 0 & -1 & 0 & 0 & -\frac{h_j}{2} & 0 \\ 0 & 0 & -1 & 0 & 0 & -\frac{h_j}{2} \\ 0 & (a_4) & (a_6) & (a_1) & 0 & 0 \\ (b_8) & (b_{10}) & 0 & (b_3) & (b_1) & (b_5) \\ (c_8) & 0 & (c_{10}) & (c_3) & (c_5) & (c_1) \end{bmatrix} \begin{bmatrix} \delta u_{J-1} \\ \delta s_{J-1} \\ \delta p_{J-1} \\ \delta f_J \\ \delta t_J \\ \delta q_J \end{bmatrix} = \begin{bmatrix} (r_1)_{J-1/2} \\ (r_2)_{J-1/2} \\ (r_3)_{J-1/2} \\ (r_4)_{J-1/2} \\ (r_5)_{J-1/2} \\ (r_6)_{J-1/2} \end{bmatrix}$$

Hence, for $j = J$ it can be written as

$$[B_j][\delta_{j-1}] + [A_j][\delta_j] = [r_j]$$

Therefore

$$\begin{aligned} j = 1 : [A_1][\delta_1] + [C_1][\delta_2] &= [r_1] \\ j = 2 : [B_2][\delta_1] + [A_2][\delta_2] + [C_2][\delta_3] &= [r_2] \\ j = 3 : [B_3][\delta_2] + [A_3][\delta_3] + [C_3][\delta_4] &= [r_3] \\ &\vdots \\ j = J-1 : [B_{J-1}][\delta_{J-2}] + [A_{J-1}][\delta_{J-1}] + [C_{J-1}][\delta_J] &= [r_{J-1}] \\ j = J : [B_J][\delta_{J-1}] + [A_J][\delta_J] &= [r_J] \end{aligned}$$

Generally in matrix form, the above system can be simplified as

$$\mathbf{A}\delta = \mathbf{r}$$

3.147

with

$$\mathbf{A} = \begin{bmatrix} [A_1] & [C_1] & & & & \\ [B_2] & [A_2] & [C_2] & & & \\ & & & \ddots & & \\ & & & & \ddots & \\ & & & & & [B_{J-1}] & [A_{J-1}] & [C_{J-1}] \\ & & & & & & [B_j] & [A_j] \end{bmatrix}, \boldsymbol{\delta} = \begin{bmatrix} [\delta_1] \\ [\delta_2] \\ \vdots \\ \vdots \\ [\delta_{J-1}] \\ [\delta_J] \end{bmatrix}$$

and

$$\mathbf{r} = \begin{bmatrix} [r_1] \\ [r_2] \\ \vdots \\ \vdots \\ [r_{J-1}] \\ [r_J] \end{bmatrix}$$

The elements of the matrices are

$$[A_1] = \begin{bmatrix} -\frac{h_j}{2} & 0 & 0 & 1 & 0 & 0 \\ 0 & -1 & 0 & 0 & -\frac{h_j}{2} & 0 \\ 0 & 0 & -\frac{h_j}{2} & 0 & 0 & -\frac{h_j}{2} \\ 0 & (a_4) & 0 & (a_1) & 0 & 0 \\ (b_8) & (b_{10}) & (b_6) & (b_3) & (b_1) & (b_5) \\ (c_8) & 0 & (c_2) & (c_3) & (c_5) & (c_1) \end{bmatrix} \quad 3.148$$

$$[A_j] = \begin{bmatrix} -\frac{h_j}{2} & 0 & 0 & 1 & 0 & 0 \\ 0 & -1 & 0 & 0 & -\frac{h_j}{2} & 0 \\ 0 & 0 & -1 & 0 & 0 & -\frac{h_j}{2} \\ 0 & (a_4) & (a_6) & (a_1) & 0 & 0 \\ (b_8) & (b_{10}) & 0 & (b_3) & (b_1) & (b_5) \\ (c_8) & 0 & (c_{10}) & (c_3) & (c_5) & (c_1) \end{bmatrix} \quad 3.149$$

$$[\mathbf{B}_j] = \begin{bmatrix} 0 & 0 & 0 & -1 & 0 & 0 \\ 0 & 0 & 0 & 0 & -\frac{h_j}{2} & 0 \\ 0 & 0 & 0 & 0 & 0 & -\frac{h_j}{2} \\ 0 & 0 & 0 & (a_2) & 0 & 0 \\ 0 & 0 & 0 & (b_4) & (b_2) & (b_6) \\ 0 & 0 & 0 & (c_4) & (c_6) & (c_2) \end{bmatrix} \quad 3.150$$

$$[\mathbf{C}_j] = \begin{bmatrix} -\frac{h_j}{2} & 0 & 0 & 0 & 0 & 0 \\ 0 & 1 & 0 & 0 & 0 & 0 \\ 0 & 0 & 1 & 0 & 0 & 0 \\ 0 & (a_3) & (a_5) & 0 & 0 & 0 \\ (b_7) & (b_9) & 0 & 0 & 0 & 0 \\ (c_7) & 0 & (c_9) & 0 & 0 & 0 \end{bmatrix} \quad 3.151$$

$$[\delta_1] = \begin{bmatrix} \delta u_0 \\ \delta s_0 \\ \delta q_0 \\ \delta f_1 \\ \delta t_1 \\ \delta q_1 \end{bmatrix}, \quad [\delta_j] = \begin{bmatrix} \delta u_{j-1} \\ \delta s_{j-1} \\ \delta p_{j-1} \\ \delta f_j \\ \delta t_j \\ \delta q_j \end{bmatrix} \quad 3.152$$

and

$$[\mathbf{r}_j] = \begin{bmatrix} (r_1)_{j-(1/2)} \\ (r_2)_{j-(1/2)} \\ (r_3)_{j-(1/2)} \\ (r_4)_{j-(1/2)} \\ (r_5)_{j-(1/2)} \\ (r_6)_{j-(1/2)} \end{bmatrix} \quad 3.153$$

The coefficient matrix \mathbf{A} is known as tridiagonal matrix due to the fact that all elements of \mathbf{A} are zero except those on the three main diagonals. To solve Equation 3.147, according to the block elimination method as described by Na (1979), we assume that \mathbf{A} is nonsingular and

we seek a factorization of the form

$$\mathbf{A} = \mathbf{LU}$$

3.154

where

$$\mathbf{L} = \begin{bmatrix} [\alpha_1] & & & & & \\ [B_2] & [\alpha_2] & & & & \\ [B_3] & & [\alpha_3] & & & \\ & & & \ddots & & \\ & & & & [B_{J-1}] & [\alpha_{J-1}] \\ & & & & [B_j] & [\alpha_j] \end{bmatrix}$$

and

$$\mathbf{U} = \begin{bmatrix} [I] & [\Gamma_1] & & & & \\ & [I] & [\Gamma_2] & & & \\ & & [I] & [\Gamma_3] & & \\ & & & \ddots & & \\ & & & & [I] & [\Gamma_{J-1}] \\ & & & & & [I] \end{bmatrix}$$

$[I]$ is the identity matrix of order 6 and $[\alpha_i]$ and $[\Gamma_i]$ are 6×6 matrices whose elements are determined by the following equations:

$$[\alpha_1] = [A_1], \quad [A_1][\Gamma_1] = [C_1] \quad 3.155$$

and

$$\begin{aligned} [\alpha_j] &= [A_j] - [B_j][\Gamma_{j-1}], \quad j = 2, 3, \dots, J \\ [\alpha_j][\Gamma_j] &= [C_j], \quad j = 2, 3, \dots, J-1 \end{aligned} \quad 3.156$$

By substituting into Equation 3.147, we get

$$\mathbf{LU}\delta = \mathbf{r}$$

3.157

If we define

$$\mathbf{U}\delta = \mathbf{W} \quad 3.158$$

Hence, equation becomes

$$\mathbf{LW} = \mathbf{r} \quad 3.159$$

where

$$\mathbf{r} = \begin{bmatrix} [W_1] \\ [W_2] \\ \vdots \\ [W_{J-1}] \\ [W_J] \end{bmatrix}$$

and $[W_j]$ are 6×1 column matrices. The elements \mathbf{W} can be solved from Equation 3.159.

$$[\alpha_1][W_1] = [r_1] \quad 3.160$$

$$[\alpha_j][W_j] = [r_j] - [B_j][W_{j-1}], \quad j = 2 \leq j \leq J \quad 3.161$$

The step in which $[W_j]$, $[\alpha_j]$ and $[\Gamma_j]$ are calculated is usually referred to as the forward sweep. Once the elements of \mathbf{W} are found, Equation 3.158 then gives the solution in the so-called backward sweep, in which the elements are obtained by the following relations:

$$[\delta_j] = [W_j] \quad 3.162$$

$$[\delta_j] = [W_j] - [\Gamma_j][\delta_{j+1}], \quad 1 \leq j \leq J-1 \quad 3.163$$

Since the elements of δ are found, Equations 3.136 to 3.141 then can be used to find $(i+1)$ iterates for Equation 3.128.

These calculations are repeated until some convergence criterion is satisfied. In the laminar boundary layer calculations, the wall shear stress parameter is commonly used as convergence criterion (Cebeci and Bradshaw, 1988). This is probably because in boundary layer calculations, the greatest errors usually occur in the wall shear stress parameter.

Therefore, the wall shear stress parameter is used as convergence criterion in this study. Calculations are stopped when

$$|\delta v_0^{(i)}| < \varepsilon_1 \quad 3.164$$

where ε_1 is a small prescribed value. The convergence criterion required that the maximum absolute error between two successive iterations be $\varepsilon_1 = 10^{-5}$, which gives the precise values until four decimal places, as suggested by Cebeci and Bradshaw (1988).

3.4 Initial Conditions

The numerical methodology was coded in MATLAB. To verify its validity, a comparison with selective data from the published literature was conducted. In the numerical calculation, the suitable step size and boundary layer thickness should be determined. Accordingly, appropriate values must be defined so that the numerical results for the quantities discussed are not affected by boundary layer thickness, y_∞ and step size of boundary layer, Δy . The computation can be initiated by determining the value concerning the velocity and temperature profile. The non suitable values of the boundary layer thickness which are too large or small may not fulfil the boundary conditions. In this study, it is found that the boundary layer thickness y_∞ from 1 to 4 is considered suitable to provide accurate numerical results depending on the problem involved.

Usually, the step size is sufficient to provide accurate numerical results (Nazar, 2003). However, the appropriate value of the step size must not affect the converged results appreciably. For example, the value of the skin friction coefficient must be free from the value of the step size chosen. Indeed, values too small may cause increased waiting time in calculation while a large values of cause minimal time in the calculation, but may produce inaccurate results (Ishak et al., 2009).

The boundary layer thickness y_∞ is almost constant for the case of the laminar boundary layer flows. Once the proper value of y_∞ has been obtained, a reasonable choice of net spacing should be determined. Usually a step size $\Delta y = 0.01$ to 0.04 is adequate to provide an accurate numerical result (Nazar, 2003). Meanwhile, the step size Δx can be arbitrary as it does not affect the converged result appreciably.

3.5 Initial Profile

The initial profiles are necessary for performing the numerical computations in MATLAB. To proceed with the numerical computation, it is necessary to make an initial guess or assumption for the function and in the boundary layer flow. The initial guess is undertaken by adopting a trial and error approach. There are several possibilities in the selection of initial guess, but it must obey and satisfy the boundary conditions stated 3.92.

The initial guess and assumption can commence with velocity, temperature distribution and concentration distribution. It is because u, s and p have both boundary conditions at $y = 0$ and y_∞ . When the initial guess of u, s and p have been defined, the other function f, v, t and q can be obtained using differentiation and integration.

$$u = \frac{df}{dy} = \frac{y \sin x}{y_\infty x} \left(\frac{3}{2} - \frac{1}{2} \left(\frac{y}{y_\infty} \right)^2 \right) \quad 3.165$$

$$s = \theta = y_\infty \left(\frac{y}{y_\infty} \right)^2 - y \quad 3.166$$

and

$$p = \phi = 1 - \frac{y}{y_\infty} \quad 3.167$$

respectively. Integrate Equation 3.165 with respect to y produce

$$f = \int_{y_\infty}^0 u dy = \frac{1}{4} y_\infty \frac{\sin x}{x} \left(\frac{y}{y_\infty} \right)^2 \left(3 - \frac{1}{2} \left(\frac{y}{y_\infty} \right)^2 \right) \quad 3.168$$

On the other hand, differentiate Equations 3.165 and 3.167 with respect to y produce

$$v = \frac{du}{dy} = \frac{3 \sin x}{2 y_\infty x} \left(1 - \left(\frac{y}{y_\infty} \right)^2 \right) \quad 3.169$$

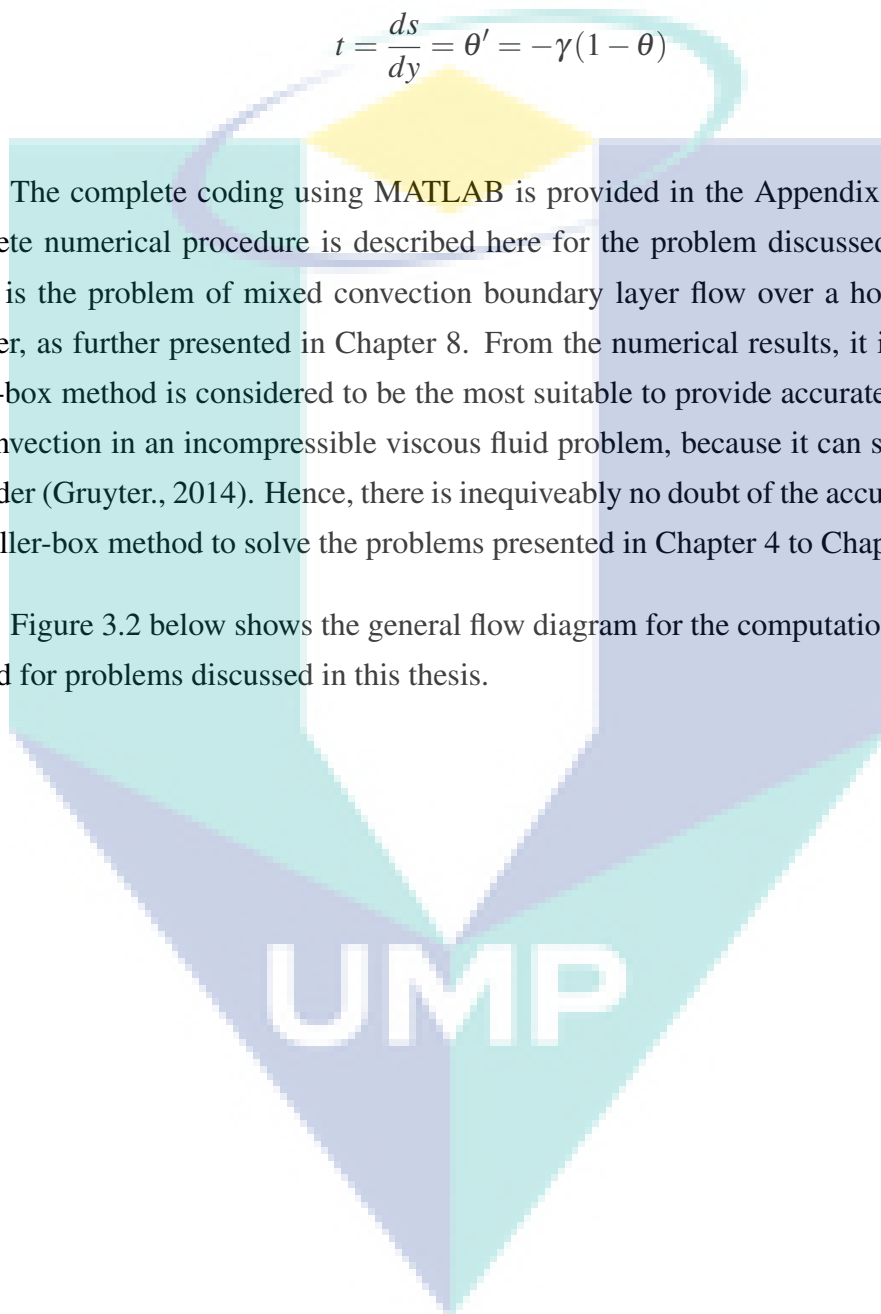
$$q = \frac{dp}{dy} = \frac{-1}{y_\infty} \quad 3.170$$

and for case s' , following the convective boundary condition

$$t = \frac{ds}{dy} = \theta' = -\gamma(1 - \theta) \quad 3.171$$

The complete coding using MATLAB is provided in the Appendix B. Notably, the complete numerical procedure is described here for the problem discussed in this chapter which is the problem of mixed convection boundary layer flow over a horizontal circular cylinder, as further presented in Chapter 8. From the numerical results, it is found that the Keller-box method is considered to be the most suitable to provide accurate results to solve the convection in an incompressible viscous fluid problem, because it can solve problem of any order (Gruyter., 2014). Hence, there is unequivocally no doubt of the accuracy in applying the Keller-box method to solve the problems presented in Chapter 4 to Chapter 8

Figure 3.2 below shows the general flow diagram for the computations of Keller-box method for problems discussed in this thesis.



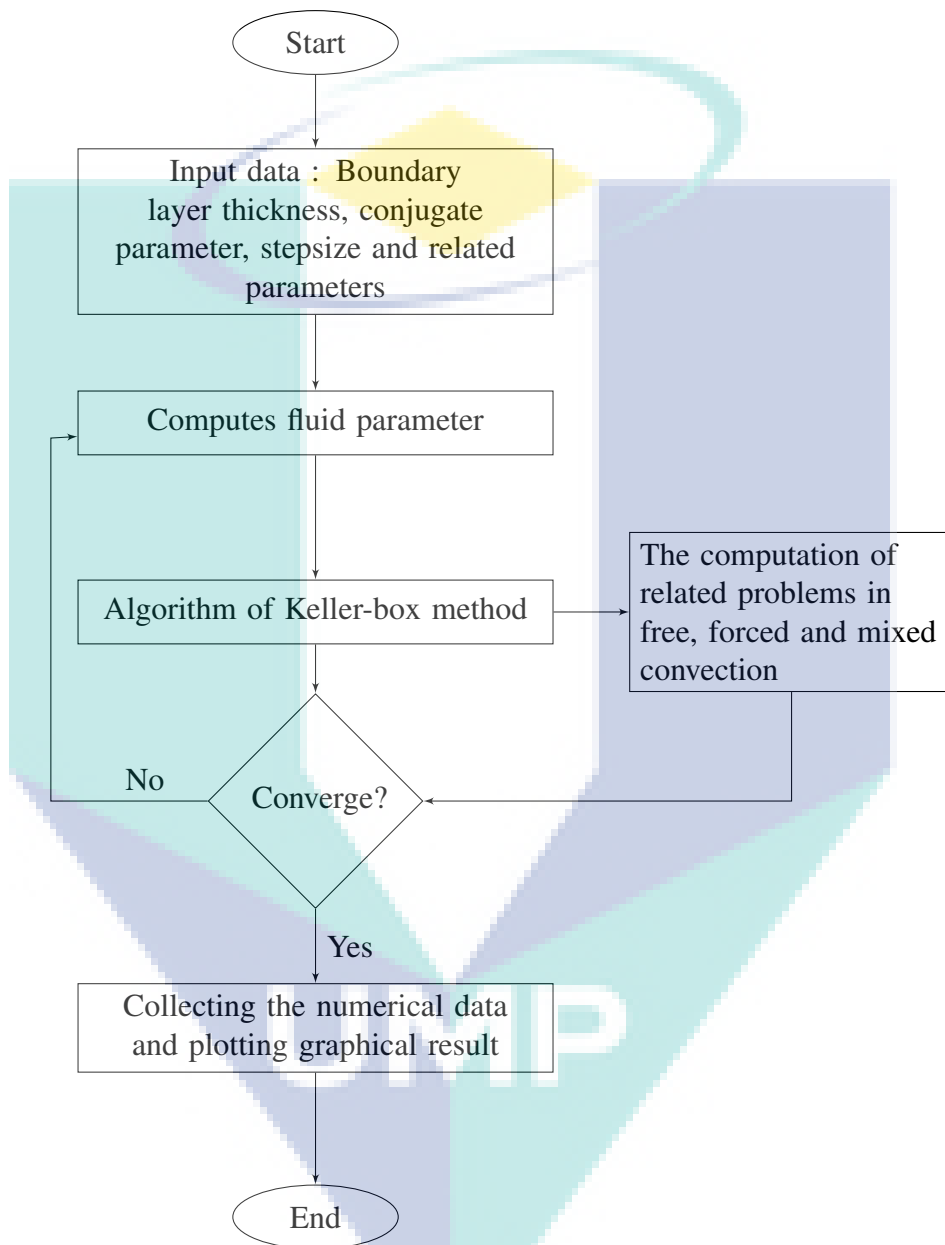


Figure 3.2. Flow diagram for Keller-box method

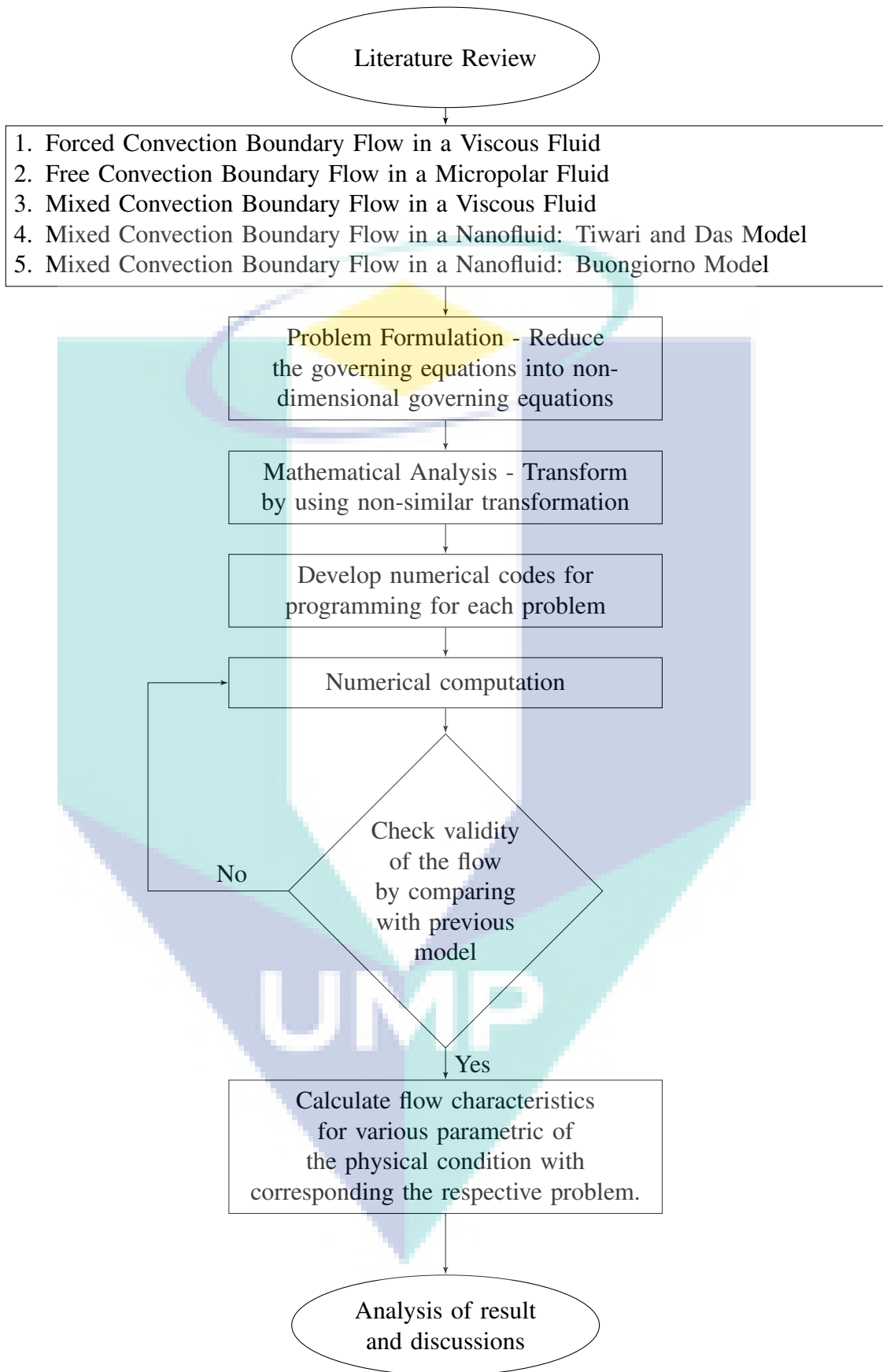


Figure 3.3. Flow chart of the solution procedure

CHAPTER 4

FORCED CONVECTION BOUNDARY LAYER FLOW OVER A HORIZONTAL CIRCULAR CYLINDER IN A VISCOUS FLUID

4.1 Introduction

Forced convection as been described in first chapter is a mechanism in which the motion of the fluid comes from an external sources such as fan, pump, blower and so forth. Applications for forced convection include systems that operate at extremely high temperatures for example transporting molten metal or liquefied plastic. Normally, forced convection is used to increase the rate of exchange. In any forced convection situation, free convection effects are also present under the presence of gravitational body forces (Nazar, 2003). In this chapter, the problem of forced convection over a horizontal circular cylinder are demonstrated.

Forced convection over a horizontal circular cylinder is a classical problem in boundary layer theory and heat transfer. The study of this problem have gained considerable attention due to its application in physical, geophysical and industrial fields. However, while often applied in applications, the study of forced convection appear less as compared to the study of free and mixed convection (Sumaily et al., 2012).

In the next section, we provides a succinct description of the governing equations and the boundary conditions for the forced convection over horizontal circular cylinder. This is followed by a presentation and discussion of the numerical results in Section 4.3, which include the variations of the skin friction coefficient and the heat transfer coefficient with the effects of the Pr number, conjugate and mixed parameter on the flow and heat transfer. Finally, Section 4.4 provides the concluding remarks about the finding of this problem.

4.2 Mathematical Formulation

The problem under consideration in this study is regarding the steadily forced convection boundary layer flow and heat transfer of a viscous and an incompressible fluid of free stream velocity U_∞ and ambient temperature T_∞ moving over a horizontal circular cylinder. The bottom of the cylinder is heated by convection from the hot fluid at temperature T_f which yields a heat transfer coefficient h_f . The physical model and coordinate system of this problem is shown in Figure 4.1.

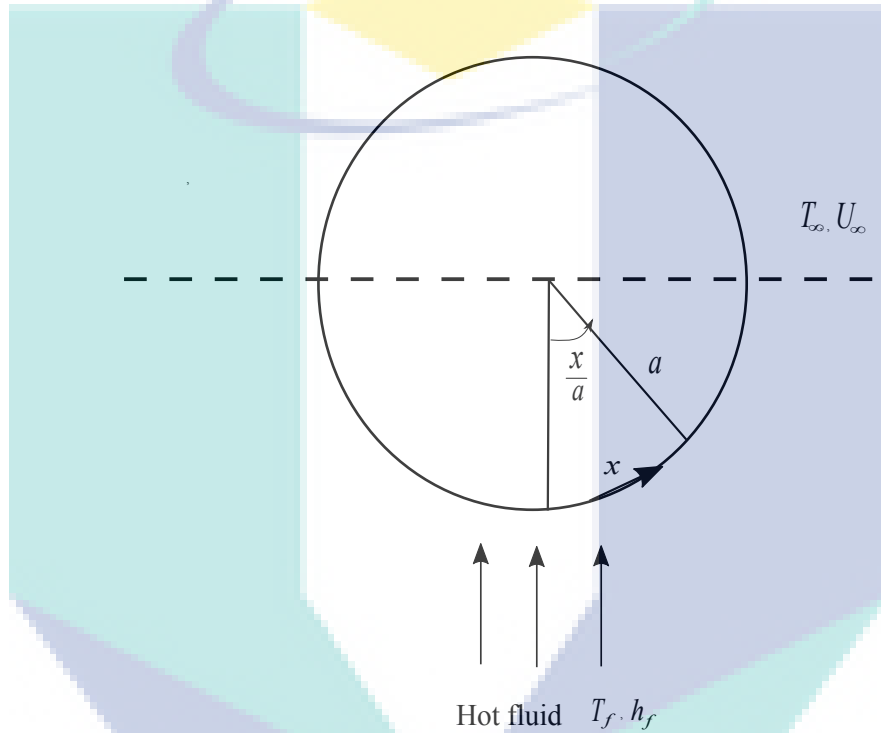


Figure 4.1. Physical model and coordinate system

The assumption has been made that the buoyancy forces and the viscous dissipation effects are neglected. The continuity equation has been given in Equation 3.67, whereas momentum and energy equations describing the flow can be written as (Salleh et al., 2011),

$$\bar{u} \frac{\partial \bar{u}}{\partial \bar{x}} + \bar{v} \frac{\partial \bar{u}}{\partial \bar{y}} = \bar{u}_e \frac{d\bar{u}_e}{d\bar{x}} + \nu \frac{\partial^2 \bar{u}}{\partial \bar{y}^2} \quad 4.1$$

$$\bar{u} \frac{\partial \bar{T}}{\partial \bar{x}} + \bar{v} \frac{\partial \bar{T}}{\partial \bar{y}} = \alpha \frac{\partial^2 \bar{T}}{\partial \bar{y}^2} \quad 4.2$$

subject to the boundary conditions

$$\begin{aligned} \bar{u} = \bar{v} = 0, \quad -k \frac{\partial \bar{T}}{\partial \bar{y}} = h_f (T_f - \bar{T}) \quad \text{at } \bar{y} = 0 \\ \bar{u} \rightarrow \bar{u}_e, \quad \bar{T} \rightarrow T_\infty \quad \text{as } \bar{y} \rightarrow \infty \end{aligned} \quad 4.3$$

where $\bar{u}_e = 2U_\infty \sin(\bar{x}/a)$, (\bar{u}, \bar{v}) are the velocity components along the (\bar{x}, \bar{y}) axes, \bar{T} is the local temperature, T_f is the temperature of the hot fluid, ν is the kinematic viscosity, k is the thermal conductivity, α is the thermal diffusivity and h_f is the heat transfer parameter for convective boundary condition. By introducing the following non-dimensional variables:

$$\begin{aligned} x = \bar{x}/a, \quad y = Re^{1/2}(\bar{y}/a), \quad u = \bar{u}/U_\infty, \quad v = Re^{1/2}(\bar{v}/U_\infty) \\ u_e = \bar{u}_e/U_\infty, \quad \theta = \frac{\bar{T} - T_\infty}{T_f - T_\infty} \end{aligned} \quad 4.4$$

where $Re = U_\infty a / \nu$ is the Reynold number. Therefore, substituting Equation 4.4 into Equations 4.1 to 4.3, the following differential equations are found

$$u \frac{\partial u}{\partial x} + v \frac{\partial u}{\partial y} = u_e \frac{\partial u_e}{\partial x} + \frac{\partial^2 u}{\partial y^2} \quad 4.5$$

$$u \frac{\partial \theta}{\partial x} + v \frac{\partial \theta}{\partial y} = \frac{1}{Pr} \frac{\partial^2 \theta}{\partial y^2} \quad 4.6$$

Boundary conditions become

$$\begin{aligned} u = v = 0, \quad \frac{\partial \theta}{\partial y} = -\gamma(1 - \theta) \quad \text{at } y = 0 \\ u \rightarrow u_e, \quad \theta \rightarrow 0 \quad \text{as } y \rightarrow \infty \end{aligned} \quad 4.7$$

where $u_e = 2 \sin x$, Pr is the Prandtl number and γ is the convective parameter defined as follow

$$Pr = \frac{\nu}{\alpha}, \quad \gamma = \frac{h_f}{k} a Re^{-1/2} \quad 4.8$$

To solve Equations 4.5 to 4.6 subjected to the boundary conditions 4.7, and by introducing ψ as

$$\psi = xf(x,y), \quad \theta = \theta(x,y) \quad 4.9$$

where ψ is the stream function which is defined as $u = \partial\psi/\partial y$ and $v = -\partial\psi/\partial x$. Using variables 4.9, Equations 4.5 and 4.6 then become

$$\frac{\partial^3 f}{\partial y^3} + f \frac{\partial^2 f}{\partial y^2} - \left(\frac{\partial f}{\partial y} \right)^2 + 4 \frac{\sin x \cos x}{x} = x \left(\frac{\partial f}{\partial y} \frac{\partial^2 f}{\partial x \partial y} - \frac{\partial f}{\partial x} \frac{\partial^2 f}{\partial y^2} \right) \quad 4.10$$

$$\frac{1}{Pr} \frac{\partial^2 \theta}{\partial y^2} + f \frac{\partial \theta}{\partial y} = x \left(\frac{\partial f}{\partial y} \frac{\partial \theta}{\partial x} - \frac{\partial f}{\partial x} \frac{\partial \theta}{\partial y} \right) \quad 4.11$$

while the boundary conditions become

$$\begin{aligned} f = \frac{\partial f}{\partial y} = 0, \quad \frac{\partial \theta}{\partial y} = -\gamma(1 - \theta) \quad \text{at } y = 0 \\ \frac{\partial f}{\partial y} \rightarrow 2 \frac{\sin x}{x}, \quad \theta \rightarrow 0 \quad \text{as } y \rightarrow \infty \end{aligned} \quad 4.12$$

Near the lower stagnation point of the cylinder $x \approx 0$, Equations 4.10 and 4.11 reduce to the following ordinary differential equations

$$f''' + ff'' - (f')^2 + 4 = 0 \quad 4.13$$

$$\frac{1}{Pr} \theta'' + f\theta' = 0 \quad 4.14$$

where the prime denotes differentiation with respect to y and the boundary conditions are

$$\begin{aligned} f(0) = f'(0) = 0, \quad \theta'(0) = -\gamma(1 - \theta(0)) \quad \text{at } y = 0 \\ f'(y) \rightarrow 2, \quad \theta(y) \rightarrow 0 \quad \text{as } y \rightarrow \infty \end{aligned} \quad 4.15$$

In practical applications, the physical quantities of interest are the skin friction coefficient, C_f and the heat transfer coefficient $Q_w(x)$ which can be written in non-dimensional form as

$$Re^{1/2}C_f = x \frac{\partial^2 f}{\partial y^2}, \quad Re^{1/2}Q_w = -\frac{\partial \theta}{\partial y} = -\gamma(1 - \theta) \quad 4.16$$

where

$$\tau_w = \mu \frac{\partial \bar{u}}{\partial \bar{y}}, \quad q_w = -k \frac{\partial \bar{T}}{\partial \bar{y}} \quad 4.17$$

$C_f = \tau_w / (\rho U_\infty^2)$ is the skin friction coefficient with $Q_w = a q_w / (k(T_f - T))$ and ρ is the fluid density. Detailed formulation can be accessed in Appendix C.

4.3 Results and Discussion

The problem is given by Equations 4.10 and 4.11 with boundary conditions 4.12 were solved numerically using the Keller-box method for the case of the convective boundary conditions. Three parameters were considered, namely the Prandtl number Pr , the convective parameter γ and the coordinate along the surface of the cylinder, x . The solutions are heavily reliant upon these parameters. In the numerical solution, the starting point was a consideration of the solution at the lower stagnation point of the cylinder i.e. $x \approx 0$ and proceeded round the cylinder up to the separation point denoted as x_s . Therefore, the solution for the local skin friction coefficient and heat transfer coefficient lies between $0 < x < x_s$. Outside this value, the solution became unstable and encountered singularity in the numerical solutions. Therefore from the numerical solution, estimation of the separation of the cylinder occurred at the point, $x_s = 1.85$ (104.50°) which is in good agreement with the results reported by Zukauskas and Ziugzda (1985), Khan et al. (2004) and Kaprawi and Santoso (2012).

Table 4.1 provides the values of the reduced skin friction coefficient $\frac{\partial^2 f}{\partial y^2}(x, 0)$ at some position x when $\gamma = 1.0$. To validate the implementation, results from this code were compared to previously published numerical results at the lower stagnation points $x \approx 0$ given by Salleh et al. (2009) and Ahmad et al. (2005). These researchers solved the similar problem under discussion, but they used different types of thermal heating process. Ahmad et al. (2005) investigate the case when constant heat flux is applied, whereas Salleh et al. (2009) using Newtonian heating. Both investigators used Keller-box method to solve the

problems. Eventhough the thermal boundary conditions are different, the momentum equation remained the same. This is due to the fact that decoupled boundary layer equation where the momentum and energy equations are independent from one and another. Change values in the thermal condition are only reflect to energy equations. Therefore, there is only a unique value the reduced skin friction $\frac{\partial^2 f}{\partial y^2}(x, 0) = 3.4866$ for all cases of CHF, NH and CBC. The comparisons between these results are found to be in a good agreement.

Table 4.1. Values of the reduced skin friction coefficient at some positions x when $\gamma = 1.0$

x	Present Result		Ahmad et al. (2005)	Salleh et al. (2009)
	x°	$\frac{\partial^2 f}{\partial y^2}(x, 0)$	$f''(0)$	$f''(0)$
0.0	0	3.4866	3.4919	3.4864
0.2	11.46	3.4302	-	-
0.4	22.92	3.2692	-	-
0.6	34.38	3.0117	-	-
0.8	45.84	2.6710	-	-
1.0	57.30	2.2637	-	-
1.2	68.75	2.8085	-	-
1.4	80.21	1.3239	-	-
1.6	91.67	0.8218	-	-
1.8	101.13	0.2688	-	-

Table 4.2. Values of the heat transfer coefficient Q_w when $Pr = 1.0$

x	γ			
	0.05	0.10	0.20	0.30
0.0	0.0471	0.0889	0.1549	0.1786
0.2	0.0510	0.1049	0.2257	0.3702
0.4	0.0517	0.1079	0.2390	0.4037
0.6	0.0520	0.1092	0.2448	0.4185
0.8	0.0522	0.1098	0.2474	0.4253
1.0	0.0522	0.1099	0.2481	0.4272
1.2	0.0522	0.1097	0.2471	0.4249
1.4	0.0522	0.1091	0.2444	0.4183
1.6	0.0517	0.1078	0.2391	0.4052
1.8	0.0509	0.1044	0.2249	0.3710

The values of the local heat transfer coefficient, Q_w for various values of the convective parameter are presented in Table 4.2, starting with $\gamma = 0.05$ up to $\gamma = 0.30$. It can be observed from these tables that the values of Q_w increase to the maximum value

when it reaches a certain point of x . After the maximum points, the values of Q_w start to decrease at the rear part of the cylinder.

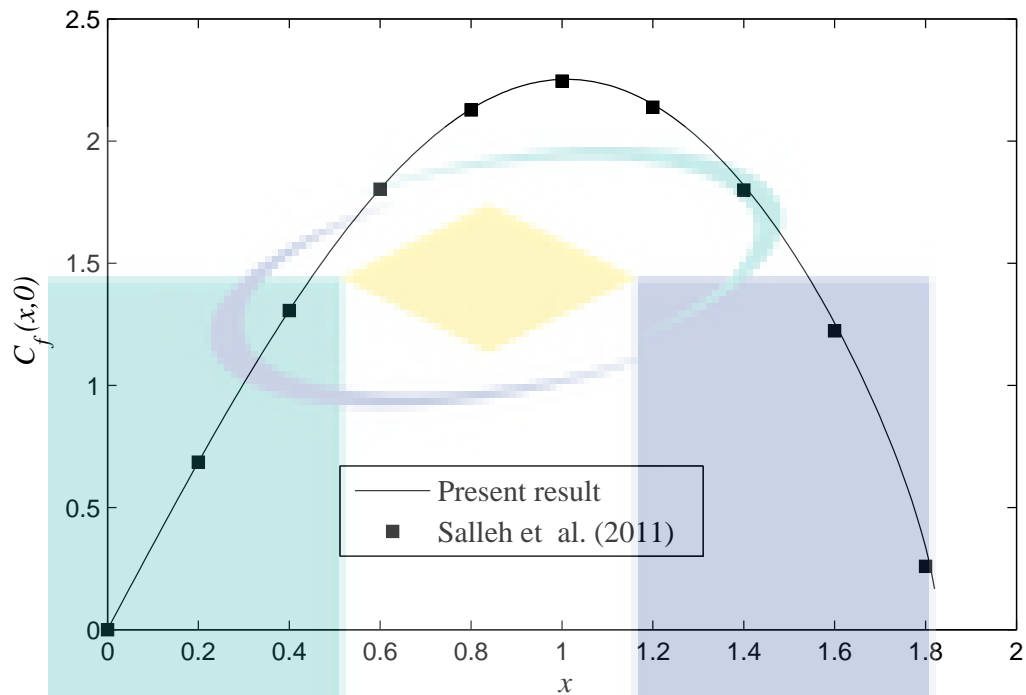


Figure 4.2. Variation of the local skin friction coefficient $C_f(x,0)$

The local skin friction coefficients, C_f are illustrated in Figure 4.2 for the present results and those reported by Salleh et al. (2011). There is no skin friction at the stagnation point (Mabood et al., 2016). The graph is almost symmetric and the point of maximum occurs at 0.96. The increase in the shear stress is caused by the deformation of the velocity profile in the boundary layer, a higher velocity gradient at the wall, and a thicker boundary layer (Kaprawi and Santoso, 2012).

Figure 4.3 shows the value of the local heat transfer coefficient for various values of Pr. As Pr increases, the heat transfer coefficient also increases. However, at the lower stagnation point $x \approx 0$, the value increases drastically before it becoming relatively constant and decrease at separation points. A similar trend is observed when γ increases as illustrates in Figure 4.4. Indeed, heat transfer coefficients increase with the increase of γ i.e. convective parameter helps in increasing the surface temperature. Figure 4.5 displays the velocity profiles near the lower stagnation points of the cylinder, $x \approx 0$. Regarding this figure, a unique graph of $\frac{\partial f}{\partial y}(x,0)$ is found for all values of Pr number and convective parameter γ due to the decoupled Equations 4.10 and 4.11.

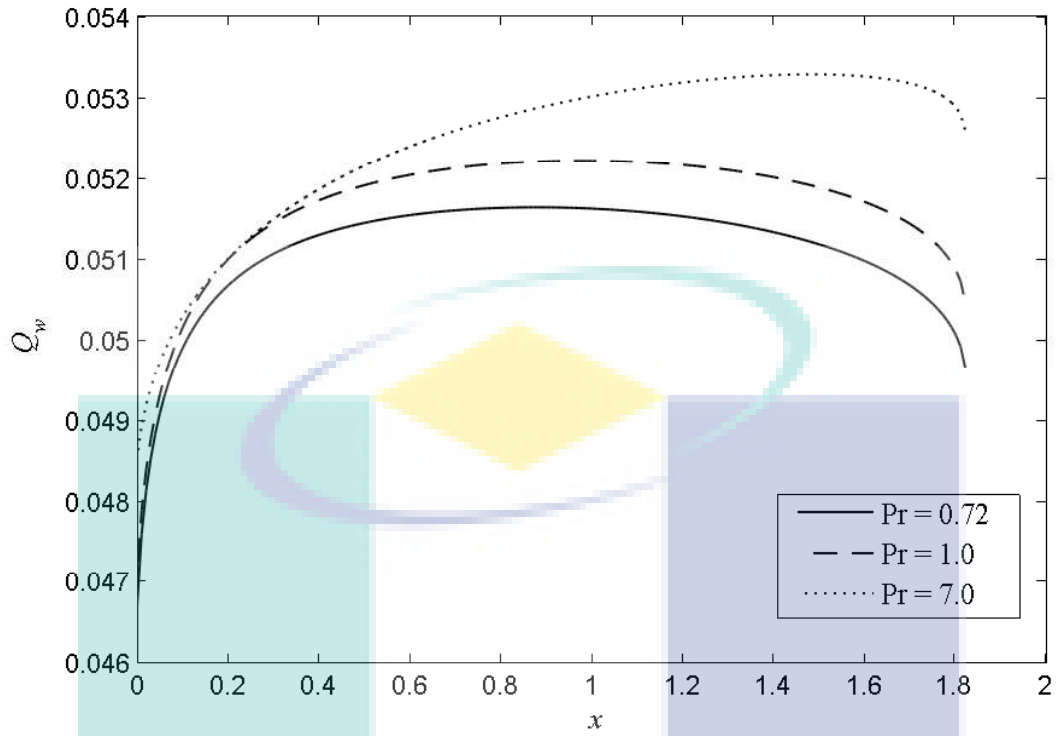


Figure 4.3. Variation of the local heat transfer coefficient for various value of Pr

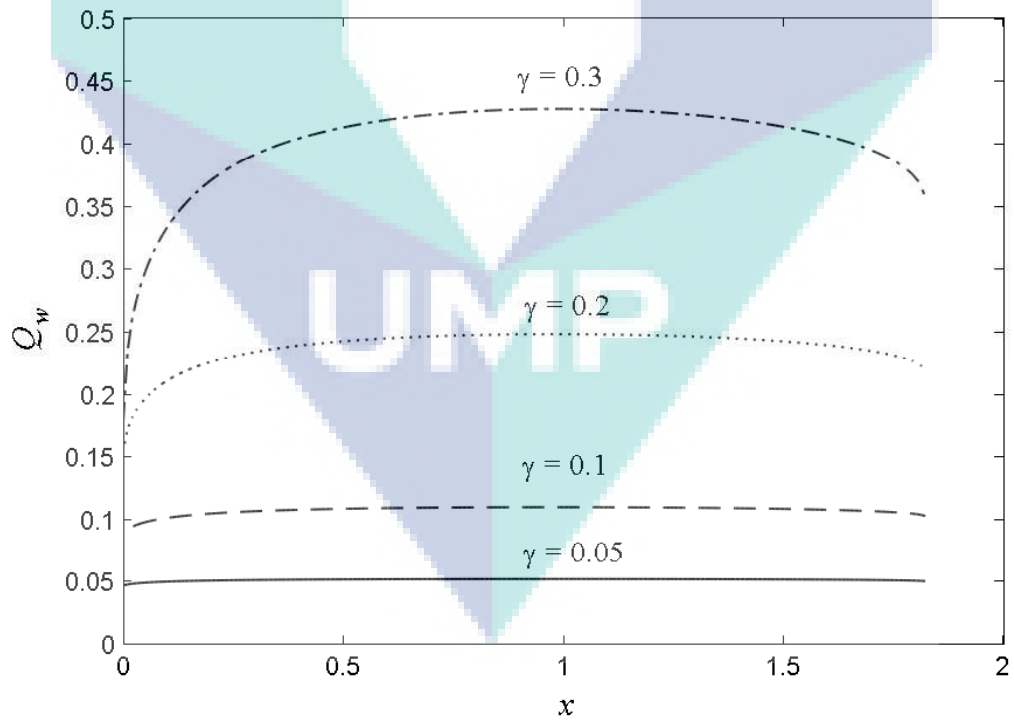


Figure 4.4. Variation of the local heat transfer coefficient for various value of γ

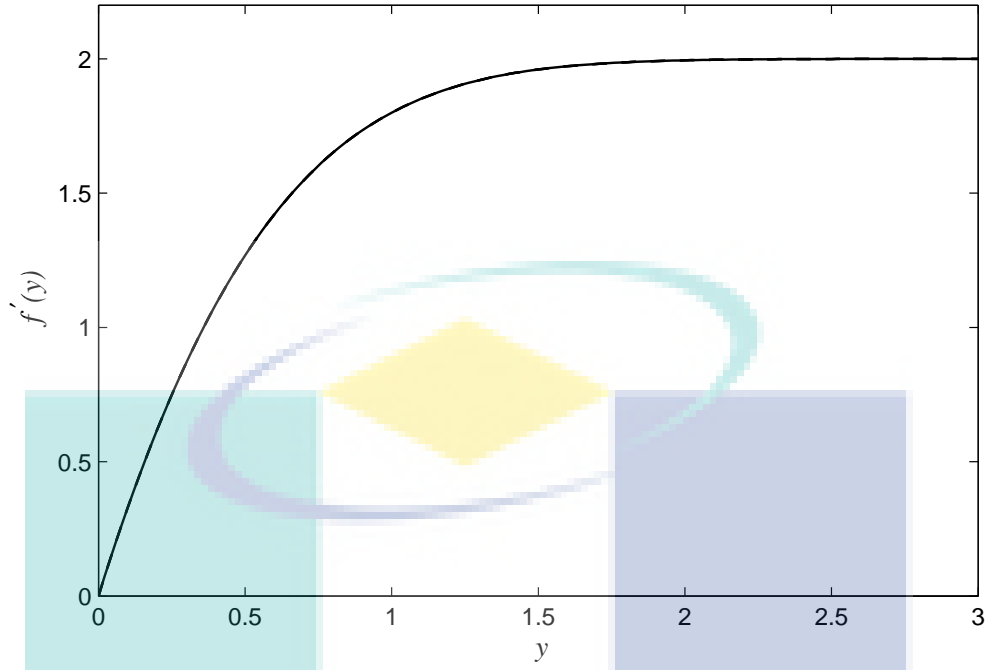


Figure 4.5. Velocity profiles $f'(y)$ near the lower stagnation point of the cylinder, $x \approx 0$

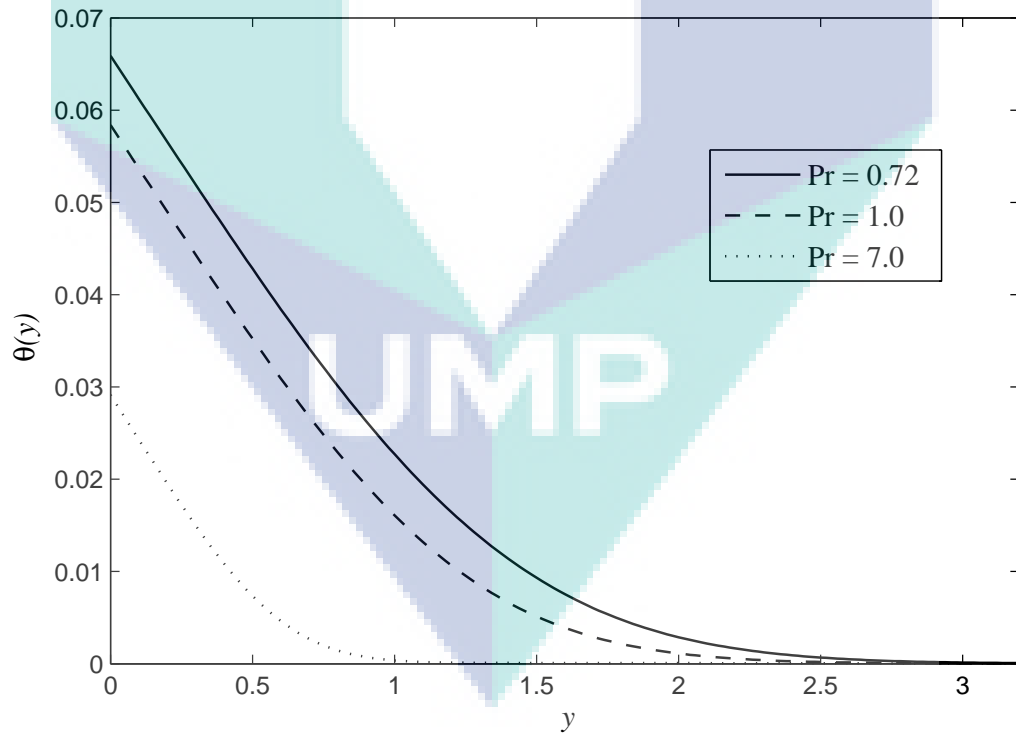


Figure 4.6. Temperature profiles $\theta(y)$ near the lower stagnation point of the cylinder, $x \approx 0$ when $\gamma = 0.1$

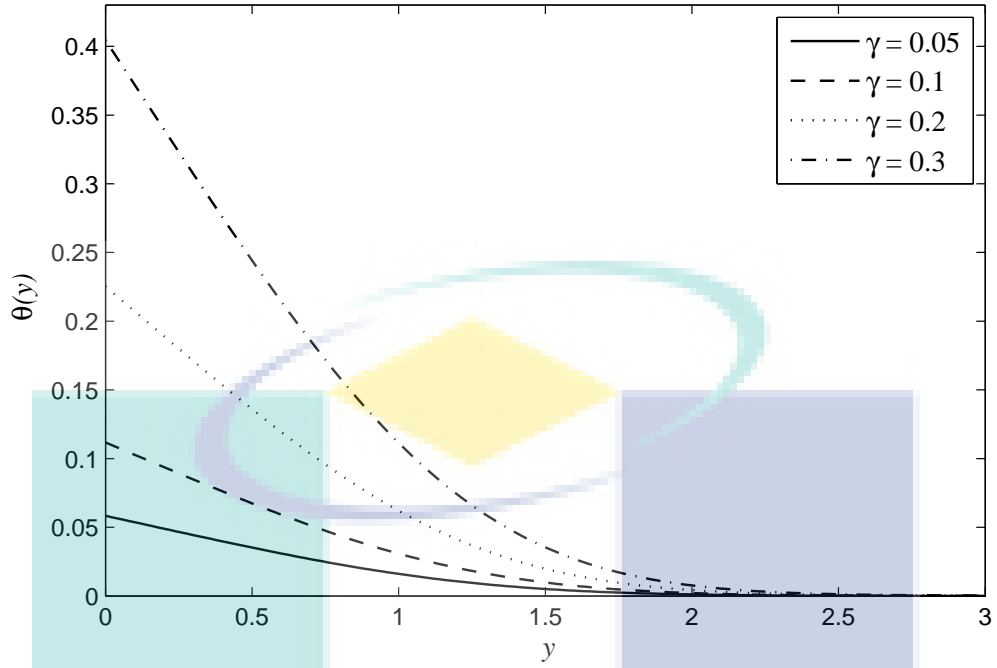


Figure 4.7. Temperature profiles $\theta(y)$ near the lower stagnation point of the cylinder, $x \approx 0$ when $Pr = 1.0$

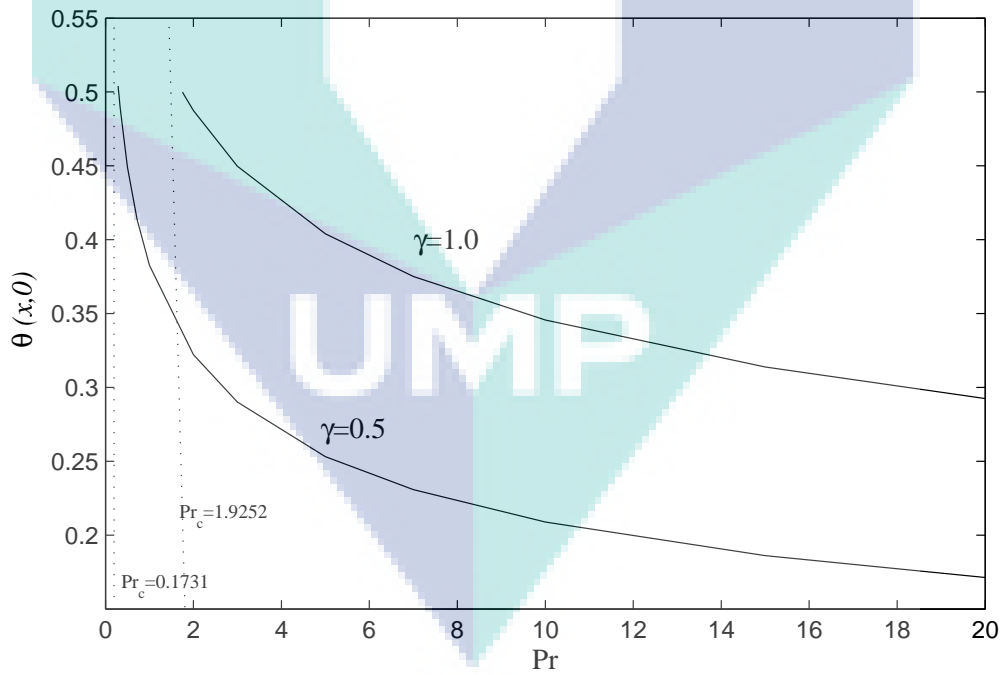


Figure 4.8. Variation of the wall temperature $\theta(x,0)$ at the lower stagnation point of the cylinder $x \approx 0$ with Pr when $\gamma = 0.5$ and 1.0 .

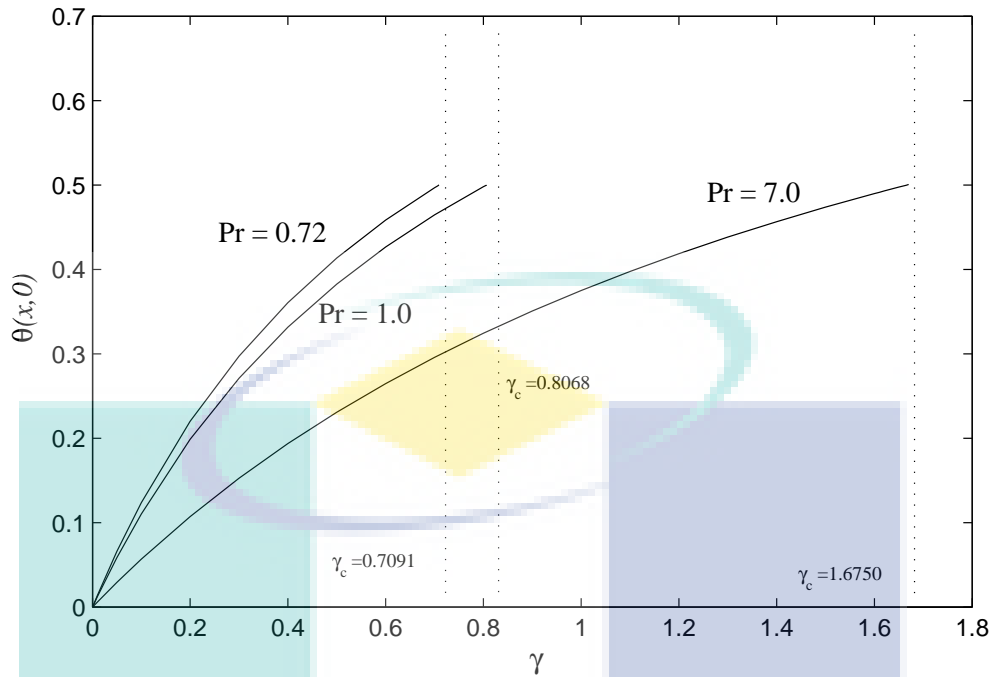


Figure 4.9. Variation of the wall temperature $\theta(x,0)$ at the lower stagnation point of the cylinder $x \approx 0$ with convective parameter γ when $Pr = 0.72, 1.0$ and 7.0

Figures 4.6 shows the temperature profiles at the stagnation point of the cylinder for various values of Pr . The temperature profile decreases when the Prandtl number Pr increases. This is due to the fact that for small values of Prandtl number $Pr (\ll 1)$, the fluid is highly conductive. Physically, if Pr increases, the thermal diffusivity decreases and this phenomenon leads to the decreasing manner of energy transfer ability that reduces the thermal boundary layer (Mohamed, 2013).

On the other hand, in 4.7 temperature profile increases as the convective parameter increases. Furthermore, the parameter γ at any location is proportional to heat transfer coefficient associated with the hot fluid h_f . Therefore, as γ increase, the hot fluid resistance increases and consequently the surface temperature increases (Aziz, 2009). From Figure 4.8, the variation of wall temperature is graphically plotted, $\theta_w(x,0)$ with $\gamma = 0.5$ and 1.0 . To achieve an acceptable solution, Pr must be greater than some critical value, say Pr_c depending on γ . As Pr approaches the critical value, $\theta(0)$ becomes large and the value of $Pr_c = 0.1713$ and 1.9252 when $\gamma = 0.5$ and 1.0 respectively.

Variation value of the wall temperature, $\theta(0)$ for different values of γ when $Pr = 0.72, 1.0$ and 7.0 are shown in Figure 4.9. Also in this case, to obtain an acceptable solution, γ must be less than some critical value, say γ_c depending on Pr . From the graph above, the critical value of γ_c is $0.7091, 0.8068$ and 1.6750 when $Pr = 0.72, 1.0$ and 7.0 , respectively.

4.4 Conclusions

The results presented in this chapter provide a better understanding regarding the influences of the presence of the convective parameter and Prandtl number Pr , on the rates of heat transfer and the hydrodynamic and thermal behaviour around a heated circular cylinder mounted in a horizontal channel. Though not surprising, the results demonstrate that the presence of the convective parameter increases the heat transfer as expected.

The separation of the cylinder for forced convection occur when position of $x = 1.85$ of cylinder where it diminishes and we have shown how convective parameter, γ and the Prandtl number affects the flow and heat transfer characteristics as well as the position of the boundary layer separation point, x_s . Therefore, we conclude that:

- i) the unique valued exists for the skin friction coefficient due to the decoupled boundary condition i.e. the flow is independent of the temperature and the maximum skin friction takes place when $x = 0.96$ (55°)
- ii) the heat transfer increases with the increase of γ as the convective parameter aids in increasing the surface temperature
- iii) an increase in the value of Pr leads to a decrease in the temperature profiles. However, the rise in γ increases the temperature profile
- iv) to achieve a physically acceptable solution, Pr must be greater or equal to Pr_c depending on γ , whereas γ must be less than or equal to γ_c depending on Pr . Outside this value, the singularity occurs and the solution becomes unstable

CHAPTER 5

FREE CONVECTION BOUNDARY LAYER FLOW OVER A HORIZONTAL CIRCULAR CYLINDER IN A MICROPOLAR FLUID

5.1 Introduction

This chapter demonstrates on a problem of free convection immersed in the micropolar fluids. Eringen (1966) was the first who proposed the theory of micropolar fluids where the structure and microrotation of fluid elements give rise to the microscopic effect. Later Eringen (1972) incorporated the thermal effects in generalizing the theory of micropolar fluid. Eringen's discovery led to the major advancement in fluid flow whereby micropolar fluid takes account into the rotation of fluid particles using an independent kinematic vector called the microrotation vector.

Accordingly, this model consider the biological fluids in thin vessels, polymeric suspensions, slurries, and colloidal fluids. Due to the vast applications, numerous problems regarding the solutions of flow of a micropolar fluid have been investigated by researchers. The historical development of the free convection flow in a micropolar fluid has already presented in Chapter 2.

In the next section, we provides a succinct description of the governing equations and the boundary conditions for the free convection over horizontal circular cylinder immersed in micropolar fluid. This is followed by a presentation and discussion of the numerical results in Section 5.3, which include the variations of the skin friction coefficient and the heat transfer coefficient with the effects of the Pr number, convective and material parameter on the flow and heat transfer. Finally, Section 5.4 provides the concluding remarks about the finding of this problem.

5.2 Mathematical Formulation

Steady free convection boundary layer flow and heat transfer of a viscous and an incompressible micropolar fluid of free stream velocity, and ambient temperature, over a horizontal circular cylinder of the radius, are next examined. Under the Boussinesq and boundary layer approximations, the basic equations are (Nazar et al., 2002b; Salleh and Nazar, 2010),

$$\rho \left(\bar{u} \frac{\partial \bar{u}}{\partial \bar{x}} + \bar{v} \frac{\partial \bar{u}}{\partial \bar{y}} \right) = (\mu + \kappa) \frac{\partial^2 \bar{u}}{\partial \bar{y}^2} + \rho g \beta (\bar{T} - T_\infty) \sin \left(\frac{\bar{x}}{a} \right) + \kappa \frac{\partial \bar{H}}{\partial \bar{y}} \quad 5.1$$

$$\bar{u} \frac{\partial \bar{T}}{\partial \bar{x}} + \bar{v} \frac{\partial \bar{T}}{\partial \bar{y}} = \alpha \frac{\partial^2 \bar{T}}{\partial \bar{y}^2} \quad 5.2$$

$$\rho J \left(\bar{u} \frac{\partial \bar{H}}{\partial \bar{x}} + \bar{v} \frac{\partial \bar{H}}{\partial \bar{y}} \right) = -\kappa \left(2\bar{H} + \frac{\partial \bar{u}}{\partial \bar{y}} \right) + \chi \frac{\partial^2 \bar{H}}{\partial \bar{y}^2} \quad 5.3$$

The physical model and coordinate system of this problem is shown in Figure 5.1.

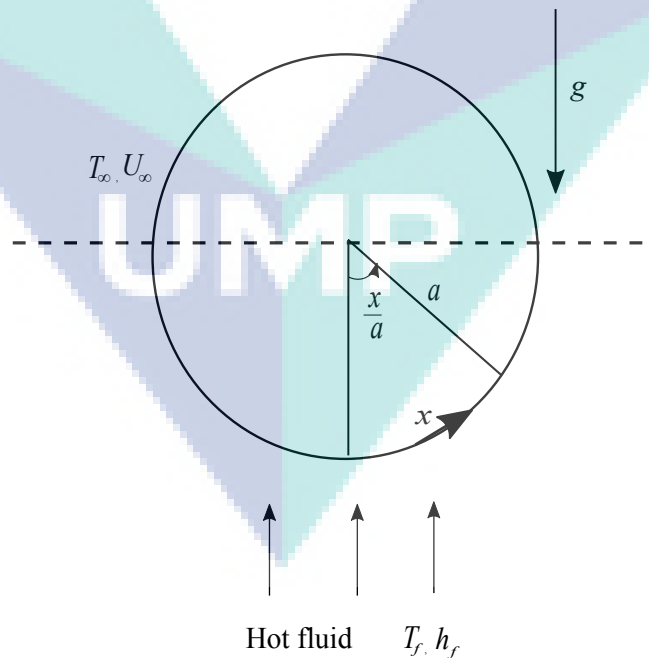


Figure 5.1. Physical model and coordinate system

Assuming the spin gradient velocity is given by $\chi = (\mu + (\kappa/2))J$. The boundary conditions for the flow and thermal field are

$$\begin{aligned} \bar{u} = \bar{v} = 0, \quad -k \frac{\partial \bar{T}}{\partial \bar{y}} = h_f(T_f - \bar{T}), \quad \bar{H} = -n \frac{\partial \bar{u}}{\partial \bar{y}} \quad \text{at } \bar{y} = 0 \\ \bar{u} \rightarrow 0, \quad \bar{T} \rightarrow T_\infty, \quad \bar{H} \rightarrow 0 \quad \text{as } \bar{y} \rightarrow \infty \end{aligned} \quad 5.4$$

where \bar{u} and \bar{v} are the velocity components along \bar{x} and \bar{y} respectively, ρ is the fluid density, ν is the kinematic viscosity, κ is the vortex viscosity, g is the gravitational acceleration, β is the thermal expansion coefficient, T is the fluid temperature in the boundary layer, \bar{H} is the angular velocity of the micropolar fluid, α is the thermal diffusivity, μ is the viscosity, and J is the microinertia per unit mass. The bottom surface of cylinder is heated by convection from hot fluid of temperature T_f which provides heat transfer coefficient h_f . Further, k is the thermal conductivity and $T_f > T_\infty$.

Therefore to solve Equations 5.1 to 5.4, the following non-dimensional variables are defined as

$$\begin{aligned} x = \bar{x}/a, \quad y = Gr^{1/4}(\bar{y}/a), \quad u = \left(\frac{a}{\nu}\right) Gr^{-1/2} \bar{u} \\ v = \left(\frac{a}{\nu}\right) Gr^{-1/4} \bar{v}, \quad \theta = \frac{\bar{T} - T_\infty}{T_f - T_\infty}, \quad H = \left(\frac{a^2}{\nu}\right) Gr^{-3/4} \bar{H} \end{aligned} \quad 5.5$$

where Gr is Grashof number which is given as

$$Gr = \frac{g\beta(T_f - T_\infty)a^3}{\nu^2} \quad 5.6$$

Substituting Equation 5.5 into Equations 5.1 to 5.4, the following boundary layer equations for the problem under consideration are given by

$$u \frac{\partial u}{\partial x} + v \frac{\partial u}{\partial y} = (1 + K) \frac{\partial^2 u}{\partial y^2} + \theta \sin x + K \frac{\partial H}{\partial y} \quad 5.7$$

$$u \frac{\partial H}{\partial x} + v \frac{\partial H}{\partial y} = \left(1 + \frac{K}{2}\right) \frac{\partial^2 H}{\partial y^2} - K \left(2H + \frac{\partial u}{\partial y}\right) \quad 5.8$$

$$u \frac{\partial \theta}{\partial x} + v \frac{\partial \theta}{\partial y} = \frac{1}{Pr} \frac{\partial^2 \theta}{\partial y^2} \quad 5.9$$

where the material or micropolar parameter K is defined as $K = \kappa/\mu$, and κ , μ are the vortex viscosity and viscosity, respectively. The boundary conditions become:

$$\begin{aligned} u = v = 0, \quad \frac{\partial \theta}{\partial y} = -\gamma(1 - \theta), \quad H = -\frac{1}{2} \frac{\partial u}{\partial y} \quad \text{at } y = 0 \\ u \rightarrow 0, \quad \theta \rightarrow 0, \quad H \rightarrow 0 \quad \text{as } y \rightarrow \infty \end{aligned} \quad 5.10$$

To solve Equations 5.7 to 5.9, subjected to the boundary conditions 5.10, we introduce the following variables

$$\psi = xf(x, y), \quad \theta = \theta(x, y), \quad H = xG(x, y) \quad 5.11$$

where ψ is the stream function defined as $u = \partial\psi/\partial y$ and $v = -\partial\psi/\partial x$. Thus, Equations 5.7 to 5.9 becomes

$$(1 + K) \frac{\partial^3 f}{\partial y^3} + f \frac{\partial^2 f}{\partial y^2} - \left(\frac{\partial f}{\partial y} \right)^2 + \frac{\sin x}{x} \theta + K \frac{\partial G}{\partial y} = x \left(\frac{\partial f}{\partial y} \frac{\partial^2 f}{\partial x \partial y} - \frac{\partial f}{\partial x} \frac{\partial^2 f}{\partial y^2} \right) \quad 5.12$$

$$\left(1 + \frac{K}{2} \right) \frac{\partial^2 G}{\partial y^2} + f \frac{\partial G}{\partial y} - \left(\frac{\partial f}{\partial y} \right) G - K \left(2G + \frac{\partial^2 f}{\partial y^2} \right) = x \left(\frac{\partial f}{\partial y} \frac{\partial G}{\partial x} - \frac{\partial f}{\partial x} \frac{\partial G}{\partial y} \right) \quad 5.13$$

$$\frac{1}{Pr} \frac{\partial^2 \theta}{\partial y^2} + f \frac{\partial \theta}{\partial y} = x \left(\frac{\partial f}{\partial y} \frac{\partial \theta}{\partial x} - \frac{\partial f}{\partial x} \frac{\partial \theta}{\partial y} \right) \quad 5.14$$

subject to the boundary conditions

$$\begin{aligned} f = \frac{\partial f}{\partial y} = 0, \quad \frac{\partial \theta}{\partial y} = -\gamma(1 - \theta), \quad G = -\frac{1}{2} \frac{\partial^2 f}{\partial y^2} \quad \text{at } y = 0 \\ \frac{\partial f}{\partial y} \rightarrow 0, \quad \theta \rightarrow 0, \quad G \rightarrow 0 \quad \text{as } y \rightarrow \infty \end{aligned} \quad 5.15$$

It can be seen that near the lower stagnation point of the cylinder, $x \approx 0$, Equations 5.12 to 5.14 reduce to the following ordinary differential equations,

$$(1 + K)f''' + ff'' - (f')^2 + \theta + KG' = 0 \quad 5.16$$

$$\left(1 + \frac{K}{2}\right)G'' + fG' - (f')G - K(2G + f'') = 0 \quad 5.17$$

$$\frac{1}{Pr}\theta'' + f\theta' = 0 \quad 5.18$$

and the boundary conditions 5.15 become

$$f(0) = f'(0) = 0, \quad \theta'(0) = -\gamma(1 - \theta(0)), \quad G(0) = -\frac{1}{2}f''(0) \quad \text{at } y = 0 \quad 5.19$$

$$f'(y) \rightarrow 0, \quad \theta(y) \rightarrow 0, \quad G(y) \rightarrow 0 \quad \text{as } y \rightarrow \infty$$

where primes denote differentiation with respect to y . Indeed, in practical applications, quantities such as surface heat flux and skin friction are very important. But, for free convection problems, the former is more important than the latter. The following equation provides both the skin friction coefficient C_f and the heat flux Q_w as

$$C_f = \frac{Gr^{-3/4}a^2}{\mu\nu}\tau_w, \quad Q_w = \frac{aGr^{-1/4}}{k_f(T_f - T_\infty)}q_w \quad 5.20$$

where τ_w is the skin friction coefficient or the shear stress at the surface of the cylinder, q_w is the heat flux from the surface of the cylinder respectively, which are given by

$$\bar{\tau}_w = \mu \left(\frac{\partial \bar{u}}{\partial \bar{y}} \right)_{\bar{y}=0}, \quad \bar{q}_w = -k_f \left(\frac{\partial \bar{T}}{\partial \bar{y}} \right)_{\bar{y}=0} \quad 5.21$$

Using Equations 5.5 and 5.11, the dimensionless quantities C_f and Q_w are obtained as

$$Gr^{1/4}C_f = \left(1 + \frac{K}{2}\right)x \frac{\partial^2 f}{\partial y^2}, \quad Q_w = -\frac{\partial \theta}{\partial y} = -\gamma(1 - \theta) \quad 5.22$$

Detailed formulation can be accessed in Appendix D.

5.3 Results and Discussion

Equations 5.12 to 5.14 with boundary conditions 5.15 were solved numerically using the same techniques as presented in Chapter 3. The numerical solution starts at the lower stagnation point of the cylinder, i.e. $x \approx 0$ and proceeds round the cylinder until the upper stagnation point, ($x = 180^\circ$). In this study, the results are also focused on the case at the lower stagnation point of the cylinder, and therefore Equations 5.17 to 5.18 are solved subject to boundary conditions 5.19. Representative results for the velocity and temperature profiles for the local heat transfer and the skin friction coefficient are obtained for various values of the convective parameter γ , material parameter K and at a different position of x . The values of material parameter considered in this problem are $K = 0$ (Newtonian fluid), $K = 1, 2$ and 3 for micropolar fluid.

To verify the accuracy of the present method, the present results are compared with those reported by Bhattacharyya and Pop (1996) as shown in Table 5.1. Bhattacharyya and Pop (1996) studied free convection from cylinders of elliptic cross-section in micropolar fluids using numerical approach. It is found that the values of Nusselt number for the previous published results with the presents results when convective parameter reduces to convective parameter i.e $\gamma \rightarrow \infty$ (CWT) are found to be in good agreement. Therefore, the result presented here is considered to be accurate.

Table 5.1. Comparison for the local Nusselt number Nu for the Newtonian case when $\gamma \rightarrow \infty$ (CWT).

x	$-\theta'(0)$	
	Bhattacharyya and Pop (1996)	Present Result
0	0.4213	0.4214
0.4	0.4183	0.4183
0.8	0.4093	0.4093
1.2	0.3942	0.3942
1.6	0.3725	0.3726
2.0	0.3440	0.3440
2.4	0.3066	0.3069
2.8	0.2568	0.2575
π	0.1963	0.1939

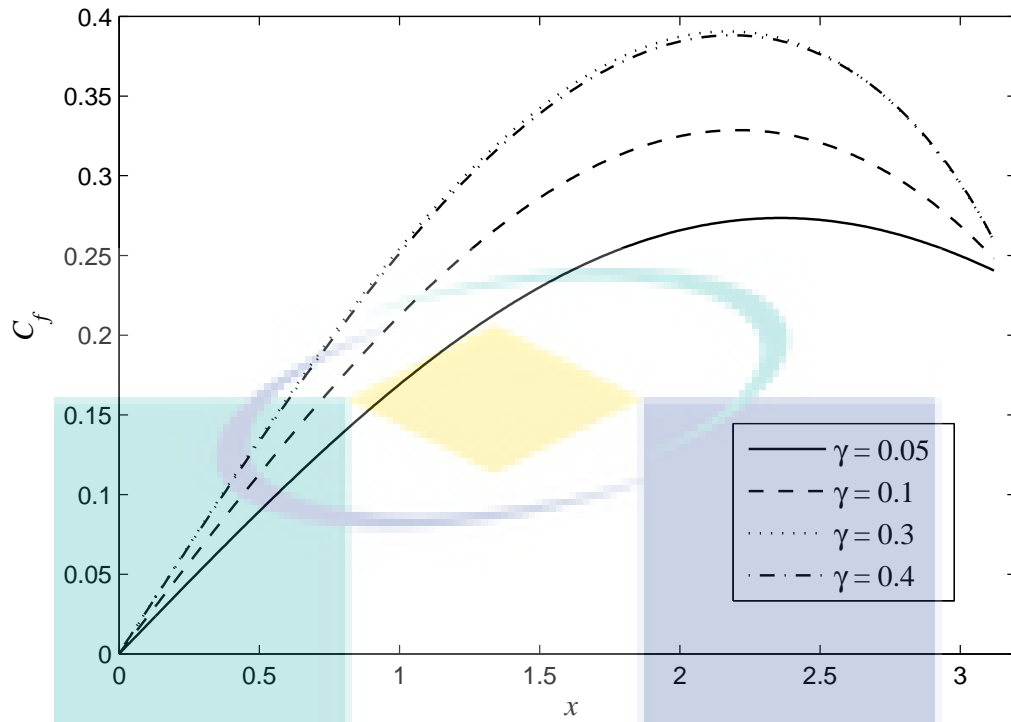


Figure 5.2. Variation of skin friction coefficient C_f for $Pr = 7$, $K = 1$ and various values of γ

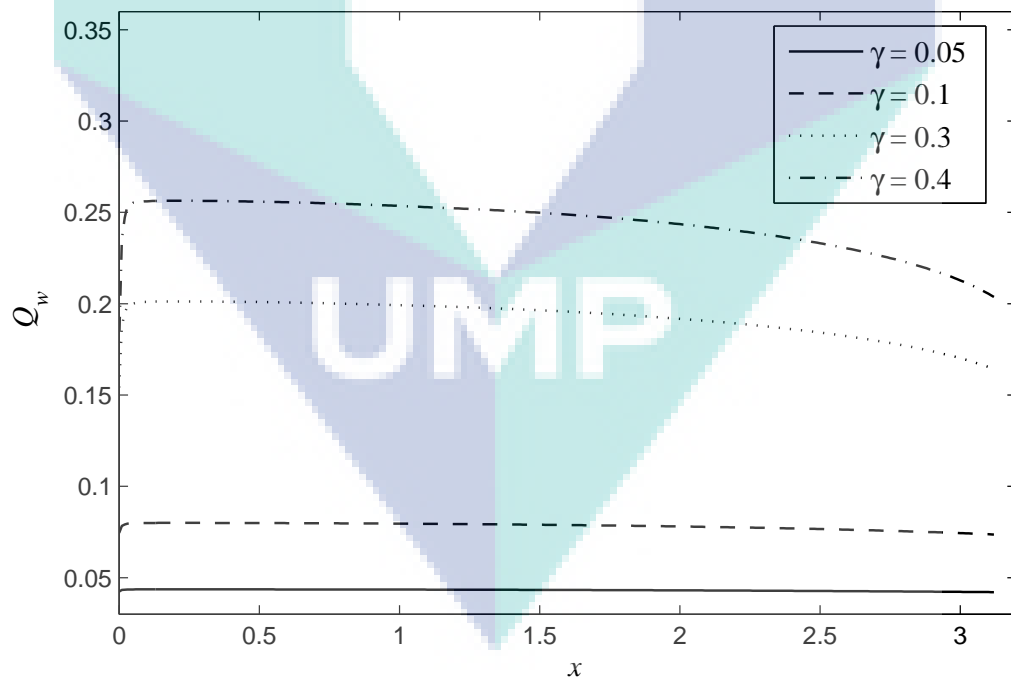


Figure 5.3. Variation of heat transfer coefficient Q_w for $Pr = 7$, $K = 1$ and various values of γ

Figures 5.2 and 5.3 illustrate the behavior of the local skin friction coefficient and local heat transfer for various values of convective parameter γ . Indeed, from these figures, it can be seen that there is no significant difference in the value of the heat transfer coefficient for the different position of x . This is possibly because the value of γ is small, and the effect of the heat transfer is not significant. However as γ increases, the heat transfer coefficient is increased. Notably, a similar pattern was observed in the case of the skin friction coefficient.

Figures 5.4 and 5.5 depict the behaviour of the local skin friction coefficient and local heat transfer for various values of the material parameter K . The skin friction coefficient increases as the value of K increases whereas the opposite pattern is observed for the heat transfer coefficient. The increasing values of C_f increase with the parameter K due to the factor of $x(1 + K/2)$. Consequently, an increase in the value of K implies a higher vortex viscosity of fluids and this resulting the higher values of local skin friction coefficients.

The corresponding variation of the skin friction coefficient C_f and heat transfer Q_w for various values of the Prandtl number are illustrated in Figures 5.6 and 5.7. From observing these figures, the values of the skin friction coefficient decrease with the increase of Pr , while those of the heat transfer increase with the increase of Pr for the fixed value of K .

Also, the temperature and velocity profiles, and angular velocity for some of the values of parameter K are displayed in Figures 5.8, 5.9 and 5.10. Noticeably, as K increases, the temperature profile increases, while the velocity and angular velocity decrease when K is increased.

The effects of the Prandtl number on velocity, temperature, and the angular velocity at the lower stagnation point are demonstrated in Figures 5.11, 5.12 and 5.13. The influence of the Prandtl number is similar to that in classical problem of the constant wall temperature case.

The effects of the convective parameter on velocity, temperature, and angular velocity at the lower stagnation point are presented in Figures 5.14, 5.15 through 5.16. It can be observed that the velocity becomes thinner as the convective parameter increases (Pantokratoras, 2014).

Note that for the case of free convection, the numerical solution demonstrates that the boundary layer reaches the top of the cylinder ($x = \pi$) without separating. Therefore, the boundary layer on each side of the cylinder must collide at ($x = \pi$) and leave the surface to form a thin buoyant plume above the cylinder.

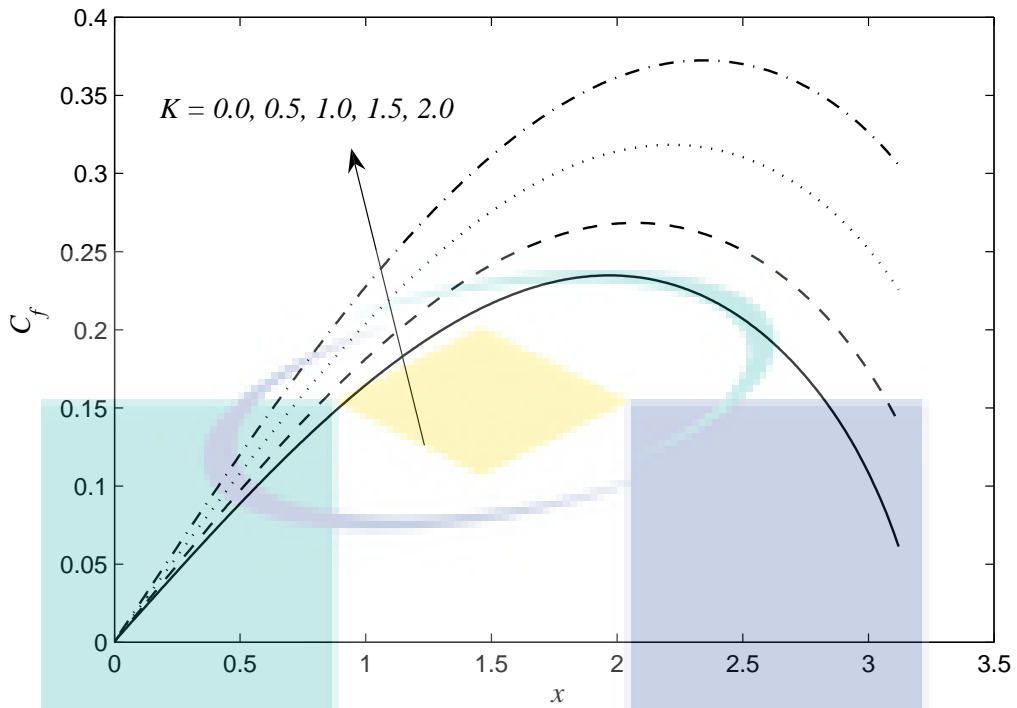


Figure 5.4. Variation of skin friction coefficient C_f for $Pr = 7$, $\gamma = 0.1$ and various values of material parameter K

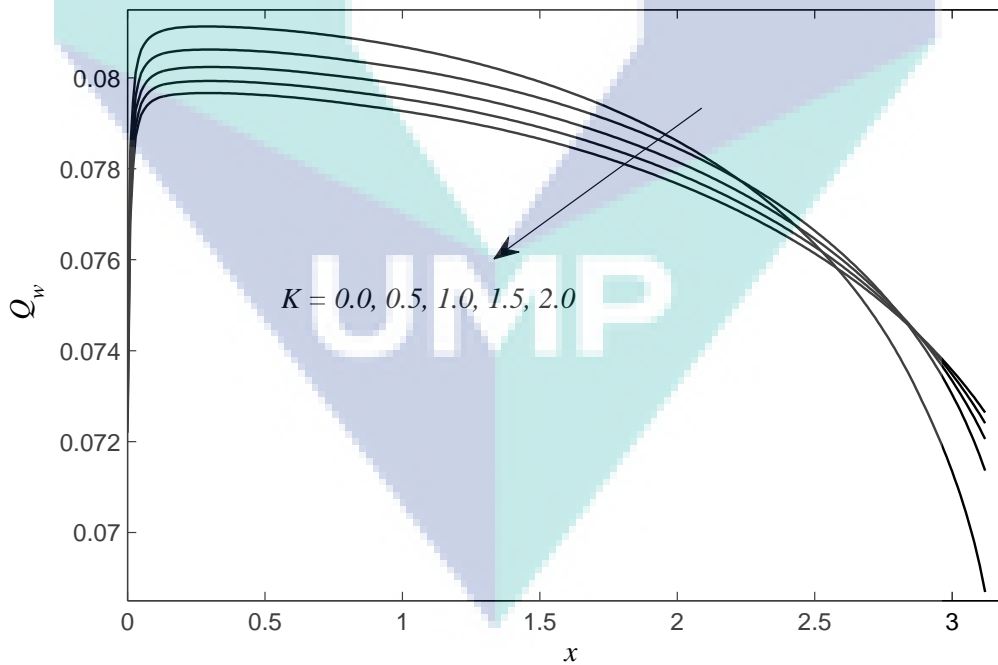


Figure 5.5. Variation of heat transfer coefficient Q_w for $Pr = 7$, $\gamma = 0.1$ and various values of material parameter K

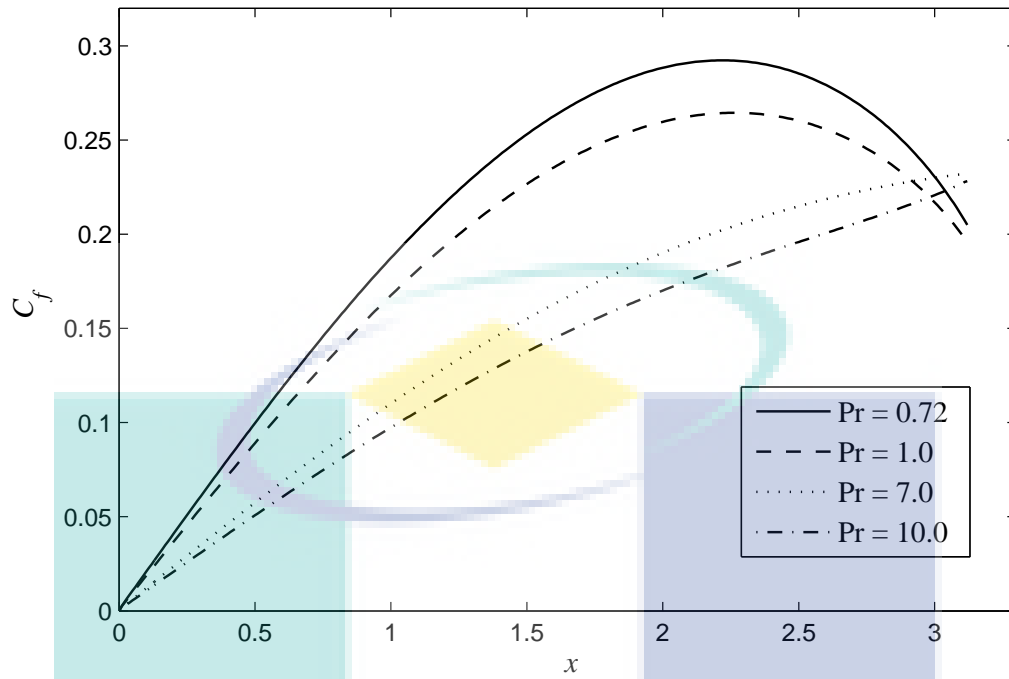


Figure 5.6. Variation of skin friction coefficient C_f for $K = 1$, $\gamma = 0.1$ and various values of Pr

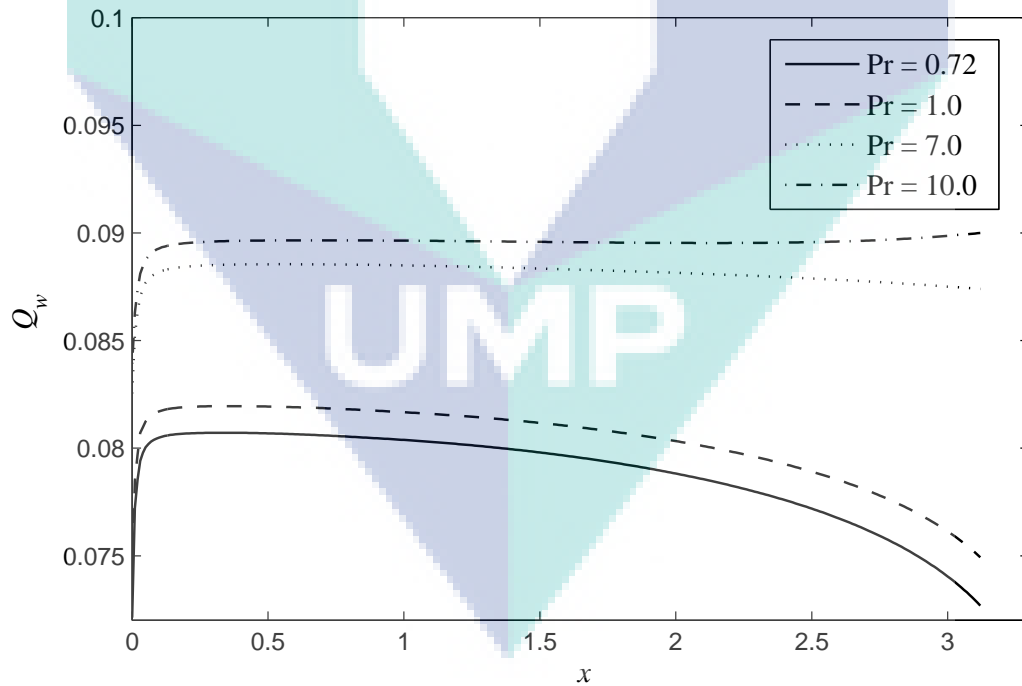


Figure 5.7. Variation of heat transfer coefficient Q_w for $K = 1$, $\gamma = 0.1$ and various values of Pr

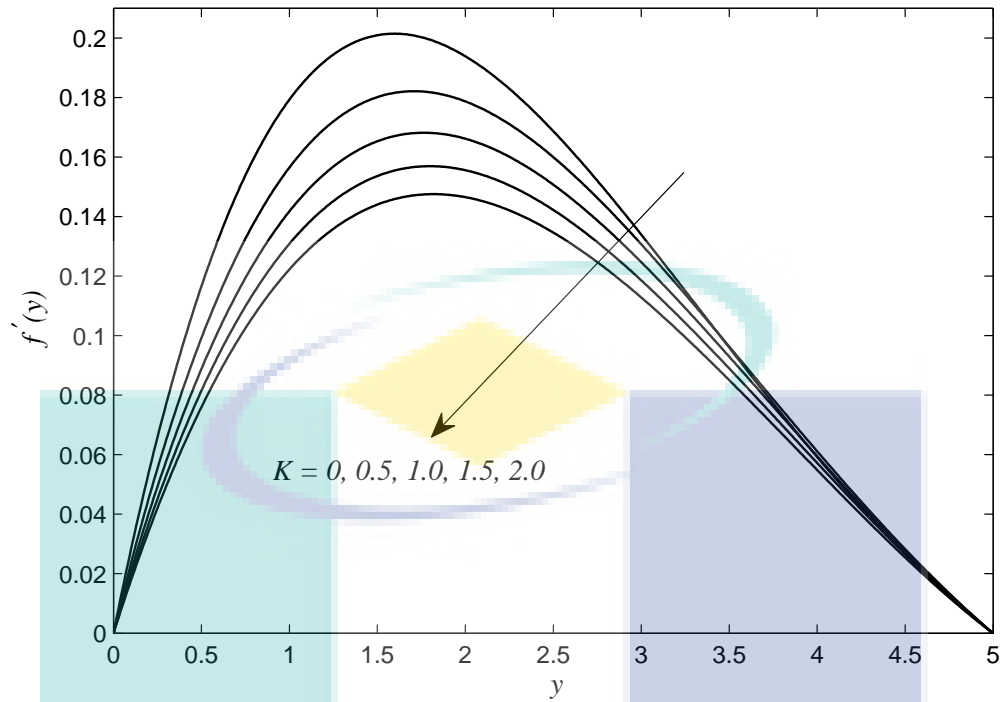


Figure 5.8. Velocity profile $f'(y)$ for various values of K when $Pr = 7.0$ and $\gamma = 0.1$

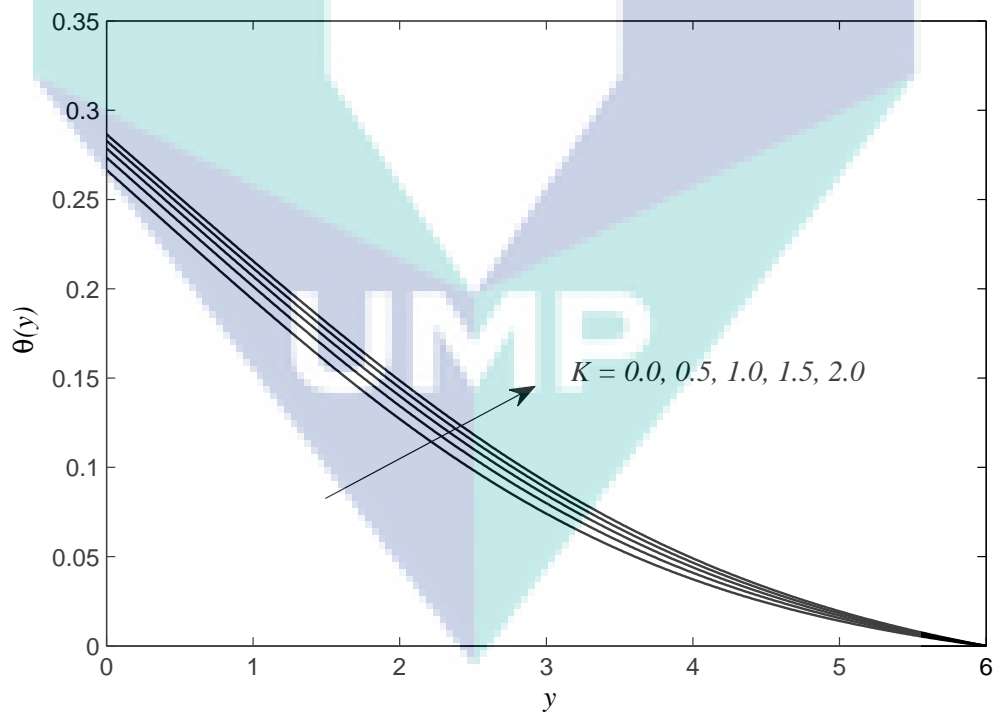


Figure 5.9. Temperature profile $\theta(y)$ for various values of K when $Pr = 7.0$ and $\gamma = 0.1$

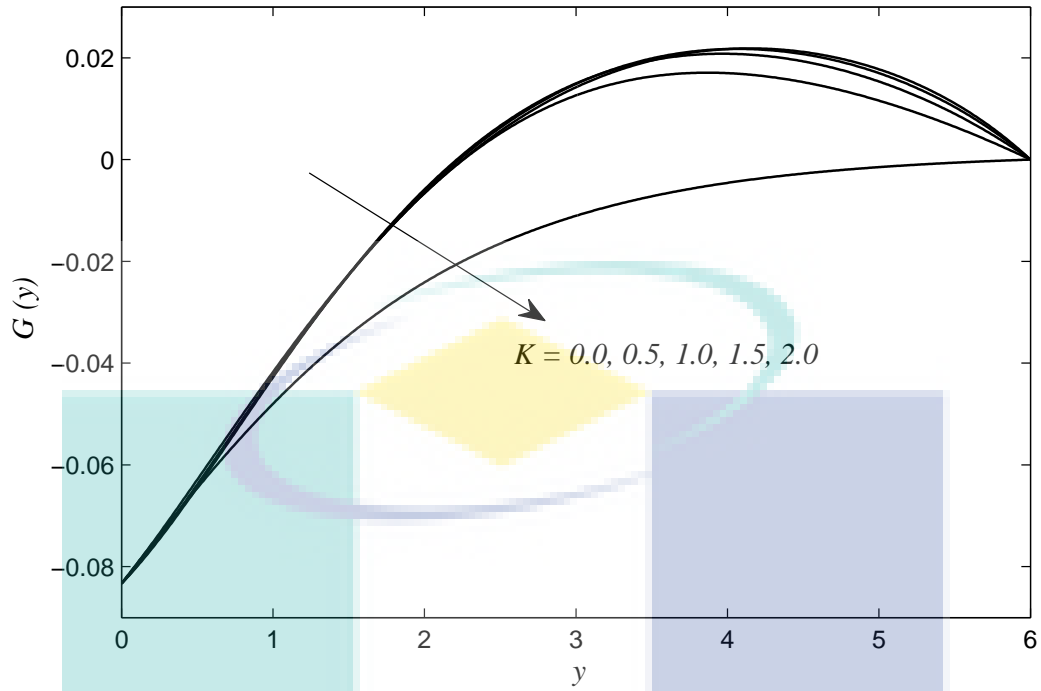


Figure 5.10. Angular velocity profile $G(y)$ for various values of K when $Pr = 7.0$ and $\gamma = 0.1$

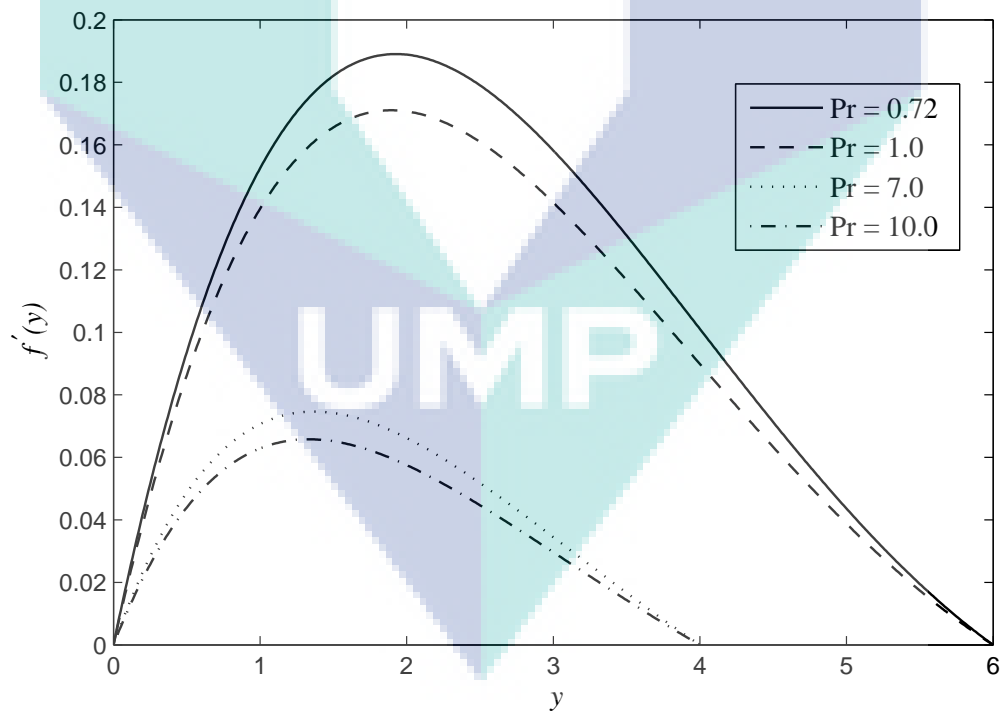


Figure 5.11. Velocity profiles $f'(y)$ for various values of Pr when $\gamma = 0.1$ and $K = 1$

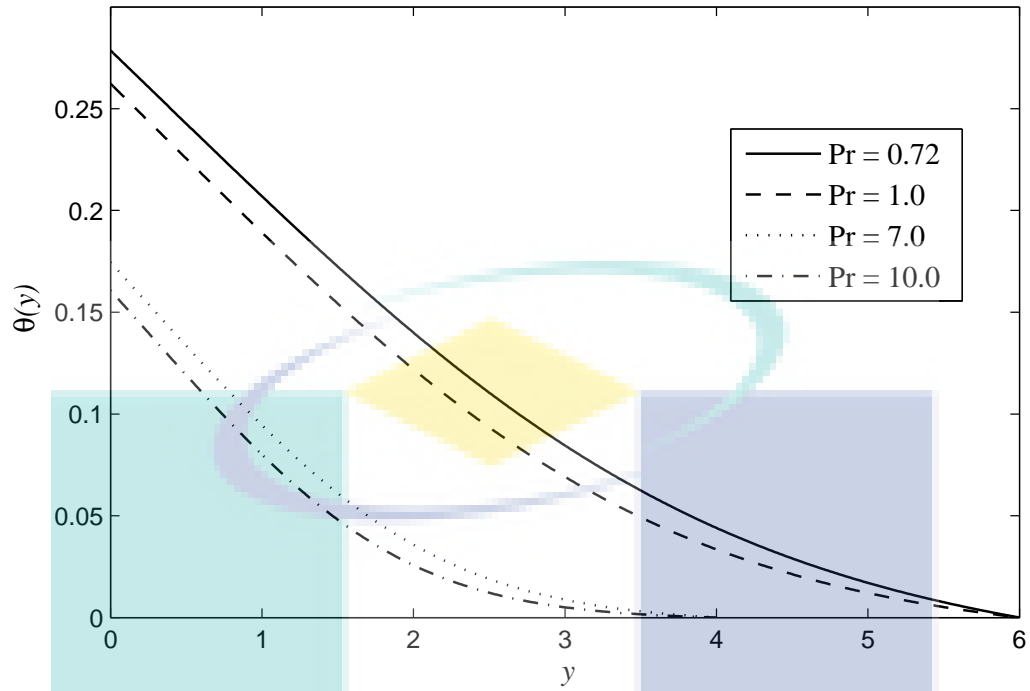


Figure 5.12. Temperature profiles $\theta(y)$ for various values of Pr when $\gamma = 0.1$ and $K = 1$

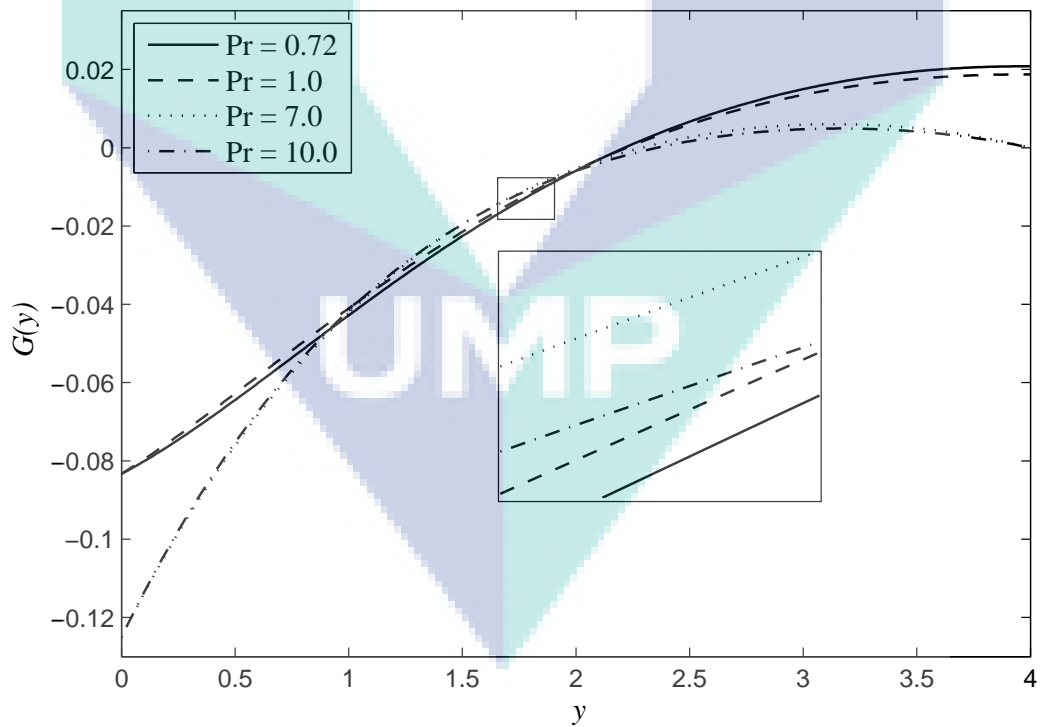


Figure 5.13. Angular velocity profiles $G(y)$ for various values of Pr when $\gamma = 0.1$ and $K = 1$

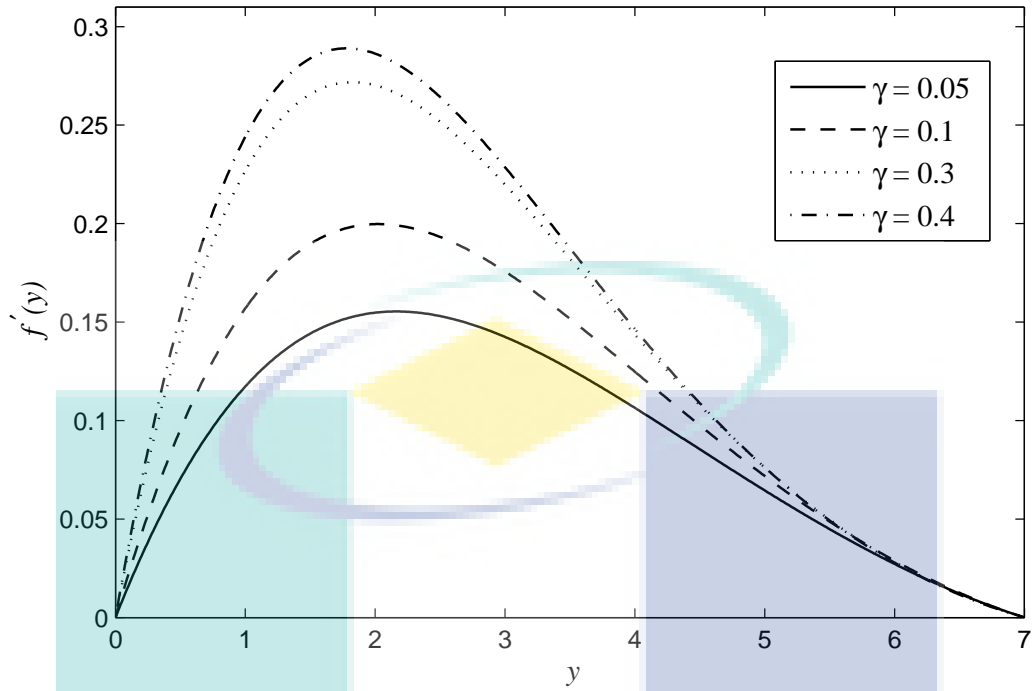


Figure 5.14. Velocity profiles $f'(y)$ for various values of γ when $Pr = 7.0$ and $K = 1$

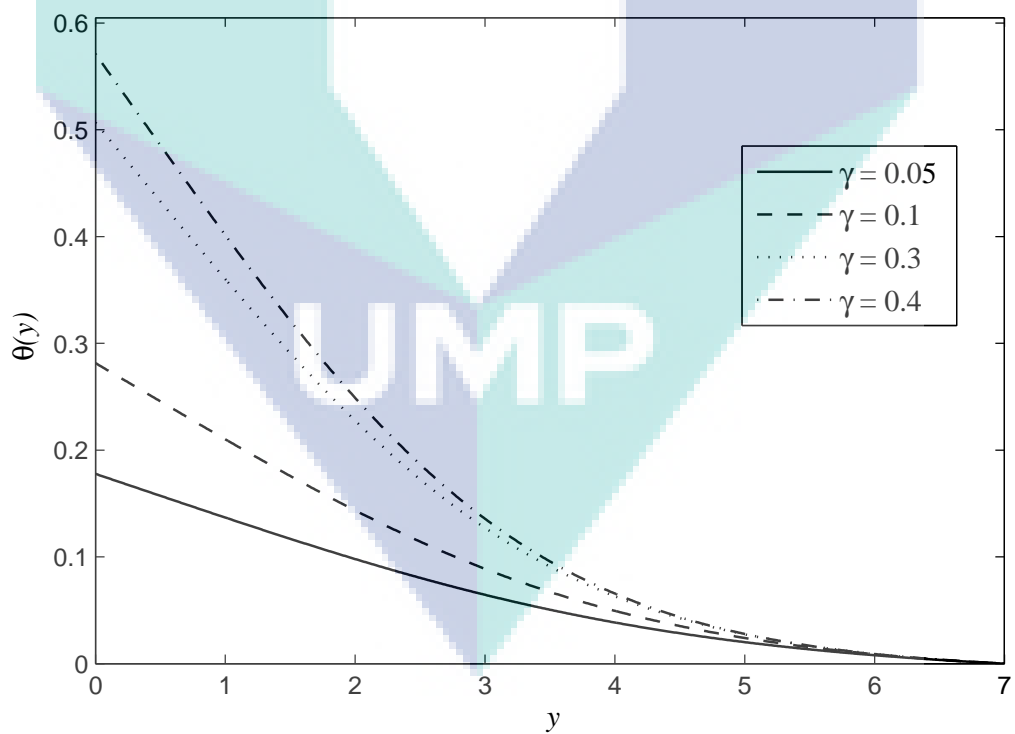


Figure 5.15. Temperature profiles $\theta(y)$ for various values of γ when $Pr = 7.0$ and $K = 1$

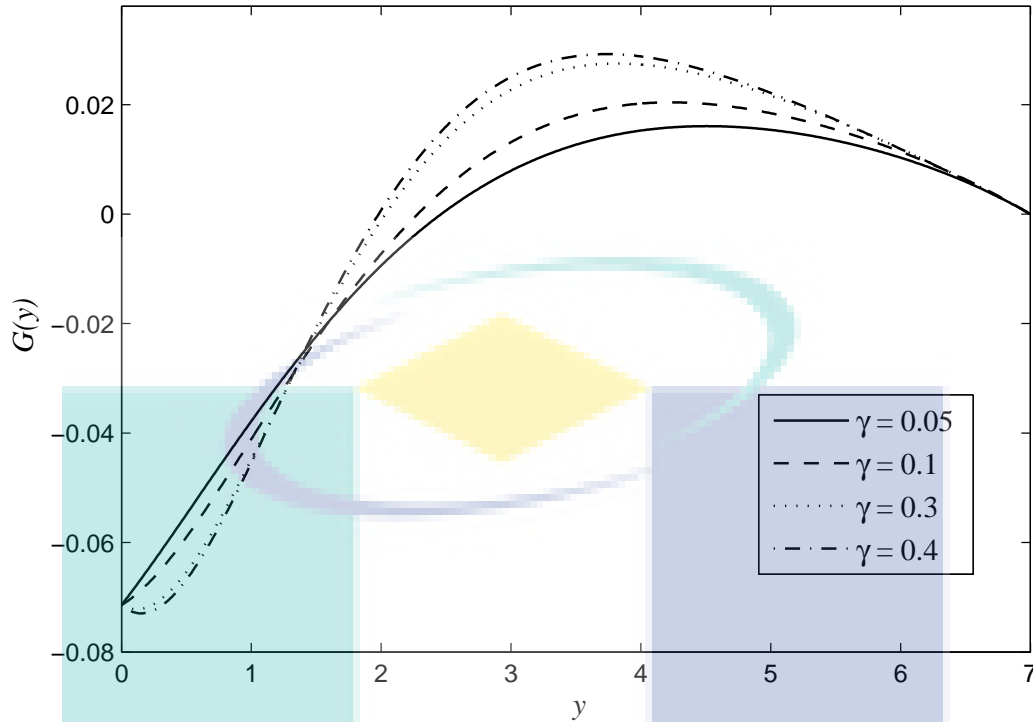


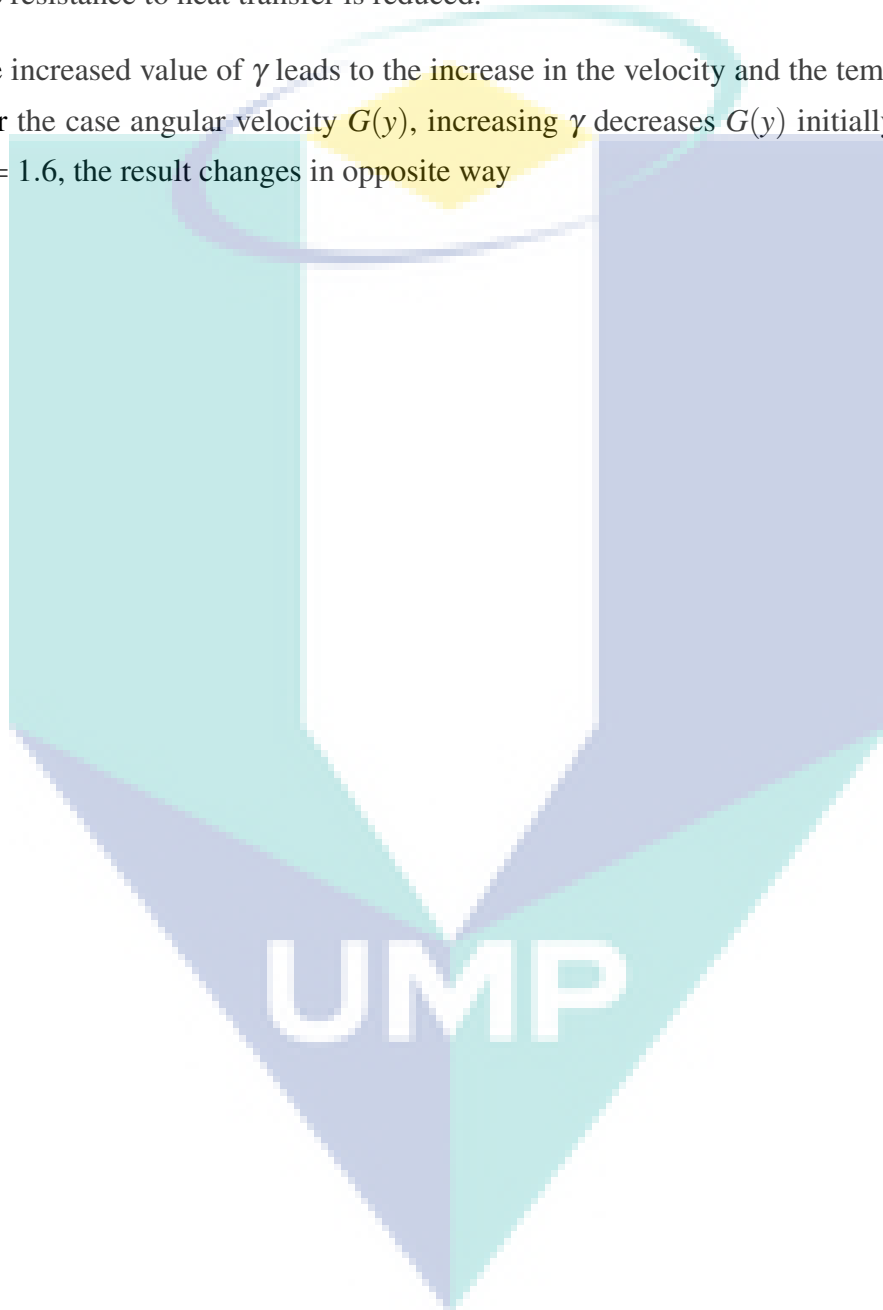
Figure 5.16. Angular velocity profiles $G(y)$ for various values of γ when $Pr = 7.0$ and $K = 1$

5.4 Conclusions

In this chapter, the problem of the free convection boundary layer of a horizontal circular cylinder immersed in a micropolar fluid with convective boundary condition was numerically studied. Notwithstanding, to determine how the convective parameter γ as well as the material parameter K and Prandtl number affect the flow and heat transfer characteristic. For the comparative result, the results were compared with the results obtained with Bhattacharyya and Pop (1996) for the case when $\gamma \rightarrow \infty$. The results were illustrated graphically and from the obtained results, the following conclusions are presented:

- i) an increase in γ and K illustrate the increment in the C_f . However the increase in Pr shows the decrease in C_f
- ii) an increase in the γ and the Pr number leads to heat transfer enhancement Q_w . Conversely, the different result are obtained with an increase of K .

- iii) an increase in the K parameter from 0 to 2 leads to decrease in velocity and the angular velocity profile. On the other hand, the temperature profile $\theta(y)$ increases with an increase of parameter K .
- iv) as the Prandtl number increases, the velocity $f'(y)$ and the temperature profile $\theta(y)$ decrease. The thermal boundary layer thickness decreases as the Pr increases. Therefore the resistance to heat transfer is reduced.
- v) the increased value of γ leads to the increase in the velocity and the temperature profile. For the case angular velocity $G(y)$, increasing γ decreases $G(y)$ initially, however after $y = 1.6$, the result changes in opposite way



CHAPTER 6

MIXED CONVECTION BOUNDARY LAYER FLOW OVER A HORIZONTAL CIRCULAR CYLINDER IN A VISCOUS FLUID

6.1 Introduction

The previous two chapters have considered both free and forced convection. In this chapter, attention is focussed on the problem of mixed convection over a horizontal circular cylinder under a convective boundary condition. Mixed convection describes the situation when the effect of the buoyancy force in forced convection, or the effect of forced flow in free convection becomes significant.

Mixed convection heat transfer exists when natural convection currents are in the same order of magnitude as the forced flow velocities (Dawood et al., 2015). Indeed, mixed convection flow from a horizontal circular cylinder constitutes an important heat transfer problem from the standpoint of engineering applications and numerical analysis (Nazar, 2003). Mixed convection boundary layer flow from general bodies in viscous fluid has been considered by numerous researchers as listed in the following paragraph. Over the past decade, the study on mixed convection over a horizontal cylinder has progressed tremendously due to the demand in industrial manufacturing processes, geothermal power generation, the dispersion of pollutants, drilling operations and more.

In the next section, we provides a succinct description of the governing equations and the boundary conditions for the mixed convection over horizontal circular cylinder. This is followed by a presentation and discussion of the numerical results in Section 6.3, which include the variations of the skin friction coefficient and the heat transfer coefficient with the effects of the Pr number, conjugate and mixed parameter on the flow and heat transfer. Finally, Section 6.4 provides the concluding remarks about the finding of this problem

6.2 Mathematical Formulation

Next, we consider the problem of mixed convection flow of a viscous and incompressible fluid impinging to a horizontal circular cylinder with radius a , where the bottom surface of the cylinder heated by convection from hot fluid. The coordinates \bar{x} and \bar{y} are measured along the surface of the cylinder, starting with the lower stagnation point and normal to it, respectively. It is assumed that the free stream velocity is in the form of U_∞ and ambient temperature T_∞ . In addition, Boussinesq equations and boundary layer approximation are proved to be valid in this problem. Under these assumptions, the steady mixed convection boundary layer flow are given as follow

$$\left(\bar{u} \frac{\partial \bar{u}}{\partial \bar{x}} + \bar{v} \frac{\partial \bar{u}}{\partial \bar{y}} \right) = \rho \bar{u}_e \frac{\partial \bar{u}_e}{\partial \bar{x}} + \nu \frac{\partial^2 \bar{u}}{\partial \bar{y}^2} + \rho g \beta (\bar{T} - T_\infty) \sin \left(\frac{\bar{x}}{a} \right) \quad 6.1$$

$$\bar{u} \frac{\partial \bar{T}}{\partial \bar{x}} + \bar{v} \frac{\partial \bar{T}}{\partial \bar{y}} = \alpha \frac{\partial^2 \bar{T}}{\partial \bar{y}^2} \quad 6.2$$

where \bar{u} and \bar{v} are the velocity components along the \bar{x} and \bar{y} respectively, ρ is the fluid density, g is the gravitational acceleration, β is the thermal expansion coefficient, T is the fluid temperature in the boundary layer, α is the thermal diffusivity, ν is the kinematic viscosity and free stream velocity \bar{u}_e for the boundary layer equations is given by

$$\bar{u}_e = U_\infty \sin \left(\frac{\bar{x}}{a} \right) \quad 6.3$$

The boundary conditions for the flow and thermal fields are as Equation 4.3

In order to solve Equations 6.1 to 6.3, we introduce the following non-dimensional variables defined as

$$\begin{aligned} x = \bar{x}/a, \quad y = Re^{1/2}(\bar{y}/a), \quad u = \bar{u}/U_\infty, \quad u_e = \bar{u}_e/U_\infty \\ v = Re^{1/2}(\bar{v}/U_\infty) \quad \theta = \frac{\bar{T} - T_\infty}{T_f - T_\infty} \end{aligned} \quad 6.4$$

Substituting Equation 6.4 into Equations 6.1 to 6.3, we obtain the following boundary layer equations for the problem under consideration

$$u \frac{\partial u}{\partial x} + v \frac{\partial u}{\partial y} = u_e \frac{\partial u_e}{\partial x} + \frac{\partial^2 u}{\partial y^2} + \lambda \theta \sin x \quad 6.5$$

$$u \frac{\partial \theta}{\partial x} + v \frac{\partial \theta}{\partial y} = \frac{1}{Pr} \frac{\partial^2 \theta}{\partial y^2} \quad 6.6$$

The transformed boundary conditions are as Equationn 4.7. Here λ is the constant mixed convection parameter which are defined as

$$\lambda = \frac{Gr}{Re^2}, \quad Gr = \frac{g\beta(T_f - T_\infty)a^3}{\nu^2} \quad 6.7$$

It is worth mentioning that (i) $\lambda > 0$ for the assisting flow, (ii) $\lambda < 0$ for the opposing flow and (iii) $\lambda = 0$ for forced convection. Further, we introduce the following similarity transformation (Anwar et al., 2008; Salleh et al., 2010b),

$$\psi = xf(x,y), \quad \theta = \theta(x,y) \quad 6.8$$

where f is the dimensionless stream function, θ is the dimensionless temperature, and ψ is the stream function defined as usual. Using stream function, we get the resulting transformed equations

$$\frac{\partial^3 f}{\partial y^3} + f \frac{\partial^2 f}{\partial y^2} - \left(\frac{\partial f}{\partial y} \right)^2 + (\cos x + \lambda \theta) \frac{\sin x}{x} = x \left(\frac{\partial f}{\partial y} \frac{\partial^2 f}{\partial x \partial y} - \frac{\partial f}{\partial x} \frac{\partial^2 f}{\partial y^2} \right) \quad 6.9$$

$$\frac{1}{Pr} \frac{\partial^2 \theta}{\partial y^2} + f \frac{\partial \theta}{\partial y} = x \left(\frac{\partial f}{\partial y} \frac{\partial \theta}{\partial x} - \frac{\partial f}{\partial x} \frac{\partial \theta}{\partial y} \right) \quad 6.10$$

the boundary conditions 4.7 become

$$f = \frac{\partial f}{\partial y} = 0, \quad \frac{\partial \theta}{\partial y} = -\gamma(1 - \theta) \quad \text{at } y = 0$$

$$\frac{\partial f}{\partial y} \rightarrow \frac{\sin x}{x}, \quad \theta \rightarrow 0 \quad \text{as } y \rightarrow \infty$$
6.11

At the lower stagnation points of the cylinder $x \approx 0$, Equations 6.9 to 6.10 reduce to the following ordinary differential equations:

$$f''' + ff'' - (f')^2 + 1 + \lambda\theta = 0$$
6.12

$$\frac{1}{\text{Pr}}\theta'' + f\theta' = 0$$
6.13

while the boundary conditions (6.11) become

$$f(0) = f'(0) = 0, \quad \theta'(0) = -\gamma(1 - \theta(0)) \quad \text{at } y = 0$$

$$f'(y) \rightarrow 1, \quad \theta(y) \rightarrow 0 \quad \text{as } y \rightarrow \infty$$
6.14

Again similar to the previous chapter, the quantities of practical interest are the skin friction coefficients, which are defined in nondimensional form as

$$C_f = Re^{1/2} \frac{\tau_w}{\rho U_\infty^2}, \quad Q_w = Re^{-1/2} \frac{aq_w}{k(T_f - T_\infty)}$$
6.15

where k is the thermal conductivity of the fluid and q_w and τ_w are the skin friction and heat transfer coefficient respectively given by

$$\tau_w = \left(\mu \frac{\partial \bar{u}}{\partial \bar{y}} \right)_{\bar{y}=0}, \quad q_w = -k \left(\frac{\partial T}{\partial \bar{y}} \right)_{\bar{y}=0}$$
6.16

Using non-dimensional variables Equation 6.4 and the transformation 6.8, we obtain

$$C_f = x \frac{\partial^2 f}{\partial y^2}, \quad Q_w = -\frac{\partial \theta}{\partial y} = -\gamma(1 - \theta)$$
6.17

Detailed formulation can be accessed in Appendix E.

6.3 Results and Discussion

Equations 6.9 to 6.10 subject to the boundary conditions 6.11 were solved numerically. Only case of the assisting flow ($\lambda > 0$) is considered. The numerical solutions begin at the lower stagnation point of the cylinder ≈ 0 and proceed round the cylinder up to the separation point. For this case, it is important to note that the separation occurs at ($x = \frac{2}{3}\pi$) while those presented by Nazar (2003) for the case of constant wall temperature reach up to ($x = \pi$). Representative results for the skin friction coefficient C_f , heat transfer coefficient Q_w are obtained at the different positions $0 < x < 120^\circ$ and for the various values of mixed convection parameter λ , the Prandtl number Pr , and the convective parameter γ .

Furthermore, to assure the accuracy of the present method, a comparison of the results have been made with those of Eckert (1942) and Anwar et al. (2008). Eckert (1942) investigated the heat transfer around bodies meanwhile Anwar et al. (2008) studied mixed convection over viscoelastic fluid over horizontal circular cylinder. Both consider constant wall temperature at the boundary and solve the problem using a combination of series and numerical method. Also, for limiting cases ($\gamma \rightarrow \infty$), constant wall temperature results were attained when large values of γ were applied in the boundary conditions. The results in Table 6.1 manifest that the numerical results obtained by the present author were found to be almost compatible to a reasonable degree with the result of Eckert (1942) and Anwar et al. (2008).

Table 6.1. Comparison results for the heat transfer coefficient with $Pr = 1$, $\lambda = -1, 0, 1$ and $\gamma \rightarrow \infty$

λ	Eckert (1942) Series	Anwar et al. (2008). Keller-box	Present results Keller-box
-1	-	0.5095	0.5072
0	0.5700	0.5706	0.5704
1	-	0.6156	0.6153

The variation of C_f and Q_w is illustrated in Figures 6.1 through 6.6. As shown in Figure 6.1, the value of C_f is higher for small Prandtl numbers while the different pattern is observed in the case of Q_w as displayed in Figure 6.2. Furthermore, the graph of C_f and Q_w at different positions of x and various values of convective parameter γ can be seen in Figure 6.3 and 6.4. Indeed, it is shown that the value of C_f decreases as γ increases and the value of Q_w increases as γ increases. For the heated cylinder ($\lambda > 0$), the values of C_f are higher for

the high value of λ as seen in Figure 6.5. Conversely in Figure 6.6, increasing λ leads to the decrease in Q_w .

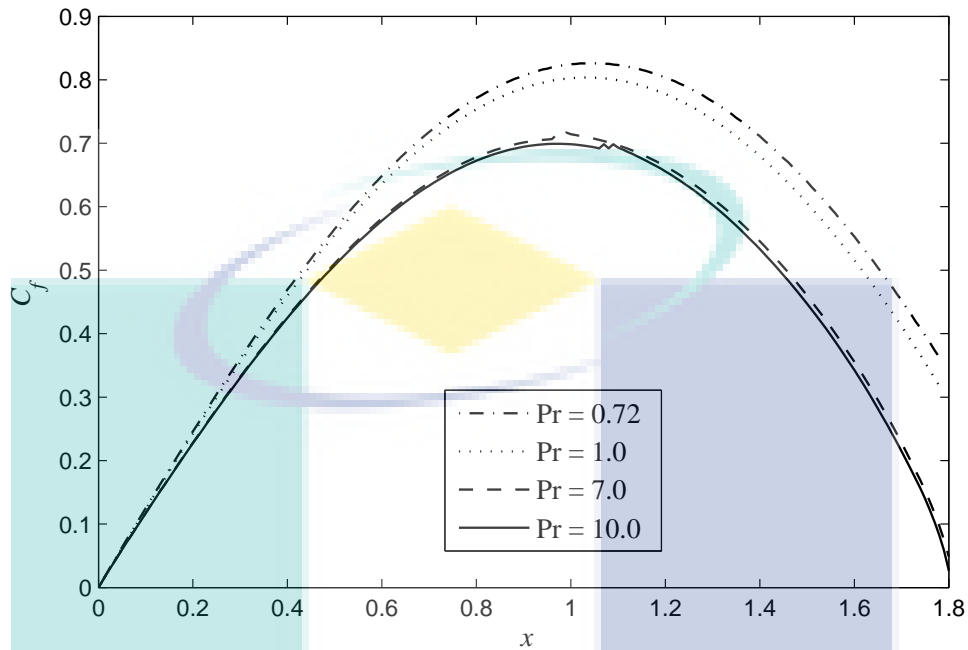


Figure 6.1. Variation of skin friction coefficient C_f for $\lambda = 1$, $\gamma = 0.1$ and various values of Pr

Figures 6.7 and 6.8 display the effect of convective parameter γ on the velocity and temperature profiles. It is observed that increasing γ leads to the increase of the temperature and velocity profiles. This is because, as γ increases, the convective heat transfer from the hot fluid on the surface of the cylinder to the cold side increase therefore, leading to an increase in both the velocity and the temperature profiles.

Figures 6.9 and 6.10 illustrate the effects of the Pr number on the velocity and temperature profiles respectively. The velocity and temperature decrease as Pr increases. The physical meaning behind this has been explained earlier in Chapter 4.

Figures 6.11 and 6.12 present the behaviour of the velocity and temperature profiles with a change in the values of mixed convection parameters λ . From these figures, it is evident that the velocity profile increases but the temperature profile decreases as λ increases. This is because when λ increases, the convection cooling effect increases and hence the fluid flow accelerates. Therefore the temperature reduces. Also, for high λ number, there exists an overshoot of the velocity profile from the free stream velocity. Finally, it is observed from the profiles in Figures 6.7 through to 6.12 that they satisfy the far field boundary conditions asymptotically, which support the numerical result obtained.

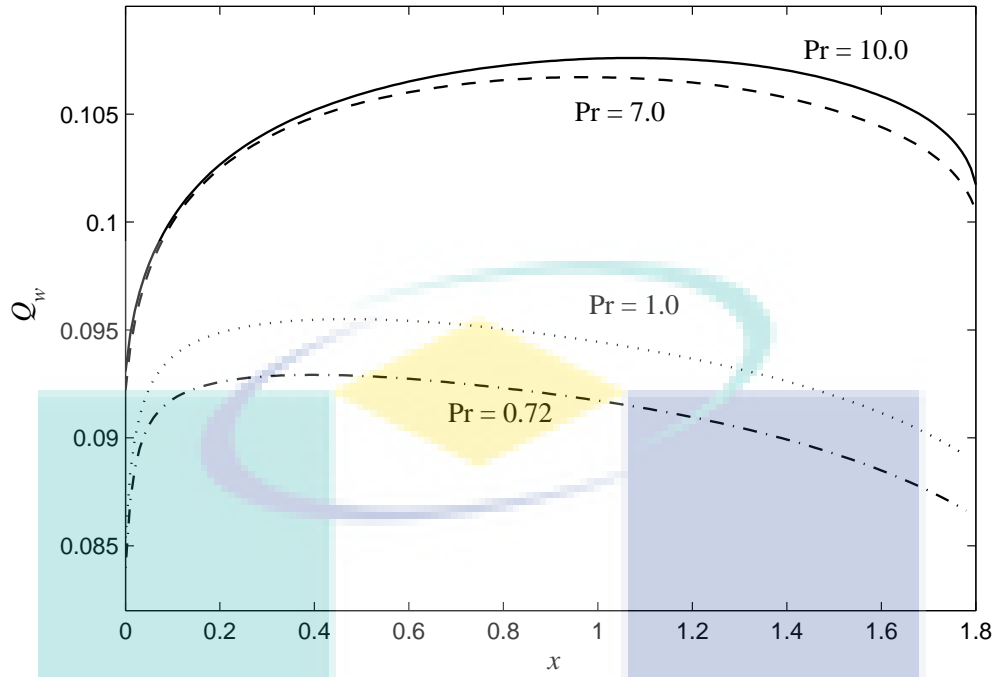


Figure 6.2. Variation of heat transfer coefficient Q_w for $\lambda = 1$, $\gamma = 0.1$ and various values of Pr

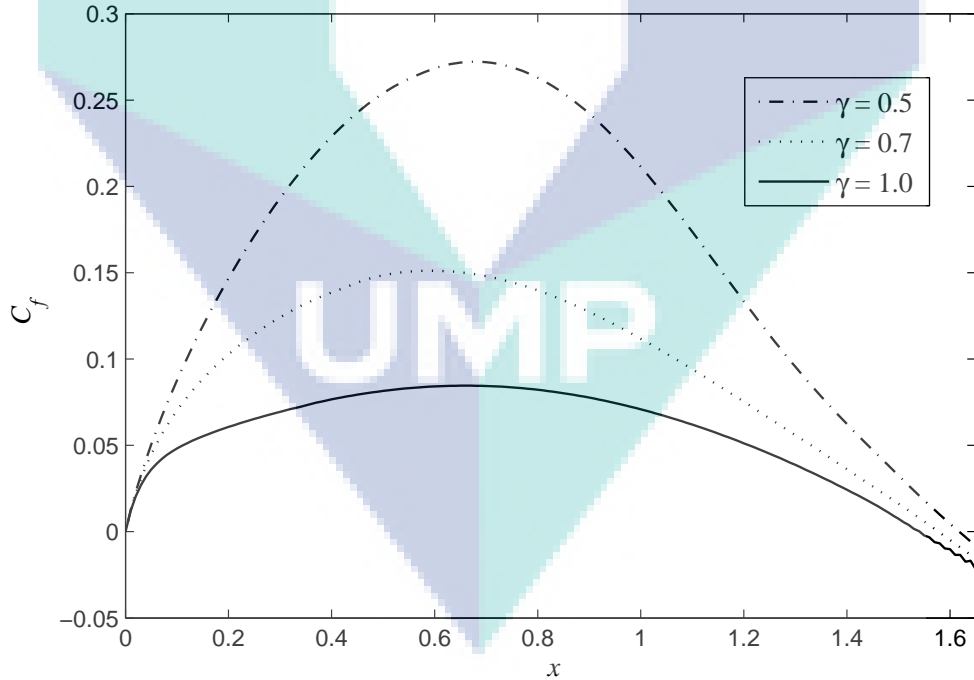


Figure 6.3. Variation of the skin friction coefficient C_f for $\lambda = 1$, $Pr = 7.0$ and various values of γ

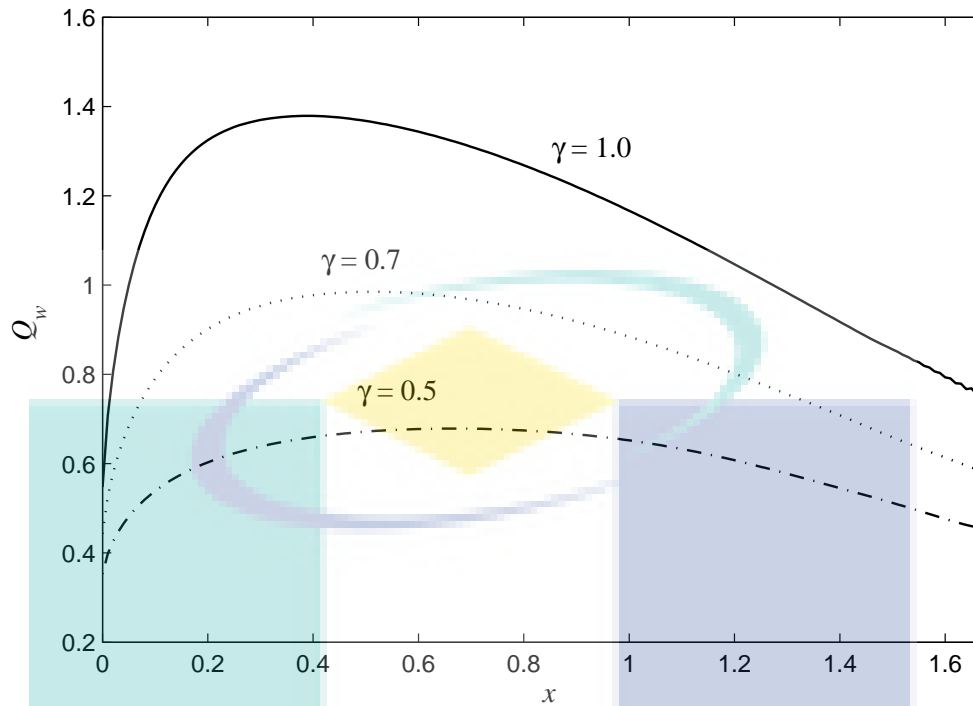


Figure 6.4. Variation of the heat transfer coefficient Q_w for $\lambda = 1$, $Pr = 7.0$ and various values of γ

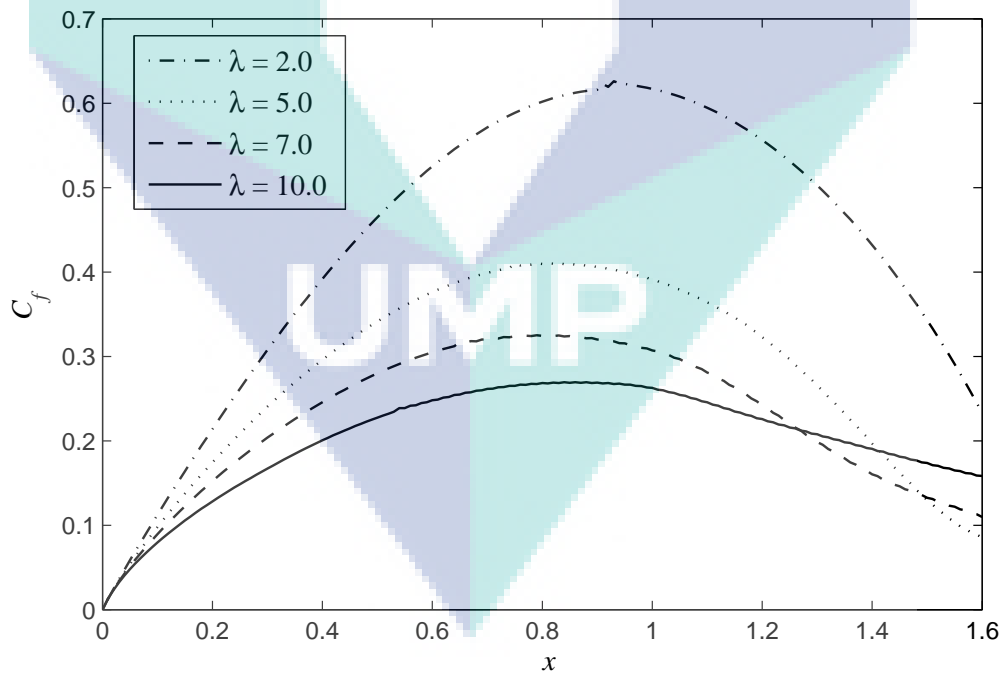


Figure 6.5. Variation of the skin friction coefficient C_f for $Pr = 7.0$, $\gamma = 0.1$ and various values of λ

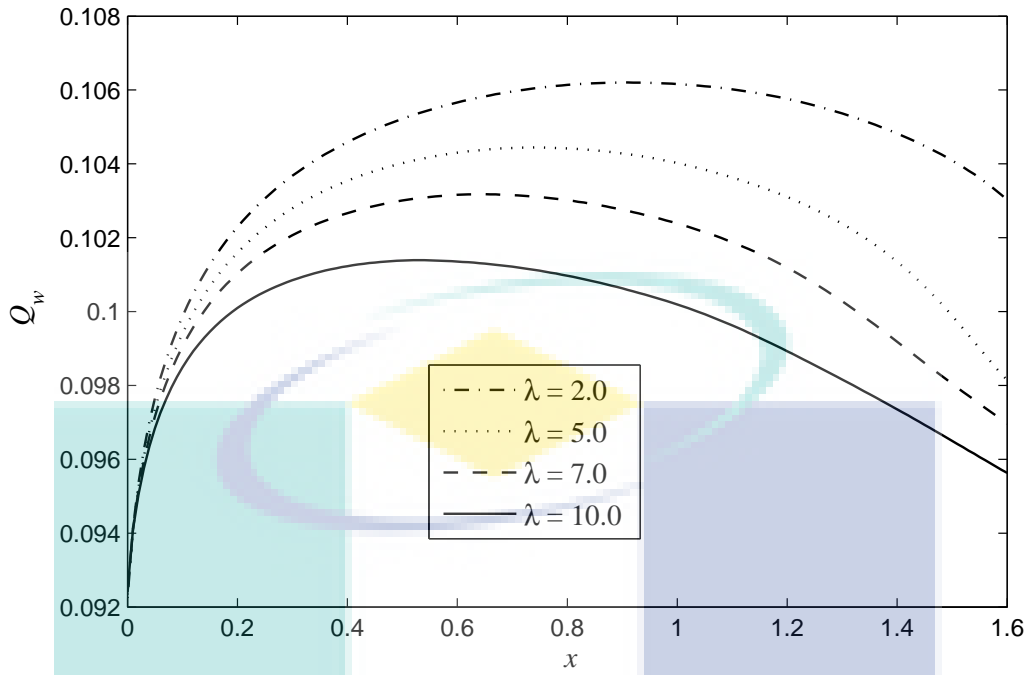


Figure 6.6. Variation of the heat transfer coefficient Q_w for $Pr = 7.0$, $\gamma = 0.1$ and various values of λ

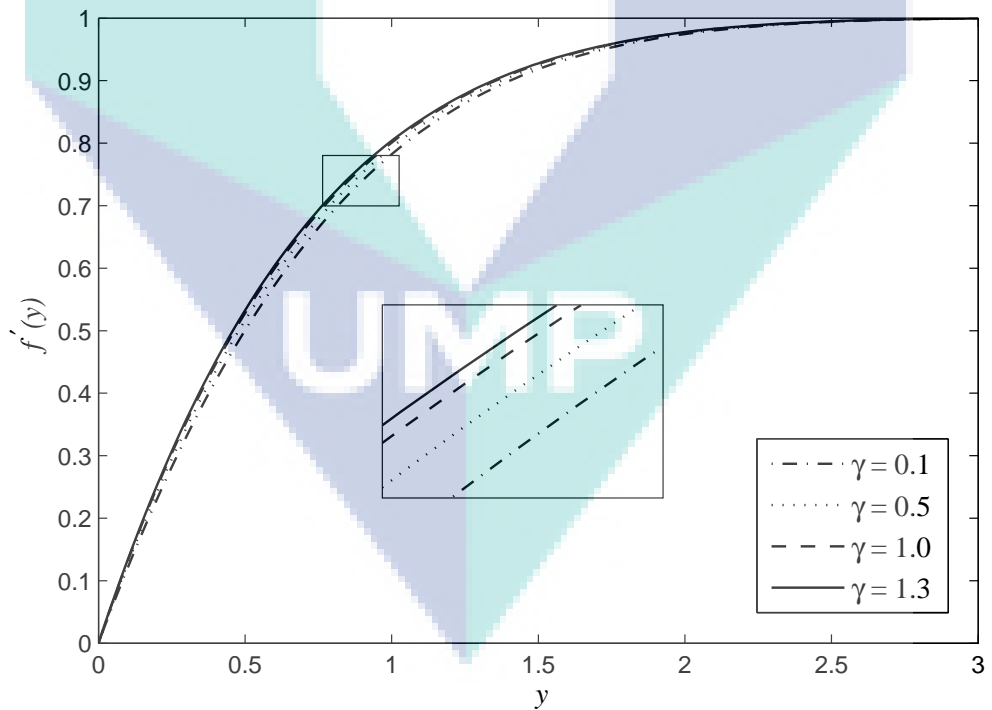


Figure 6.7. Velocity profiles $f'(y)$ for various values of γ when $Pr = 7$ and $\lambda = 1.0$

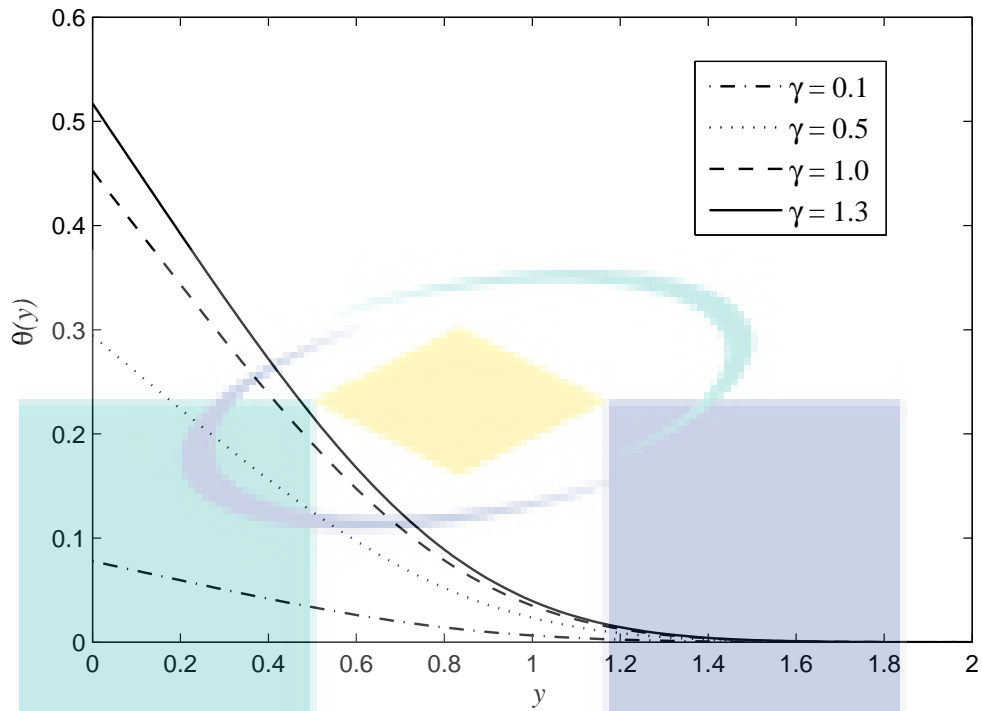


Figure 6.8. Temperature profiles $\theta(y)$ for various values of γ when $Pr = 7$ and $\lambda = 1.0$

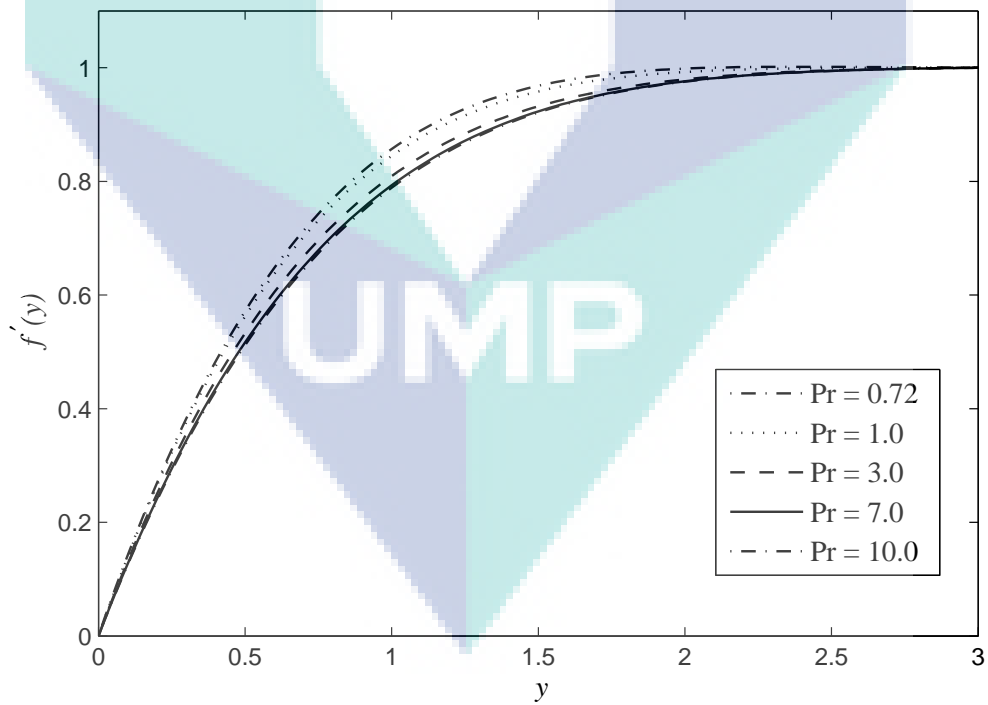


Figure 6.9. Velocity profiles $f'(y)$ for various values of Pr when $\gamma = 0.1$ and $\lambda = 1.0$

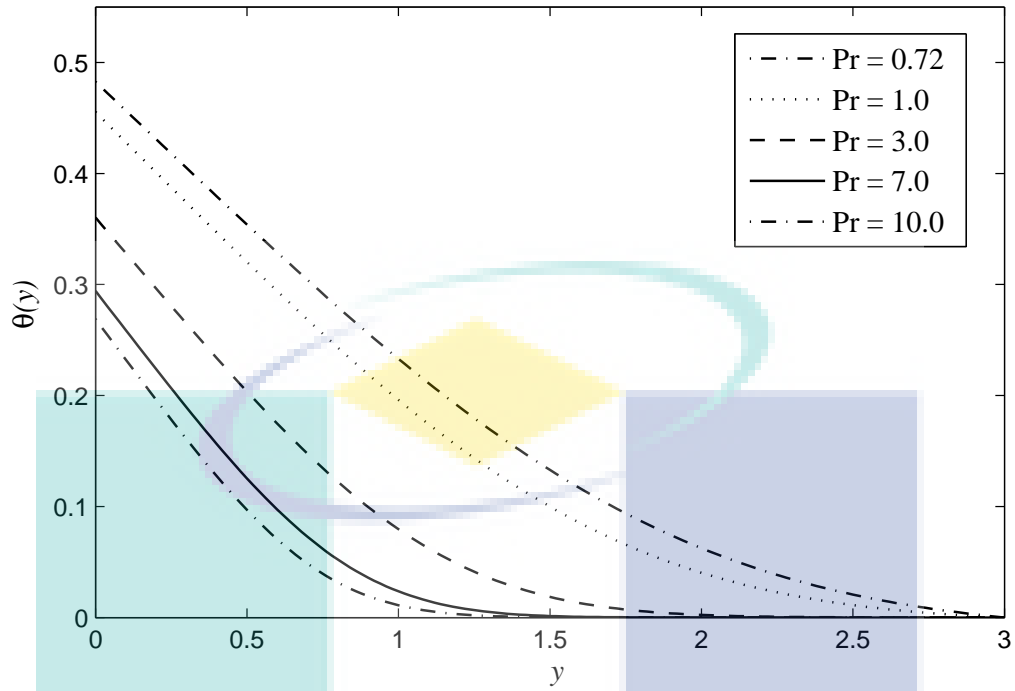


Figure 6.10. Temperature profiles $\theta(y)$ for various values of Pr when $\gamma = 0.1$ and $\lambda = 1.0$

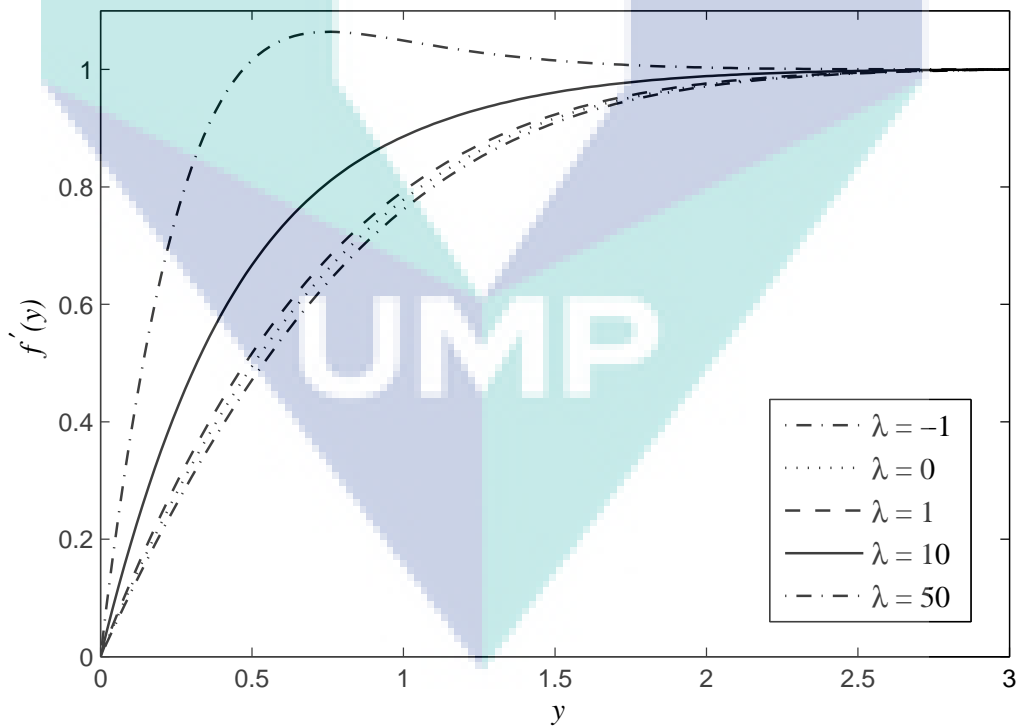


Figure 6.11. Velocity profiles $f'(y)$ for various values of λ when $Pr = 7.0$ and $\gamma = 0.1$

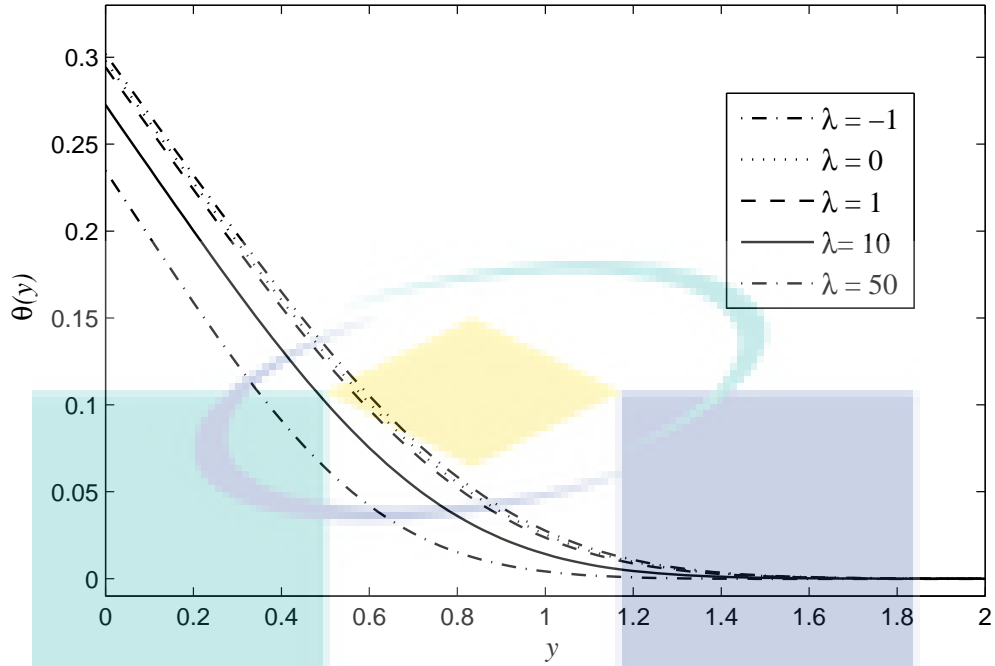


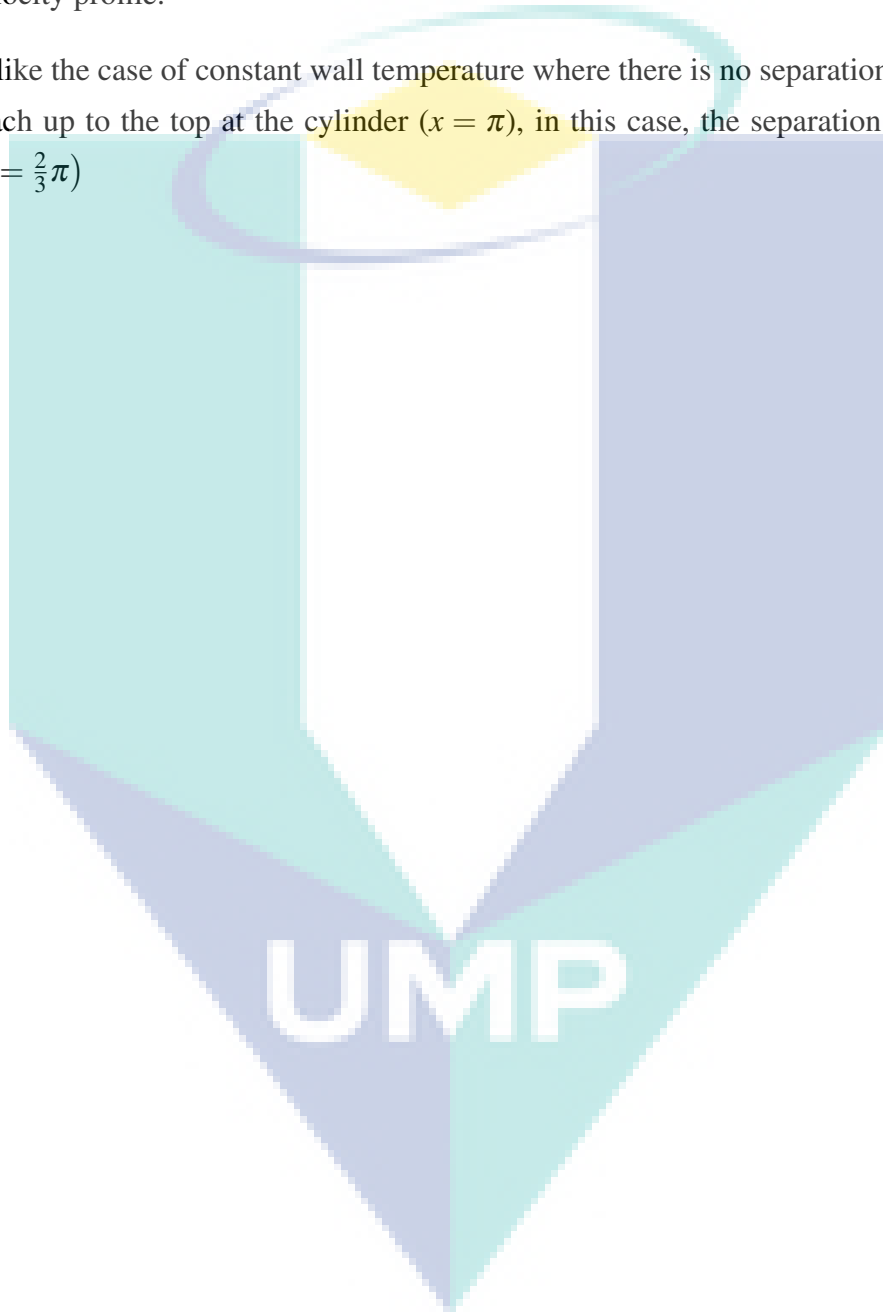
Figure 6.12. Temperature profiles $\theta(y)$ for various values of λ when $Pr = 7.0$ and $\gamma = 1.0$

6.4 Conclusions

The mixed convection boundary layer on a horizontal circular cylinder was considered where there was a convective boundary condition relating the surface temperature to the surface heat flux. By taking specific forms for the outer flow and surface heat transfer parameter, it reduced the problem to a system of non-similarity equations. Apart from the convective parameter γ , the problem involved two other parameters: the Prandtl number Pr and the mixed convection parameter λ . Besides that, we also looked into the effects of the skin friction coefficient and the heat transfer coefficient on the flow and heat transfer characteristics. Numerical results for the velocity and temperature profiles were reported in figurative form. Therefore, from this study, the following conclusions can be drawn:

- i) skin friction coefficient C_f is higher for small Prandtl number and convective parameter, however as the mixed convection λ increases, C_f is increases
- ii) heat transfer coefficient Q_w shows an increase for the increase value of Prandtl number and convective parameter, and opposite trend is observed when λ increase

- iii) the temperature profile $\theta(y)$ increases when the convective parameter γ increases, and different patterns are observed for the increase in the Pr number and the mixed convection parameter λ .
- iv) as the value of the convective parameter γ and mixed convection parameter λ increase, the velocity profile increases, while the increase in Pr number led to a decrease in the velocity profile.
- v) unlike the case of constant wall temperature where there is no separation as the flow can reach up to the top at the cylinder ($x = \pi$), in this case, the separation occur earlier at ($x = \frac{2}{3}\pi$)



CHAPTER 7

MIXED CONVECTION BOUNDARY LAYER FLOW OVER A HORIZONTAL CIRCULAR CYLINDER IN A NANOFUID: TIWARI AND DAS MODEL

7.1 Introduction

In this chapter, the problem associated with the mixed convection boundary layer flow over the horizontal circular cylinder immersed in nanofluid is considered and discussed. Early research on the mixed convection in a viscous fluid has previously been discussed in Chapter 5. Therefore this chapter will focus on the development of the mixed convection immersed in a nanofluid.

Conventional fluids such as oil, ethylene glycol mixture, and water are attributed with low thermal conductivity and thus resulting in the limitation to enhance the performance of many engineering devices. Due to this drawback, there is a strong need among researchers to develop advanced heat transfer fluids producing higher conductivities and consequently improve the thermal characteristics. An innovative method of improving the thermal conductivities of a fluid is to suspend metallic nanoparticles within the fluid (Tiwari and Das, 2007). The thermal conductivities of fluids with suspended particle are expected to be higher than those of common fluids.

The process of suspended metallic, non-metallic or polymeric nano-sized particle in a fluid is called nanofluids. The procedure of preparing the suspended particle of nanofluid is given in the paper by Xuan (2000) where they highlight that thermal conductivity of nanofluid remarkably increases with the volume fraction of the particle.

Two successful models for convective transport in nanofluids are found in the literature namely the Tiwari and Das, and Buongiorno model. Tiwari and Das focus on heat transfer enhancement via the solid volume fraction of different nanoparticles and base fluid. On the other hand, Buongiorno proposed that the nanoparticle absolute velocity can be viewed as the sum of base fluid velocity and relative velocity (slip velocity) which

addresses the important aspect of the Brownian motion, and thermophoresis parameters. There are many excellent reviews on convective transport in nanofluids have been reported by Daungthongsuk and Wongwises (2007) and Sheikholeslami and Ganji (2016). In this chapter, the model of nanofluid proposed by Tiwari and Das is applied as the model which notably has been successfully used in many of the research journals.

In the next section, we provides a succinct description of the governing equations and the boundary conditions for the mixed convection boundary layer over cylinder in nanofluids using Tiwari and Das model. This is followed by a presentation and discussion of the numerical results in Section 7.3, which include the effects of the governing parameter on the heat and flow. Finally, Section 7.4 provides the concluding remarks about the findings of the problem.

7.2 Mathematical Formulation

Consider the steady two-dimensional mixed convection flow of a nanofluid past a circular cylinder of radius a and wall temperature T_w . It is assumed that the free stream velocity is in the form of $\bar{u}_e(\bar{x})$ and the ambient temperature is T_∞ . The coordinates \bar{x} and \bar{y} are measured along the surface of the cylinder, starting with the lower stagnation point and normal to it, respectively.

The basic steady mixed convection boundary layer flow for a nanofluid in Cartesian coordinates are (Tiwari and Das, 2007),

$$\bar{u} \frac{\partial \bar{u}}{\partial \bar{x}} + \bar{v} \frac{\partial \bar{u}}{\partial \bar{y}} = -\frac{1}{\rho_{nf}} \frac{\partial \bar{p}}{\partial \bar{x}} + \frac{\mu_{nf}}{\rho_{nf}} \frac{\partial^2 \bar{u}}{\partial \bar{y}^2} + \frac{\phi \rho_s \beta_s + (1 - \phi) \rho_f \beta_f}{\rho_{nf}} g (\bar{T} - T_\infty) \sin\left(\frac{\bar{x}}{a}\right) \quad 7.1$$

$$\bar{u} \frac{\partial \bar{T}}{\partial \bar{x}} + \bar{v} \frac{\partial \bar{T}}{\partial \bar{y}} = \alpha_{nf} \left(\frac{\partial^2 \bar{T}}{\partial \bar{x}^2} + \frac{\partial^2 \bar{T}}{\partial \bar{y}^2} \right) \quad 7.2$$

The boundary conditions for the flow and thermal field are same as Equation 4.3. Here \bar{u} and \bar{v} are the velocity components along the \bar{x} and \bar{y} axes respectively, T is the fluid temperature, \bar{p} is the fluid pressure, β_f is the thermal coefficient expansion of the fluid fraction, β_s is the thermal expansion coefficient of solid fraction, α_{nf} is the thermal

diffusivity of the nanofluid, ρ_{nf} is the density of the nanofluid, ρ_f is the density of the fluid fraction, ρ_s is the density of the solid fraction, μ_f is the viscosity of the fluid fraction and μ_{nf} is the viscosity of the nanofluid, which are given by Oztop and Abu-Nada (2008). The bottom surface of cylinder is heated by convection from hot fluid of temperature T_f which provides heat transfer coefficient h_f . Further, k is the thermal conductivity and $T_f > T_\infty$.

In order to solve Equations 7.1 to 7.2, we introduce the following non-dimensional variables defined as

$$\begin{aligned} x &= \bar{x}/a, & y &= Re^{1/2}(\bar{y}/a), & u &= \bar{u}/U_\infty, & v &= Re^{1/2}(\bar{v}/U_\infty) \\ \theta &= \frac{T - T_\infty}{T_f - T_\infty}, & p &= \frac{\bar{p} - p_\infty}{\rho_{nf} U_\infty^2} \end{aligned} \quad 7.3$$

where ν_f is the kinematic viscosity of the fluid. Substituting these variables into Equations 7.1 to 7.2 and making use of the boundary layer approximation, namely that $Re \rightarrow \infty$, we obtain the following boundary layer equations for the problem under consideration in dimensionless form:

$$u \frac{\partial u}{\partial x} + v \frac{\partial u}{\partial y} = -\frac{\partial p}{\partial x} + \frac{\mu_{nf}}{\rho_{nf} \nu_f} \frac{\partial^2 u}{\partial y^2} + \frac{\phi \rho_s (\beta_s / \beta_f) + (1 - \phi) \rho_f}{\rho_{nf}} \lambda \theta \sin x \quad 7.4$$

$$u \frac{\partial \theta}{\partial x} + v \frac{\partial \theta}{\partial y} = \frac{1}{Pr} \frac{\alpha_{nf}}{\alpha_f} \frac{\partial^2 \theta}{\partial y^2} \quad 7.5$$

The boundary conditions become 4.7. From Equation 7.4 that $p = p(x)$, we have

$$-\frac{\partial p}{\partial x} = u_e \frac{\partial u_e}{\partial x} \quad 7.6$$

Therefore we have to solve the following boundary layer

$$\begin{aligned} u \frac{\partial u}{\partial x} + v \frac{\partial u}{\partial y} &= u_e \frac{\partial u_e}{\partial x} + \frac{1}{(1 - \phi)^{2.5} [1 - \phi + (\phi \rho_s / \rho_f)]} \frac{\partial^2 u}{\partial y^2} \\ &+ \left[\frac{\phi \rho_s}{(1 - \phi) \rho_f + \phi \rho_s} \left(\frac{\beta_s}{\beta_f} \right) + \frac{(1 - \phi) \rho_f}{\phi \rho_s + (1 - \phi) \rho_f} \right] \lambda \sin x \end{aligned} \quad 7.7$$

$$u \frac{\partial \theta}{\partial x} + v \frac{\partial \theta}{\partial y} = \frac{1}{Pr} \frac{k_{nf}/k_f}{(1-\phi) + (\phi(\rho C_p)_s/(\rho C_p)_f)} \frac{\partial^2 \theta}{\partial y^2} \quad 7.8$$

where k_{nf} is effective thermal conductivity of the nanofluids, k_f is the thermal conductivity of the fluid, k_s is the thermal conductivity of the solid, $(\rho C_p)_{nf}$ is the heat capacity of the nanofluid, ϕ is the nanoparticles volume fraction or solid volume fraction of the nanofluid defined as

$$\begin{aligned} \alpha_{nf} &= \frac{k_{nf}}{(\rho C_p)_{nf}}, & \rho_{nf} &= (1-\phi)\rho_f + \phi\rho_s, & \mu_{nf} &= \frac{\mu_f}{(1-\phi)^{2.5}} \\ (\rho C_p)_{nf} &= (1-\phi)(\rho C_p)_f + \phi(\rho C_p)_s, & \frac{k_{nf}}{k_f} &= \frac{(k_s + 2k_f) - 2\phi(k_f - k_s)}{(k_s + 2k_f) + \phi(k_f - k_s)} \end{aligned} \quad 7.9$$

with the boundary conditions 4.7. The solution of Equations 7.7 to 7.8 are in the form of

$$\psi = xf(x,y), \quad \theta = \theta(x,y) \quad 7.10$$

where ψ is the stream function. By substituting Equation 7.10 into Equations 7.7 and 7.8, and taking account that $u_e(x) = \sin x$, we obtain:

$$\begin{aligned} & \frac{1}{(1-\phi)^{2.5}[1-\phi + (\phi\rho_s/\rho_f)]} \frac{\partial^3 f}{\partial y^3} + f \frac{\partial^2 f}{\partial y^2} - \left(\frac{\partial^2 f}{\partial y^2} \right)^2 + \frac{\sin x \cos x}{x} \\ & + \left[\frac{\phi\rho_s}{(1-\phi)\rho_f + \phi\rho_s} \left(\frac{\beta_s}{\beta_f} \right) + \frac{(1-\phi)\rho_f}{\phi\rho_s + (1-\phi)\rho_f} \right] \frac{\lambda \theta \sin x}{x} \\ & = x \left(\frac{\partial f}{\partial y} \frac{\partial^2 f}{\partial x \partial y} - \frac{\partial f}{\partial x} \frac{\partial^2 f}{\partial y^2} \right) \end{aligned} \quad 7.11$$

$$\frac{1}{Pr} \frac{k_{nf}/k_f}{(1-\phi) + (\phi(\rho C_p)_s/(\rho C_p)_f)} \frac{\partial^2 \theta}{\partial y^2} + f \frac{\partial \theta}{\partial x} = x \left(\frac{\partial f}{\partial y} \frac{\partial \theta}{\partial x} - \frac{\partial f}{\partial x} \frac{\partial \theta}{\partial y} \right) \quad 7.12$$

along with boundary conditions Equation 6.11. Near the lower stagnation point of the cylinder $x \approx 0$, Equations 7.11 and 7.12 reduce to the ordinary differential equations:

$$\frac{1}{(1-\phi)^{2.5} \left[1 - \phi + (\phi \rho_s / \rho_f) \right]} f''' + f f'' - (f')^2 + 1 + \left[\frac{\phi \rho_s}{(1-\phi) \rho_f + \phi \rho_s} \left(\frac{\beta_s}{\beta_f} \right) + \frac{(1-\phi) \rho_f}{\phi \rho_s + (1-\phi) \rho_f} \right] \lambda \theta = 0 \quad 7.13$$

$$\frac{1}{Pr (1-\phi) + \phi (\rho C_p)_s / (\rho C_p)_f} \frac{k_{nf}/k_f}{\theta''} + f \theta' = 0 \quad 7.14$$

and the boundary conditions becomes as Equation 6.14. It is worth to mention here that when $(\phi = 0)$ this is the case for regular fluid and Equations (7.13) and (7.14) reduced to those derived by Merkin (1977). Meanwhile, for the case when $\gamma \rightarrow \infty$ this case reduced to constant wall temperature as solved by Tham et al. (2012).

Therefore, the primary objective of this study is to estimate the skin friction coefficient C_f , and the Nusselt number Nu_x . Importantly, these parameters characterise the surface drag and the wall heat, respectively. The physical quantities of interest in this case are the skin friction coefficient C_f and the Nusselt number Nu_x which are defined as

$$C_f = \frac{\tau_w}{\rho_f U_\infty^2}, \quad Nu = \frac{aq_w}{k_f (T_f - T_\infty)} \quad 7.15$$

where τ_w is the skin friction coefficient or the shear stress at the surface of the cylinder and q_w is the heat flux from the surface of the cylinder, which are given by

$$\tau_w = \mu_{nf} \left(\frac{\partial \bar{u}}{\partial \bar{y}} \right), \quad q_w = -k_{nf} \left(\frac{\partial \bar{T}}{\partial \bar{y}} \right) \quad 7.16$$

Substituting Equations 7.3 and 7.10 into Equations 7.16 and 7.17, we get

$$Re_x^{1/2} C_f = \frac{1}{(1-\phi)^{2.5} x} \frac{\partial^2 y}{\partial y^2}(x, 0), \quad Re_x^{-1/2} Nu = -\frac{k_{nf}}{k_f} \frac{\partial \theta}{\partial y}(x, 0) \quad 7.17$$

Detailed formulation can be accessed in Appendix F.

7.3 Results and Discussion

The partial differential Equations 7.11 and 7.12 with corresponding boundary conditions 6.11 were solved numerically using an efficient implicit difference scheme. The numerical investigation of the boundary problem has been carried out for the following parameters : the solid volume fraction parameter ($\phi = 0.0$ to 0.2), the mixed conjugate parameter ($\lambda = -1.0$ to 5.0), the convective parameter ($\gamma = 0$ to 0.3), and the Prandtl number $Pr = 6.2$ (water-based fluid). Three different types of nanoparticles, namely Al_2O_3 , Cu , and TiO_2 (with water as their base fluid) have been considered in this study as these nanoparticles are well known and have been excessively used in many experimental works. Representative results for the skin friction coefficient $Re_x^{1/2}C_f$ and the local Nusselt number $Re_x^{-1/2}Nu$, have been obtained for the following range of the nanoparticle volume fraction $\phi = 0$ (regular fluids) at different positions x with a different number of parameters. Notably, this study reduces those of a viscous or regular fluid when $\phi = 0$. Data is applied to the thermophysical properties of the the fluid and nanoparticles as listed in Table 7.1 (Oztop and Abu-Nada, 2008) to compute each case of nanofluid.

Table 7.1. Thermophysical properties of fluid and nanoparticles

Physical properties	Fluid phase	Cu	Al_2O_3	TiO_2
$C_p(J/kgK)$	4179	3.85	765	686.2
$\rho(kg/m^3)$	997.1	8933	3970	4250
$k(W/mK)$	0.613	400	40	8.9538
$\beta \times 10^{-5}(1/K)$	21	167	0.85	0.9

The solution process starts at $x \approx 0$ where the Equations 7.11 and 7.12 are solved moving forward to reach the solutions. Based on the computation, the separation point for this case is limited at ($x = 120^\circ$). Indeed, this result differs when applying the constant wall temperature where the separation process can reach up to ($x = 180^\circ$). Therefore, the separation process occurs faster when the convective boundary condition is applied. The present models have been validated successfully against the works of Merkin (1977) and Tham et al. (2012) for problem of mixed convection over horizontal circular cylinder at $\gamma \rightarrow \infty$ (CWT) as shown in Table 7.2. In the report by Merkin (1977), two series solutions are obtained, one of which is valid near the leading edge of the cylinder and the other is valid asymptotically. The comparison indicates that the previous results and the current ones are found to be in good agreement. Therefore, the present numerical result obtained is found to be reliable and accurate.

Table 7.2. Values of local Nusselt number, $Re_x^{-1/2}Nu$ for $\phi = 0.0, Pr = 1, \gamma \rightarrow \infty$, and various values of λ

λ	Merkin (1977)	Tham et al. (2012)	Present result
	Series	Keller-box	Keller-box
0.0	0.5705	0.5705	0.5700
0.5	0.5943	0.5945	0.5938
1.0	0.6156	0.6156	0.6148
2.0	0.6497	0.6515	0.6510
5.0	0.7315	0.7315	0.7302

Figures 7.1 to 7.3 demonstrate the skin friction coefficient $Re_x^{1/2}C_f$ and Figures 7.4 to 7.6 demonstrate the local Nusselt number $Re_x^{-1/2}Nu$ of each nanoparticle with the nanoparticle volume fraction $\phi = 0.0, 0.1$ and 0.2 respectively. Naturally for each and all three nanoparticles cases, the skin friction coefficient increases with the increment of ϕ . The similar pattern is observed for the local Nusselt number $Re_x^{-1/2}Nu$ where the increases in ϕ increases the local Nusselt number. However, both the skin friction and the local Nusselt number decrease as λ increases.

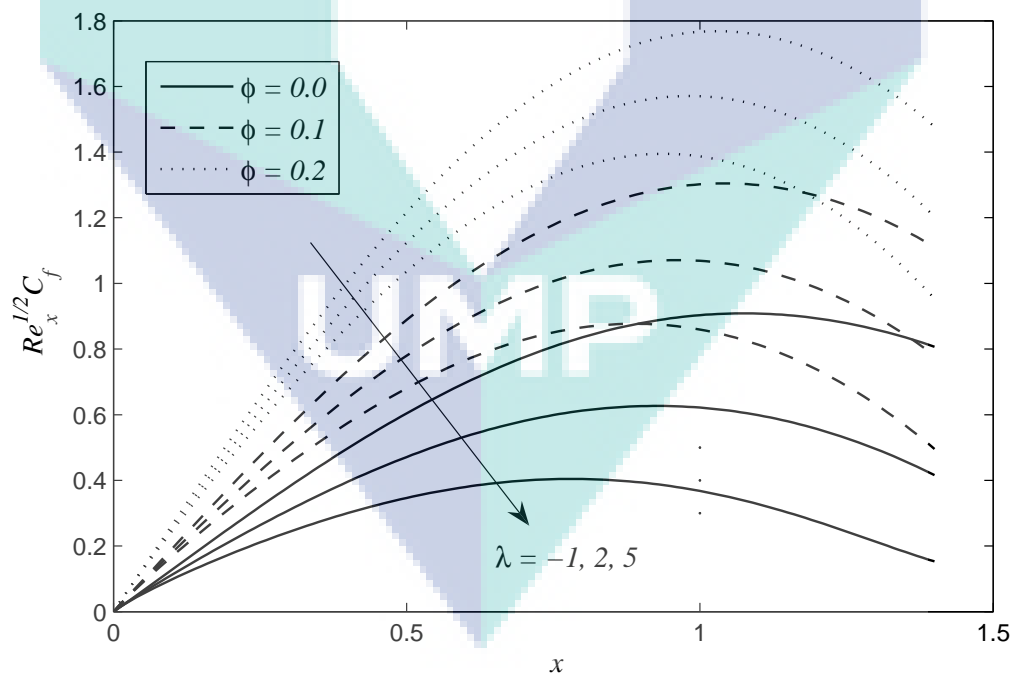


Figure 7.1. Comparison of the skin friction coefficient $Re_x^{1/2}C_f$ using Cu nanoparticles with $\phi = 0, 0.1, 0.2, \gamma = 0.1, Pr = 6.2$ and various values of λ

Figure 7.7 and 7.9 illustrate the velocity profiles, f' and meanwhile Figure 7.10 and 7.12 display the temperature profile $\theta(y)$ at the lower stagnation point of the cylinder $x \approx 0$ of the each nanoparticles (Cu, Al_2O_3 and TiO_2) respectively with $\phi = 0.0, 0.1$ and 0.2 . For each and all three nanoparticles, the velocity layer thickness increases with the increment of λ . Also, the thermal boundary layer thickness increases as λ increases.

On the other hand, Figure 7.13 displays the skin friction coefficient $Re_x^{1/2}C_f$ and Figure 7.14 illustrates the local Nusselt number $Re_x^{-1/2}Nu$ of each nanoparticle for various values of the convective parameter γ . Indeed, these figures show that for each nanoparticles cases, the skin friction coefficient $Re_x^{1/2}C_f$ decreases with the increment of γ . The different situation occurs for the local Nusselt number $Re_x^{-1/2}Nu$ as it increases with the increment of γ . Increasing γ leads to an increase in the velocity and temperature profile as seen in Figures 7.15 and 7.16. This is because as γ increases, the convective heat transfer from the hot nanofluid side on the surface of the cylinder to the cold nanofluid side increases, thereby leading to an increase in both the velocity and temperature gradient. From all the velocity and temperature profiles, it is also observed that the profiles satisfy the far field boundary conditions asymptotically, as such, this supports the validity of the numerical result obtained.

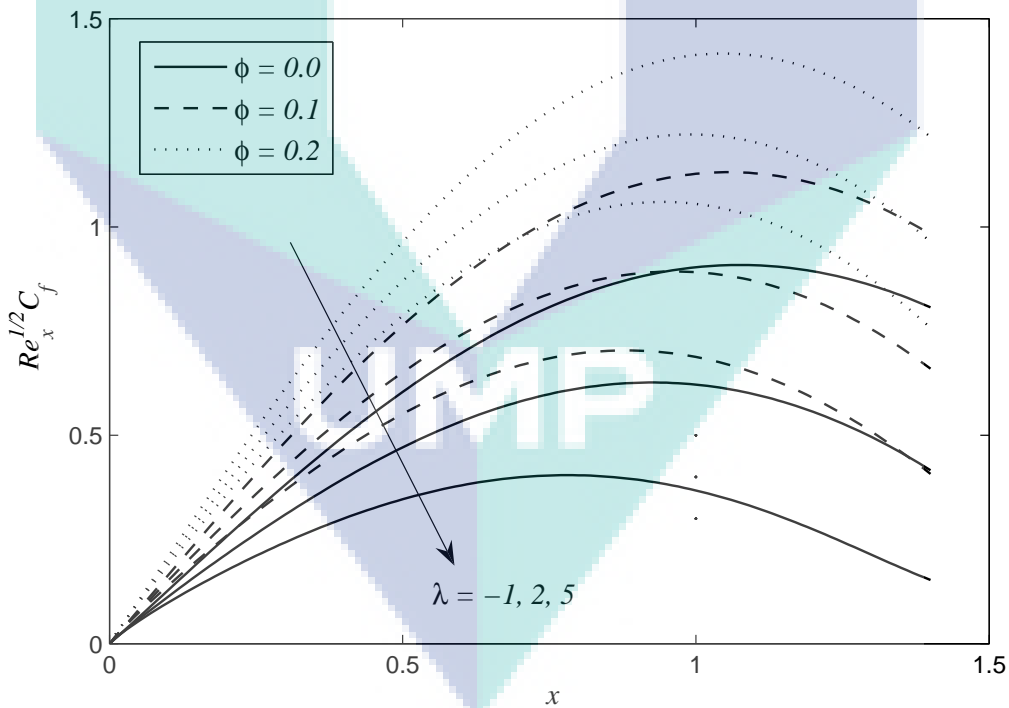


Figure 7.2. Comparison of the skin friction coefficient $Re_x^{1/2}C_f$ using Al_2O_3 nanoparticles with $\phi = 0, 0.1, 0.2$, $\gamma = 0.1$, $\text{Pr} = 6.2$ and various values of λ

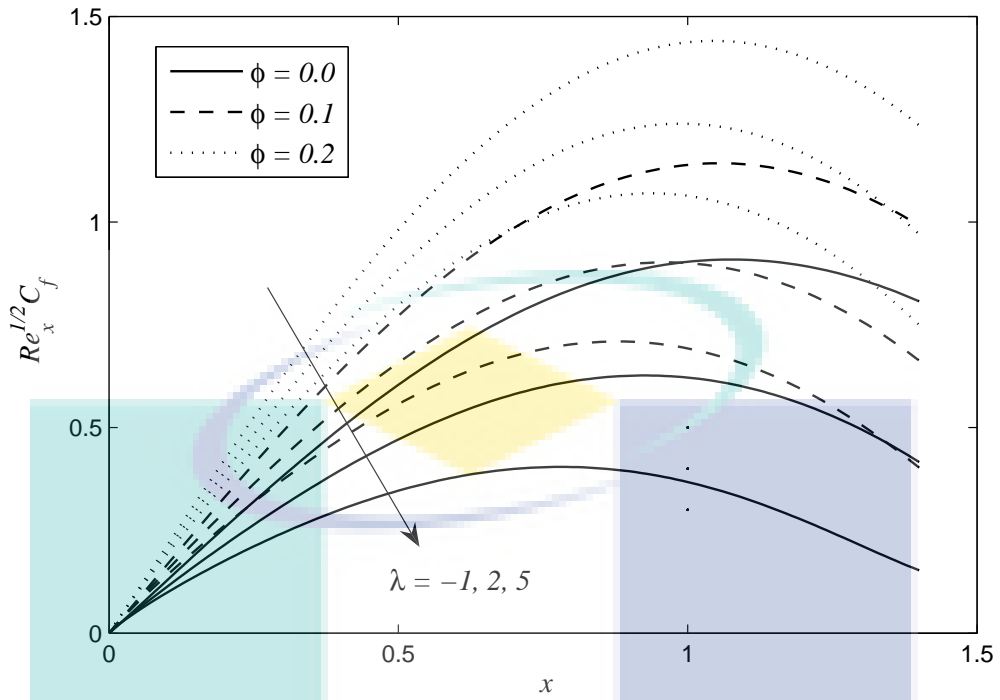


Figure 7.3. Comparison of the skin friction coefficient $Re_x^{1/2} C_f$ using TiO_2 nanoparticles with $\phi = 0, 0.1, 0.2$, $\gamma = 0.1$, $Pr = 6.2$ and various values of λ

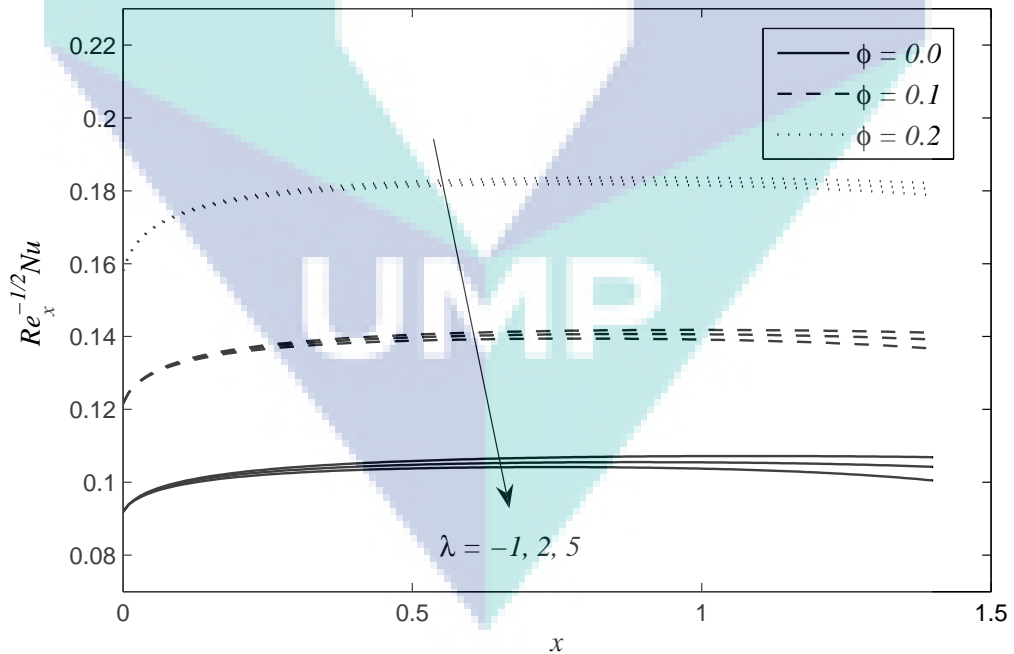


Figure 7.4. Comparison of the local Nusselt number $Re_x^{-1/2} Nu$ using Cu nanoparticles with $\phi = 0, 0.1, 0.2$, $\gamma = 0.1$, $Pr = 6.2$ and various values of λ

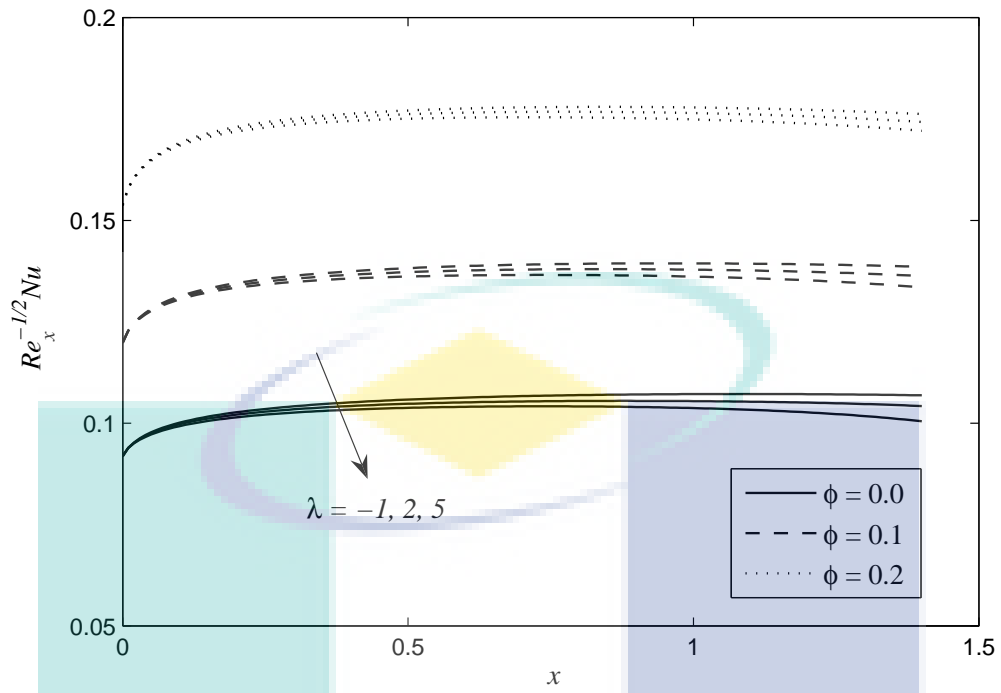


Figure 7.5. Comparison of the local Nusselt number $Re_x^{-1/2}Nu$ using Al_2O_3 nanoparticles with $\phi = 0, 0.1, 0.2$, $\gamma = 0.1$, $Pr = 6.2$ and various values of λ

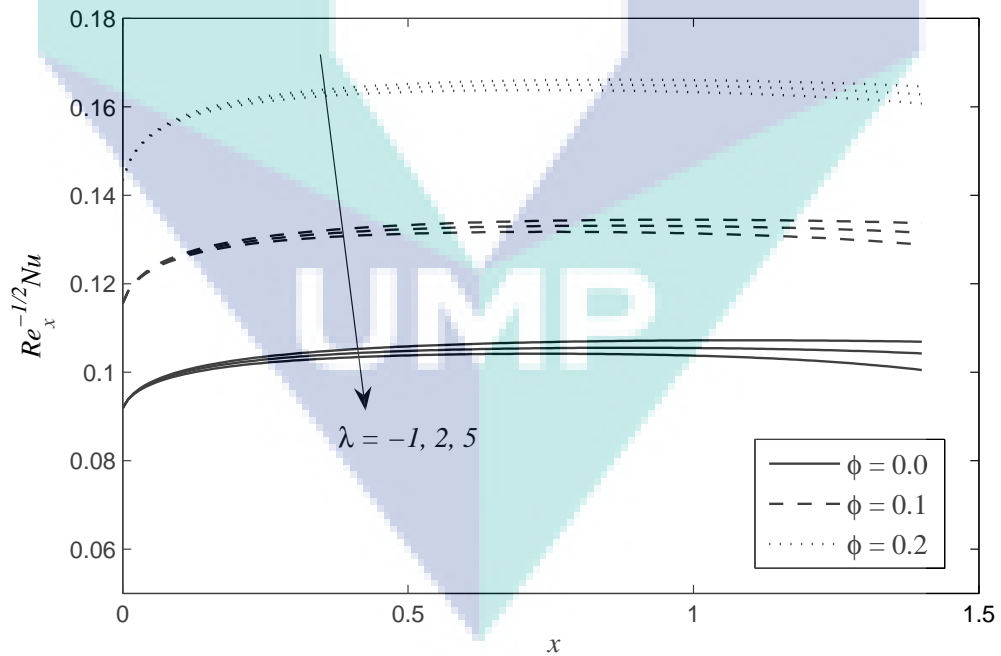


Figure 7.6. Comparison of the local Nusselt number $Re_x^{-1/2}Nu$ using TiO_2 nanoparticles with $\phi = 0, 0.1, 0.2$, $\gamma = 0.1$, $Pr = 6.2$ and various values of λ

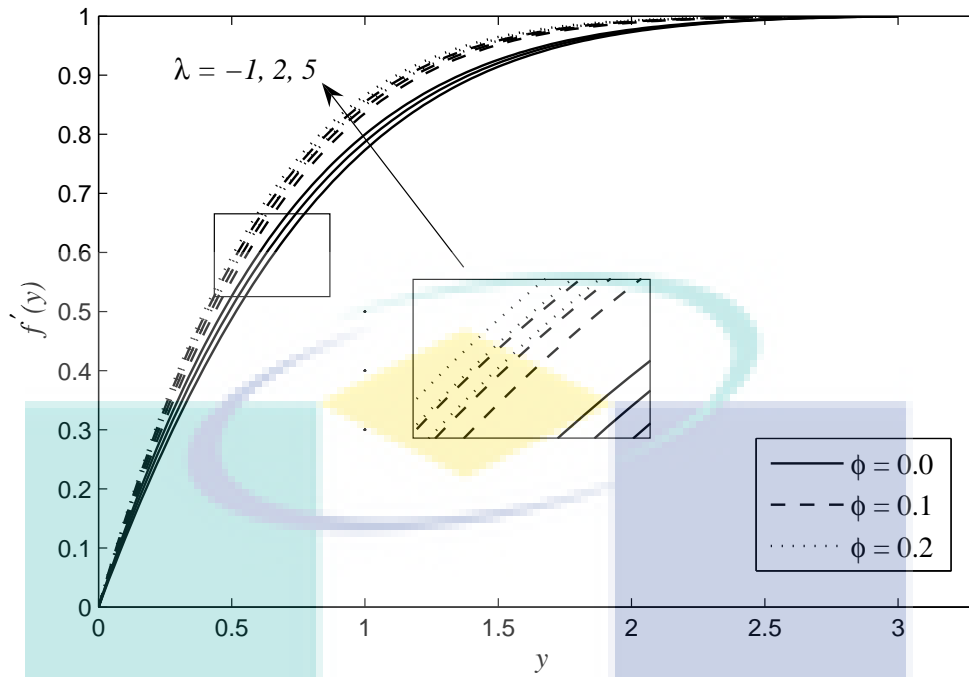


Figure 7.7. Velocity profiles $f'(y)$ using Cu nanoparticles with $\gamma = 0.1$, $Pr = 6.2$, $\phi = 0, 0.1, 0.2$ and various values of λ

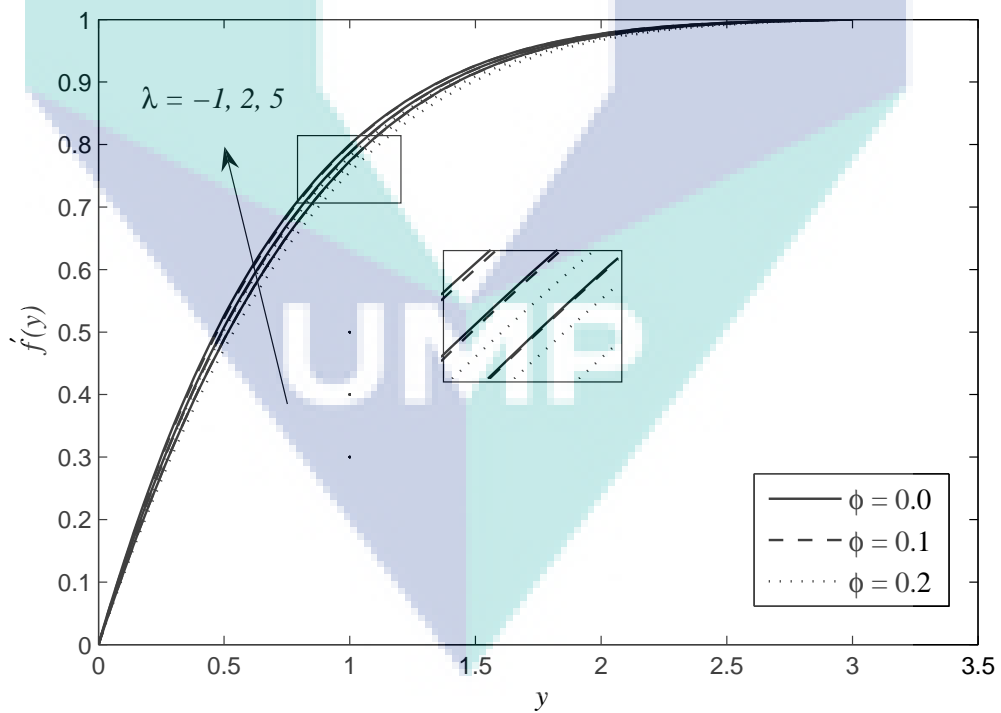


Figure 7.8. Velocity profiles $f'(y)$ using Al_2O_3 nanoparticles with $\gamma = 0.1$, $Pr = 6.2$, $\phi = 0, 0.1, 0.2$ and various values of λ

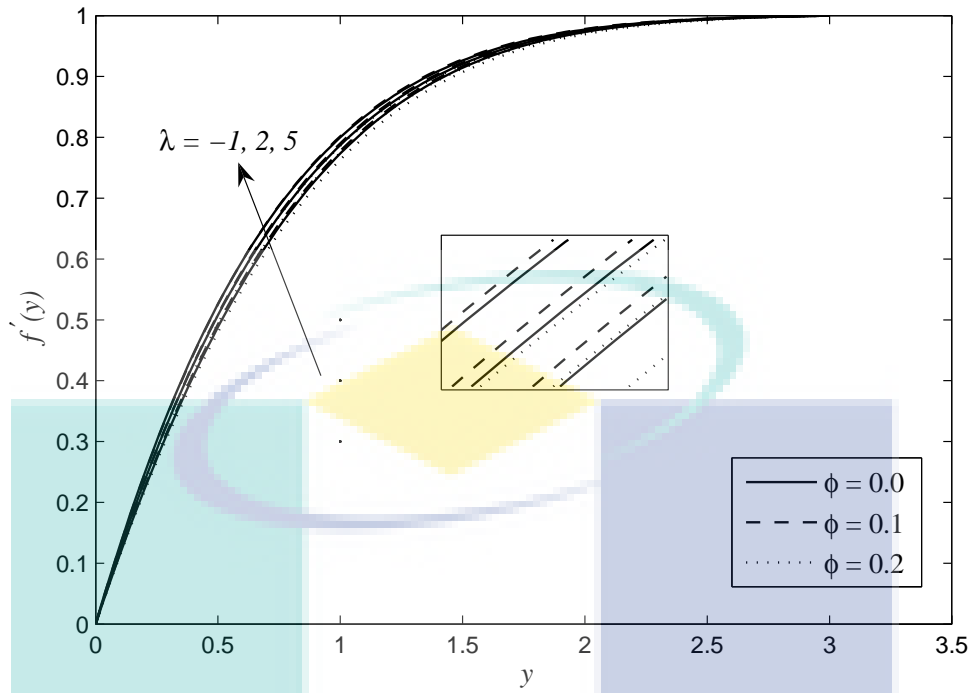


Figure 7.9. Velocity profiles $f'(y)$ using TiO_2 nanoparticles with $\gamma = 0.1$, $\text{Pr} = 6.2$, $\phi = 0, 0.1, 0.2$ and various values of λ

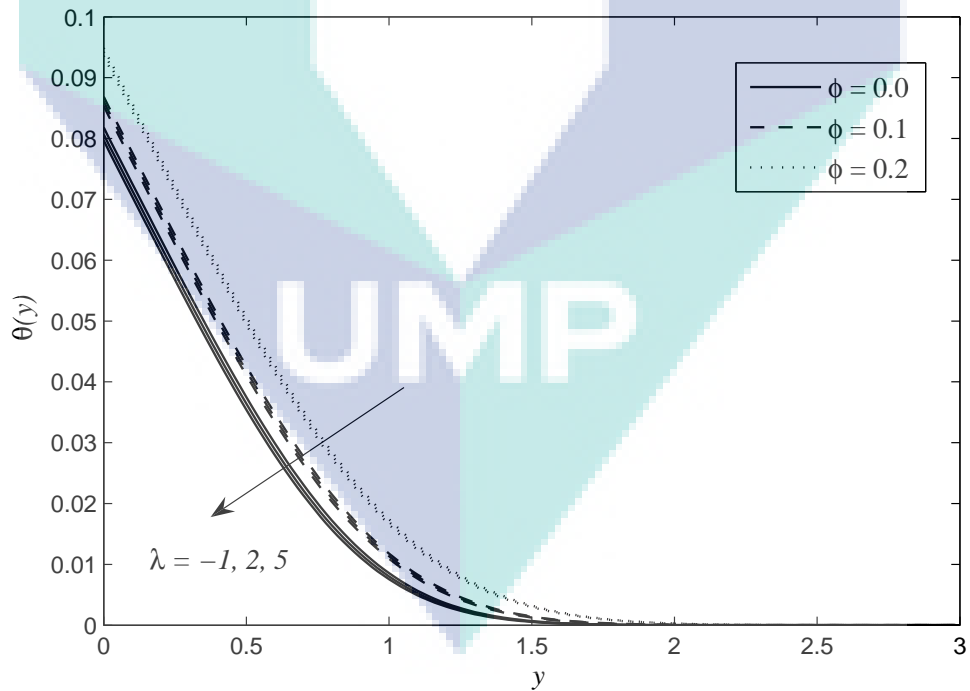


Figure 7.10. Temperature profiles $\theta(y)$ using Cu nanoparticles with $\gamma = 0.1$, $\text{Pr} = 6.2$, $\phi = 0, 0.1, 0.2$ and various values of λ

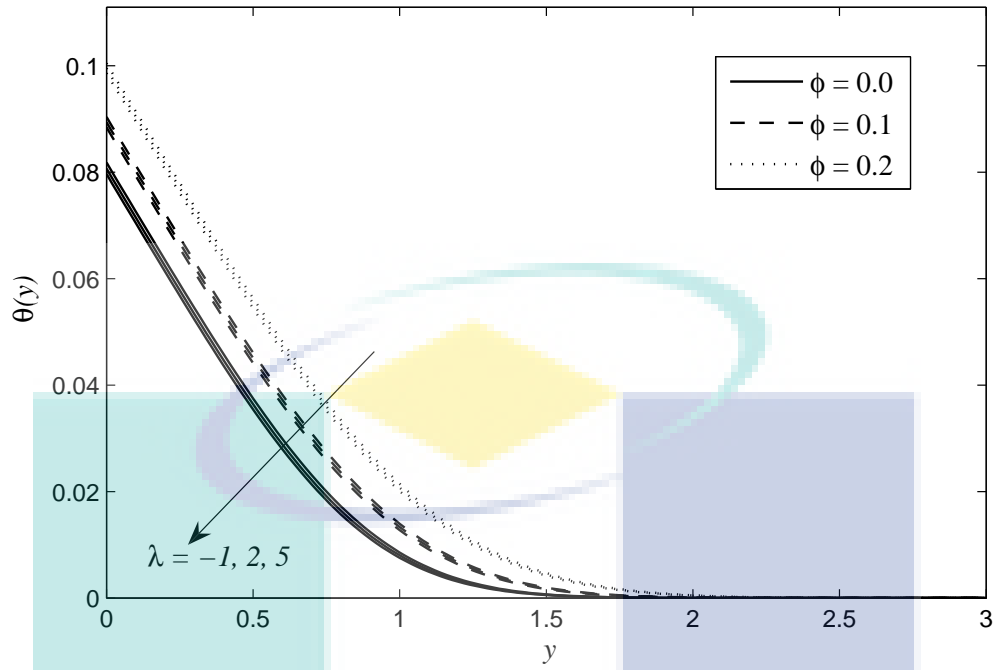


Figure 7.11. Temperature profiles $\theta(y)$ using Al_2O_3 nanoparticles with $\gamma = 0.1$, $\text{Pr} = 6.2$, $\phi = 0, 0.1, 0.2$ and various values of λ

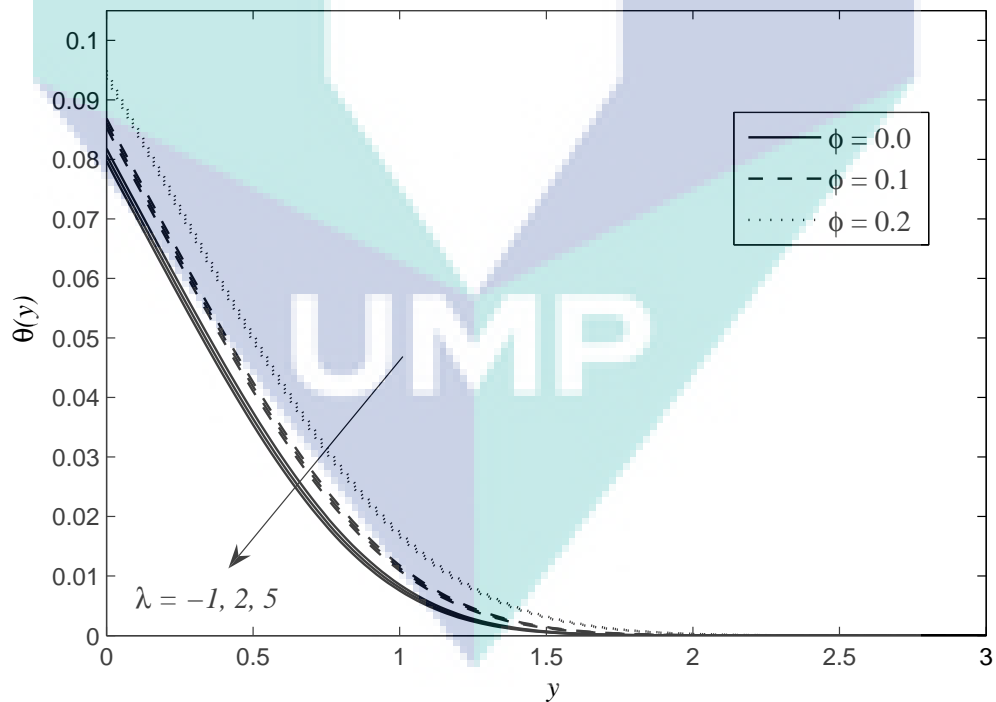


Figure 7.12. Temperature profiles $\theta(y)$ using TiO_2 nanoparticles with $\gamma = 0.1$, $\text{Pr} = 6.2$, $\phi = 0, 0.1, 0.2$ and various values of λ

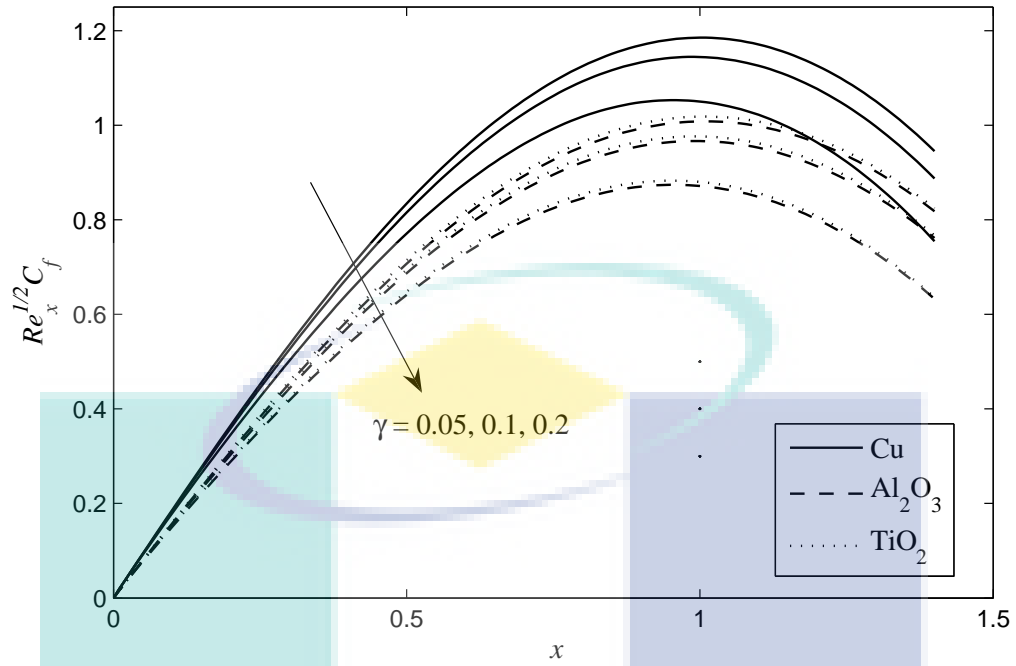


Figure 7.13. Comparison of the skin friction coefficient $Re_x^{1/2} C_f$ with $\phi = 0.1$, $\lambda = 1$, $Pr = 6.2$ and various values of γ

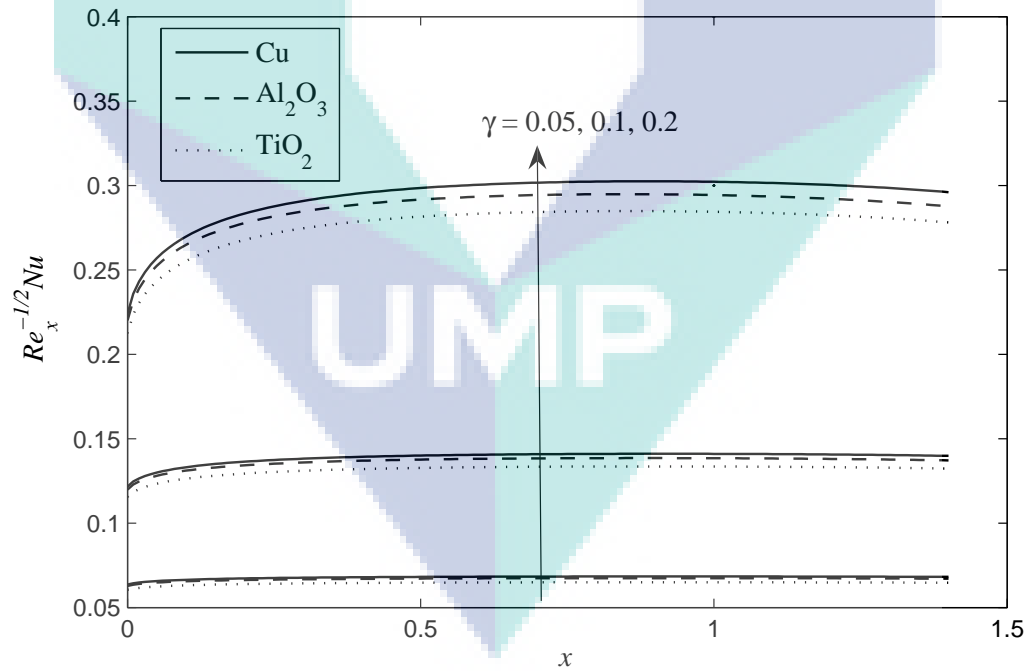


Figure 7.14. Comparison of the local Nusselt number $Re_x^{-1/2} Nu$ with $\phi = 0.1$, $\lambda = 1$, $Pr = 6.2$ and various values of γ

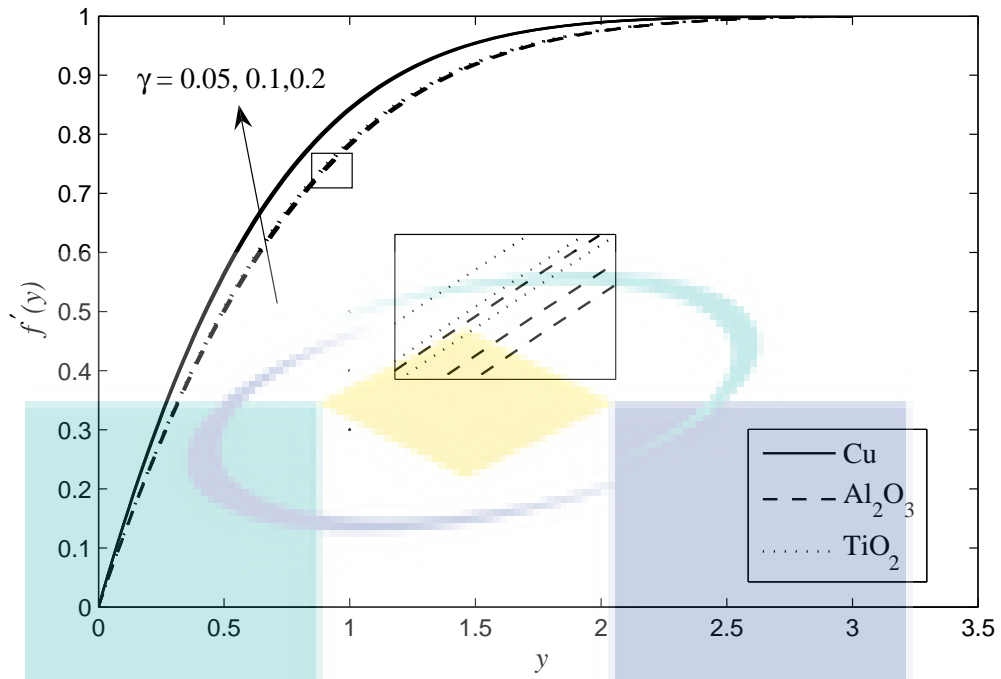


Figure 7.15. Velocity profiles $f'(y)$ using various nanoparticles with $Pr= 6.2$, $\phi = 0.1$, $\lambda = 1$ and various values of γ

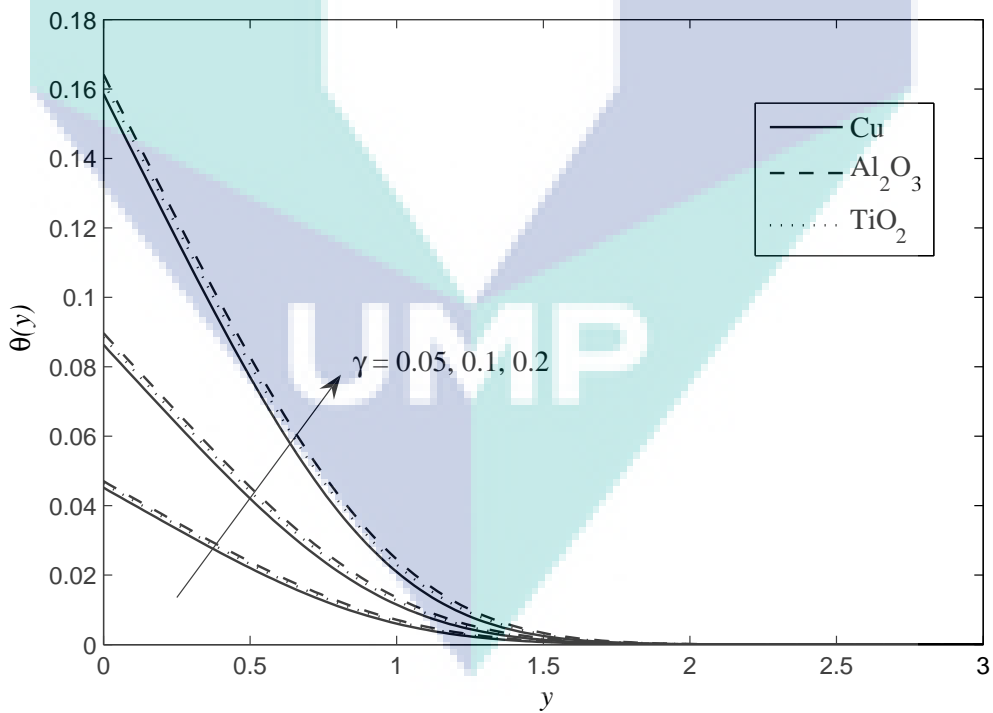


Figure 7.16. Temperature profiles $\theta(y)$ using using various nanoparticles with $Pr= 6.2$, $\phi = 0$, 0.1 and 0.2 , $\lambda = 1$ and various values of γ

7.4 Conclusions

In this chapter, the problem of mixed convection boundary layer flow over an isothermal horizontal circular cylinder immersed in a nanofluid is studied. The effects of mixed convection parameter λ , the type of nanoparticles (Al_2O_3 , Cu, TiO_2), the convective parameter γ and the nanoparticle volume fraction ϕ on the flow and heat transfer characteristics, have been investigated. The governing non-similar boundary layer equations were solved numerically using the Keller-box method. Therefore, based on the results the following conclusions are presented:

- i) an increase in the value of mixed convection parameter λ led to the reduction of the value of both the skin friction coefficient $Re_x^{1/2}C_f$ and the local Nusselt number $Re_x^{-1/2}Nu$
- ii) an increase in the value of nanoparticle volume fraction ϕ led to the increment of both the skin friction coefficient $Re_x^{1/2}C_f$ and the local Nusselt number $Re_x^{-1/2}Nu$.
- iii) an increase in the value of the convective parameter γ led to the increment of the local Nusselt number $Re_x^{-1/2}Nu$. However a different pattern is observed for both the skin friction coefficient $Re_x^{1/2}C_f$
- iv) nanoparticle Cu has a higher value of the local Nusselt number $Re_x^{-1/2}Nu$, as well as the skin friction coefficient $Re_x^{1/2}C_f$ compared to nanoparticles TiO_2 and Al_2O_3 .
- v) the increasing value of the mixed convection parameter λ is found to increase the velocity profile $f'(y)$ for all three nanoparticles. Conversely for all nanoparticles, the temperature profile $\theta(y)$ decrease as λ increases.
- vi) an increase in the value of the convective parameter γ led to the increment of both the velocity $f'(y)$ and temperature profile $\theta(y)$.

CHAPTER 8

MIXED CONVECTION BOUNDARY LAYER FLOW OVER A HORIZONTAL CIRCULAR CYLINDER IN A NANOFUID: BUONGIORNO MODEL

8.1 Introduction

The influence of thermal conductivities in many fields of applications such as in producing energy electronic and transportation sectors have contributed towards an ever-accelerating interest in the development of nanofluids. As a result, various models for solving the nanofluid problem have developed. In this chapter, the leading and notorious nanofluid model is demonstrated besides the Tiwari and Das (2007) which is Buongiorno's model proposed by Buongiorno (2006).

Indeed, Buongiorno conducted an extensive study of convective transport in nanofluids, focusing more on the heat transfer enhancement observed during convective situations. Buongiorno refuted the ideas of several other authors concerning the abnormal increase seen in the dispersion of suspended nanoparticles. From this study, the effect of the significant agent for heat transfer such as suspension, particle rotation, the dispersion, however is too small to explain the observed enhancement. Also, the marked improvement cannot be explained by turbulence as turbulence is not affected by the presence of nanoparticles. Furthermore, Buongiorno claimed that a satisfactory explanation for the abnormal increase of the thermal conductivity and viscosity is still to be found. Buongiorno went further to suggest a new model based on the mechanics of nanoparticles/base-fluid relative velocity. Moreover, he took the absolute velocity of nanoparticles to be the total sum of the base fluid velocity and relative velocity, which he called a slip velocity. Buongiorno's model consists of seven slip mechanisms; brownian diffusion, thermophoresis, inertia, diffusiophoresis, gravity settling, Magnus effect and fluid drainage. Subsequently, he concluded that in the absence of turbulent effects, brownian diffusion and thermophoresis dominate. Based on these two effects, Buongiorno derived the conservation equations.

In the next section, we provides a succinct description of the governing equations and the boundary conditions for the mixed convection boundary layer over horizontal circular cylinder in a nanofluid using the Buongiorno-Darcy model. This is followed by presenting and discussion of the numerical results in Section 8.3, which include the variations of the skin friction coefficient and, heat flux and mass flux as well as the velocity, temperature and nanoparticle volume fraction profile. Finally, Section 8.4 provides the concluding remarks about the finding of this problem.

8.2 Mathematical Formulation

Consider the steady mixed convection boundary layer flow past a heated horizontal circular cylinder embedded in a porous medium filled by water-based nanofluid for the present problem. It is assumed that hot temperature from the bottom of surface and the uniform nanoparticle volume fraction of the surface of the cylinder are T_f and C_w , respectively, while the ambient values, attained as y tends to infinity are T_∞ , and C_∞ , where $T_f > T_\infty$ for a heated cylinder (assisting flow) and $T_f < T_\infty$ for a cooled cylinder (opposing flow) and, $C_w > C_\infty$. The physical model and coordinate system is shown in Figure 8.1.

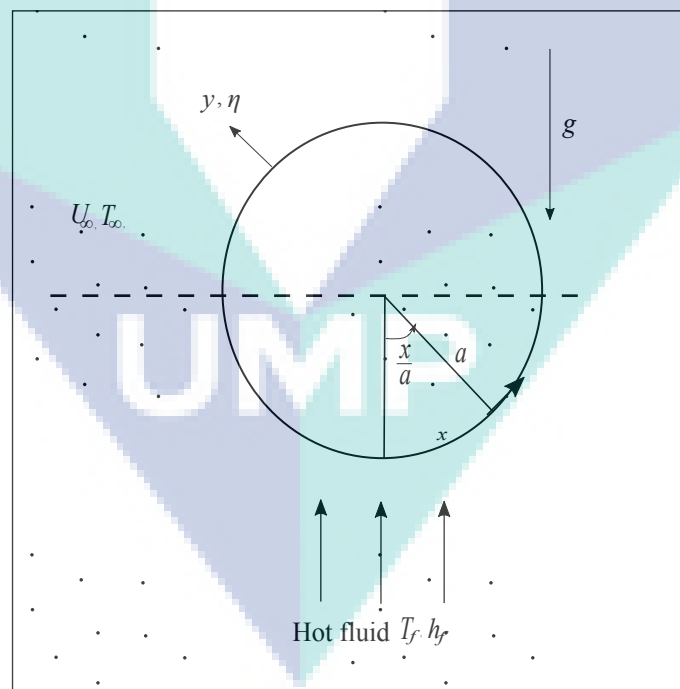


Figure 8.1. Physical model and coordinate system

It is also assumed that the velocity of the external flow (inviscid flow) is $\bar{u}_e(\bar{x})$, where x is the coordinate measured along the surface of the cylinder starting from the lower

stagnation point and y is the coordinate measured in the direction normal to the surface of the cylinder. It is assumed that there are homogeneity and local thermal equilibrium in the porous medium. Further, it is assumed that the Oberbeck-Boussinesq approximation takes place and that the nanoparticle concentration is dilute. Under these assumptions, the governing equations are based on the models proposed by Buongiorno (2006), Tham et al. (2014) are given in details in Chapter 3. To conserve space and avoid any form of repetition, see Equations 3.84 to 3.86 in Chapter 3.

The corresponding equations for the case of a regular (base) fluid ($Nb = Nt = Nr = 0$) for the mixed convection problem about the horizontal cylinder described by the following equations base fluid when

$$\frac{\partial f}{\partial y} = (1 + \theta\lambda) \frac{\sin x}{x} \quad 8.1$$

$$\frac{\partial^2 \theta}{\partial y^2} + f \frac{\partial \theta}{\partial y} = x \left(\frac{\partial f}{\partial y} \frac{\partial \theta}{\partial x} - \frac{\partial f}{\partial x} \frac{\partial \theta}{\partial y} \right) \quad 8.2$$

$$f(x, 0) = 0, \quad \theta(x, 0) = 1, \quad \theta(x, \infty) = 0 \quad 8.3$$

Near the lower stagnation point, $x \approx 0$, Equations 3.84 to 3.86 for the case of mixed convection reduce to the following ordinary differential equations

$$f' = 1 + (\theta - Nr\phi)\lambda \quad 8.4$$

$$\theta'' + f\theta' + Nb\theta'\phi' + Nt\theta'' = 0 \quad 8.5$$

$$\phi'' + Le f \phi' + \frac{Nt}{Nb} \theta'' = 0 \quad 8.6$$

subjected to boundary conditions

$$f(0) = 0, \quad \theta'(0) = -\gamma(1 - \theta(0)), \quad \phi(0) = 1 \quad \text{at } y = 0 \quad 8.7$$

$$\theta(y) \rightarrow 0, \quad \phi(y) \rightarrow 0 \quad \text{as } y \rightarrow \infty$$

where the term for porous medium filled by nanofluid is modified in Rayleigh number Ra is

$$Ra = (1 - C_\infty)gK\rho_f\beta(T_f - T_\infty)/(\mu\alpha_m) \text{ in term of } \lambda = \frac{Ra}{Pe}.$$

The quantity of interest in this study are the skin friction C_f , Nusselt number Nu and the Sherwood number Sh which are defined as

$$C_f = \frac{\tau_w}{\rho U_\infty^2}, \quad Nu = \frac{aq_w}{k_f(T_f - T_\infty)}, \quad Sh = \frac{aq_m}{D_B(C_w - C_\infty)} \quad 8.8$$

where τ_w is the skin friction coefficient or the shear stress at the surface of the cylinder, q_w and q_m is the heat and mass flux from the surface of the cylinder respectively, which are given by

$$\bar{\tau}_w = \mu \left(\frac{\partial \bar{u}}{\partial \bar{y}} \right)_{\bar{y}=0}, \quad \bar{q}_w = -k_f \left(\frac{\partial \bar{T}}{\partial \bar{y}} \right)_{\bar{y}=0}, \quad \bar{q}_m = -D_B \left(\frac{\partial \bar{C}}{\partial \bar{y}} \right)_{\bar{y}=0} \quad 8.9$$

Using Equations 3.12 and 3.27, the dimensionless quantities C_f , Nu and Sh are obtained as

$$\frac{Pe^{1/2}}{Pr} C_f = x \frac{\partial^2 f}{\partial y^2}, \quad Pe^{-1/2} Nu = -\frac{\partial f}{\partial y}, \quad Pe^{-1/2} Sh = -\frac{\partial \phi}{\partial y} \quad 8.10$$

Detailed formulation can be accessed in Appendix G.

8.3 Results and Discussion

The partial differential Equations 3.84 to 3.86 with corresponding boundary conditions 3.87 were solved numerically. The numerical investigation of the boundary problem has been carried out for different values of parameters; Lewis number Le , Brownian number Nb , thermophoresis parameter Nt , buoyancy ratio parameter Nr , convective parameter γ and at some streamwise positions x .

The dimensionless skin friction C_f , the dimensionless heat flux Nu , the dimensionless mass flux Sh , the velocity profiles $f'(y)$, the temperature profiles $\theta(y)$ and the nanoparticles volume fraction profiles $\phi(y)$ have been obtained. It appears that the values of the parameters considered usually exist in geophysical and engineering applications (Nield and Kuznetsov, 2009). The choice of Lewis number range is made on the basis of scale analysis, as described in Section 9.2.1 of Bejan (2013). Also, as observed from Nield and Kuznetsov (2009), since

most nanofluids examined to date incorporating large values of the Lewis number, the interest here is mainly in the case of $Le \geq 1$.

For validation purposes, given there is presently no experimental data available in the literature for the present problem, possibly due to the difficulties in considering all the factors, the problem is solved for limiting case when $\gamma \rightarrow \infty$. Accordingly, this is where the thermal heating becomes a case of constant wall temperature. The results are compared for the values of heat transfer coefficient $-\theta(0)$ with those reported by Cheng (1982) and Tham et al. (2014) as shown in Table 8.1. Cheng (1982) and Tham et al. (2014) perform a numerical investigation on mixed convection about a horizontal cylinder in a fluid-saturated porous medium for case of constant wall temperature. Cheng (1982) solved the problem by integrated numerically using Runge-Kutta method with a systematic guessing of $\theta'(0)$ by the shooting technique. On the other hand, Tham et al. (2014) implement finite difference method using Keller-box method which is the same as the current study. The comparison between these results is found to be excellent, based on the obtained numerical result.

Table 8.1. Values of the heat coefficient $-\theta'(0)$ in viscous fluid

λ	$-\theta'(0)$		
	Cheng (1982) Runge-Kutta	Tham et al. (2014) Keller-box	Present result Keller-box
0.0	0.7980	0.7979	0.7973
0.5	0.9157	0.9156	0.9146
1.0	1.0192	1.0191	1.0178
2.0	1.1988	1.1987	1.1968

Table 8.2 illustrate the effect of mixed convection parameter λ on the skin friction C_f , Nusselt Nu , Sherwood number Sh . In this thesis, only case $\lambda > 0$ (heated cylinder) are considered. Increasing λ increases the buoyancy effect in a mixed convection flow which finally leads to the acceleration of the fluid flow. This yield an enhancement in the local skin friction coefficient and the reduction in the local Nusselt and Sherwood number. Furthermore, from observing Table 8.2, near the lower stagnation point $x \approx 0$, C_f is minimum while Nu and Sh are maximum at this point, respectively.

The aim therefore is to observe the influence of the convective parameter γ as well as other parameters such as Le , λ , Nb and Nt on the heat and mass flow characteristics. Also the results are presented graphically for the effect of the above parameters. Figures 8.2 to 8.7 present the effects of the convective parameter γ on the skin friction coefficient C_f , local Nusselt number Nu , and local Sherwood number Sh , velocity f' , temperature θ and the nanoparticle volume fraction ϕ , respectively. Indeed, it can be observed that increasing

γ leads to the increase in the local Nusselt number. However, a different pattern is found for the local skin friction coefficient and local Sherwood number. Both the skin friction and Sherwood number show opposite behaviour with an increasing value of γ .

The influence of γ on the temperature profile $\theta(y)$ is demonstrated in Figure 8.6. From the figure, the thermal boundary layer increases as γ increases which are due to the convective heat transfer from the hot fluid side on the surface of the cylinder to the cold nanofluid side increasing, therefore leading to an increase in the temperature gradients. As γ increases, the convective heating increases (i.e. $\gamma \rightarrow \infty$). In fact, the high γ produces strong surface convection and subsequently supplies more heat to the cylinder's surface. This results in the temperature difference between the surface and nanofluid intensifies. As a result, the figures illustrate the increasing value of γ , therefore leading to an increase in the velocity, temperature profile and nanoparticle volume fraction profile.

Table 8.2. Values of the dimensionless skin friction, heat flux and mass flux for various values of λ

$x \backslash \lambda$	$(Pe^{1/2}/Pr)C_f$			$Pe^{-1/2}Nu$			$Pe^{-1/2}Sh$		
	1	2	5	1	2	5	1	2	5
0	0.0000	0.0000	0.0000	0.1466	0.1444	0.1380	1.0234	0.9599	0.8022
0.2	0.0499	0.0683	0.1168	0.1819	0.1681	0.1401	0.8663	0.6799	0.5155
0.4	0.0879	0.126	0.2243	0.1875	0.1698	0.1402	0.8264	0.6631	0.5109
0.6	0.118	0.1738	0.3213	0.1893	0.1699	0.1401	0.7966	0.6474	0.5078
0.8	0.1369	0.2107	0.4014	0.1898	0.1694	0.1398	0.7613	0.6325	0.5034
1.0	0.1463	0.2319	0.4604	0.1893	0.1684	0.1394	0.7265	0.6124	0.4976
1.2	0.1435	0.2364	0.4948	0.1881	0.1671	0.1388	0.6842	0.5880	0.4899
1.4	0.1301	0.2246	0.5020	0.1862	0.1654	0.1380	0.6364	0.5589	0.4798
1.6	0.1080	0.1973	0.4814	0.1836	0.1633	0.137	0.5833	0.5241	0.4667
1.8	0.0796	0.1566	0.4337	0.1804	0.1608	0.1358	0.5243	0.4823	0.4497
2.0	0.0482	0.1078	0.3586	0.1765	0.1576	0.1341	0.4590	0.4338	0.4260
2.2	0.0177	0.0573	0.2631	0.1718	0.1538	0.1320	0.3874	0.3785	0.3941
2.4	-0.0076	0.0119	0.1598	0.1660	0.1489	0.1291	0.3095	0.3155	0.3527
2.6	-0.0236	-0.0214	0.0625	0.1583	0.1426	0.1250	0.2252	0.2436	0.2986
2.8	-0.027	-0.0358	-0.0110	0.1475	0.1335	0.1190	0.1340	0.1599	0.2248
3.0	-0.0158	-0.025	-0.0356	0.1286	0.1174	0.1074	0.0338	0.0577	0.1138
π	-0.0024	-0.0042	-0.0092	0.0946	0.0881	0.0843	-0.0287	-0.0198	-0.0024

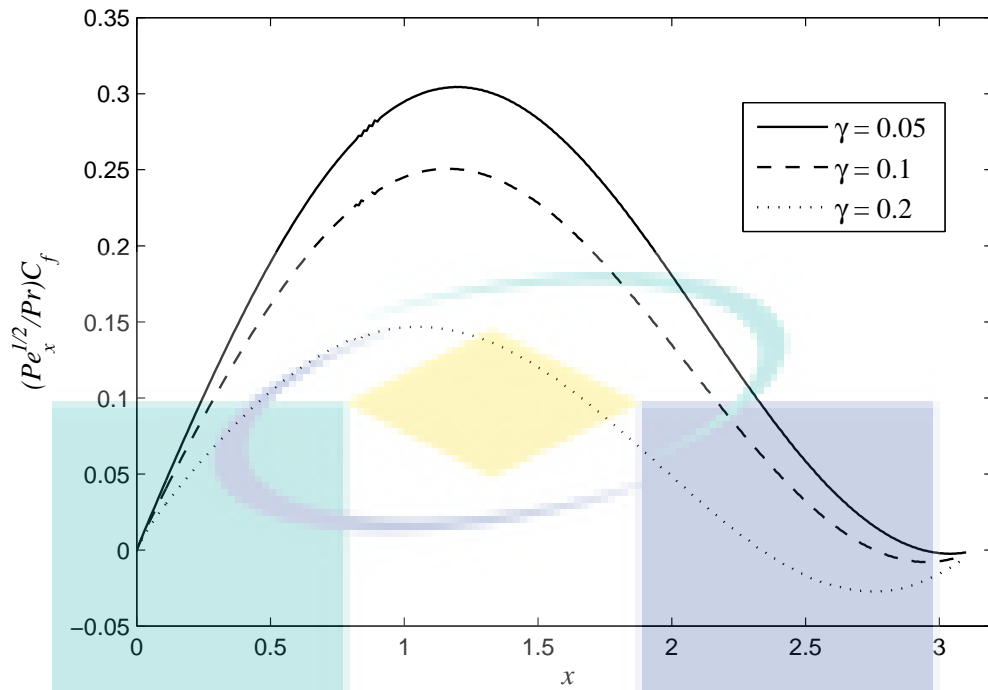


Figure 8.2. Variation of the dimensionless skin friction coefficient $(Pe^{1/2}/Pr)C_f$ for $Le = 2$, $\gamma = 0.05, 0.1, 0.2$, $Nb = 0.5$, $Nr = 0.5$, $Nt = 0.5$ and $\lambda = 1$

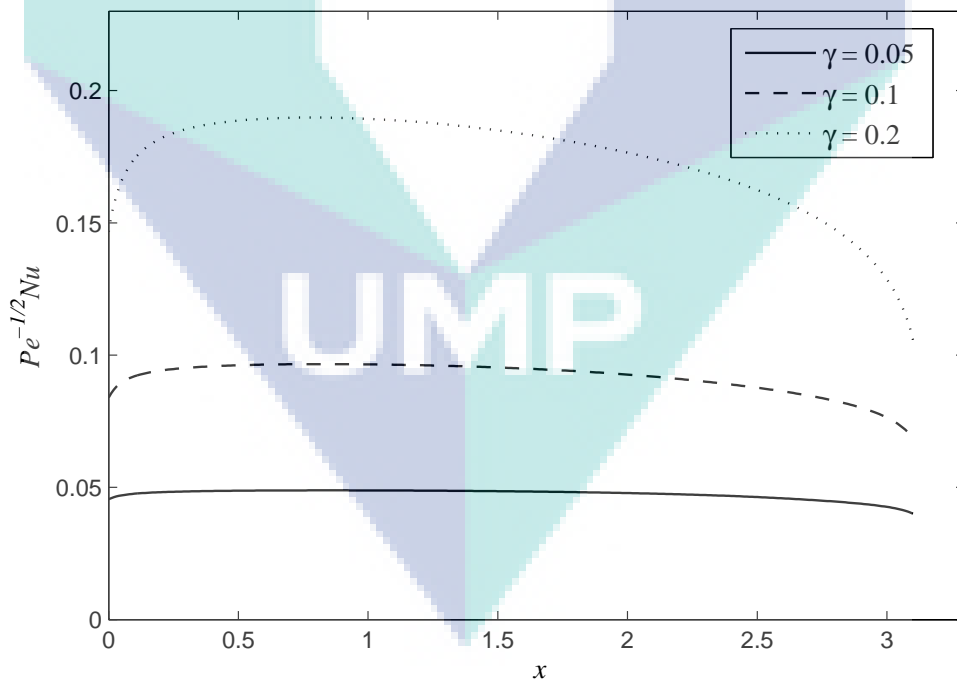


Figure 8.3. Variation of the dimensionless heat flux $Pe^{-1/2}Nu$ for $Le = 2$, $\gamma = 0.05, 0.1, 0.2$, $Nb = 0.5$, $Nr = 0.5$, $Nt = 0.5$ and $\lambda = 1$

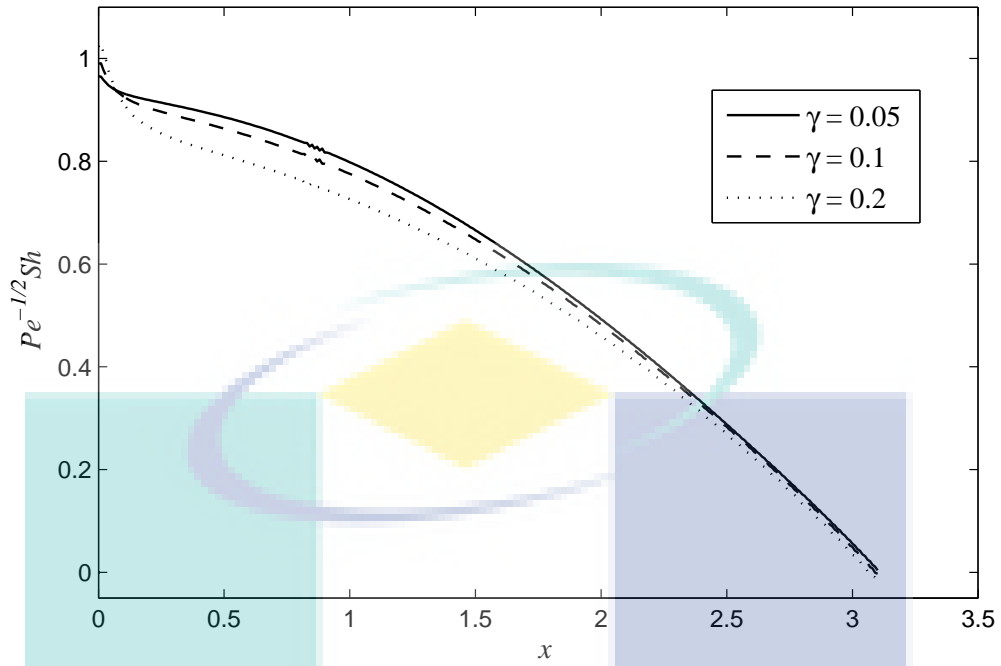


Figure 8.4. Variation of the dimensionless mass flux $Pe^{-1/2}Sh$ for $Le = 2$, $\gamma = 0.05, 0.1, 0.2$, $Nb = 0.5$, $Nr = 0.5$, $Nt = 0.5$ and $\lambda = 1$

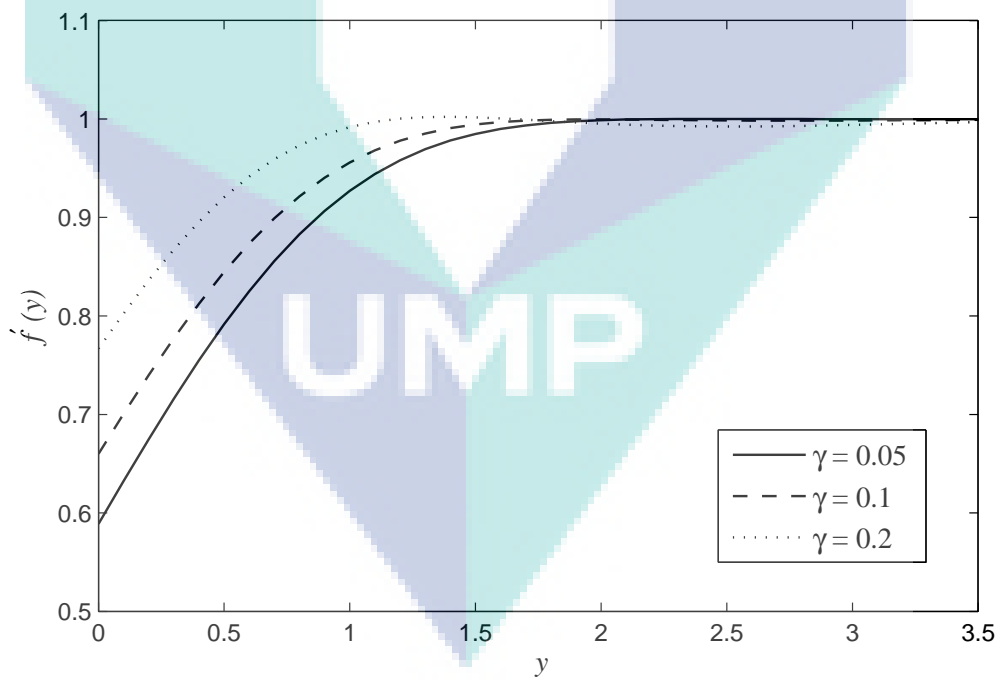


Figure 8.5. Velocity profile $f'(y)$ for various values of γ for $Le = 2$, $Nb = 0.5$, $Nr = 0.5$, $Nt = 0.5$ and $\lambda = 1$

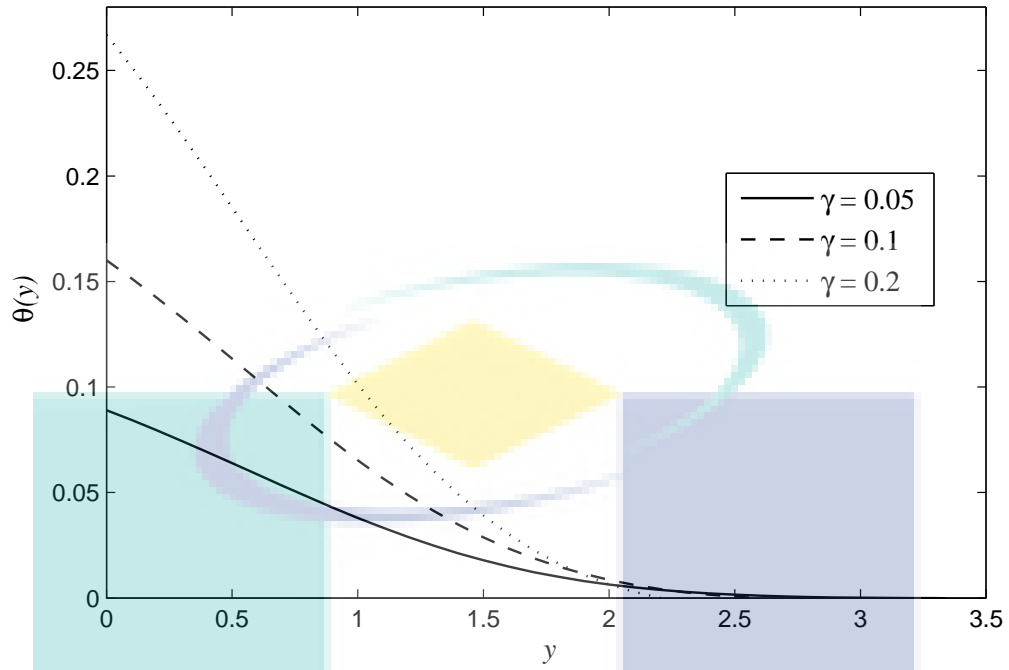


Figure 8.6. Temperature profile $\theta(y)$ for various values of γ for $Le = 2, Nb = 0.5, Nr = 0.5, Nt = 0.5$ and $\lambda = 1$

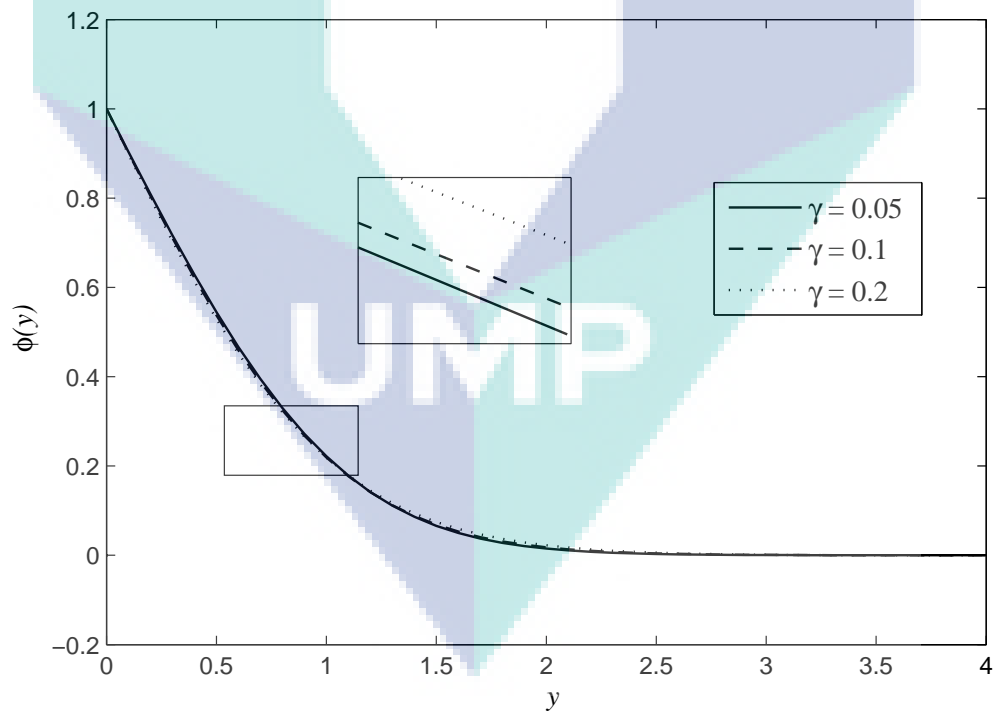


Figure 8.7. Nanoparticle volume fraction profile $\phi(y)$ for various values of γ for $Le = 2, Nb = 0.5, Nr = 0.5, Nt = 0.5$ and $\lambda = 1$

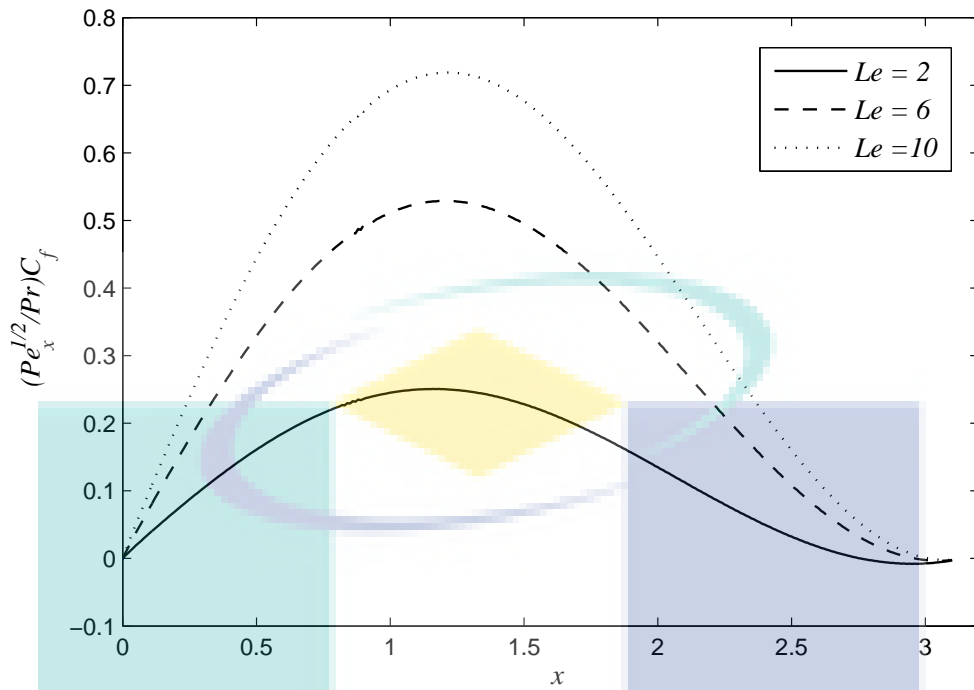


Figure 8.8. Variation of the dimensionless skin friction coefficient $(Pe_x^{1/2}/Pr)C_f$ for $\lambda = 1$, $Le = 2, 6, 10$, $Nb = 0.5$, $Nr = 0.5$, $Nb = 0.5$ and $\gamma = 0.1$

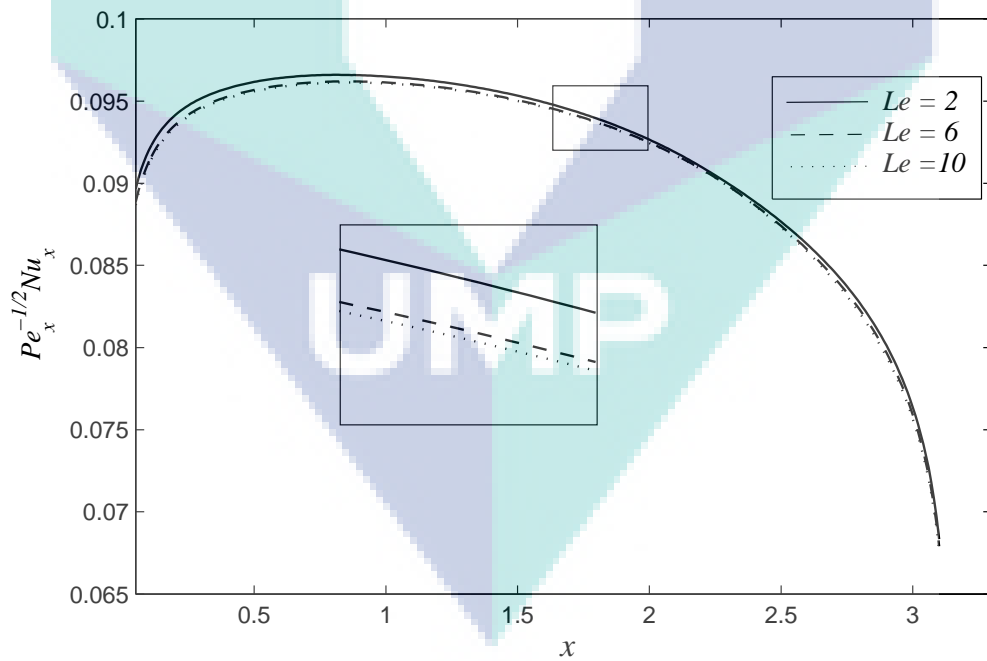


Figure 8.9. Variation of the dimensionless heat flux $Pe_x^{-1/2}Nu$ for $\lambda = 1$, $Le = 2, 6, 10$, $Nb = 0.5$, $Nr = 0.5$, $Nt = 0.5$ and $\gamma = 0.1$

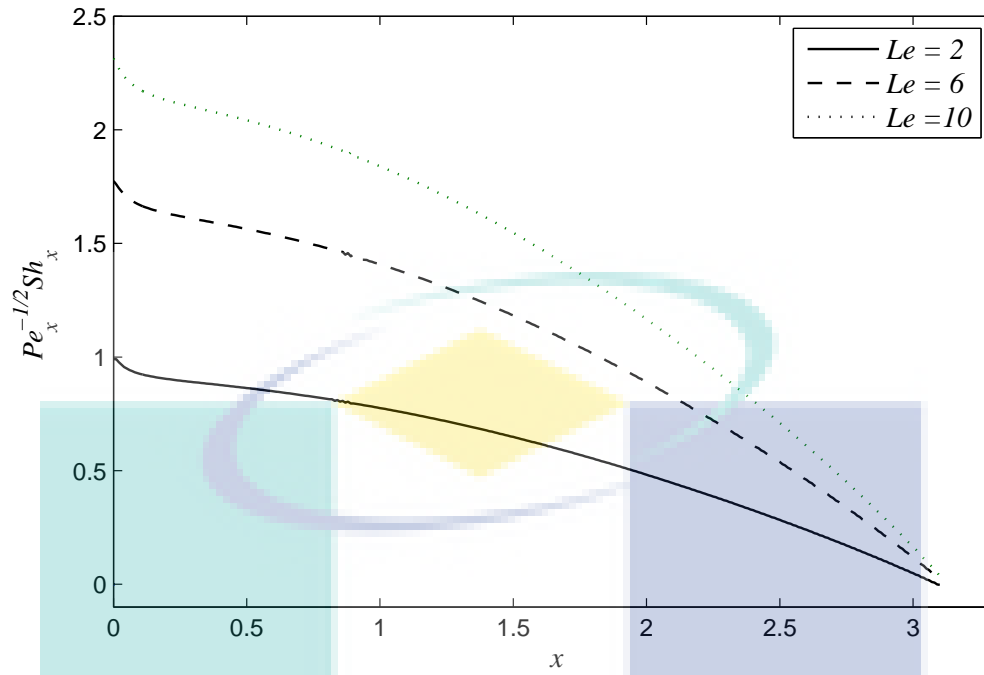


Figure 8.10. Variation of the dimensionless mass flux $Pe_x^{-1/2} Sh_x$ for $\lambda = 1$, $Le = 2, 6, 10$, $Nb = 0.5$, $Nr = 0.5$, $Nt = 0.5$ and $\gamma = 0.1$

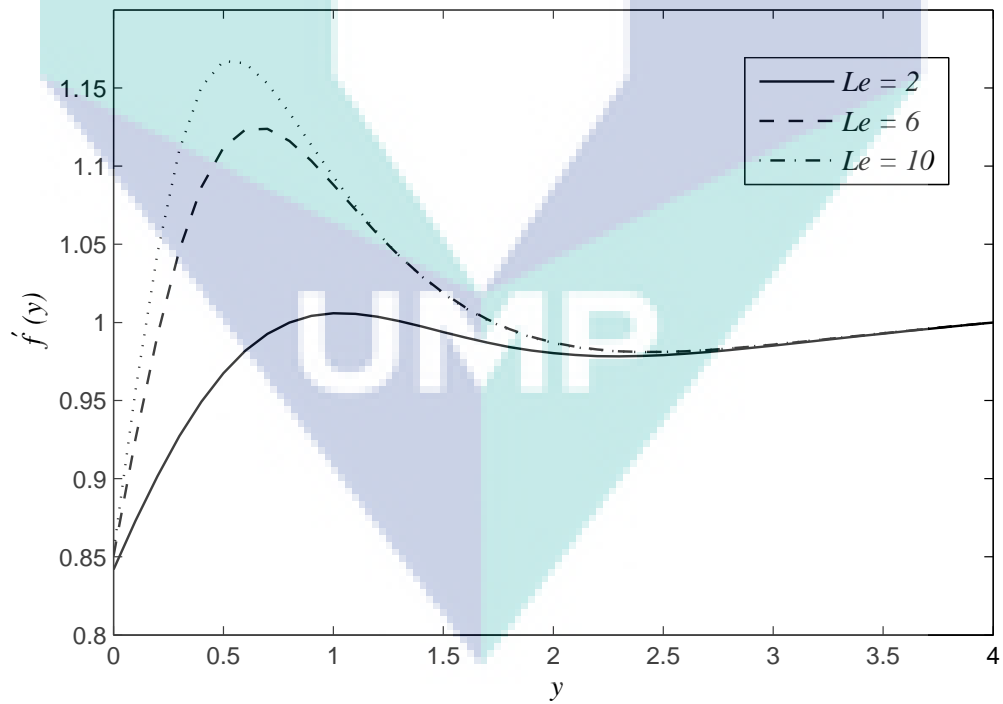


Figure 8.11. Velocity profile $f'(y)$ for various values of Le for $Nb = 0.5$, $Nr = 0.5$, $Nt = 0.5$, $\lambda = 1$ and $\gamma = 0.1$

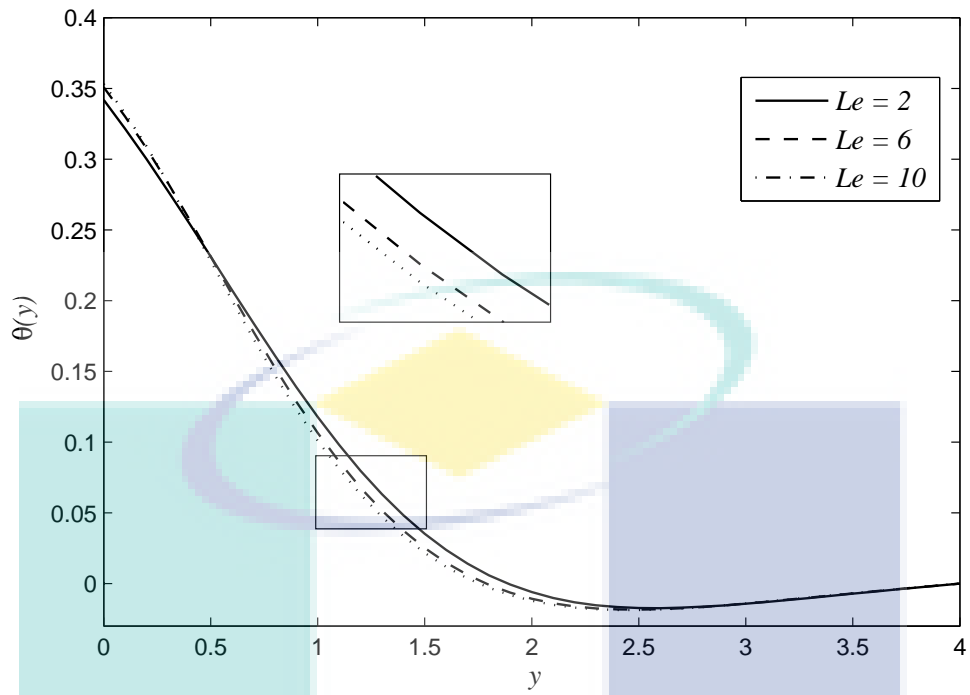


Figure 8.12. Temperature profile $\theta(y)$ for various values of Le for $Nb = 0.5$, $Nr = 0.5$, $Nt = 0.5$, $\lambda = 1$ and $\gamma = 0.1$

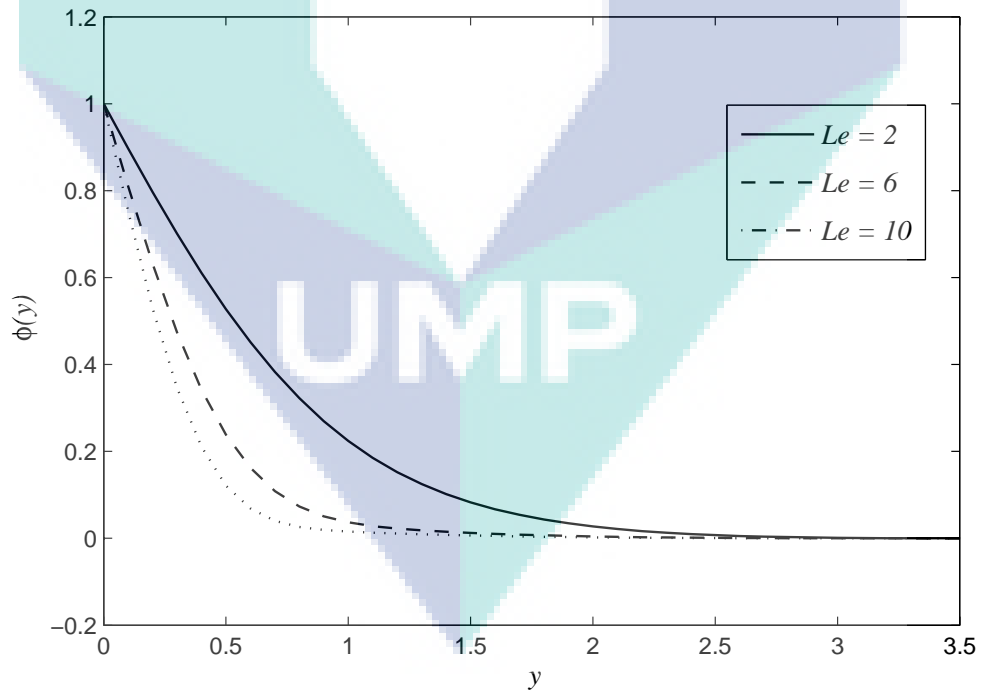


Figure 8.13. Nanoparticles volume fraction profile $\phi(y)$ for various values of Le for $Nb = 0.5$, $Nr = 0.5$, $Nt = 0.5$, $\lambda = 1$ and $\gamma = 0.1$

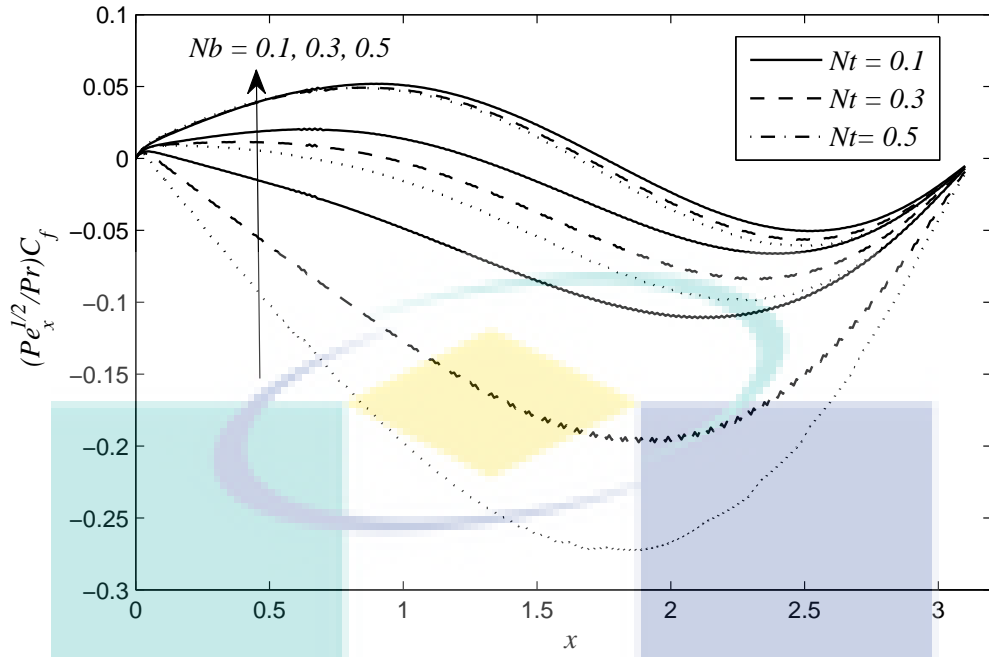


Figure 8.14. Variation of the dimensionless skin friction coefficient $(Pe^{1/2}/Pr)C_f$ for $Le = 2$, $Nb = 0.1, 0.3, 0.5$, $Nr = 0.5$, $Nt = 0.1, 0.3, 0.5$, $\lambda = 1$ and $\gamma = 0.1$

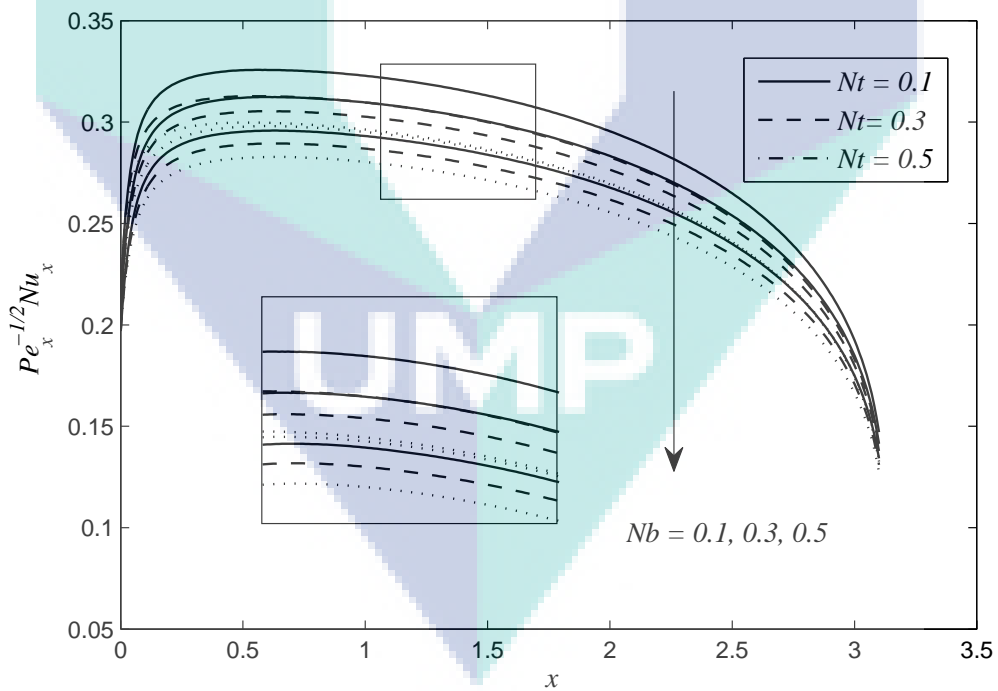


Figure 8.15. Variation of the dimensionless heat flux $Pe^{-1/2}Nu_x$ for $Le = 2$, $Nb = 0.1, 0.3, 0.5$, $Nr = 0.5$, $Nt = 0.1, 0.3, 0.5$, $\lambda = 1$ and $\gamma = 0.1$

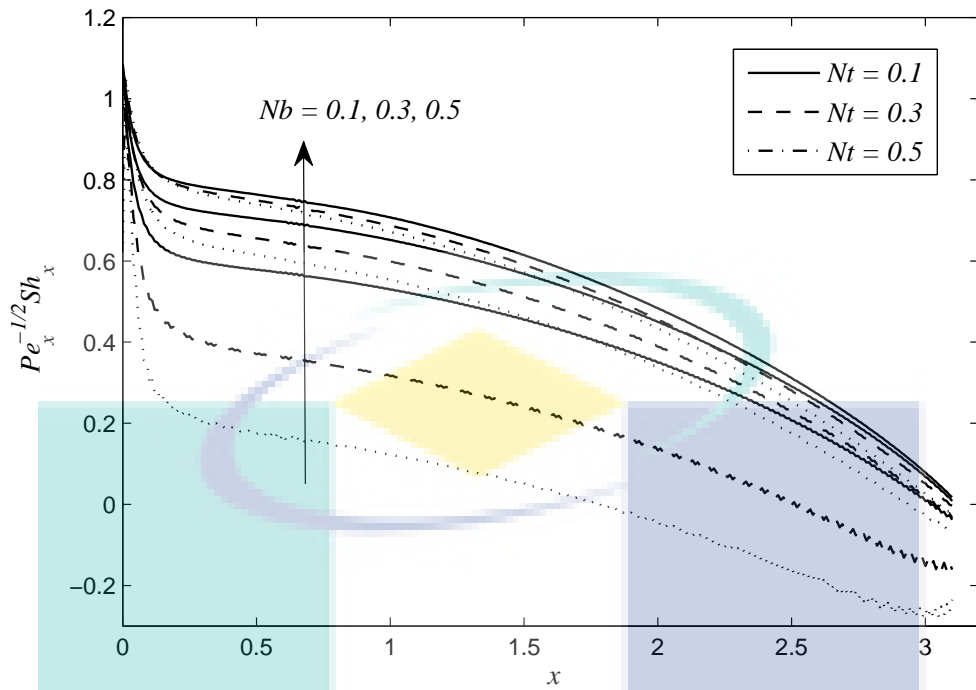


Figure 8.16. Variation of the dimensionless mass flux $Pe_x^{-1/2} Sh_x$ for $Le = 2$, $Nb = 0.1, 0.3, 0.5$, $Nr = 0.5$, $Nt = 0.1, 0.3, 0.5$, $\lambda = 1$ and $\gamma = 0.1$

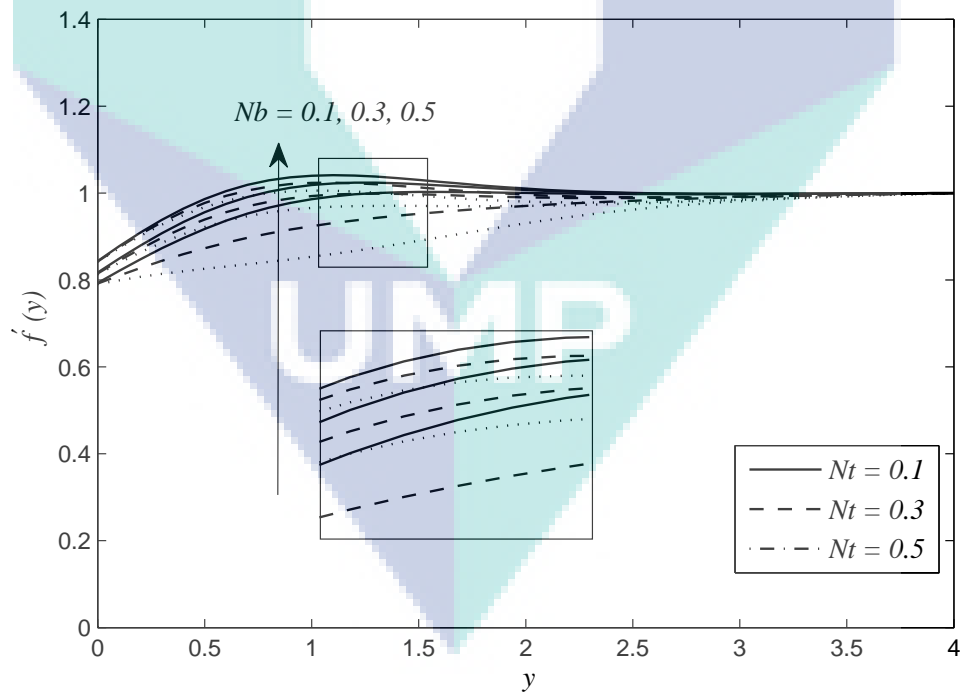


Figure 8.17. Velocity profile $f'(y)$ for various values of Nb and Nt for $Nr = 0.5$, $Le = 2$, $\lambda = 1$ and $\gamma = 0.1$

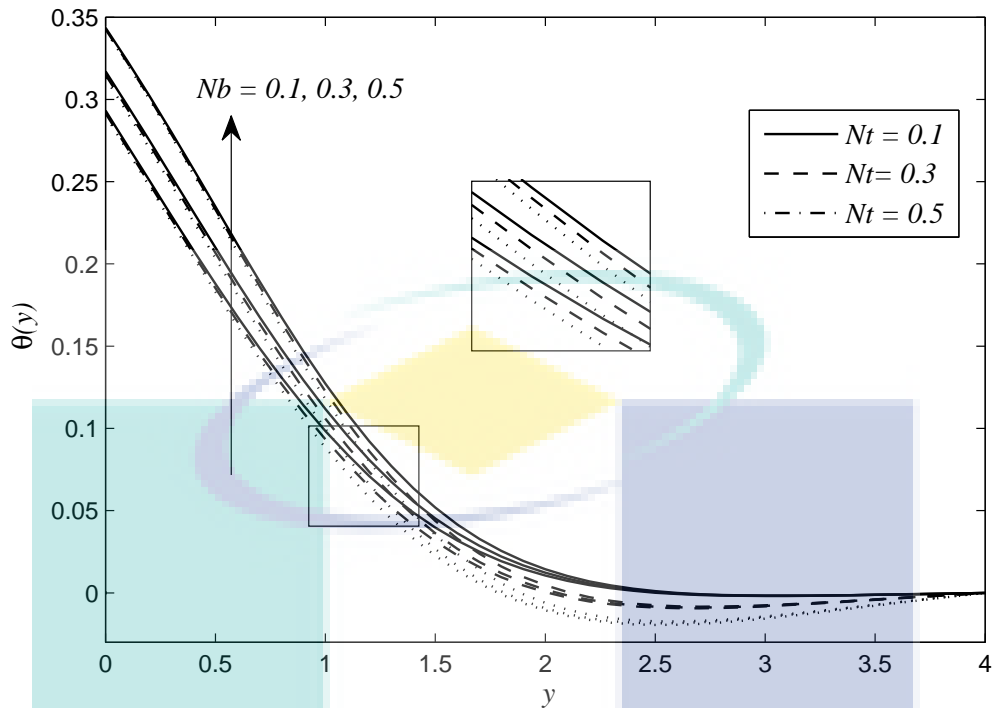


Figure 8.18. Temperature profile $\theta(y)$ for various values of Nb and Nt for $Nr = 0.5$, $Le = 2$, $\lambda = 1$ and $\gamma = 0.1$

Figures 8.8 to 8.13 illustrate the behaviour of the skin friction coefficients C_f , the local Nusselt number Nu , the local Sherwood number Sh , velocity f' , temperature θ , and the nanoparticle volume fraction with changes in the values of the Lewis number Le . Increasing the values of Le produces increases in both the skin friction coefficient and the Sherwood number. However, the Nusselt number shows a decrease in the increase in the Le number. From the definition of the skin friction coefficient $c_f \propto \tau_w/(\rho U_\infty^2)$, the density of the fluid decreases as the values of Le increase. Thus, the value of the skin friction coefficient is proportional to the increase of Le . From the Figures 8.12 and 8.13, it is also noticeable that the thickness of the thermal and the mass fraction boundary layers decrease with increasing values of Le . This is due to the increase in the Lewis number which tends to increase the buoyancy-induced flow along the surface at the expense of the reduced concentration and its boundary layer thickness (Tham et al., 2014).

The corresponding variation of the skin friction, the Nusselt and Sherwood number for some of the values of Brownian motion parameter Nb and thermophoresis parameter Nt are also presented in Figure 8.14 to 8.16. It is shown in the Figure 8.15 where Nu decreases with the increase in the parameters Nb and Nt which corresponds to an increase in the thermal boundary layer thickness. A further reason for such phenomena occurring is that when the higher values of Nb and Nt are subsequently higher in the volume of nanoparticles migrating

away from the vicinity of the wall, this in turn reduces the rate of heat transfer. Conversely, for the case of Nb , different patterns were observed in the local skin friction coefficient and the Sherwood number. It is therefore evident from the figures that both the skin friction coefficient C_f and the Sherwood number Sh increase with the increase in the parameters Nb , but decreases in the parameter of Nt .

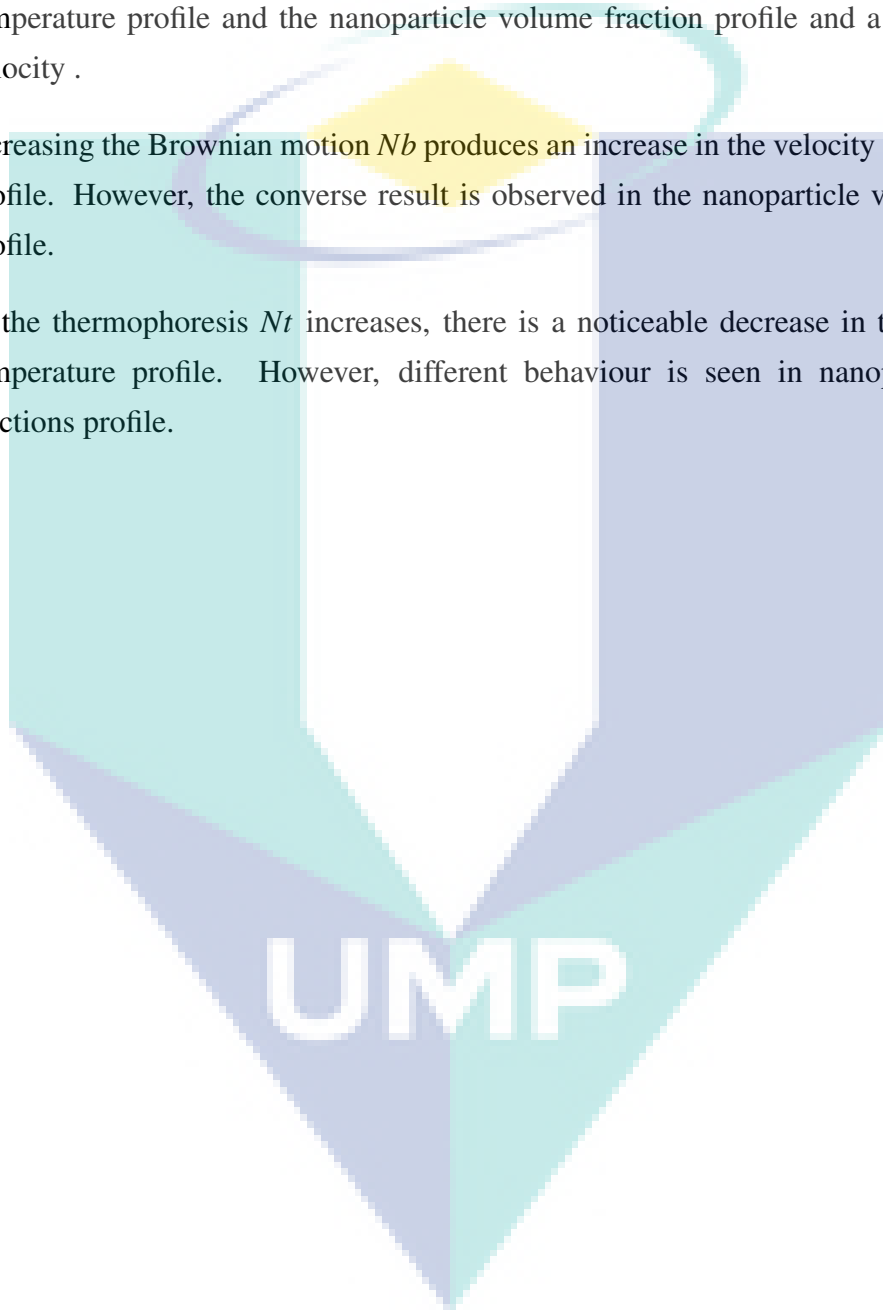
The effects of Nb and Nt on the velocity f' , temperature and nanoparticles volume fraction are shown in Figures 8.17 to 8.18. Increasing the Brownian motion Nb produces an increase in the velocity and temperature profile with a slight decrease in the volume fraction profiles. This possibly occurs because for the small particles, the Brownian motion is strong, and the parameter Nb will have high values. On the other hand, in case of a large particle, Brownian motion does exert a significant effect on both the temperature and volume fraction. In addition, a positive Nb indicates a cold surface, whereas a negative Nb corresponds to a hot surface. Increasing the thermophoresis parameter Nt leads to increases in the volume fraction profiles. However, a different pattern is observed for the velocity and temperature profile.

8.4 Conclusions

The mixed convection boundary layer over a horizontal circular cylinder embedded in porous medium saturated by a nanofluid with Darcy model and Buongiorno equation model is studied considering the convective boundary condition. Based on Buongiorno's theory, the effects of Brownian motion and thermophoresis are included for the nanofluids. Besides convective parameter γ , we looked into the effects of the Lewis number Le , Brownian number Nb , and thermophoresis parameter Nt on the flow and heat transfer characteristic. Therefore, from the results, the following conclusions are presented:

- i) the dimensionless skin friction coefficient C_f increased when the value of the Lewis number Le , mixed convection parameter λ , and Brownian number Nb increased. However, C_f demonstrated the opposite pattern for the convective parameter γ and thermophoresis parameter Nt .
- ii) the Nusselt number Nu decreased when the value of the Le , λ , Nb , Nt increased. On the other hand, as γ increases, Nu also increases.
- iii) the Sherwood number Sh increased when the value of the Le and Nb increased; but not for the case of γ , λ and Nt .

- iv) an increase in the convective parameter γ leads towards the increase in both of velocity and temperature profile with a slight decrease in the nanoparticle volume fraction profile.
- v) velocity and temperature profile increase when the Le increases, and different patterns are observed for the nanoparticle volume fractions profile.
- vi) an increase in the mixed convection parameter λ leads to the increase in both the temperature profile and the nanoparticle volume fraction profile and a decrease in the velocity .
- vii) increasing the Brownian motion Nb produces an increase in the velocity and temperature profile. However, the converse result is observed in the nanoparticle volume fractions profile.
- viii) as the thermophoresis Nt increases, there is a noticeable decrease in the velocity and temperature profile. However, different behaviour is seen in nanoparticle volume fractions profile.



CHAPTER 9

CONCLUSIONS

9.1 Summary of Research

This thesis was conducted to obtain the numerical solution of convection flow when the new heating condition namely the convective boundary condition is applied. Therefore, this research aims to formulate the mathematical model of convection flow and to examine the convective effect as well as the effects of other parameters in five separate flow problems. Motivated by the previous studies of CWT, CHF and more recently NH on the flow problem, this has driven the authors of this study to investigate the behaviour of CBC in simulating the solution regarding skin friction coefficient, velocity, temperature and other parameters. To the best of the author's knowledge, the mathematical model applying CWT and CHF has been fully developed for various geometries. However, CBC is yet to be established and there are very limited number of studies of CBC especially involving the horizontal cylinder. Notwithstanding, this study is expected to be an incremental step towards the determining the effect of CBC in the convection flow problem. The results in this research will bridge the existing void that exists between the evolvement of the heating condition of CWT, CHF, NH and lastly CBC.

The introductory chapter which is Chapter 1 presented the research background including the problem statement, objectives and scope of research, methodology, the significance of the study and outline of the thesis. The basic concept of the convection and theory were presented in Chapter 2 to provide a further understanding of the flow and heat transfer problem. In addition, literature review for the problem under discussion were also demonstrated in this chapter.

The governing equations are in the system of PDE, therefore the numerical technique known as the Keller-box method was executed in this research for all five problems stated. The Keller-box method is established method and are found to be efficient and suitable to solve all flow problem. The detailed of Keller-box procedure are thoroughly discussed in

Chapter 3 for the specific problem of mixed convection boundary layer flow in nanofluids. The Keller-box algebraic computation is performed in MATLAB, and numerical scheme of Keller box for CBC is developed. The MATLAB code is additionally provided herein Appendix B.

The thesis consists of nine chapters with the main research were contributed in Chapter 4 to Chapter 8. Chapter 4 presented the analysis on the problem of steady forced convection boundary layer flow past over a horizontal circular cylinder in viscous fluid. The comparison on numerical results of skin friction coefficient concurs very well with those reported previously. The numerical results for the skin friction heat transfer coefficient and are presented in tabular form from the lower stagnation point, $x \approx 0$ up to case when $x = 101^\circ$. It is noticed that in this problem, the unique valued exists for the skin friction coefficient due to the decoupled boundary condition. In addition, to achieve a physically acceptable solution, Pr must be greater or equal to Pr_c depending on γ , whereas γ must be less than or equal to γ_c depending on Pr . Outside this value, the singularity occurs and the solution becomes unstable.

The solution for the problem of free convection boundary layer flow in micropolar fluid is discussed in Chapter 5. With the increase in values of material parameter K , the values of velocity distribution and angular velocity profiles also increase, while the values of temperature profile decrease. Moreover, convective parameter γ and material parameter number had significant effects on the fluid flow characteristics in terms of values skin friction and heat transfer coefficient as well as for temperature profile.

In Chapter 6, the problem of mixed convection flow in viscous fluid is presented. It is observed that increasing convective parameter leads to the increase of the temperature and velocity profiles. Further, it is shown in the figure that the value of skin friction coefficient decreases as γ increases and the value of heat transfer coefficient increases as γ increases. The results on the increment of mixed convection parameter λ for this problem shows that the value of skin friction, heat transfer coefficient and velocity profile is increased as well.

The study on nanofluids has been given in Chapter 7 and 8. Chapter 7 focus on the mixed convection in nanofluid using Tiwari and Das model. Three different types of nanoparticles, namely Al_2O_3 , Cu , and TiO_2 have been considered in this study. Finding shows that nanoparticle Cu has a higher value of the local Nusselt number $Re_x^{-1/2}Nu$, as well as the skin friction coefficient $Re_x^{1/2}C_f$ compared to nanoparticles TiO_2 and Al_2O_3 . Besides that, an increase in the value of the convective parameter led to the increment of the local Nusselt number. However a different pattern is observed for both the skin friction coefficient.

The other nanofluids model known as Buongiorno has also been covered in this study. Chapter 8 provides an analysis on the problem of mixed convection boundary layer flow in nanofluid by using Buongiorno model. Two important mechanism in Buongiorno model is Brownian motion and thermophoresis. It is noticed that increasing the Brownian motion Nb produces an increase in the velocity and temperature profile. However, the converse result is observed in the nanoparticle volume fractions profile. In additions, as the thermophoresis Nt increases, there is a noticeable decrease in the velocity and temperature profile. However, different behaviour is seen in nanoparticle volume fractions profile.

The cylinder exhibit boundary layer separation; the case where the boundary layer separate from the cylinder surface and the flow become unstable. If the flow can succesfully reach the upper cylinder i.e $x = 180^\circ$, then no separation occur. Therefore, by incorporating CBC in the boundary conditions in the five problem under discussion, we found that for the problem of free convection in micropolar Chapter 5 and mixed convection in nanofluid using Buongiorno in Chapter 8, the numerical solutions start from the lower stagnation point ($x \approx 0$) and proceeds round the cylinder until upper stagnation point ($x = 180^\circ$) of the circular cylinder. However for case forced convection in viscous fluid Chapter 4, the estimation of separation of the cylinder occured at $x = 104.50^\circ$. In addition, in Chapter 6 for problem of mixed convection of viscous fluid and Chapter 7 problem of nanofluid Tiwari and Das model, the flow can reach up to $x = 120^\circ$. Beyond this point, the boundary layer simply lift off the cylinder surface.

From the research findings, naturally incorporating CBC in a mathematical model of convection flow produces a different result in the separation process, velocity, temperature, skin friction and so forth. Since different industries require different heating processes, presumably CBC will provide a better result when the heat transfer at the surface relies on the wall temperature instead of being continually constant. Therefore, using CBC possibly offers more significant impact on producing better output in heat transfer flow. Thus, from the findings of this thesis, the following contributions are hereby presented:

- (i) The research gaps about CWT, CHF, NH and CBC become closer when the mathematical model of convective flow using CBC is developed especially over the horizontal circular cylinder. Most of the CBC focus on the stretching sheet and plate, and research on the circular cylinder is extremely limited in the literature.
- (ii) Most researchers have considered constant wall temperature or constant heat flux to model the system due to its simplicity. This research is expected to be relevant to broad range of applications since CBC appears to be a more realistics system to apply since not all situations can be considered as constant. Therefore, real phenomena can

be described through developing a mathematical model regarding convective boundary condition and can thus be solved via the numerical method.

- (iii) Moreover, the findings in this study have provided a platform that hopefully can facilitate further research and study to explore this area in another geometries and other types of fluids.

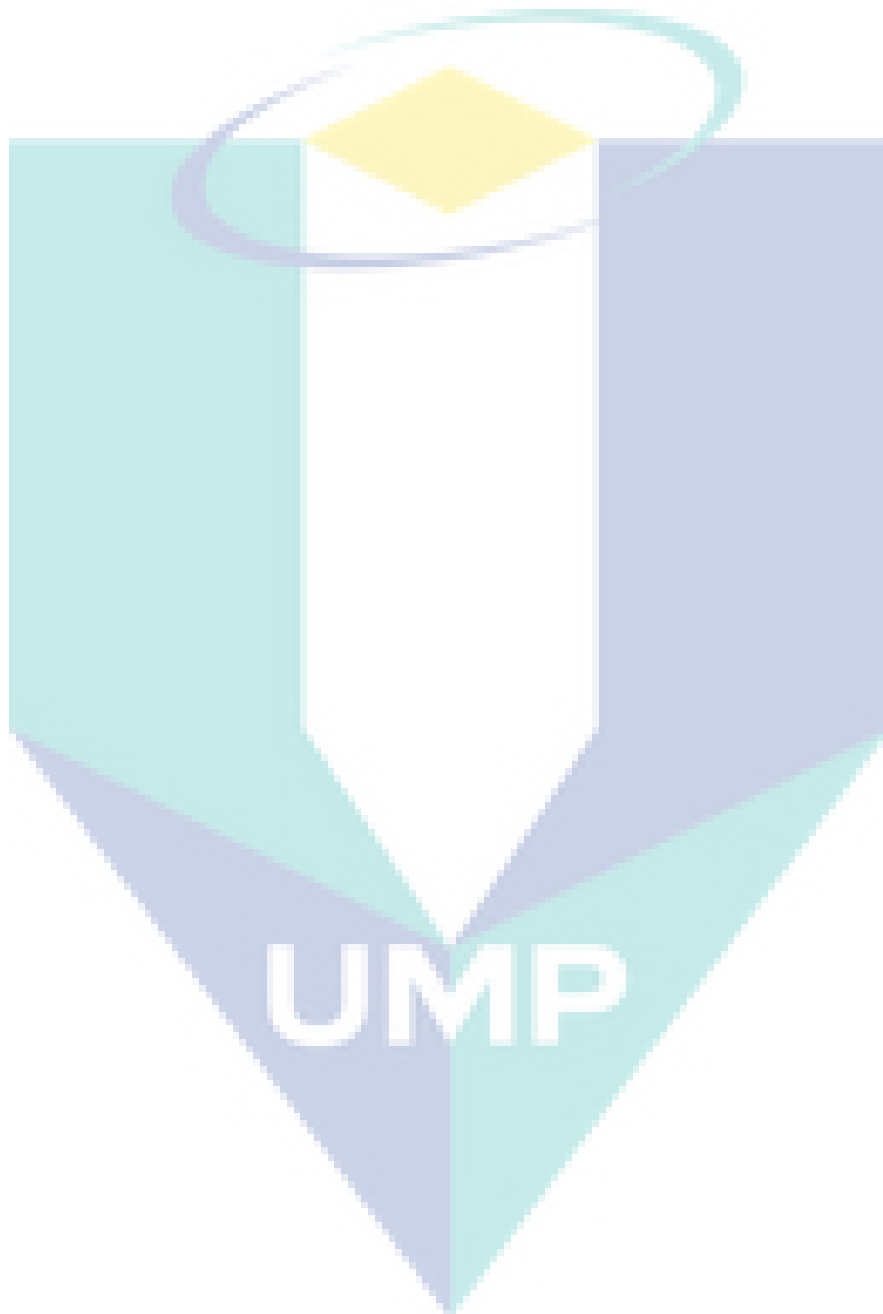
9.2 Suggestion for Future Research

Indeed, the implementation of CBC in the boundary condition is not as straightforward as compared to CWT and CHF. As observed in the figures and tables in Chapter 4 to Chapter 8, only small values of convective parameter are used. For the of case $\gamma \geq 1$, singularities were encountered from the result in the numerical scheme. Until now, this problem remains unsolved, even many approaches introduced in the initial profile in MATLAB. Therefore this research is not complete and there are possibly numerous approaches that could be adopted to improve research in this area. Further, there are some interesting research studies as yet not carried out regarding the problem of boundary layer flow. The problems presented in this thesis concentrate on the horizontal circular cylinder only. Therefore, this problem could be extended based on the following suggestions;

- i) Examine the new types of boundary conditions; mixed thermal Newtonian heating.
- ii) Incorporate other effects like chemical reaction, radiation and Soret/ Dufour which are also important in industrial applications.
- iii) Investigate other types of geometries such as microtubes or rotating down-pointing cone.
- iv) Consider further types of non-Newtonian fluids. For instance Maxwell, Walter's, Burger's fluid and others.
- v) Extend the value of convective parameter γ in CBC so that more accurate results are discovered.

Undoubtedly, the suggested future work that highlighted here is not an easy task to be explored. The most challenging aspect in extending the boundary flow problem by regarding convective boundary conditions is to develop a suitable initial profile to suit or fit the boundary condition perfectly for small number of convective parameters, γ up to a vast number, so that the case of CWT would be recovered. If the initial profile can be successfully discovered, then the remaining parts will be much easier to determine.

Therefore, as a sequel to this thesis, it is hoped that the impasse in finding the initial profile of convective boundary condition can be solved entirely and other suggested area could be taken into account into the problems.



REFERENCES

- Abbasi, F., Shehzad, S., Hayat, T., and Alhuthali, M. (2016). Mixed convection flow of jeffrey nanofluid with thermal radiation and double stratification. *Journal of Hydrodynamics, Ser. B*, 28(5):840 – 849.
- Abdallaoui, M. E., Hasnaoui, M., and Amahmid, A. (2015). Numerical simulation of natural convection between a decentered triangular heating cylinder and a square outer cylinder filled with a pure fluid or a nanofluid using the lattice boltzmann method. *Powder Technology*, 277:193 – 205.
- Abou-Ziyan, H., Kalender, A., Shedid, M., and Abdel-Hameed, H. (2017). Experimental investigation of free convection from short horizontal cylinder to newtonian and power-law liquids of large prandtl numbers. *Experimental Thermal and Fluid Science*, 86:102 – 116.
- Abu-Nada, E. and Oztop, H. F. (2009). Effect of inclination angle on natural convection in enclosures filled with Cu-water nanofluid. *International Journal Heat Fluid Flow*, 30(4):669 – 678.
- Acheson, D. (1990). *Elementary Fluid Dynamics*. Clarendon Press, Oxford, London.
- Acrivos, A. (1966). On the combined effect of forced and free convection heat transfer in laminar boundary layer flows. *Chemical Engineering Science*, 21(4):343 – 352.
- Ahmad, K., Nazar, R., and Pop, I. (2012). Mixed convection in laminar film flow of a micropolar fluid. *International Communications in Heat and Mass Transfer*, 39(1):36 – 39.
- Ahmad, S., Arifin, N., Nazar, R., and Pop, I. (2009). Mixed convection boundary layer flow past an isothermal horizontal circular cylinder with temperature-dependent viscosity. *International Journal of Thermal Sciences*, 48(10):1943 – 1948.
- Ahmad, S., Nazar, R., and Pop, I. (2005). Forced convection boundary layer flow over a horizontal circular cylinder with constant surface heat flux. Kedah Malaysia. Proceeding of the Symposium Kebangsaan Sains Matematik ke XIII.
- Alsaedi, A., Awais, M., and Hayat, T. (2012). Effects of heat generation/absorption on stagnation point flow of nanofluid over a surface with convective boundary conditions. *Communications in Nonlinear Science and Numerical Simulation*, 17(11):4210 – 4223.
- Altunkaya, A. N., Avci, M., and Aydin, O. (2017). Effects of viscous dissipation on mixed convection in a vertical parallel-plate microchannel with asymmetric uniform wall heat fluxes: The slip regime. *International Journal of Heat and Mass Transfer*, 111:495 – 499.
- Amin, N. and Riley, N. (1990). Horizontal free convection. *Proceedings of the Royal Society of London A: Mathematical, Physical and Engineering Sciences*, 427(1873):371–384.
- Anderson, J. D. J. (2005). Ludwig Prandtl's boundary layer. *American Institute of Physics*, 58(12):42 – 48.

- Anwar, I., Amin, N., and Pop, I. (2008). Mixed convection boundary layer flow of a viscoelastic fluid over a horizontal circular cylinder. *International Journal of Non-Linear Mechanics*, 43(9):814 – 821.
- Ariman, T., Turk, M., and Sylvester, N. (1973). Microcontinuum fluid mechanics —a review. *International Journal of Engineering Science*, 11(8):905 – 930.
- Ashorynejad, H. R., Mohamad, A. A., and Sheikholeslami, M. (2013). Magnetic field effects on natural convection flow of a nanofluid in a horizontal cylindrical annulus using Lattice Boltzmann method. *International Journal of Thermal Sciences*, 64:240 – 250.
- Aziz, A. (2009). A similarity solution for laminar thermal boundary layer over a flat plate with a convective surface boundary condition. *Communications in Nonlinear Science and Numerical Simulation*, 14(4):1064 – 1068.
- Aziz, A. and Khan, W. (2012). Natural convective boundary layer flow of a nanofluid past a convectively heated vertical plate. *International Journal of Thermal Sciences*, 52:83 – 90.
- Bachok, N., Ishak, A., and Pop, I. (2010). Boundary-layer flow of nanofluids over a moving surface in a flowing fluid. *International Journal of Thermal Sciences*, 49(9):1663 – 1668.
- Bachok, N., Ishak, A., and Pop, I. (2012). Unsteady boundary layer flow of a nanofluid over a permeable stretching/shrinking sheet. *International Journal and Heat Mass Transfer*, 55:2102 – 2109.
- Balaram, M. and Sastri, V. (1973). Micropolar free convection flow. *International Journal of Heat and Mass Transfer*, 16(2):437 – 441.
- Bejan, A. (2013). *Convection heat transfer (4th edition)*. John Wiley and Sons., New York.
- Bhargava, R. and Takhar, H. (2000). Numerical study of heat transfer characteristics of the micropolar boundary layer near a stagnation point on a moving wall. *International Journal of Engineering Science*, 38(4):383 – 394.
- Bharti, R. P., Chhabra, R. P., and Eswaran, V. (2007). Steady forced convection heat transfer from a heated circular cylinder to power-law fluids. *International Journal of Heat and Mass Transfer*, 50(7):977 – 990.
- Bhattacharyya, S. and Pop, I. (1996). Free convection from cylinders of elliptic cross-section in micropolar fluids. *International Journal of Engineering Science*, 34(11):1301 – 1310.
- Bhowmick, S., Molla, M. M., Mia, M., and Saha, S. C. (2014). Non-newtonian mixed convection flow from a horizontal circular cylinder with uniform surface heat flux. *Procedia Engineering*, 90:510 – 516.
- Birkhauser, G. L. (1999). Micropolar fluids: Theory and applications. *Journal of Fluid Mechanics*, 401(1):378 – 381.
- Blasius, H. (1908). The boundary layer in fluid with little friction. *Journal of Applied Mathematics and Physics*, 56(60):397 – 398.

- Borrelli, A., Giantesio, G., and Patria, M. C. (2013). Numerical simulations of three-dimensional mhd stagnation-point flow of a micropolar fluid. *Computers & Mathematics with Applications*, 66(4):472 – 489.
- Botte, G. G., Subramanian, V. R., and White, R. E. (2000). Mathematical modeling of secondary lithium batteries. *Electrochimica Acta*, 45:25952609.
- Buongiorno, J. (2006). Convective transport in nanofluids. *Journal of Heat Transfer*, 128:240 – 250.
- Cebeci, T. and Bradshaw, P. (1988). *Physical and Computational Aspects of Convective Heat Transfer*. Springer, New York.
- Chaudhary, R. C. and Jain, P. (2006). Unsteady free convection boundary-layer flow past an impulsively started vertical surface with newtonian heating. *Romanian Journal of Physics*, 9:911 – 925.
- Cheng, P. (1982). Mixed convection about a horizontal cylinder and sphere in a fluid-saturated porous medium. *International Journal of Heat and Mass Transfer*, 25:1245 – 1246.
- Cheng, P. and Minkowycz, W. J. (1977). Free convection about a vertical flat plate embedded in a porous medium with application to heat transfer from a dike. *Journal of Geophysical Research*, 82(14):2040 – 2044.
- Choi, U. S. (1995). Enhancing thermal conductivity of fluids with nanoparticles. San Francisco, CA. ASME International Mechanical Engineering Congress and Exposition.
- Darus, A. N. (1994). *Analisis Pemindahan Haba*. Dewan Bahasa dan Pustaka, Kuala Lumpur.
- Das, K., Duari, P. R., and Kundu, P. K. (2015). Numerical simulation of nanofluid flow with convective boundary condition. *Journal of the Egyptian Mathematical Society*, 23(2):435 – 439.
- Daunghongsuk, W. and Wongwises, S. (2007). A critical review of convective heat transfer of nanofluids. *Renewable and Sustainable Energy Reviews*, 11(5):797 – 817.
- Dawood, H., Mohammed, H., Sidik, N. A. C., Munisamy, K., and Wahid, M. (2015). Forced, natural and mixed-convection heat transfer and fluid flow in annulus: A review. *International Communications in Heat and Mass Transfer*, 62:45 – 57.
- Deka, R. K., Paul, A., and Chaliha, A. (2017). Transient free convection flow past vertical cylinder with constant heat flux and mass transfer. *Ain Shams Engineering Journal*, 8(4):643 – 651.
- Dhanai, R., Rana, P., and Kumar, L. (2016). Mhd mixed convection nanofluid flow and heat transfer over an inclined cylinder due to velocity and thermal slip effects: Buongiorno's model. *Powder Technology*, 288:140 – 150.
- Dinarvand, S. and Pop, I. (2017). Free-convective flow of copper/water nanofluid about a rotating down-pointing cone using Tiwari-Das nanofluid scheme. *Advanced Powder Technology*, 28(3):900 – 909.

- Ding, Y., Chen, H., Wang, L., Yang, C.-Y., He, Y., Yang, W., Lee, W. P., Zhang, L., and Huo, R. (2007). Heat transfer intensification using nanofluids. *KONA Powder and Particle Journal*, 25:23 – 38.
- Durgam, S., Venkateshan, S., and Sundararajan, T. (2017). Experimental and numerical investigations on optimal distribution of heat source array under natural and forced convection in a horizontal channel. *International Journal of Thermal Sciences*, 115:125 – 138.
- Eastman, J. A., Choi, U. S., Li, S., Thompson, L. J., and Lee, S. (1997). Enhanced thermal conductivity through the development of nanofluids. Pittsburgh. MRS.
- Eckert, E. (1942). The calculation of the heat transfer in the laminar boundary layer around bodies. *VDI-Forschungsheft*, 416:1 – 24.
- Eiyad, A.-N., Ziyad, K., Saleh, M., and Ali, Y. (2008). Heat transfer enhancement in combined convection around a horizontal cylinder using nanofluids. *Journal of Heat Transfer*, 130(8):084505.
- Elgazery, N. S. and Elazem, N. Y. A. (2009). The effect of variable thermal conductivity on micro-polar fluid flow by chebyshev collocation method. *Chemical Engineering Communications*, 197(3):400 – 422.
- Elliott, L. (1970). Free convection on a two dimensional or axisymmetric body. *Journal Mechanical Applied Mathematics*, 23(5):153 – 162.
- Elsherbiny, S. M., Teamah, M. A., and Moussa, A. R. (2017). Experimental mixed convection heat transfer from an isothermal horizontal square cylinder. *Experimental Thermal and Fluid Science*, 82:459 – 471.
- Eringen, A. (1966). Theory of micropolar fluids. *Journal of Mathematics and Mechanics*, 16:1 – 18.
- Eringen, A. (1972). Theory of thermomicrofluids. *Journal of Mathematical Analysis and Applications*, 38(2):480 – 496.
- Frössling, N. (1940). Evaporation, heat transfer and velocity distribution in two-dimensional and rotationally symmetrical laminar boundary-layer flow. *Lunds. University Arsskr. NF Avdanced 2*, 35(4):2 – 38.
- Garoosi, F., Jahanshaloo, L., and Garoosi, S. (2015). Numerical simulation of mixed convection of the nanofluid in heat exchangers using a buongiorno model. *Powder Technology*, 269:296 – 311.
- Gibanov, N. S., Sheremet, M. A., and Pop, I. (2016). Free convection in a trapezoidal cavity filled with a micropolar fluid. *International Journal of Heat and Mass Transfer*, 99:831 – 838.
- Gorla, R. S. R. (1995). Unsteady mixed convection in micropolar boundary layer flow on a vertical plate. *Fluid Dynamics Research*, 15(4):237.
- Gruyter., D. (2014). *Keller-Box Method and Its Application*. Higher Education Press., Berlin, Boston.

- Hajmohammadi, M., Maleki, H., Lorenzini, G., and Nourazar, S. (2015). Effects of Cu and Ag nano-particles on flow and heat transfer from permeable surfaces. *Advanced Powder Technology*, 26(1):193 – 199.
- Hassani, M., Tabar, M. M., Nemati, H., Domairry, G., and Noori, F. (2011). An analytical solution for boundary layer flow of a nanofluid past a stretching sheet. *International Journal of Thermal Sciences*, 50(11):2256 – 2263.
- Hassanien, A. I. (1997). Combined forced and free convection in boundary layer flow of a micropolar fluid over a horizontal plate. *Journal Applied Mathematics and Physics*, 48(4):571 – 583.
- Hassanien, I. A. and Gorla, R. S. R. (1990). Combined forced and free convection in stagnation flows of micropolar fluids over vertical non-isothermal surfaces. *International Journal of Engineering Science*, 28(8):783 – 792.
- Hayat, T., Khan, M. I., Waqas, M., and Alsaedi, A. (2017). Newtonian heating effect in nanofluid flow by a permeable cylinder. *Results in Physics*, 7:256 – 262.
- Hussanan, A., Salleh, M. Z., Khan, I., and Shafie, S. (2017). Convection heat transfer in micropolar nanofluids with oxide nanoparticles in water, kerosene and engine oil. *Journal of Molecular Liquids*, 229:482 – 488.
- Ibrahim, F. and Hassanien, I. (2001). Local nonsimilarity solutions for mixed convection boundary layer flow of a micropolar fluid on horizontal flat plates with variable surface temperature. *Applied Mathematics and Computation*, 122(2):133 – 153.
- Incropera, F. P., DeWitt, D. P., Bergman, T. L., and Lavine, A. S. (2006). *Fundamentals of Heat and Mass Transfer*. John Wiley and Sons., New York.
- Ishak, A. (2010). Thermal boundary layer flow over a stretching sheet in a micropolar fluid with radiation effect. *Meccanica*, 45(3):367 – 373.
- Ishak, A., Nazar, R., and Pop, I. (2009). Dual solutions in mixed convection boundary layer flow of micropolar fluids. *Communications in Nonlinear Science and Numerical Simulation*, 14(4):1324 – 1333.
- Ishak, A., Yacob, N. A., and Bachok, N. (2011). Radiation effects on the thermal boundary layer flow over a moving plate with convective boundary condition. *Meccanica*, 46(4):795 – 801.
- Ismael, M. A., Mansour, M., Chamkha, A. J., and Rashad, A. (2016). Mixed convection in a nanofluid filled-cavity with partial slip subjected to constant heat flux and inclined magnetic field. *Journal of Magnetism and Magnetic Materials*, 416:25 – 36.
- Jena, S. and Mathur, M. (1981). Similarity solutions for laminar free convection flow of a thermomicro-polar fluid past a non-isothermal vertical flat plate. *International Journal of Engineering Science*, 19(11):1431 – 1439.
- Joshi, N. and Sukhatme, S. (1971). An analysis of combined free and forced convection heat transfer from a horizontal circular cylinder to a transverse flow. *ASME. J. Heat Transfer*, 93(4):343 – 352.

- Kaprawi, S. and Santoso, S. (2012). Convective heat transfer from a heated elliptical cylinder at uniform wall temperature. *International Journal of Energy and Environment*, 3(1):133 – 140.
- Kasim, A. R. M. (2014). *Convective Boundary Layer Flow of Viscoelastic Fluid*. Ph.D Thesis, Universiti Teknologi Malaysia.
- Kefayati, G. (2017). Mixed convection of non-newtonian nanofluid in an enclosure using Buongiorno's mathematical model. *International Journal of Heat and Mass Transfer*, 108, Part B:1481 – 1500.
- Keller, H. (1970). *A New Difference Method for Parabolic Problems In: Bramble, J., Ed., Numerical Methods for Partial Differential Equations*. Academic Press, New York.
- Kelson, N. and Desseaux, A. (2001). Effect of surface conditions on flow of a micropolar fluid driven by a porous stretching sheet. *International Journal of Engineering Science*, 39(16):1881 – 1897.
- Khan, J. A., Mustafa, M., and Mushtaq, A. (2016). On three-dimensional flow of nanofluids past a convectively heated deformable surface: A numerical study. *International Journal of Heat and Mass Transfer*, 94:49 – 55.
- Khan, W. and Aziz, A. (2011). Double-diffusive natural convective boundary layer flow in a porous medium saturated with a nanofluid over a vertical plate: Prescribed surface heat, solute and nanoparticle fluxes. *International Journal of Thermal Sciences*, 50(11):2154 – 2160.
- Khan, W., Culham, J., and Yovanovich, M. (2004). Fluid flow around and heat transfer from an infinite circular cylinder. *ASME. Journal Heat Transfer*, 127(7):785 – 790.
- Khan, W. and Pop, I. (2010). Boundary-layer flow of a nanofluid past a stretching sheet. *International Journal of Heat and Mass Transfer*, 53(11):2477 – 2483.
- Khanafer, K., Vafai, K., and Lightstone, M. (2003). Buoyancy-driven heat transfer enhancement in a two-dimensional enclosure utilizing nanofluids. *International Journal of Heat and Mass Transfer*, 46(19):3639 – 3653.
- Kim, Y. J. and Lee, J.-C. (2003). Analytical studies on mhd oscillatory flow of a micropolar fluid over a vertical porous plate. *Surface and Coatings Technology*, 171(13):187 – 193.
- Kuznetsov, A. and Nield, D. (2010). Natural convective boundary-layer flow of a nanofluid past a vertical plate. *International Journal of Thermal Sciences*, 49(2):243 – 247.
- Kuznetsov, A. and Nield, D. (2011). Double-diffusive natural convective boundary-layer flow of a nanofluid past a vertical plate. *International Journal of Thermal Sciences*, 50(5):712 – 717.
- Mabood, F., Ibrahim, S., Kumar, P., and Khan, W. (2017). Viscous dissipation effects on unsteady mixed convective stagnation point flow using Tiwari-Das nanofluid model. *Results in Physics*, 7:280 – 287.
- Mabood, F., Khan, W., and Yovanovich, M. (2016). Forced convection of nanofluid flow across horizontal circular cylinder with convective boundary condition. *Journal of Molecular Liquids*, 222:172 – 180.

- Magyari, E. (2011). Comment on a similarity solution for laminar thermal boundary layer over a flat plate with a convective surface boundary condition by A. Aziz. *Communications in Nonlinear Science and Numerical Simulation*, 16(1):599 – 601.
- Magyari, E. and Keller, B. (2001). Exact analytical solutions of forced convection flow in a porous medium. *International Communication. Heat Mass Transfer*, 28(2):233 – 241.
- Mahfouz, F. (2013). Numerical simulation of free convection within an eccentric annulus filled with micropolar fluid using spectral method. *Applied Mathematics and Computation*, 219(10):5397 – 5409.
- Mahgoub, S. (2013). Forced convection heat transfer over a flat plate in a porous medium. *Ain Shams Engineering Journal*, 4(4):605 – 613.
- Maiti, G. (1975). Convective heat transfer in micropolar fluid flow through a horizontal parallel plate channel. *Journal of Applied Mathematics and Mechanics*, 55(2):105–111.
- Makinde, O. and Aziz, A. (2011). Boundary layer flow of a nanofluid past a stretching sheet with a convective boundary condition. *International Journal of Thermal Sciences*, 50(7):1326 – 1332.
- Malik, M., Jamil, H., Salahuddin, T., Bilal, S., Rehman, K., and Mustafa, Z. (2016). Mixed convection dissipative viscous fluid flow over a rotating cone by way of variable viscosity and thermal conductivity. *Results in Physics*, 6:1126 – 1135.
- Mansour, M., El-Hakiem, M., and Kabeir, S. E. (2000). Heat and mass transfer in magnetohydrodynamic flow of micropolar fluid on a circular cylinder with uniform heat and mass flux. *Journal of Magnetism and Magnetic Materials*, 220(23):259 – 270.
- Mansur, S. and Ishak, A. (2013). The flow and heat transfer of a nanofluid past a stretching/shrinking sheet with a convective boundary condition. *Abstract and Applied Analysis*, 2013:1 – 9.
- Martynenko, O. and Khramtsov, P. (2005). *Free Convective Heat Transfer*. Springer, Springer Berlin Heidelberg, New York.
- Mathur, M., Ojha, S., and Ramachandran, P. (1978). Thermal boundary layer of a micropolar fluid on a circular cylinder. *International Journal of Heat and Mass Transfer*, 21:923 – 933.
- Merkin, J. (1976). Free convection boundary layer on an isothermal horizontal circular cylinders. St. Louis, Mo. ASME/AIChE Heat transfer conference.
- Merkin, J. (1977). Mixed convection from a horizontal circular cylinder. *International Journal of Heat and Mass Transfer*, 20(1):73 – 77.
- Merkin, J. (1994). Natural-convection boundary-layer flow on a vertical surface with newtonian heating. *International Journal of Heat and Fluid Flow*, 15(5):392 – 398.
- Merkin, J. and Pop, I. (2011). The forced convection flow of a uniform stream over a flat surface with a convective surface boundary condition. *Communications in Nonlinear Science and Numerical Simulation*, 16(9):3602 – 3609.

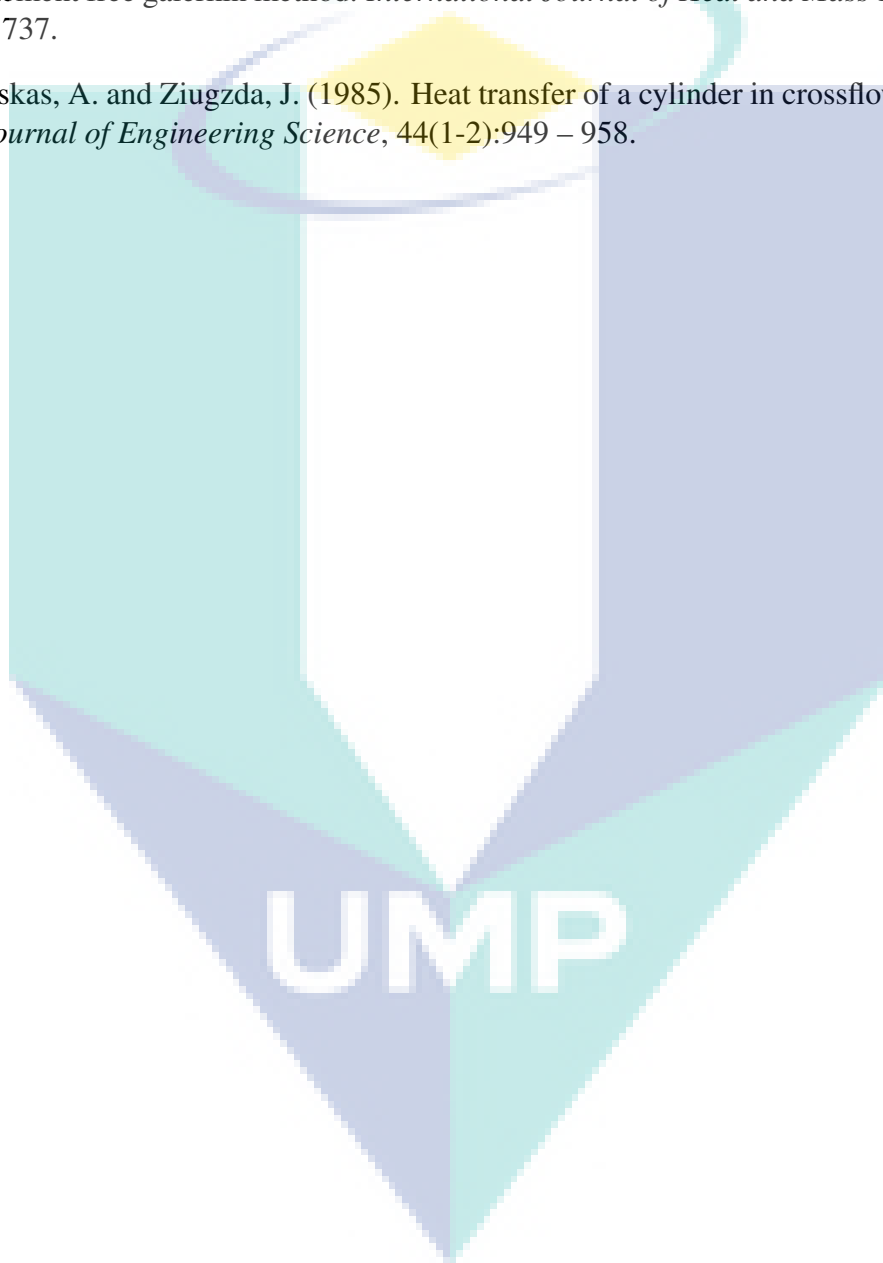
- Merkin, J. H. and Pop, I. (1988). A note on the free convection boundary layer on a horizontal circular cylinder with constant heat flux. *Wärme - und Stoffübertragung*, 22(1):79 – 81.
- Mirgolbabaeei, H., Barari, A., Ibsen, L., and Sfahani, M. (2010). Analytical solution of forced-convective boundary-layer flow over a flat plate. *Archives of Civil and Mechanical Engineering*, 10(2):41 – 51.
- Mohamed, M. K. A. (2013). *Mathematical modelling for the convection boundary layer flow in a viscous fluid with Newtonian heating and convective boundary conditions*. MSc Thesis, Universiti Malaysia Pahang.
- Mohammed, H. A. and Salman, Y. K. (2007). Free and forced convection heat transfer in the thermal entry region for laminar flow inside a circular cylinder horizontally oriented. *Energy Conversion and Management*, 48(7):2185 – 2195.
- Mohd Rohni, A., Ahmad, S., and Pop, I. (2013). Forced convection boundary layer flow along a horizontal cylinder in porous medium filled by nanofluid. *International Journal of Humanities and Management Sciences*, 1(1):23 – 27.
- Moshizi, S., Zamani, M., Hosseini, S., and Malvandi, A. (2017). Mixed convection of magnetohydrodynamic nanofluids inside microtubes at constant wall temperature. *Journal of Magnetism and Magnetic Materials*, 430:36 – 46.
- Mukhopadhyay, S. (2012). Mixed convection boundary layer flow along a stretching cylinder in porous medium. *Journal of Petroleum Science and Engineering*, 9697:73 – 78.
- Mukhopadhyay, S. and Mandal, I. C. (2015). Magnetohydrodynamic (MHD) mixed convection slip flow and heat transfer over a vertical porous plate. *Engineering Science and Technology, an International Journal*, 18(1):98 – 105.
- Na, T. Y. (1979). *Computational Methods in Engineering Boundary Value Problems*. Academic Press, New York.
- Nadeem, S., Mehmood, R., and Akbar, N. S. (2014). Optimized analytical solution for oblique flow of a Casson-nano fluid with convective boundary conditions. *International Journal of Thermal Sciences*, 78:90 – 100.
- Nakai, S. and Okazaki, T. (1975). Heat transfer from a horizontal circular wire at small Reynolds and Grashof numbers. *International Journal Heat Mass Transfer*, 18:397 – 413.
- Nayak, R., Bhattacharyya, S., and Pop, I. (2015). Numerical study on mixed convection and entropy generation of Cu - water nanofluid in a differentially heated skewed enclosure. *International Journal of Heat and Mass Transfer*, 85:620 – 634.
- Nazar, R. (2003). *Mathematical model for free and mixed convection boundary layer flows of micropolar fluids*. Ph.D Thesis, Universiti Teknologi Malaysia.
- Nazar, R., Amin, N., Groan, T., and Pop, I. (2002a). Free convection boundary layer on a sphere with constant surface heat flux in a micropolar fluid. *International Communications in Heat and Mass Transfer*, 29(8):1129 – 1138.
- Nazar, R., Amin, N., and Pop, I. (2002b). Free convection boundary layer on an isothermal horizontal circular cylinder in a micropolar fluid. *Heat Transfer*, 2:525 – 530.

- Nazar, R., Amin, N., and Pop, I. (2003). Mixed convection boundary layer flow from a horizontal circular cylinder in micropolar fluids: case of constant wall temperature. *International Journal of Numerical Methods for Heat & Fluid Flow*, 13(1):86 – 109.
- Nazar, R., Amin, N., and Pop, I. (2004). Mixed convection boundary-layer flow from a horizontal circular cylinder with a constant surface heat flux. *Heat and Mass Transfer*, 40(3-4):219 – 227.
- Nield, D. and Kuznetsov, A. (2009). The Cheng-Minkowycz problem for natural convective boundary-layer flow in a porous medium saturated by a nanofluid. *International Journal of Heat and Mass Transfer*, 52(25-26):5792 – 5795.
- Nield, D. A. and Kuznetsov, A. V. (2011). The Cheng-Minkowycz problem for the double-diffusive natural convective boundary layer flow in a porous medium saturated by a nanofluid. *International Journal of Heat and Mass Transfer*, 54:5 – 9.
- Othman, N. A., Yacob, N. A., Bachok, N., Ishak, A., and Pop, I. (2017). Mixed convection boundary-layer stagnation point flow past a vertical stretching/shrinking surface in a nanofluid. *Applied Thermal Engineering*, 115:1412 – 1417.
- Oztop, H. F. and Abu-Nada, E. (2008). Numerical study of natural convection in partially heated rectangular enclosures filled with nanofluids. *International Journal of Heat and Fluid Flow*, 29(5):1326 – 1336.
- Pantokratoras, A. (2014). A note on natural convection along a convectively heated vertical plate. *International Journal of Thermal Sciences*, 76:221 – 224.
- Peddieson, J. and McNitt, R. P. (1970). Boundary layer theory for micropolar fluid. *Recent Advance Engineering Science*, 5:405 – 426.
- Rahmati, A. R., Roknabadi, A. R., and Abbaszadeh, M. (2016). Numerical simulation of mixed convection heat transfer of nanofluid in a double lid-driven cavity using Lattice Boltzmann method. *Alexandria Engineering Journal*, 55(4):3101 – 3114.
- RamReddy, C., Murthy, P., Chamkha, A. J., and Rashad, A. (2013). Soret effect on mixed convection flow in a nanofluid under convective boundary condition. *International Journal of Heat and Mass Transfer*, 64:384 – 392.
- Ramzan, M., Bilal, M., Farooq, U., and Chung, J. D. (2016). Mixed convective radiative flow of second grade nanofluid with convective boundary conditions: An optimal solution. *Results in Physics*, 6:796 – 804.
- Rebhi, A. D., Tariq, A. A., Benbella, A. S., and Mahmoud, A. (2007). Unsteady natural convection heat transfer of micropolar fluid over a vertical surface with constant heat flux. *Turkish Journal Engineering Environment Science*, 31:225 – 233.
- Roca, N. C. and Pop, I. (2013). Mixed convection stagnation point flow past a vertical flat plate with a second order slip: Heat flux case. *International Journal of Heat and Mass Transfer*, 65:102 – 109.
- Sajid, M., Abbas, Z., and Hayat, T. (2009). Homotopy analysis for boundary layer flow of a micropolar fluid through a porous channel. *Applied Mathematical Modelling*, 33(11):4120 – 4125.

- Sakai, F., Li, W., and Nakayama, A. (2014). A rigorous derivation and its applications of volume averaged transport equations for heat transfer in nanofluids saturated metal foam. *Proc. 15th International Heat Transfer Conference*, 23(2):435 – 439.
- Salleh, M. Z. and Nazar, R. (2010). Free convection boundary layer flow over a horizontal circular cylinder with Newtonian heating. *Sains Malaysiana*, 39(4):671 – 676.
- Salleh, M. Z., Nazar, R., Arifin, N., and Pop, I. (2011). Numerical solutions of forced convection boundary layer flow on a horizontal circular cylinder with Newtonian heating. *Malaysian Journal of Mathematical Sciences*, 5(2):161 – 184.
- Salleh, M. Z., Nazar, R., and Pop, I. (2009). Forced convection boundary layer flow at a forward stagnation point with Newtonian heating. *Chemical Engineering Communications*, 196(9):987 – 996.
- Salleh, M. Z., Nazar, R., and Pop, I. (2010a). Boundary layer flow and heat transfer over a stretching sheet with Newtonian heating. *Journal of the Taiwan Institute of Chemical Engineers*, 41(6):651 – 655.
- Salleh, M. Z., Nazar, R., and Pop, I. (2010b). Mixed convection boundary layer flow over a horizontal circular cylinder with Newtonian heating. *Heat and Mass Transfer*, 46(11):1411 – 1418.
- Samyuktha, N. and Ravindran, R. (2015). Thermal radiation effect on mixed convection flow over a vertical stretching sheet embedded in a porous medium with suction (injection). *Procedia Engineering*, 127:767 – 774.
- Sanitjai, S. and Goldstein, R. (2004). Forced convection heat transfer from a circular cylinder in crossflow to air and liquids. *International Journal of Heat and Mass Transfer*, 47(22):4795 – 4805.
- Sastry, V. U. K. and Maity, G. (1976). Numerical solution of combined convective heat transfer of micropolar fluid in an annulus of two vertical pipes. *International Journal of Heat and Mass Transfer*, 19:207 – 211.
- Schlichting, H. (1968). *Boundary Layer Theory 8th Edition*. Springer Inc.
- Seshadri, R. and Munjam, S. R. (2016). Mixed convection flow due to a vertical plate in the presence of heat source and chemical reaction. *Ain Shams Engineering Journal*, 7(2):671 – 682.
- Seyyedi, S., Dayyan, M., Soleimani, S., and Ghasemi, E. (2015). Natural convection heat transfer under constant heat flux wall in a nanofluid filled annulus enclosure. *Ain Shams Engineering Journal*, 6(1):267 – 280.
- Sheikholeslami, M. and Bhatti, M. (2017). Forced convection of nanofluid in presence of constant magnetic field considering shape effects of nanoparticles. *International Journal of Heat and Mass Transfer*, 111:1039 – 1049.
- Sheikholeslami, M. and Ganji, D. (2016). Nanofluid convective heat transfer using semi analytical and numerical approaches: A review. *Journal of the Taiwan Institute of Chemical Engineers*, 65:43 – 77.

- Sheremet, M. A., Grosan, T., and Pop, I. (2015). Free convection in a square cavity filled with a porous medium saturated by nanofluid using Tiwari and Das' nanofluid model. *Transport in Porous Media*, 106(3):595 – 610.
- Sheremet, M. A. and Pop, I. (2015). Free convection in a porous horizontal cylindrical annulus with a nanofluid using Buongiorno's model. *Computers Fluids*, 118:182 – 190.
- Shu, J. J. and Wilks, G. (1995). An accurate numerical method for systems of differentio-integral equations associated with multiphase flow. *Computers & Fluids*, 24(6):625 – 652.
- Soares, A. A., Ferreira, J. M., and Chhabra, R. P. (2005). Flow and forced convection heat transfer in crossflow of non-newtonian fluids over a circular cylinder. *Industrial & Engineering Chemistry Research*, 44(15):5815 – 5827.
- Soleimani, S., Sheikholeslami, M., Ganji, D., and Gorji-Bandpay, M. (2012). Natural convection heat transfer in a nanofluid filled semi-annulus enclosure. *International Communications in Heat and Mass Transfer*, 39(4):565 – 574.
- Sparrow, E. and Lee, L. (1976). Analysis of mixed convection about a horizontal cylinder. *International Journal of Heat and Mass Transfer*, 19(2):229 – 232.
- Sumaily, G. F. A., Sheridan, J., Ibsen, and Thompson, M. C. (2012). Analysis of forced convection heat transfer from a circular cylinder embedded in a porous medium. *International Journal of Thermal Sciences*, 51:121 – 131.
- Takhar, H. S., Agarwal, R. S., and Bhargava, R. (1998). Mixed convection flow of a micropolar fluid over a stretching sheet. *Heat and Mass Transfer*, 34(2):213 – 219.
- Tham, L., Nazar, R., and Pop, I. (2012). Mixed convection boundary layer flow from a horizontal circular cylinder in a nanofluid. *International Journal of Numerical Methods for Heat & Fluid Flow*, 22(5):576 – 606.
- Tham, L., Nazar, R., and Pop, I. (2014). Mixed convection flow from a horizontal circular cylinder embedded in a porous medium filled by a nanofluid: Buongiorno-Darcy model. *International Journal of Thermal Sciences*, 84:21 – 33.
- Tiwari, R. K. and Das, M. K. (2007). Heat transfer augmentation in a two-sided lid-driven differentially heated square cavity utilizing nanofluids. *International Journal of Heat and Mass Transfer*, 50(910):2002 – 2018.
- Vimala, S., Damodaran, S., Sivakumar, R., and Sekhar, T. (2016). The role of magnetic Reynolds number in Magnetohydrodynamic forced convection heat transfer. *Applied Mathematical Modelling*, 40(1314):6737 – 6753.
- Waqas, M., Farooq, M., Khan, M. I., Alsaedi, A., Hayat, T., and Yasmeen, T. (2016). Magnetohydrodynamic mixed convection flow of micropolar liquid due to nonlinear stretched sheet with convective condition. *International Journal of Heat and Mass Transfer*, 102:766 – 772.
- Willson, A. J. (1969). Basic flows of a micropolar liquid. *Applied Scientific Research*, 20(1):338 – 355.

- Xuan, Y. and Li, Q. (2000). Heat transfer enhancement of nanofluids. *International Journal Heat Fluid Flow*, 21:58 – 64.
- Yacob, N. A., Ishak, A., Pop, I., and Vajravelu, K. (2011). Boundary layer flow past a stretching/shrinking surface beneath an external uniform shear flow with a convective surface boundary condition in a nanofluid. *Nanoscale Research Letters*, 6(1):314.
- Zhang, P., Zhang, X., Deng, J., and Song, L. (2016). A numerical study of natural convection in an inclined square enclosure with an elliptic cylinder using variational multiscale element free galerkin method. *International Journal of Heat and Mass Transfer*, 99:721 – 737.
- Zukauskas, A. and Ziugzda, J. (1985). Heat transfer of a cylinder in crossflow. *International Journal of Engineering Science*, 44(1-2):949 – 958.



APPENDIX A

LIST OF SYMBOLS IN MATLAB PROGRAM

MATLAB	Keller-box
np, nx	J, N
x, delx	$x, \Delta x$
eta, etainf, deleta	$y, y_\infty, \Delta y$
f, u, v, s, t, p, q	$f, f', f'', \theta, \theta', \phi, \phi'$
cfb, cub, csb	$f_{j-1/2}^{n-1}, u_{j-1/2}^{n-1}, s_{j-1/2}^{n-1}$
ctb, cpb, cqb	$t_{j-1/2}^{n-1}, p_{j-1/2}^{n-1}, q_{j-1/2}^{n-1}$
cfsb, cftb, cfqb	$f_{j-1/2}^{n-1} s_{j-1/2}^{n-1}, f_{j-1/2}^{n-1} t_{j-1/2}^{n-1}, f_{j-1/2}^{n-1} q_{j-1/2}^{n-1}$
cqtb, cusb, cupb, cttb	$q_{j-1/2}^{n-1} t_{j-1/2}^{n-1}, u_{j-1/2}^{n-1} s_{j-1/2}^{n-1}, u_{j-1/2}^{n-1} p_{j-1/2}^{n-1}, (t_{j-1/2}^{n-1})^2$
cderfb, cdertb, cderqb	$(f_j^{n-1} - f_{j-1}^{n-1})h_j^{-1}, (t_j^{n-1} - t_{j-1}^{n-1})h_j^{-1}, (q_j^{n-1} - q_{j-1}^{n-1})h_j^{-1}$
fb, ub, sb, tb, pb, qb	$f_{j-1/2}, u_{j-1/2}, s_{j-1/2}, t_{j-1/2}, p_{j-1/2}, q_{j-1/2}$
fsb, ftb, fqb	$f_{j-1/2} s_{j-1/2}, f_{j-1/2} t_{j-1/2}, f_{j-1/2} q_{j-1/2}$
usb, upb, qtb	$s_{j-1/2} s_{j-1/2}, u_{j-1/2} p_{j-1/2}, q_{j-1/2} t_{j-1/2}$
derfb, dertb, derqb	$(f_j - f_{j-1})h_j^{-1}, (t_j - t_{j-1})h_j^{-1}, (q_j - q_{j-1})h_j^{-1}$
a1 to a6	$(a_1)_j$ to $(a_6)_j$
b1 to b10	$(b_1)_j$ to $(b_{10})_j$
c1 to c10	$(c_1)_j$ to $(c_{10})_j$
r1 to r6	$(r_1)_j$ to $(r_6)_j$
R1, R2, R3	$(R_1)_{j-1/2}^{n-1}, (R_2)_{j-1/2}^{n-1}, (R_3)_{j-1/2}^{n-1}$
a, b, c	$[A_j], [B_j], [C_j]$
alfa, gamma	$[\alpha_j], [\Gamma_j]$
ww, rr, dell	$[W_j], [r_j], [\delta_j]$
delf, delu, dels, delt, delp,	$\delta f, \delta u, \delta s, \delta t, \delta p$

APPENDIX B

MATLAB PROGRAM

```

## Mixed Convection Boundary Layer Flow Over a Horizontal
## Circular Cylinder Porous Medium in a Nanofluid: Buongiorno Model
## Convective Boundary Condition (CBC)
## Method: Keller-Box Method
## Refer page 55 (Chapter 3)

%%%%%%%%%%%%%%%%%%%%%%%%%%%%%%%%%%%%%%%%%%%%%%%%%%%%%%%%%%%%%%%%%%%%%%%%
% Darcy's Model
%%%%%%%%%%%%%%%%%%%%%%%%%%%%%%%%%%%%%%%%%%%%%%%%%%%%%%%%%%%%%%%%%%%%%%%%
% The answer displayed in the result sheet will be started from
% number 1 instead of 0
%%%%%%%%%%%%%%%%%%%%%%%%%%%%%%%%%%%%%%%%%%%%%%%%%%%%%%%%%%%%%%%%%%%%%%%%
clear all;

for Le = [2 6]
    blt = 4; % Input boundary layer thickness
    xend = 3.1; % Input endpoint of x = 3.142
    delx = 0.01; % Input stepsize for x
    deleta = 0.1; % Input stepsize for boundary thickness
    ge = 1; % Input mixed parameter

    Le = 2; % Input Lewis Number = 2, 4, 6, 10, 50
    Nb = 0.5; % Input Brownian Number = 0.5, 1.0, 1.5, 2.0
    Nr = 0.1; % Input Buoyancy Ratio Parameter = 0.5, 1.0, 1.5, 2.0
    Nt = 0.5; % Input Thermophoresis parameter = 0.5, 1.0, 1.5, 2.0
    fs = 0.1; % Input convective parameter

% Equation 3.144

    if ( Nt == 0 && Nb == 0 )
        divide = 0;
    else
        divide = Nt/Nb;
    end

% To generate the initial value for velocity and temperature profiles

    x(1) = 0.0;
    xx(1) = 0.0;
    M(1) = 1.0;

```

```

% Equation 3.94

nx    = ( xend / delx ) + 1;
np    = ( blt / deleta ) + 1;

for i = 2:nx
x(i)  = x(i-1) + delx;
xx(i) = x(i) / (x(i) - x(i-1));
M(i)  = sin(x(i)) / x(i);
end

for i = 1:nx
dbstop if warning

stop  = 1.0;
k     = 1;
eselon = 0.00001;

while stop > eselon

eta(1,1) = 0.0;

for j = 2:np
eta(j,1) = eta(j-1,1) + deleta;
end

% Equations 3.165 to 3.171 - To generate initial value of velocity and temperature profiles :

etau15 = 1 / eta(np,1);

for j = 1:np
deta(j,k) = deleta;
etab      = eta(j,1) / eta(np,1);
etab1     = etab^2;
eqs       = (1 + (1 - Nr) * ge) * M(i);
eqsa      = 0.5 * eta(np,1) * (M(i) - eqs);
eqsb      = eta(np,1) * eqs;

if i == 1
f(j,1,i) = 0.25 * eta(np,1) * M(i) * etab1 * (3 - 0.5 * etab1);
u(j,1,i) = etab * M(i) * (1.5 - 0.5 * etab1);
v(j,1,i) = 1.5 * etau15 * M(i) * (1 - etab1);
s(j,1,i) = eta(np,1)*etab1 - eta(np,1) * etab;
t(j,1,i) = -fs * (1 - s(j,1,i));
p(j,1,i) = 1 - etab;

```

```

q(j,1,i) = -1 * etau15;

else

% from shift profile
f(j,1,i) = ff(j);
u(j,1,i) = uu(j);
s(j,1,i) = ss(j);
t(j,1,i) = tt(j);
p(j,1,i) = pp(j);
q(j,1,i) = qq(j);
end
end

% To define the coefficients of the linearized equations momentum and energy

for j = 2:np
% Previous station
if i == 1
cfb(j,i) = 0.0;
cub(j,i) = 0.0;
csb(j,i) = 0.0;
ctb(j,i) = 0.0;
cpb(j,i) = 0.0;
cqb(j,i) = 0.0;
cfsb(j,i) = cfb(j,i) * csb(j,i);
cqtb(j,i) = cqb(j,i) * ctb(j,i);
cttb(j,i) = ctb(j,i) * ctb(j,i);
cusb(j,i) = cub(j,i) * csb(j,i);
cftb(j,i) = cfb(j,i) * ctb(j,i);
cfqb(j,i) = cfb(j,i) * cqb(j,i);
cupb(j,i) = cub(j,i) * cpb(j,i);
cderfb(j,i) = 0.0;
cdertb(j,i) = 0.0;
cderqb(j,i) = 0.0;

else
cfb(j,i) = ffb(j);
cub(j,i) = uub(j);
csb(j,i) = ssb(j);
ctb(j,i) = ttb(j);
cpb(j,i) = ppb(j);
cqb(j,i) = qqb(j);
cfsb(j,i) = cfb(j,i) * csb(j,i);
cqtb(j,i) = cqb(j,i) * ctb(j,i);

```



```

cttb(j,i) = ctb(j,i) * ctb(j,i);
cusb(j,i) = cub(j,i) * csb(j,i);
cftb(j,i) = cfb(j,i) * ctb(j,i);
cfqb(j,i) = cfb(j,i) * cqj(j,i);
cupb(j,i) = cub(j,i) * cpb(j,i);
cderfb(j,i) = dderfb(j);
cdertb(j,i) = ddertb(j);
cderqb(j,i) = dderqb(j);
end

% Equations 3.95 to 3.98 - Present station (centered-difference derivatives)

fb(j,k,i) = 0.5 * ( f(j,k,i) + f(j-1,k,i) );
ub(j,k,i) = 0.5 * ( u(j,k,i) + u(j-1,k,i) );
sb(j,k,i) = 0.5 * ( s(j,k,i) + s(j-1,k,i) );
tb(j,k,i) = 0.5 * ( t(j,k,i) + t(j-1,k,i) );
pb(j,k,i) = 0.5 * ( p(j,k,i) + p(j-1,k,i) );
qb(j,k,i) = 0.5 * ( q(j,k,i) + q(j-1,k,i) );
fsb(j,k,i) = fb(j,k,i) * sb(j,k,i);
qtb(j,k,i) = qb(j,k,i) * tb(j,k,i);
ttb(j,k,i) = tb(j,k,i) * tb(j,k,i);
usb(j,k,i) = ub(j,k,i) * sb(j,k,i);
ftb(j,k,i) = fb(j,k,i) * tb(j,k,i);
fqj(j,k,i) = fb(j,k,i) * qb(j,k,i);
upb(j,k,i) = ub(j,k,i) * pb(j,k,i);
derfb(j,k,i) = ( f(j,k,i) - f(j-1,k,i) ) / deta(j,k);
dertb(j,k,i) = ( t(j,k,i) - t(j-1,k,i) ) / deta(j,k);
derqb(j,k,i) = ( q(j,k,i) - q(j-1,k,i) ) / deta(j,k);

% Equation 3.142 - Coefficients of the difference momentum equation

a1(j,k) = 1;
a2(j,k) = -1;
a3(j,k) = -0.5 * deta(j,k) * ge * M(i);
a4(j,k) = a3(j,k);
a5(j,k) = 0.5 * deta(j,k) * Nr * ge * M(i);
a6(j,k) = a5(j,k);

% Equation 3.143 - Coefficients of the difference energy equation

b1(j,k) = 1 + (1 + xx(i)) * 0.5 * deta(j,k) * fb(j,k,i) ...
+ 0.5 * Nb * deta(j,k) * qb(j,k,i)...
+ 0.5 * Nt * deta(j,k) * tb(j,k,i)...
+ 0.5 * Nt * deta(j,k) * tb(j,k,i)...
- 0.5 * xx(i) * deta(j,k) * cfb(j,i);
b2(j,k) = -2 + b1(j,k);

```

```

b3(j,k) = (1 + xx(i)) * 0.5 * deta(j,k) * tb(j,k,i) ...
+ 0.5 * xx(i) * deta(j,k) * ctb(j,i);
b4(j,k) = b3(j,k);
b5(j,k) = 0.5 * Nb * deta(j,k) * tb(j,k,i);
b6(j,k) = b5(j,k);
b7(j,k) = - 0.5 * xx(i) * deta(j,k) * sb(j,k,i) + 0.5 * xx(i) * deta(j,k) * csb(j,i);
b8(j,k) = b7(j,k);
b9(j,k) = - 0.5 * xx(i) * deta(j,k) * ub(j,k,i) - 0.5 * xx(i) * deta(j,k) * cub(j,i);
b10(j,k) = b9(j,k);

```

```

% Equation 3.144 - Coefficients of the difference concentration equation

```

```

c1(j,k) = 1 + (1 + xx(i)) * 0.5 * deta(j,k) * Le * fb(j,k,i) ...
- 0.5 * xx(i) * deta(j,k) * Le * cfb(j,i);
c2(j,k) = - 2 + c1(j,k);
c3(j,k) = (1 + xx(i)) * 0.5 * deta(j,k) * Le * qb(j,k,i) ...
+ 0.5 * xx(i) * deta(j,k) * Le * cqj(j,i);
c4(j,k) = c3(j,k);
c5(j,k) = divide;
c6(j,k) = - 1 * (divide);
c7(j,k) = - 0.5 * xx(i) * deta(j,k) * Le * pb(j,k,i)...
+ 0.5 * xx(i) * deta(j,k) * Le * cpj(j,i);
c8(j,k) = c7(j,k);
c9(j,k) = - 0.5 * deta(j,k) * xx(i) * Le * ub(j,k,i)...
- 0.5 * xx(i) * deta(j,k) * Le * cub(j,i);
c10(j,k) = c9(j,k);

```

```

% Equations 3.125 to 3.127- Expressions of Rj

```

```

R1 = deta(j,k) * (- cderfb(j,i)) + deta(j,k) * M(i) +deta(j,k) * csb(j,i) * ge * M(i) ;
R2 = deta(j,k) * (- cdertb(j,i)) - deta(j,k) * cftb(j,i) -deta(j,k) * Nb
    * cqtb(j,i) - deta(j,k) * Nt * cttb(j,i) - deta(j,k) * xx(i) *
    cusb(j,i) + deta(j,k) * xx(i) * cftb(j,i);Le * deta(j,k) *
    xx(i) * cfqb(j,i);
R3 = deta(j,k) * (- cderqb(j,i)) - deta(j,k) * Le * cfqb(j,i) -
    deta(j,k) * cdertb(j,i) * (divide)-Le * deta(j,k) *
    xx(i) * cupb(j,i) + - deta(j,k) * Nr * cpb(j,i) * ge * M(i);

```

```

% Equation 3.145 - Expressions of rj-1/2

```

```

r1(j,k) = f(j-1,k,i) - f(j,k,i) + ( deta(j,k) * ub(j,k,i) );
r2(j,k) = s(j-1,k,i) - s(j,k,i) + ( deta(j,k) * tb(j,k,i) );
r3(j,k) = p(j-1,k,i) - p(j,k,i) + ( deta(j,k) * qb(j,k,i) );

```

```

if i == 1
r4(j,k) = R1 - f(j,k,i) + f(j-1,k,i) + deta(j,k) * ge * M(i) * sb(j,k,i) ...
        - deta(j,k) * Nr * ge * M(i) * pb(j,k,i);
else
r4(j,k) = R1 - f(j,k,i) + f(j-1,k,i)+ M(i) * deta(j,k) + deta(j,k) * ...
        ge * M(i) * sb(j,k,i) - deta(j,k) * Nr * ge * M(i) * pb(j,k,i);
end

r5(j,k) = R2 - t(j,k,i) + t(j-1,k,i)- (1 + xx(i)) * deta(j,k) * ftb(j,k,i)...
        - deta(j,k) * Nb * qtb(j,k,i) - deta(j,k) * Nt * ttb(j,k,i)...
        + xx(i) * deta(j,k) * usb(j,k,i)- xx(i) * deta(j,k) * ub(j,k,i)...
        * csb(j,i)+ xx(i) * deta(j,k) * sb(j,k,i) * cub(j,i)+ xx(i) *...
        deta(j,k) * tb(j,k,i) * cfb(j,i)- xx(i) * deta(j,k) * fb(j,k,i) * ctb(j,i);

r6(j,k) = R3 - q(j,k,i) + q(j-1,k,i) - (1 + xx(i)) * Le * deta(j,k) * fqb(j,k,i) ...
        - (divide) * (t(j,k,i) - t(j-1,k,i))+ Le * xx(i) * deta(j,k) * upb(j,k,i) ...
        - Le * xx(i) * deta(j,k) * ub(j,k,i) * cpb(j,i) + Le * xx(i) * deta(j,k)...
        * pb(j,k,i) * cub(j,i) + Le * xx(i) * deta(j,k) * qb(j,k,i) * cfb(j,i) ...
        - Le * xx(i) * deta(j,k) * fb(j,k,i) * cqb(j,i);
end

% Obtain the elements of the matrices

% Equation 3.148
a{2,k} = [ -0.5*deta(2,k) 0 0 1 0 0; 0 -1 0 0 -0.5*deta(2,k) 0; ...
0 0 -0.5*deta(2,k) 0 0 -0.5*deta(2,k); 0 a4(2,k) 0 a1(2,k) 0 0; ...
b8(2,k) b10(2,k) b6(2,k) b3(2,k) b1(2,k) b5(2,k); ...
c8(2,k) 0 c2(2,k) c3(2,k) c5(2,k) c1(2,k)];

% Equation 3.149
for j = 3:np
a{j,k} = [ -0.5*deta(j,k) 0 0 1 0 0; 0 -1 0 0 -0.5*deta(j,k) 0; ...
0 0 -1 0 0 -0.5*deta(j,k); 0 a4(j,k) a6(j,k) a1(j,k) 0 0; ...
b8(j,k) b10(j,k) 0 b3(j,k) b1(j,k) b5(j,k); ...
c8(j,k) 0 c10(j,k) c3(j,k) c5(j,k) c1(j,k)];

% Equation 3.150
b{j,k} = [ 0 0 0 -1 0 0; 0 0 0 0 -0.5*deta(j,k) 0; ...
0 0 0 0 -0.5*deta(j,k); 0 0 0 a2(j,k) 0 0; ...
0 0 0 b4(j,k) b2(j,k) b6(j,k); 0 0 0 c4(j,k) c6(j,k) c2(j,k)];
end

```

```

% Equation 3.151

for j = 2:np
c{j,k} = [ -0.5*deta(j,k) 0 0 0 0 0; 0 1 0 0 0 0; ...
0 0 1 0 0 0; 0 a3(j,k) a5(j,k) 0 0 0; ...
b7(j,k) b9(j,k) 0 0 0 0; c7(j,k) 0 c9(j,k) 0 0 0];
end

% The recursion formulas : forward sweep
alfa{2,k} = a{2,k};
gamma{2,k} = inv(alfa{2,k}) * c{2,k};

% Equation 3.156

for j = 3:np
alfa{j,k} = a{j,k} - ( b{j,k} * gamma{j-1,k});
gamma{j,k} = inv(alfa{j,k}) * c{j,k};
end

% Equation 3.153

for j = 2:np
rr{j,k} = [ r1(j,k); r2(j,k); r3(j,k); r4(j,k); r5(j,k); r6(j,k)];
end

% Equation 3.160

ww{2,k} = inv(alfa{2,k}) * rr{2,k};

% Equation 3.161

for j = 3:np
ww{j,k} = inv(alfa{j,k}) * (rr{j,k} - (b{j,k} * ww{j-1,k}));
end

% backward sweep
delf(1,k) = 0.0;
delt(1,k) = 0.0;
delp(1,k) = 0.0;
delu(np,k) = 0.0;
dels(np,k) = 0.0;
delp(np,k) = 0.0;

dell{np,k} = ww{np,k};

```

```

% Equation 3.163

for j = np-1:-1:2
dell{j,k} = ww{j,k} - (gamma{j,k} * dell{j+1,k});
end

% Equation 3.152

delu(1,k) = dell{2,k}(1,1);
dels(1,k) = dell{2,k}(2,1);
delq(1,k) = dell{2,k}(3,1);
delf(2,k) = dell{2,k}(4,1);
delt(2,k) = dell{2,k}(5,1);
delq(2,k) = dell{2,k}(6,1);

for j = np:-1:3
delu(j-1,k) = dell{j,k}(1,1);
dels(j-1,k) = dell{j,k}(2,1);
delp(j-1,k) = dell{j,k}(3,1);
delf(j,k) = dell{j,k}(4,1);
delt(j,k) = dell{j,k}(5,1);
delq(j,k) = dell{j,k}(6,1);
end

% Equation 3.128 - Newton's method

for j = 1:np
f(j,k+1,i) = f(j,k,i) + delf(j,k);
u(j,k+1,i) = u(j,k,i) + delu(j,k);
s(j,k+1,i) = s(j,k,i) + dels(j,k);
t(j,k+1,i) = t(j,k,i) + delt(j,k);
p(j,k+1,i) = p(j,k,i) + delp(j,k);
q(j,k+1,i) = q(j,k,i) + delq(j,k);
end

% Check for convergence of the iterations

stop = abs(dels(1,k));
kmax(i) = k;
k = k+1;
end

% Shift profile
for j = 1:np
ff(j) = f(j,k,i);
uu(j) = u(j,k,i);

```

```

ss(j) = s(j,k,i);
tt(j) = t(j,k,i);
pp(j) = p(j,k,i);
qq(j) = q(j,k,i);
end

for j = 1:np
ffb(j) = fb(j,kmax(i),i);
uub(j) = ub(j,kmax(i),i);
ssb(j) = sb(j,kmax(i),i);
ttb(j) = tb(j,kmax(i),i);
ppb(j) = pb(j,kmax(i),i);
qqb(j) = qb(j,kmax(i),i);
dderfb(j) = derfb(j,kmax(i),i);
ddertb(j) = dertb(j,kmax(i),i);
dderqb(j) = derqb(j,kmax(i),i);
end

Nu(i) = -1.0 * t(1,kmax(i),i);
Sh(i) = -1.0 * q(1,kmax(i),i);
Cf(i) = (t(1,kmax(i),i) - (Nr*q(1,kmax(i),i))) * ge * x(i) * M(i);
%Cf(i) = x(i) * v(1,kmax(i),i);

end

figure(1)% plot dimensionless skin friction
plot(x, Cf,'--','LineWidth',1, 'LineSmoothing','on');
% create MANUAL legend STARTS
% hold on
% p1 = plot(0, 0,'-', 'linewidth',2);
% p2 = plot(0, 0,'--', 'linewidth',2);
% LegendSetting = legend([p1 p2], '\it {Nr} = 0.1', '\it {Nr} = 0.5',
% 'Location', 'NorthEast');
% set(LegendSetting, 'FontName','Times New Roman', 'FontSize',12)
% hold off
xlabel('\it x','Fontname', 'Times New Roman','FontSize',18)
ylabel('\it ({Pe_x^{1/2}/Pr})C_f','Fontname', 'Times New Roman','FontSize',18)
%xlim([0 3.5])
hold all;

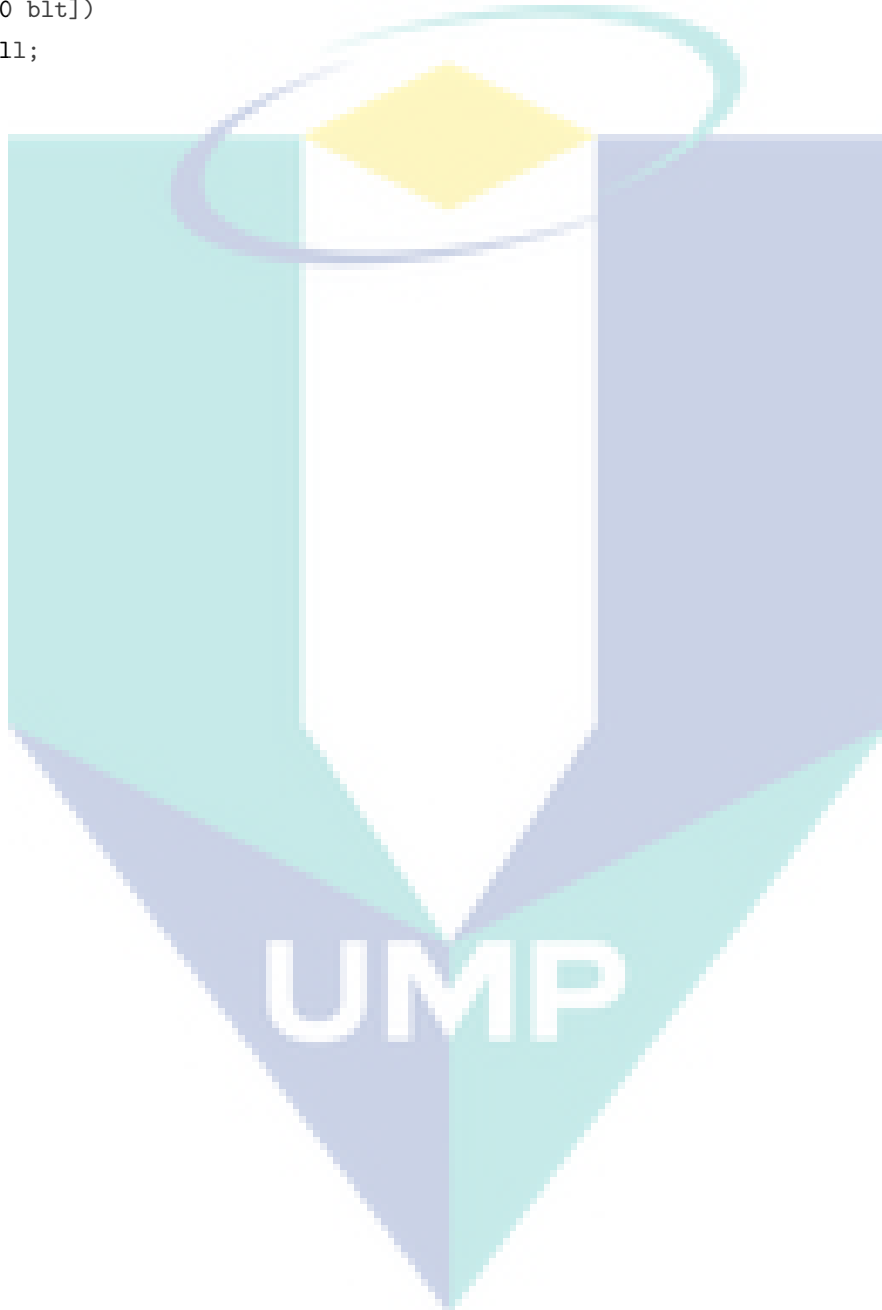
figure(2) % plot velocity profile
plot(eta, u(:,kmax(1),1),'--','LineWidth',1, 'LineSmoothing','on');
% create MANUAL legend STARTS
% hold on
% p1 = plot(0, 0,'-', 'linewidth',2);
% p2 = plot(0, 0,'--', 'linewidth',2);

```

```

% p3 = plot(0, 0,'-.', 'linewidth',2);
% LegendSetting = legend([p1 p2 p3], '\it {Nr} = 0.1', '\it {Nr} = 0.3',
% 'Location', 'NorthEast');
% set(LegendSetting, 'FontName','Times New Roman', 'FontSize',12)
% hold off
xlabel('\it y','Fontname', 'Times New Roman','FontSize',18)
ylabel( '\it f\prime (y)','Fontname', 'Times New Roman','FontSize',18)
xlim([0 blt])
hold all;

```



APPENDIX C

FORMULATION OF FORCED CONVECTION IN VISCOUS FLUID (CHAPTER 4, PAGE 83)

Basic dimensional boundary layer equations are

$$\frac{\partial \bar{u}}{\partial \bar{x}} + \frac{\partial \bar{v}}{\partial \bar{y}} = 0 \quad \text{C1}$$

$$\bar{u} \frac{\partial \bar{u}}{\partial \bar{x}} + \bar{v} \frac{\partial \bar{u}}{\partial \bar{y}} = \bar{u}_e \frac{d\bar{u}_e}{d\bar{x}} + \nu \frac{\partial^2 \bar{u}}{\partial \bar{y}^2} \quad \text{C2}$$

$$\bar{u} \frac{\partial \bar{T}}{\partial \bar{x}} + \bar{v} \frac{\partial \bar{T}}{\partial \bar{y}} = \alpha \frac{\partial^2 \bar{T}}{\partial \bar{y}^2} \quad \text{C3}$$

subject to boundary conditions

$$\bar{u} = \bar{v} = 0, \quad -k \frac{\partial \bar{T}}{\partial \bar{y}} = h_f (T_f - \bar{T}) \quad \text{at } \bar{y} = 0$$

$$\bar{u} \rightarrow \bar{u}_e, \quad \bar{T} \rightarrow T_\infty \quad \text{as } \bar{y} \rightarrow \infty \quad \text{C4}$$

By introducing non-dimensionalised using the following variables

$$x = \bar{x}/a, \quad y = Re^{1/2}(\bar{y}/a), \quad u = \bar{u}/U_\infty, \quad v = Re^{1/2}(\bar{v}/U_\infty)$$

$$u_e = \bar{u}_e/U_\infty, \quad \theta = \frac{\bar{T} - T_\infty}{T_f - T_\infty} \quad \text{C5}$$

Substituting C5 into continuity, momentum and energy equations, the differential equation are found as follows:

Continuity equation

$$\frac{\partial \bar{u}}{\partial \bar{x}} + \frac{\partial \bar{v}}{\partial \bar{y}} = 0$$

$$\frac{\partial(uU_\infty)}{\partial(xa)} + \frac{\partial(vU_\infty Re^{-1/2})}{\partial(ya Re^{-1/2})} = 0 \quad C6$$

$$\frac{U_\infty}{a} \left[\frac{\partial u}{\partial x} + \frac{\partial v}{\partial y} \right] = 0$$

$$\frac{\partial u}{\partial x} + \frac{\partial v}{\partial y} = 0$$

Momentum equation

$$\bar{u} \frac{\partial \bar{u}}{\partial \bar{x}} + \bar{v} \frac{\partial \bar{u}}{\partial \bar{y}} = \bar{u}_e \frac{\partial \bar{u}_e}{\partial \bar{x}} + \nu \frac{\partial^2 \bar{u}}{\partial \bar{y}^2}$$

$$uU_\infty \frac{\partial(uU_\infty)}{\partial(xa)} + vU_\infty Re^{-1/2} \frac{\partial(uU_\infty)}{\partial(ya Re^{-1/2})} = u_e U_\infty \frac{\partial(u_e U_\infty)}{\partial(xa)} + \nu \frac{\partial^2(uU_\infty)}{\partial(ya Re^{-1/2})^2}$$

$$\frac{U_\infty^2}{a} \left(u \frac{\partial u}{\partial x} + v \frac{\partial u}{\partial y} \right) = \frac{U_\infty^2}{a} u_e \frac{\partial u_e}{\partial x} + \frac{\nu U_\infty}{a} Re \frac{\partial^2 u}{\partial y^2} \quad C7$$

$$u \frac{\partial u}{\partial x} + v \frac{\partial u}{\partial y} = u_e \frac{\partial u_e}{\partial x} + \frac{\nu}{a U_\infty} Re \frac{\partial^2 u}{\partial y^2}$$

$$u \frac{\partial u}{\partial x} + v \frac{\partial u}{\partial y} = u_e \frac{\partial u_e}{\partial x} + \frac{\partial^2 u}{\partial y^2}$$

where Reynold number is given by $Re = U_\infty a / \nu$.

Energy equation

$$\bar{u} \frac{\partial \bar{T}}{\partial \bar{x}} + \bar{v} \frac{\partial \bar{T}}{\partial \bar{y}} = \alpha \frac{\partial^2 \bar{T}}{\partial \bar{y}^2}$$

$$uU_\infty \frac{\partial(\theta(T_f - T_\infty) + T_\infty)}{\partial(xa)} + vU_\infty Re^{-1/2} \frac{\partial(\theta(T_f - T_\infty) + T_\infty)}{\partial(ya Re^{-1/2})} = \alpha \frac{\partial^2(\theta(T_f - T_\infty) + T_\infty)}{\partial(ya Re^{-1/2})^2}$$

$$\frac{uU_\infty}{a} (T_f - T_\infty) \left(u \frac{\partial \theta}{\partial x} + v \frac{\partial \theta}{\partial y} \right) = \frac{\alpha}{a^2} Re (T_f - T_\infty) \frac{\partial^2 \theta}{\partial y^2} \quad C8$$

$$u \frac{\partial \theta}{\partial x} + v \frac{\partial \theta}{\partial y} = \frac{\alpha}{aU_\infty} Re \frac{\partial^2 \theta}{\partial y^2}$$

$$u \frac{\partial \theta}{\partial x} + v \frac{\partial \theta}{\partial y} = \frac{1}{Pr} \frac{\partial^2 \theta}{\partial y^2}$$

Boundary conditions

$$u = v = 0, \quad -k \frac{\partial \theta}{\partial y} = -\gamma(1 - \theta) \quad \text{at } y = 0$$

$$u \rightarrow u_e, \quad \theta \rightarrow 0 \quad \text{as } y \rightarrow \infty$$

C9

To solve continuity, momentum, energy equations subject to boundary conditions, the following assumption has been made

$$\psi = xf(x,y), \quad \theta = \theta(x,y)$$

C10

Using variables in C10, continuity equation is identically satisfied. The momentum equation becomes

$$u \frac{\partial u}{\partial x} + v \frac{\partial u}{\partial y} = u_e \frac{\partial u_e}{\partial x} + \frac{\partial^2 u}{\partial y^2}$$

$$x \frac{\partial f}{\partial y} \left(\frac{\partial f}{\partial y} + x \frac{\partial^2 f}{\partial x \partial y} \right) + \left(-f - x \frac{\partial f}{\partial x} \right) x \frac{\partial^2 f}{\partial y^2} = 2 \sin x \frac{\partial(2 \sin x)}{\partial y} + x \frac{\partial^3 f}{\partial y^3}$$

$$x \frac{\partial^3 f}{\partial y^3} + f x \frac{\partial^2 f}{\partial y^2} - x \left(\frac{\partial f}{\partial y} \right)^2 + 4 \sin x \cos x = x^2 \left(\frac{\partial f}{\partial y} \frac{\partial^2 f}{\partial x \partial y} - \frac{\partial f}{\partial x} \frac{\partial^2 f}{\partial y^2} \right)$$

C11

$$\frac{\partial^3 f}{\partial y^3} + f \frac{\partial^2 f}{\partial y^2} - \left(\frac{\partial f}{\partial y} \right)^2 + 4 \sin x \cos x = x \left(\frac{\partial f}{\partial y} \frac{\partial^2 f}{\partial x \partial y} - \frac{\partial f}{\partial x} \frac{\partial^2 f}{\partial y^2} \right)$$

Energy equation becomes

$$u \frac{\partial \theta}{\partial x} + v \frac{\partial \theta}{\partial y} = \frac{1}{\text{Pr}} \frac{\partial^2 \theta}{\partial y^2}$$

$$x \frac{\partial f}{\partial y} \frac{\partial \theta}{\partial x} + \left(-f - x \frac{\partial f}{\partial x} \right) \frac{\partial \theta}{\partial y} = \frac{1}{\text{Pr}} \frac{\partial^2 \theta}{\partial y^2} \quad \text{C12}$$

$$\frac{1}{\text{Pr}} \frac{\partial^2 \theta}{\partial y^2} + f \frac{\partial \theta}{\partial y} = x \left(\frac{\partial f}{\partial y} \frac{\partial \theta}{\partial x} - \frac{\partial f}{\partial x} \frac{\partial \theta}{\partial y} \right)$$

and the boundary are

$$f = \frac{\partial f}{\partial y} = 0, \quad \frac{\partial \theta}{\partial y} = -\gamma(1 - \theta) \quad \text{at } y = 0$$

$$\frac{\partial f}{\partial y} \rightarrow 2 \frac{\sin x}{x}, \quad \theta \rightarrow 0 \quad \text{as } y \rightarrow \infty \quad \text{C13}$$

UMP

APPENDIX D
FORMULATION OF FREE CONVECTION IN MICROPOLAR FLUID
(CHAPTER 5, PAGE 95)

Basic dimensional boundary layer equations are

$$\frac{\partial \bar{u}}{\partial \bar{x}} + \frac{\partial \bar{v}}{\partial \bar{y}} = 0 \quad \text{D1}$$

$$\rho \left(\bar{u} \frac{\partial \bar{u}}{\partial \bar{x}} + \bar{v} \frac{\partial \bar{u}}{\partial \bar{y}} \right) = (\mu + \kappa) \frac{\partial^2 \bar{u}}{\partial \bar{y}^2} + \rho g \beta (T - T_\infty) \sin\left(\frac{x}{a}\right) + \kappa \frac{\partial \bar{H}}{\partial \bar{y}} \quad \text{D2}$$

$$\bar{u} \frac{\partial \bar{T}}{\partial \bar{x}} + \bar{v} \frac{\partial \bar{T}}{\partial \bar{y}} = \alpha \frac{\partial^2 \bar{T}}{\partial \bar{y}^2} \quad \text{D3}$$

$$\rho J \left(\bar{u} \frac{\partial \bar{H}}{\partial \bar{x}} + \bar{v} \frac{\partial \bar{H}}{\partial \bar{y}} \right) = -\kappa \left(2\bar{H} + \frac{\partial \bar{u}}{\partial \bar{y}} \right) + \chi \frac{\partial^2 \bar{H}}{\partial \bar{y}^2} \quad \text{D4}$$

subject to boundary conditions

$$\bar{u} = \bar{v} = 0, \quad -k \frac{\partial \bar{T}}{\partial \bar{y}} = h_f (T_f - \bar{T}), \quad \bar{H} = -n \frac{\partial \bar{u}}{\partial \bar{y}} \quad \text{at } \bar{y} = 0$$

$$\bar{u} \rightarrow 0, \quad \bar{T} \rightarrow T_\infty, \quad \bar{H} \rightarrow 0 \quad \text{as } \bar{y} \rightarrow \infty \quad \text{D5}$$

By introducing non-dimensionalised using the following variables

$$x = \bar{x}/a, \quad y = Gr^{1/4}(\bar{y}/a), \quad u = \left(\frac{a}{v}\right) Gr^{-1/2} \bar{u}$$

$$v = \left(\frac{a}{v}\right) Gr^{-1/4} \bar{v}, \quad \theta = \frac{\bar{T} - T_\infty}{T_f - T_\infty}, \quad H = \left(\frac{a^2}{v}\right) Gr^{-3/4} \bar{H} \quad \text{D6}$$

Substituting D6 into continuity, momentum and energy equations, the differential equation are found as follows:

Continuity equation

$$\frac{\partial \bar{u}}{\partial \bar{x}} + \frac{\partial \bar{v}}{\partial \bar{y}} = 0$$

$$\frac{\partial \left(\frac{uv}{a} Gr^{1/2} \right)}{\partial (xa)} + \frac{\partial \left(\frac{uv}{a} Gr^{1/4} \right)}{\partial (yaGr^{-1/4})} = 0$$

$$\frac{vGr^{1/2}}{a^2} \left(\frac{\partial u}{\partial x} + \frac{\partial v}{\partial y} \right) = 0$$

$$\frac{\partial u}{\partial x} + \frac{\partial v}{\partial y} = 0$$

D7

Momentum equation

$$\rho \left(\bar{u} \frac{\partial \bar{u}}{\partial \bar{x}} + \bar{v} \frac{\partial \bar{u}}{\partial \bar{y}} \right) = (\mu + \kappa) \frac{\partial^2 \bar{u}}{\partial \bar{y}^2} + \rho g \beta (T - T_\infty) \sin\left(\frac{x}{a}\right) + \kappa \frac{\partial \bar{H}}{\partial \bar{y}}$$

$$\rho \left[\frac{uv}{a} Gr^{1/2} \frac{\left(\frac{uv}{a} Gr^{1/2} \right)}{\partial (xa)} + \frac{uv}{a} Gr^{1/4} \frac{\left(\frac{uv}{a} Gr^{1/2} \right)}{\partial (yaGr^{-1/4})} \right]$$

$$= (\mu + \kappa) \frac{\partial^2 \frac{uv}{a} Gr^{1/2}}{\partial (yaGr^{-1/4})^2} + \rho g \beta (T - T_\infty) \sin\left(\frac{xa}{a}\right) + \kappa \frac{\partial \left(\frac{vH}{a^2} Gr^{3/4} \right)}{\partial (yaGr^{-1/4})}$$

D8a

$$\rho \frac{v^2}{a^3} Gr \left(u \frac{\partial u}{\partial x} + v \frac{\partial u}{\partial y} \right) = \frac{v}{a^3} Gr (\mu + \kappa) \frac{\partial^2 u}{\partial y^2} + \rho g \beta (T - T_\infty) \sin(x) + \kappa Gr \frac{v}{a^3} \frac{\partial H}{\partial y}$$

$$u \frac{\partial u}{\partial x} + v \frac{\partial u}{\partial y} = \left(\frac{\mu + \kappa}{\rho v} \right) \frac{\partial^2 u}{\partial y^2} + \frac{g \beta a^3}{v^2 Gr} (T - T_\infty) \sin(x) + \frac{\kappa}{\rho v} \frac{\partial H}{\partial y}$$

where $Gr = g\beta(T_f - T_\infty)a^3/v^2$, $K = \kappa/\mu$ and $\rho = \mu/v$. Substituting Gr , K , and ρ into D8a, we obtain

$$u \frac{\partial u}{\partial x} + v \frac{\partial u}{\partial y} = \frac{\mu}{\rho \nu} \frac{\partial^2 u}{\partial y^2} + \frac{\kappa}{\rho \nu} \frac{\partial^2 u}{\partial y^2} + \frac{g\beta a^3}{\nu^2 Gr} (T - T_\infty) \sin(x) + \frac{\kappa}{\rho \nu} \frac{\partial H}{\partial y}$$

$$u \frac{\partial u}{\partial x} + v \frac{\partial u}{\partial y} = \frac{\partial^2 u}{\partial y^2} + K \frac{\partial^2 u}{\partial y^2} + \frac{T - T_\infty}{T_f - T_\infty} \sin x + K \frac{\partial H}{\partial y} \quad \text{D8b}$$

$$u \frac{\partial u}{\partial x} + v \frac{\partial u}{\partial y} = (1 + K) \frac{\partial^2 u}{\partial y^2} + \theta \sin x + K \frac{\partial H}{\partial y}$$

Energy equation

$$\bar{u} \frac{\partial \bar{T}}{\partial \bar{x}} + \bar{v} \frac{\partial \bar{T}}{\partial \bar{y}} = \alpha \frac{\partial^2 \bar{T}}{\partial \bar{y}^2}$$

$$\frac{uv}{a} Gr^{1/2} \frac{\partial (\theta(T_f - T_\infty) + T_\infty)}{\partial (xa)} + \frac{uv}{a} Gr^{1/4} \frac{\partial (\theta(T_f - T_\infty) + T_\infty)}{\partial (yaGr^{-1/4})} = \alpha \frac{\partial^2 (\theta(T_f - T_\infty) + T_\infty)}{\partial (yaGr^{-1/4})^2}$$

$$\frac{\nu Gr^{1/2}}{a^2} (T_f - T_\infty) \left(u \frac{\partial \theta}{\partial x} + v \frac{\partial \theta}{\partial y} \right) = \frac{\alpha Gr^{1/2}}{a^2} (T_f - T_\infty) \frac{\partial^2 \theta}{\partial y^2} \quad \text{D9}$$

$$u \frac{\partial \theta}{\partial x} + v \frac{\partial \theta}{\partial y} = \frac{\alpha}{\nu} \frac{\partial^2 \theta}{\partial y^2}$$

$$u \frac{\partial \theta}{\partial x} + v \frac{\partial \theta}{\partial y} = \frac{1}{Pr} \frac{\partial^2 \theta}{\partial y^2}$$

Micropolar equation

$$\rho J \left(\bar{u} \frac{\partial \bar{H}}{\partial \bar{x}} + \bar{v} \frac{\partial \bar{H}}{\partial \bar{y}} \right) = -\kappa \left(2\bar{H} + \frac{\partial \bar{u}}{\partial \bar{y}} \right) + \chi \frac{\partial^2 \bar{H}}{\partial \bar{y}^2}$$

$$\rho J \left[\frac{uv}{a} Gr^{1/2} \frac{\partial \left(\frac{H\nu Gr^{3/4}}{a^2} \right)}{\partial (xa)} + \frac{\nu v}{a} Gr^{1/4} \frac{\partial \left(\frac{H\nu Gr^{3/4}}{a^2} \right)}{\partial (yaGr^{-1/4})} \right]$$

D10a

$$= -\kappa \left[2 \left(\frac{H\nu Gr^{3/4}}{a^2} \right) + \frac{\partial \left(\frac{uv}{a} Gr^{1/2} \right)}{(yaGr^{-1/4})} \right] + \chi \frac{\partial^2 \left(\frac{H\nu Gr^{3/4}}{a^2} \right)}{\partial (yaGr^{-1/4})^2}$$

$$\rho J \frac{v^2 Gr^{5/4}}{a^4} \left(u \frac{\partial H}{\partial y} + v \frac{\partial H}{\partial y} \right) = -\kappa \frac{v Gr^{3/4}}{a^2} \left(2H + \frac{\partial u}{\partial y} \right) + \chi \frac{Gr^{5/4} v}{a^4} \frac{\partial^2 H}{\partial y^2}$$

$$u \frac{\partial H}{\partial x} + v \frac{\partial H}{\partial y} = -\frac{\kappa a^2}{\rho J v Gr^{1/2}} \left(2H + \frac{\partial u}{\partial y} \right) + \frac{\chi}{\rho J v} \frac{\partial^2 H}{\partial y^2}$$

$$u \frac{\partial H}{\partial x} + v \frac{\partial H}{\partial y} = -\frac{\kappa}{\rho v} \left[2H + \frac{\partial u}{\partial y} \right] + \frac{(\mu + \kappa/2)}{\rho v} \frac{\partial^2 H}{\partial y^2}$$

D10b

$$u \frac{\partial H}{\partial x} + v \frac{\partial H}{\partial y} = -K \left[2H + \frac{\partial u}{\partial y} \right] + \left(1 + \frac{K}{2} \right) \frac{\partial^2 H}{\partial y^2}$$

Boundary conditions

$$u = v = 0, \quad -k \frac{\partial \theta}{\partial y} = -\gamma(1 - \theta), \quad H = -\frac{1}{2} \frac{\partial u}{\partial y} \quad \text{at } y = 0$$

$$u \rightarrow 0, \quad \theta \rightarrow 0, \quad H \rightarrow 0 \quad \text{as } y \rightarrow \infty$$

D11

To solve the governing equation subject to boundary conditions, the following assumption has been made

$$\psi = x f(x, y), \quad \theta = \theta(x, y) \quad N = x G(x, y)$$

D12

Using variables in D12, continuity equation is identically satisfied. The momentum equation becomes

$$u \frac{\partial u}{\partial x} + v \frac{\partial u}{\partial y} = (1 + K) \frac{\partial^2 u}{\partial y^2} + \theta \sin x + K \frac{\partial H}{\partial y}$$

$$x \frac{\partial f}{\partial y} \left(\frac{\partial f}{\partial y} + x \frac{\partial^2 f}{\partial x \partial y} \right) + \left(-f - x \frac{\partial f}{\partial x} \right) + x \frac{\partial^2 f}{\partial y^2} = (1 + K) x \frac{\partial^3 f}{\partial y^3} + \theta \sin x + K \left(x \frac{\partial G}{\partial y} \right)$$

$$(1 + K) x \frac{\partial^3 f}{\partial y^3} + \theta \sin x + K x \left(\frac{\partial G}{\partial y} \right) + f x \frac{\partial^2 f}{\partial y^2}$$

$$-x \left(\frac{\partial f}{\partial y} \right)^2 = x^2 \left(\frac{\partial f}{\partial y} \frac{\partial^2 f}{\partial x \partial y} - \frac{\partial f}{\partial x} \frac{\partial^2 f}{\partial y^2} \right)$$

D13

$$(1 + K) \frac{\partial^3 f}{\partial y^3} + \frac{\theta \sin x}{x} + K \left(\frac{\partial G}{\partial y} \right) + f \frac{\partial^2 f}{\partial y^2} - \left(\frac{\partial f}{\partial y} \right)^2 = x \left(\frac{\partial f}{\partial y} \frac{\partial^2 f}{\partial x \partial y} - \frac{\partial f}{\partial x} \frac{\partial^2 f}{\partial y^2} \right)$$

Meanwhile for micropolar equation, we obtain

$$\begin{aligned} \rho J \left(\bar{u} \frac{\partial \bar{H}}{\partial \bar{x}} + \bar{v} \frac{\partial \bar{H}}{\partial \bar{y}} \right) &= -\kappa \left(2\bar{H} + \frac{\partial \bar{u}}{\partial \bar{y}} \right) + \chi \frac{\partial^2 \bar{H}}{\partial \bar{y}^2} \\ x \frac{\partial f}{\partial y} \left(G + x \frac{\partial G}{\partial x} \right) + \left(-f - x \frac{\partial f}{\partial x} \right) x \frac{\partial G}{\partial y} &= \left(1 + \frac{K}{2} \right) \frac{\partial^2 G}{\partial y^2} - K \left(2xG + x \frac{\partial^2 f}{\partial y^2} \right) \\ \left(1 + \frac{K}{2} \right) x \frac{\partial^2 G}{\partial y^2} - Kx \left(2G + \frac{\partial^2 f}{\partial y^2} \right) - Gx \frac{\partial f}{\partial y} + fx \frac{\partial G}{\partial y} &= x^2 \left(\frac{\partial f}{\partial y} \frac{\partial G}{\partial y} - \frac{\partial f}{\partial x} \frac{\partial G}{\partial y} \right) \\ \left(1 + \frac{K}{2} \right) \frac{\partial^2 G}{\partial y^2} - K \left(2G + \frac{\partial^2 f}{\partial y^2} \right) - G \frac{\partial f}{\partial y} + f \frac{\partial G}{\partial y} &= x \left(\frac{\partial f}{\partial y} \frac{\partial G}{\partial y} - \frac{\partial f}{\partial x} \frac{\partial G}{\partial y} \right) \end{aligned} \quad \text{D14}$$

Energy equation becomes

$$\begin{aligned} u \frac{\partial \theta}{\partial x} + v \frac{\partial \theta}{\partial y} &= \frac{1}{\text{Pr}} \frac{\partial^2 \theta}{\partial y^2} \\ x \frac{\partial f}{\partial y} x \frac{\partial \theta}{\partial x} + \left(-f - x \frac{\partial f}{\partial x} \right) \frac{\partial \theta}{\partial y} &= \frac{1}{\text{Pr}} \frac{\partial^2 \theta}{\partial y^2} \\ \frac{1}{\text{Pr}} \frac{\partial^2 \theta}{\partial y^2} + f \frac{\partial \theta}{\partial y} &= x \left(\frac{\partial f}{\partial y} \frac{\partial \theta}{\partial x} - \frac{\partial f}{\partial x} \frac{\partial \theta}{\partial y} \right) \end{aligned} \quad \text{D15}$$

and the boundary are

$$\begin{aligned} f = \frac{\partial f}{\partial y} = 0, \quad \frac{\partial \theta}{\partial y} = -\gamma(1 - \theta), \quad G = -\frac{1}{2} \frac{\partial^2 f}{\partial y^2} \quad \text{at } y = 0 \\ \frac{\partial f}{\partial y} \rightarrow 0, \quad \theta \rightarrow 0, \quad G \rightarrow 0 \quad \text{as } y \rightarrow \infty \end{aligned} \quad \text{D16}$$

APPENDIX E
FORMULATION OF MIXED CONVECTION IN VISCOUS FLUID
(CHAPTER 6, PAGE 111)

Basic dimensional boundary layer equations are

$$\frac{\partial \bar{u}}{\partial \bar{x}} + \frac{\partial \bar{v}}{\partial \bar{y}} = 0 \quad \text{E1}$$

$$\bar{u} \frac{\partial \bar{u}}{\partial \bar{x}} + \bar{v} \frac{\partial \bar{u}}{\partial \bar{y}} = \bar{u}_e \frac{d\bar{u}_e}{d\bar{x}} + \nu \frac{\partial^2 \bar{u}}{\partial \bar{y}^2} + g\beta(T - T_\infty) \sin\left(\frac{\bar{x}}{a}\right) \quad \text{E2}$$

$$\bar{u} \frac{\partial \bar{T}}{\partial \bar{x}} + \bar{v} \frac{\partial \bar{T}}{\partial \bar{y}} = \alpha \frac{\partial^2 \bar{T}}{\partial \bar{y}^2} \quad \text{E3}$$

subject to boundary conditions

$$\bar{u} = \bar{v} = 0, \quad -k \frac{\partial \bar{T}}{\partial \bar{y}} = h_f(T_f - \bar{T}) \quad \text{at } \bar{y} = 0$$

$$\bar{u} \rightarrow \bar{u}_e, \quad \bar{T} \rightarrow T_\infty \quad \text{as } \bar{y} \rightarrow \infty \quad \text{E4}$$

By introducing non-dimensionalised using the following variables

$$x = \bar{x}/a, \quad y = Re^{1/2}(\bar{y}/a), \quad u = \bar{u}/U_\infty, \quad v = Re^{1/2}(\bar{v}/U_\infty)$$

$$u_e = \bar{u}_e/U_\infty, \quad \theta = \frac{\bar{T}_f - T_\infty}{T_w - T_\infty} \quad \text{E5}$$

Substituting E5 into continuity, momentum and energy equations, the differential equation are found as follows:

Continuity equation

$$\frac{\partial \bar{u}}{\partial \bar{x}} + \frac{\partial \bar{v}}{\partial \bar{y}} = 0$$

$$\frac{\partial(uU_\infty)}{\partial(xa)} + \frac{\partial(vU_\infty Re^{-1/2})}{\partial(ya Re^{-1/2})} = 0 \quad \text{E6a}$$

$$\frac{U_\infty}{a} \left(\frac{\partial u}{\partial x} + \frac{\partial v}{\partial y} \right) = 0$$

$$\frac{\partial u}{\partial x} + \frac{\partial v}{\partial y} = 0$$

E6b

Momentum equation

$$\bar{u} \frac{\partial \bar{u}}{\partial \bar{x}} + \bar{v} \frac{\partial \bar{u}}{\partial \bar{y}} = \bar{u}_e \frac{\partial \bar{u}_e}{\partial \bar{x}} + \nu \frac{\partial^2 \bar{u}}{\partial \bar{y}^2} + g\beta(T - T_\infty) \sin\left(\frac{\bar{x}}{\bar{a}}\right)$$

$$uU_\infty \frac{\partial(uU_\infty)}{\partial(xa)} + \nu U_\infty Re^{-1/2} \frac{\partial(uU_\infty)}{\partial(yaRe^{-1/2})} = u_e U_\infty \frac{\partial(u_e U_\infty)}{\partial(xa)} + \nu \frac{\partial^2(uU_\infty)}{\partial(yaRe^{-1/2})^2} + g\beta(T - T_\infty) \sin\left(\frac{xa}{a}\right)$$

$$\frac{U_\infty^2}{a} \left(u \frac{\partial u}{\partial x} + v \frac{\partial u}{\partial y} \right) = \frac{U_\infty^2}{a} u_e \frac{\partial u_e}{\partial x} + \frac{\nu U_\infty}{a} Re \frac{\partial^2 u}{\partial y^2} + g\beta(T - T_\infty) \sin$$

E7

$$u \frac{\partial u}{\partial x} + v \frac{\partial u}{\partial y} = u_e \frac{\partial u_e}{\partial x} + \frac{\nu}{aU_\infty} Re \frac{\partial^2 u}{\partial y^2} + \frac{ga\beta(T - T_\infty) \sin x}{U_\infty^2}$$

$$u \frac{\partial u}{\partial x} + v \frac{\partial u}{\partial y} = u_e \frac{\partial u_e}{\partial x} + \frac{\partial^2 u}{\partial y^2} + \lambda \theta \sin x$$

where lambda is given by $\lambda = Gr/Re^2$.

Energy equation

$$\bar{u} \frac{\partial \bar{T}}{\partial \bar{x}} + \bar{v} \frac{\partial \bar{T}}{\partial \bar{y}} = \alpha \frac{\partial^2 \bar{T}}{\partial \bar{y}^2}$$

$$uU_\infty \frac{\partial(\theta(T_f - T_\infty) + T_\infty)}{\partial(xa)} + \nu U_\infty Re^{-1/2} \frac{\partial(\theta(T_f - T_\infty) + T_\infty)}{\partial(yaRe^{-1/2})} = \alpha \frac{\partial^2(\theta(T_f - T_\infty) + T_\infty)}{\partial(yaRe^{-1/2})^2}$$

$$\frac{uU_\infty}{a} (T_f - T_\infty) \left(u \frac{\partial \theta}{\partial x} + v \frac{\partial \theta}{\partial y} \right) = \frac{\alpha}{a^2} Re (T_f - T_\infty) \frac{\partial^2 \theta}{\partial y^2}$$

E8a

$$u \frac{\partial \theta}{\partial x} + v \frac{\partial \theta}{\partial y} = \frac{\alpha}{aU_\infty} Re \frac{\partial^2 \theta}{\partial y^2}$$

$$u \frac{\partial \theta}{\partial x} + v \frac{\partial \theta}{\partial y} = \frac{1}{Pr} \frac{\partial^2 \theta}{\partial y^2}$$

E8b

Boundary conditions

$$u = v = 0, \quad -k \frac{\partial \theta}{\partial y} = -\gamma(1 - \theta) \quad \text{at } y = 0$$

$$u \rightarrow u_e, \quad \theta \rightarrow 0 \quad \text{as } y \rightarrow \infty$$

E9

To solve continuity, momentum, energy equations subject to boundary conditions, the following assumption has been made

$$\psi = xf(x,y), \quad \theta = \theta(x,y)$$

E10

Using variables in E10, continuity equation is identically satisfied. The momentum equation becomes

$$u \frac{\partial u}{\partial x} + v \frac{\partial u}{\partial y} = u_e \frac{\partial u_e}{\partial x} + \frac{\partial^2 u}{\partial y^2} + \lambda \theta \sin x$$

$$x \frac{\partial f}{\partial y} \left(\frac{\partial f}{\partial y} + x \frac{\partial^2 f}{\partial x \partial y} \right) + \left(-f - x \frac{\partial f}{\partial x} \right) x \frac{\partial^2 f}{\partial y^2} = \sin x \frac{\partial(\sin x)}{\partial y} + x \frac{\partial^3 f}{\partial y^3} + \lambda \theta \sin x$$

$$x \frac{\partial^3 f}{\partial y^3} + f_x \frac{\partial^2 f}{\partial y^2} - x \left(\frac{\partial f}{\partial y} \right)^2 + \sin x \cos x + \lambda \theta \sin x = x^2 \left(\frac{\partial f}{\partial y} \frac{\partial^2 f}{\partial x \partial y} - \frac{\partial f}{\partial x} \frac{\partial^2 f}{\partial y^2} \right)$$

E11

$$\frac{\partial^3 f}{\partial y^3} + f \frac{\partial^2 f}{\partial y^2} - \left(\frac{\partial f}{\partial y} \right)^2 + (\cos x + \lambda \theta) \frac{\sin x}{x} = x \left(\frac{\partial f}{\partial y} \frac{\partial^2 f}{\partial x \partial y} - \frac{\partial f}{\partial x} \frac{\partial^2 f}{\partial y^2} \right)$$

where $u_e = \sin x$.

Energy equation becomes

$$u \frac{\partial \theta}{\partial x} + v \frac{\partial \theta}{\partial y} = \frac{1}{\text{Pr}} \frac{\partial^2 \theta}{\partial y^2}$$

$$x \frac{\partial f}{\partial y} \frac{\partial \theta}{\partial x} + \left(-f - x \frac{\partial f}{\partial x} \right) \frac{\partial \theta}{\partial y} = \frac{1}{\text{Pr}} \frac{\partial^2 \theta}{\partial y^2} \quad \text{E12}$$

$$\frac{1}{\text{Pr}} \frac{\partial^2 \theta}{\partial y^2} + f \frac{\partial \theta}{\partial y} = x \left(\frac{\partial f}{\partial y} \frac{\partial \theta}{\partial x} - \frac{\partial f}{\partial x} \frac{\partial \theta}{\partial y} \right)$$

and the boundary condition

$$f = \frac{\partial f}{\partial y} = 0, \quad \frac{\partial \theta}{\partial y} = -\gamma(1 - \theta) \quad \text{at } y = 0$$

$$\frac{\partial f}{\partial y} \rightarrow \frac{\sin x}{x}, \quad \theta \rightarrow 0 \quad \text{as } y \rightarrow \infty \quad \text{E13}$$

UMP

APPENDIX F

FORMULATION OF MIXED CONVECTION IN NANOFLUID: TIWARI AND DAS MODEL (CHAPTER 7, PAGE 124)

Basic dimensional boundary layer equations are

$$\frac{\partial \bar{u}}{\partial \bar{x}} + \frac{\partial \bar{v}}{\partial \bar{y}} = 0 \quad \text{F1}$$

$$\bar{u} \frac{\partial \bar{u}}{\partial \bar{x}} + \bar{v} \frac{\partial \bar{u}}{\partial \bar{y}} = -\frac{1}{\rho_{nf}} \frac{\partial \bar{p}}{\partial \bar{x}} + \frac{\mu_{nf}}{\rho_{nf}} \frac{\partial^2 \bar{u}}{\partial \bar{y}^2} + \frac{\phi \rho_s \beta_s + (1 - \phi) \rho_f \beta_f}{\rho_{nf}} g(\bar{T} - T_\infty) \sin\left(\frac{\bar{x}}{a}\right) \quad \text{F2}$$

$$\bar{u} \frac{\partial \bar{T}}{\partial \bar{x}} + \bar{v} \frac{\partial \bar{T}}{\partial \bar{y}} = \alpha \frac{\partial^2 \bar{T}}{\partial \bar{y}^2} \quad \text{F3}$$

subject to boundary conditions

$$\bar{u} = \bar{v} = 0, \quad -k \frac{\partial \bar{T}}{\partial \bar{y}} = h_f(T_f - \bar{T}) \quad \text{at } \bar{y} = 0$$

$$\bar{u} \rightarrow \bar{u}, \quad \bar{T} \rightarrow T_\infty \quad \text{as } \bar{y} \rightarrow \infty \quad \text{F4}$$

By introducing non-dimensionalised using the following variables

$$x = \bar{x}/a, \quad y = Re^{1/2}(\bar{y}/a), \quad u = \bar{u}/U_\infty, \quad v = Re^{1/2}(\bar{v}/U_\infty)$$

$$\theta = \frac{T - T_\infty}{T_f - T_\infty}, \quad p = \frac{\bar{p} - p_\infty}{\rho_{nf} U_\infty^2} \quad \text{F5}$$

Substituting F5 into continuity, momentum and energy equations, the differential equation are found as follows:

Continuity equation

$$\frac{\partial \bar{u}}{\partial \bar{x}} + \frac{\partial \bar{v}}{\partial \bar{y}} = 0$$

$$\frac{\partial(uU_\infty)}{\partial(xa)} + \frac{\partial(vU_\infty Re^{-1/2})}{\partial(ya Re^{-1/2})} = 0 \quad \text{F6a}$$

$$\frac{U_\infty}{a} \left(\frac{\partial u}{\partial x} + \frac{\partial v}{\partial y} \right) = 0$$

$$\frac{\partial u}{\partial x} + \frac{\partial v}{\partial y} = 0$$

F6b

Momentum equation

$$\bar{u} \frac{\partial \bar{u}}{\partial \bar{x}} + \bar{v} \frac{\partial \bar{u}}{\partial \bar{y}} = -\frac{1}{\rho_{nf}} \frac{\partial \bar{p}}{\partial \bar{x}} + \frac{\mu_{nf}}{\rho_{nf}} \frac{\partial^2 \bar{u}}{\partial \bar{y}^2} + \frac{\phi \rho_s \beta_s + (1-\phi) \rho_f \beta_f}{\rho_{nf}} g(\bar{T} - T_\infty) \sin \left(\frac{\bar{x}}{a} \right)$$

$$uU_\infty \frac{\partial(uU_\infty)}{\partial(xa)} + vU_\infty Re^{-1/2} \frac{\partial(uU_\infty)}{\partial(yaRe^{-1/2})} = -\frac{1}{\rho_{nf}} \frac{\partial(\rho_{nf}U_\infty^2 p + p_\infty)}{\partial(xa)} + \frac{\mu_{nf}}{\rho_{nf}} \frac{\partial^2(uU_\infty)}{\partial(yaRe^{-1/2})^2} + \frac{\phi \rho_s \beta_s + (1-\phi) \rho_f \beta_f}{\rho_{nf}} g\beta(T - T_\infty) \sin \left(\frac{xa}{a} \right)$$

$$\frac{U_\infty^2}{a} \left(u \frac{\partial u}{\partial x} + \frac{\partial u}{\partial y} \right) = -\frac{U_\infty^2}{a} \frac{\partial p}{\partial x} + \frac{\mu_{nf}}{\rho_{nf}} \frac{U_\infty^2}{a} Re \frac{\partial^2 u}{\partial y^2} + \frac{\phi \rho_s \beta_s + (1-\phi) \rho_f \beta_f}{\rho_{nf}} g\beta(T - T_\infty) \sin \left(\frac{xa}{a} \right)$$

F7

$$u \frac{\partial u}{\partial x} + v \frac{\partial u}{\partial y} = -\frac{\partial p}{\partial x} + \frac{1}{aU_\infty} \frac{\mu_{nf}}{\rho_{nf}} Re \frac{\partial^2 u}{\partial y^2} + \left(\frac{\phi \rho_s \beta_s + (1-\phi) \rho_f \beta_f}{\rho_{nf}} \right) \frac{ga\beta(T - T_\infty) \sin x}{U_\infty^2}$$

$$u \frac{\partial u}{\partial x} + v \frac{\partial u}{\partial y} = -\frac{\partial p}{\partial x} + \frac{\mu_{nf}}{\rho_{nf} \nu_f} \frac{\partial^2 u}{\partial y^2} + \frac{\phi \rho_s (\beta_s / \beta_f) + (1-\phi) \rho_f}{\rho_{nf}} \lambda \theta \sin x$$

Energy equation

$$\bar{u} \frac{\partial \bar{T}}{\partial \bar{x}} + \bar{v} \frac{\partial \bar{T}}{\partial \bar{y}} = \frac{1}{Pr} \frac{\alpha_{nf}}{\alpha_f} \frac{\partial^2 \bar{T}}{\partial \bar{y}^2}$$

$$uU_\infty \frac{\partial(\theta(T_f - T_\infty) + T_\infty)}{\partial(xa)} + vU_\infty Re^{-1/2} \frac{\partial(\theta(T_f - T_\infty) + T_\infty)}{\partial(yaRe^{-1/2})} = \frac{1}{Pr} \frac{\alpha_{nf}}{\alpha_f} \frac{\partial^2(\theta(T_f - T_\infty) + T_\infty)}{\partial(yaRe^{-1/2})^2}$$

$$\frac{U_\infty}{a} (T_f - T_\infty) \left(u \frac{\partial \theta}{\partial x} + v \frac{\partial \theta}{\partial y} \right) = \frac{1}{Pr} \frac{\alpha_{nf}}{\alpha_f} \frac{Re}{a^2} (T_f - T_\infty) \frac{\partial^2 \theta}{\partial y^2}$$

F8a

$$u \frac{\partial \theta}{\partial x} + v \frac{\partial \theta}{\partial y} = \frac{1}{\text{Pr}} \frac{\alpha_{nf}}{\alpha_f} \frac{Re}{aU_\infty} \frac{\partial^2 \theta}{\partial y^2}$$

$$u \frac{\partial \theta}{\partial x} + v \frac{\partial \theta}{\partial y} = \frac{1}{\text{Pr}} \frac{\alpha_{nf}}{\alpha_f} \frac{\partial^2 \theta}{\partial y^2}$$

F8b

Boundary conditions

$$u = v = 0, \quad -k \frac{\partial \theta}{\partial y} = -\gamma(1 - \theta) \quad \text{at } y = 0$$

$$u \rightarrow 0, \quad \theta \rightarrow 0 \quad \text{as } y \rightarrow \infty$$

F9

To solve continuity, momentum, energy equations subject to boundary conditions, the following assumption has been made

$$\psi = xf(x, y), \quad \theta = \theta(x, y)$$

F10

Using variables in F10, continuity equation is identically satisfied. The momentum equation becomes

$$u \frac{\partial u}{\partial x} + v \frac{\partial u}{\partial y} = -\frac{\partial p}{\partial x} + \frac{\mu_{nf}}{\rho_{nf} \nu_f} \frac{\partial^2 u}{\partial y^2} + \frac{\phi \rho_s (\beta_s / \beta_f) + (1 - \phi) \rho_f}{\rho_{nf}} \lambda \theta \sin x$$

$$u \frac{\partial u}{\partial x} + v \frac{\partial u}{\partial y} = u_e \frac{\partial u_e}{\partial x} + \frac{\mu_{nf}}{\rho_{nf} \nu_f} \frac{\partial^2 u}{\partial y^2} + \frac{\phi \rho_s (\beta_s / \beta_f) + (1 - \phi) \rho_f}{\rho_{nf}} \lambda \theta \sin x$$

$$x \frac{\partial f}{\partial y} \left(\frac{\partial f}{\partial y} + x \frac{\partial^2 f}{\partial x \partial y} \right) + \left(-f - x \frac{\partial f}{\partial x} \right) x \frac{\partial^2 f}{\partial y^2} = \sin x \frac{\partial(\sin x)}{\partial y}$$

$$+ \frac{1}{(1 - \phi)^{2.5} [1 - \phi + (\phi \rho_s / \rho_f)]} x \frac{\partial^3 f}{\partial y^3} + \frac{\phi \rho_s (\beta_s / \beta_f) + (1 - \phi) \rho_f}{\rho_{nf}} \lambda \theta \sin x \quad \text{F11}$$

$$\frac{1}{(1 - \phi)^{2.5} [1 - \phi + (\phi \rho_s / \rho_f)]} \frac{\partial^3 f}{\partial y^3} + \frac{\phi \rho_s (\beta_s / \beta_f) + (1 - \phi) \rho_f}{\rho_{nf}} \lambda \theta \sin x$$

$$+ f \frac{\partial^2 f}{\partial y^2} - \left(\frac{\partial f}{\partial y} \right)^2 + \frac{\sin x \cos x}{x} = x \left(\frac{\partial f}{\partial y} \frac{\partial^2 f}{\partial x \partial y} - \frac{\partial f}{\partial x} \frac{\partial^2 f}{\partial y^2} \right)$$

Energy equation becomes

$$u \frac{\partial \theta}{\partial x} + v \frac{\partial \theta}{\partial y} = \frac{1}{\text{Pr}} \frac{\alpha_{nf}}{\alpha_f} \frac{\partial^2 \theta}{\partial y^2}$$

$$x \frac{\partial f}{\partial y} \frac{\partial \theta}{\partial x} + \left(-f - x \frac{\partial f}{\partial x} \right) \frac{\partial \theta}{\partial y} = \frac{1}{\text{Pr}} \frac{k_{nf}}{(\rho C_p)_f} \frac{1}{\alpha_f} \frac{\partial^2 \theta}{\partial y^2} \quad \text{F12}$$

$$x \frac{\partial f}{\partial y} \frac{\partial \theta}{\partial x} + \left(-f - x \frac{\partial f}{\partial x} \right) \frac{\partial \theta}{\partial y} = \frac{1}{\text{Pr}} \frac{(\rho)C_p}{k_f} \frac{k_{nf}}{(1-\phi) + (\phi(\rho C_p)_s/(\rho C_p)_f)} \frac{\partial^2 \theta}{\partial y^2}$$

$$\frac{1}{\text{Pr} (1-\phi) + (\phi(\rho C_p)_s/(\rho C_p)_f)} \frac{k_{nf}/k_f}{\alpha_f} \frac{\partial^2 \theta}{\partial y^2} + f \frac{\partial \theta}{\partial x} = x \left(\frac{\partial f}{\partial y} \frac{\partial \theta}{\partial x} - \frac{\partial f}{\partial x} \frac{\partial \theta}{\partial y} \right)$$

and the boundary condition

$$f = \frac{\partial f}{\partial y} = 0, \quad \frac{\partial \theta}{\partial y} = -\gamma(1-\theta) \quad \text{at } y=0$$

$$\frac{\partial f}{\partial y} \rightarrow \frac{\sin x}{x}, \quad \theta \rightarrow 0 \quad \text{as } y \rightarrow \infty$$

F13

UMP

APPENDIX G

FORMULATION OF MIXED CONVECTION IN NANOFLUID: BUONGIORNO MODEL (CHAPTER 8, PAGE 141)

Basic dimensional boundary layer equations are

$$\frac{\partial \bar{u}}{\partial \bar{x}} + \frac{\partial \bar{v}}{\partial \bar{y}} = 0 \quad \text{G1}$$

$$\frac{\mu}{K} \frac{\partial \bar{u}}{\partial \bar{y}} = \left[(1 - \bar{C}_\infty) \beta \rho_{f\infty} \frac{\partial \bar{T}}{\partial \bar{y}} - (\rho_p - \rho_{f\infty}) \frac{\partial \bar{C}}{\partial \bar{y}} \right] g \sin \left(\frac{\bar{x}}{a} \right) \quad \text{G2}$$

$$\bar{u} \frac{\partial \bar{T}}{\partial \bar{x}} + \bar{v} \frac{\partial \bar{T}}{\partial \bar{y}} = \alpha_m \frac{\partial^2 \bar{T}}{\partial \bar{y}^2} + \tau \left[D_B \frac{\partial \bar{T}}{\partial \bar{y}} \frac{\partial \bar{C}}{\partial \bar{y}} + \left(\frac{D_T}{T_\infty} \right) \left(\frac{\partial \bar{T}}{\partial \bar{y}} \right)^2 \right] \quad \text{G3}$$

$$\frac{1}{\varepsilon} \left(\bar{u} \frac{\partial \bar{C}}{\partial \bar{x}} + \bar{v} \frac{\partial \bar{C}}{\partial \bar{y}} \right) = D_B \frac{\partial^2 \bar{C}}{\partial \bar{y}^2} + \left(\frac{D_T}{T_\infty} \right) \frac{\partial^2 \bar{T}}{\partial \bar{y}^2} \quad \text{G4}$$

subject to boundary conditions

$$\bar{v}(\bar{x}, \bar{y}) = 0, \quad -k \frac{\partial \bar{T}}{\partial \bar{y}} = h_f (T_f - \bar{T}), \quad \bar{C}(\bar{x}, \bar{y}) = \bar{C}_w \quad \text{at } \bar{y} = 0, \quad 0 \leq \bar{x} \leq \pi$$

$$\bar{u}(\bar{x}, \bar{y}) \rightarrow \bar{u}_e(\bar{x}), \quad \bar{T}(\bar{x}, \bar{y}) \rightarrow \bar{T}_\infty, \quad \bar{C}(\bar{x}, \bar{y}) \rightarrow \bar{C}_\infty \quad \text{as } \bar{y} \rightarrow \infty, \quad 0 \leq \bar{x} \leq \pi \quad \text{G5}$$

By introducing non-dimensionalised using the following variables

$$x = \frac{\bar{x}}{a}, \quad y = \frac{Pe^{1/2} \bar{y}}{a}, \quad u = \frac{\bar{u}}{U_\infty}, \quad v = \frac{Pe^{1/2} \bar{v}}{U_\infty}$$

$$\theta = \frac{\bar{T} - T_\infty}{T_f - T_\infty}, \quad \phi = \frac{\bar{C} - C_\infty}{C_w - C_\infty} \quad \text{G6}$$

Substituting G6 into continuity, momentum, energy equations and nanoparticle volume fraction equations, the differential equation are found as follows:

Continuity equation

$$\frac{\partial \bar{u}}{\partial \bar{x}} + \frac{\partial \bar{v}}{\partial \bar{y}} = 0$$

$$\frac{\partial(uU_\infty)}{\partial(xa)} + \frac{\partial(vU_\infty Re^{-1/2})}{\partial(ya Re^{-1/2})} = 0$$

$$\frac{U_\infty}{a} \left(\frac{\partial u}{\partial x} + \frac{\partial v}{\partial y} \right) = 0$$

G7

$$\frac{\partial u}{\partial x} + \frac{\partial v}{\partial y} = 0$$

Momentum equation

$$\frac{\mu}{K} \frac{\partial \bar{u}}{\partial \bar{y}} = \left[(1 - \bar{C}_\infty) \beta \rho_{f\infty} \frac{\partial \bar{T}}{\partial \bar{y}} - (\rho_p - \rho_{f\infty}) \frac{\partial \bar{C}}{\partial \bar{y}} \right] g \sin \left(\frac{\bar{x}}{a} \right)$$

$$\frac{\mu}{K} \frac{\partial(uU_\infty)}{\partial(ya Pe^{-1/2})} = \beta(1 - C_\infty) \rho_\infty \frac{\partial(\theta(T_f - T_\infty) + T_\infty)}{\partial(ya Pe^{-1/2})} g \sin \frac{xa}{a}$$

$$- (\rho_p - \rho_{f\infty}) \frac{\partial(\phi(C_w - C_\infty) + C_\infty)}{\partial(ya Pe^{-1/2})} g \sin \left(\frac{xa}{a} \right)$$

$$Pe^{1/2} \frac{\mu U_\infty}{Ka} \frac{\partial u}{\partial y} = \frac{\beta(1 - C_\infty)(T_f - T_\infty) \rho_{f\infty}}{a} Pe^{1/2} \frac{\partial \theta}{\partial y} g \sin x$$

$$- \frac{(\rho_p - \rho_{f\infty})(C_w - C_\infty)}{a} Pe^{1/2} \frac{\partial \phi}{\partial y} g \sin x$$

G8

$$\frac{\partial u}{\partial y} = \frac{Ka\beta(1 - C_\infty)(T_f - T_\infty) \rho_{f\infty}}{\mu U_\infty} \frac{\partial \theta}{\partial y} g \sin x$$

$$- \frac{(\rho_p - \rho_{f\infty})(C_w - C_\infty)K}{\mu U_\infty} \frac{\partial \phi}{\partial y} g \sin x$$

$$\frac{\partial u}{\partial y} = \lambda \frac{\partial \theta}{\partial y} \sin x - \lambda Nr \frac{\partial \phi}{\partial y} \sin x$$

$$\frac{\partial u}{\partial y} = \left(\frac{\partial \theta}{\partial y} - Nr \frac{\partial \phi}{\partial y} \right) \lambda \sin x$$

Energy equation

$$\begin{aligned}
 \bar{u} \frac{\partial \bar{T}}{\partial \bar{x}} + \bar{v} \frac{\partial \bar{T}}{\partial \bar{y}} &= \alpha_m \frac{\partial^2 \bar{T}}{\partial \bar{y}^2} + \tau \left[D_B \frac{\partial \bar{T}}{\partial \bar{y}} \frac{\partial \bar{C}}{\partial \bar{y}} + \left(\frac{D_T}{T_\infty} \right) \left(\frac{\partial \bar{T}}{\partial \bar{y}} \right)^2 \right] \\
 u U_\infty \frac{\partial (\theta(T_f - T_\infty) + T_\infty)}{\partial (xa)} + v U_\infty Pe^{-1/2} \frac{\partial (\theta(T_f - T_\infty) + T_\infty)}{\partial (yaPe^{-1/2})} &= \alpha_m \frac{\partial^2 (\theta(T_f - T_\infty) + T_\infty)}{\partial (yaPe^{-1/2})^2} \\
 + \tau \left[D_B \frac{\partial (\theta(T_f - T_\infty) + T_\infty)}{\partial (yaPe^{-1/2})} \frac{\partial (\phi(C_w - C_\infty) + C_\infty)}{\partial (yaPe^{-1/2})} + \frac{D_T}{T_\infty} \left(\frac{\partial (\phi(C_w - C_\infty) + C_\infty)}{\partial (yaPe^{-1/2})} \right)^2 \right] \\
 u U_\infty (T_f - T_\infty) \left(u \frac{\partial \theta}{\partial x} + v \frac{\partial \theta}{\partial y} \right) &= \frac{\alpha_m}{a^2} Pe (T_f - T_\infty) \frac{\partial^2 \theta}{\partial y^2} + \tag{G9} \\
 \tau \frac{(T_f - T_\infty)}{a^2} Pe \left[D_B (C_w - C_\infty) \frac{\partial \theta}{\partial y} \frac{\partial \phi}{\partial y} + \frac{D_T}{T_\infty} (T_f - T_\infty) \left(\frac{\partial \theta}{\partial y} \right)^2 \right] \\
 u \frac{\partial \theta}{\partial x} + v \frac{\partial \theta}{\partial y} &= \frac{\alpha_m}{a U_\infty} Pe (T_f - T_\infty) \frac{\partial^2 \theta}{\partial y^2} + \frac{\tau}{a U_\infty} Pe \left[D_B (C_w - C_\infty) \frac{\partial \theta}{\partial y} \frac{\partial \phi}{\partial y} + \frac{D_T}{T_\infty} (T_f - T_\infty) \left(\frac{\partial \theta}{\partial y} \right)^2 \right] \\
 u \frac{\partial \theta}{\partial x} + v \frac{\partial \theta}{\partial y} &= \frac{\partial^2 \theta}{\partial y^2} + Nb \frac{\partial \theta}{\partial y} \frac{\partial \phi}{\partial y} + Nt \left(\frac{\partial \theta}{\partial y} \right)^2
 \end{aligned}$$

Nanoparticle volume fraction equation

$$\begin{aligned}
 \frac{1}{\varepsilon} \left(\bar{u} \frac{\partial \bar{C}}{\partial \bar{x}} + \bar{v} \frac{\partial \bar{C}}{\partial \bar{y}} \right) &= D_B \frac{\partial^2 \bar{C}}{\partial \bar{y}^2} + \left(\frac{D_T}{T_\infty} \right) \frac{\partial^2 \bar{T}}{\partial \bar{y}^2} \\
 \frac{1}{\varepsilon} \left(u U_\infty \frac{\partial (\phi(C_w - C_\infty) + C_\infty)}{\partial (xa)} + v U_\infty Pe^{-1/2} \frac{\partial (\phi(C_w - C_\infty) + C_\infty)}{\partial (yaPe^{-1/2})} \right) \\
 &= D_B \frac{\partial^2 (\phi(C_w - C_\infty) + C_\infty)}{\partial (yaPe^{-1/2})^2} + \frac{D_T}{T_\infty} \frac{\partial^2 (\theta(T_f - T_\infty) + T_\infty)}{\partial (yaPe^{-1/2})^2} \\
 \frac{1}{\varepsilon} \frac{u U_\infty}{a} (C_w - C_\infty) \left(u \frac{\partial \phi}{\partial x} + v \frac{\partial \phi}{\partial y} \right) &= D_B (C_w - C_\infty) Pe \frac{\partial^2 \theta}{\partial y^2} + \frac{D_T}{T_\infty} (T_f - T_\infty) \frac{\partial^2 \theta}{\partial y^2} \tag{G10} \\
 \frac{1}{\varepsilon} \frac{a U_\infty}{D_B Pe} \left(u \frac{\partial \phi}{\partial x} + v \frac{\partial \phi}{\partial y} \right) &= \frac{\partial^2 \theta}{\partial y^2} + \frac{D_T}{D_B T_\infty} \frac{T_f - T_\infty}{(C_w - C_\infty)} \frac{\partial^2 \theta}{\partial y^2} \\
 Le \left(u \frac{\partial \phi}{\partial x} + v \frac{\partial \phi}{\partial y} \right) &= \frac{\partial^2 \theta}{\partial y^2} + \frac{Nt}{Nb} \frac{\partial^2 \theta}{\partial y^2}
 \end{aligned}$$

Boundary conditions

$$v(x,y) = 0, \quad \theta'(x,y) = -\gamma(1 - \theta(x,y)), \quad \phi(x,y) = 1 \quad \text{at } y = 0, \quad 0 \leq x \leq \pi$$

$$u(x,y) \rightarrow u_e(x), \quad \theta(x,y) \rightarrow 0, \quad \phi(x,y) \rightarrow 0 \quad \text{as } y \rightarrow \infty, \quad 0 \leq x \leq \pi \quad \text{G11}$$

To solve governing equations subject to boundary conditions, the following assumption has been made

$$\psi = xf(x,y), \quad \theta = \theta(x,y), \quad \phi = \phi(x,y) \quad \text{G12}$$

Using variables in G12, continuity equation is identically satisfied. Integrating G8 and using the boundary conditions G11, we obtain the following for momentum equation

$$\int \partial u = \int \left(\left(\frac{\partial \theta}{\partial y} - Nr \frac{\partial \phi}{\partial y} \right) \lambda \sin x \right) \partial y$$

$$u = (\theta - Nr\phi) \lambda \sin x + c$$

$$u = (\theta - Nr\phi) \lambda \sin x + \sin x$$

G13

$$u = \left(1 + (\theta - Nr\phi) \lambda \right) \sin x$$

Substituting variables G12 into G13 yields

$$x \frac{\partial f}{\partial y} = \left(1 + (\theta - Nr\phi) \lambda \right) \sin x$$

$$\frac{\partial f}{\partial y} = \left(1 + (\theta - Nr\phi) \lambda \right) \frac{\sin x}{x}$$

G14

Energy equation becomes

$$u \frac{\partial \theta}{\partial x} + v \frac{\partial \theta}{\partial y} = \frac{\partial^2 \theta}{\partial y^2} + Nb \frac{\partial \theta}{\partial y} \frac{\partial \phi}{\partial y} + Nt \left(\frac{\partial \theta}{\partial y} \right)^2$$

$$x \frac{\partial f}{\partial y} \frac{\partial \theta}{\partial x} + \left(-f - x \frac{\partial f}{\partial x} \right) \frac{\partial \theta}{\partial y} = \frac{\partial^2 \theta}{\partial y^2} + Nb \frac{\partial \theta}{\partial y} \frac{\partial \phi}{\partial y} + Nt \left(\frac{\partial \theta}{\partial y} \right)^2 \quad \text{G15}$$

$$\frac{\partial^2 \theta}{\partial y^2} + Nb \frac{\partial \theta}{\partial y} \frac{\partial \phi}{\partial y} + Nt \left(\frac{\partial \theta}{\partial y} \right)^2 + f \frac{\partial \theta}{\partial x} = x \left(\frac{\partial f}{\partial y} \frac{\partial \theta}{\partial x} - \frac{\partial f}{\partial x} \frac{\partial \theta}{\partial y} \right)$$

Nanoparticle volume fraction yields

$$Le \left(u \frac{\partial \phi}{\partial x} + v \frac{\partial \phi}{\partial y} \right) = \frac{\partial^2 \theta}{\partial y^2} + \frac{Nt}{Nb} \frac{\partial^2 \theta}{\partial y^2}$$

$$Le \left(x \frac{\partial f}{\partial y} \frac{\partial \phi}{\partial x} + \left(-f - x \frac{\partial f}{\partial x} \right) \frac{\partial \phi}{\partial y} \right) = \frac{\partial^2 \theta}{\partial y^2} + \frac{Nt}{Nb} \frac{\partial^2 \theta}{\partial y^2} \quad \text{G16}$$

$$\frac{\partial^2 \theta}{\partial y^2} + \frac{Nt}{Nb} \frac{\partial^2 \theta}{\partial y^2} + Le f \frac{\partial \phi}{\partial y} = x Le \left(\frac{\partial f}{\partial y} \frac{\partial \phi}{\partial x} - \frac{\partial f}{\partial x} \frac{\partial \phi}{\partial y} \right)$$

and the boundary condition

$$f(x,y) = 0, \quad \theta'(x,y) = -\gamma(1 - \theta(x,y)), \quad \phi(x,y) = 1 \quad \text{at } y = 0, \quad 0 \leq x \leq \pi$$

$$\theta(x,y) \rightarrow 0, \quad \phi(x,y) \rightarrow 0 \quad \text{as } y \rightarrow \infty, \quad 0 \leq x \leq \pi \quad \text{G17}$$

UMP

APPENDIX H
LIST OF PUBLICATIONS

A Journal

1. **Sarif, N. M.**, Salleh, M. Z., and Nazar, R., 2016. Numerical study of mixed convection boundary layer flow near the lower stagnation point of a horizontal circular cylinder in nanofluids, *ARPN Journal of Engineering and Applied Sciences*, 11 (11), 7274–7278.
2. **Sarif, N. M.**, Salleh, M. Z., and Nazar, R., 2016. Mixed convection flow over a horizontal circular cylinder in viscous Fluid at lower stagnation point with convective boundary conditions, *ScienceAsia Journal*, 42, 5–10.
3. **Sarif, N. M.**, Salleh, M. Z., and Nazar, R., 2013. Numerical solution of flow and heat transfer over a stretching sheet with Newtonian heating using the Keller-Box method, *Procedia Engineering*, 53, 542–554.
4. Hussanan, A., Khan, I., Hashim, H., Mohamed, M. K. A., Ishak, N., **Sarif, N. M.**, and Salleh, M. Z., 2016. Unsteady MHD Flow of some nanofluid past an accelerated vertical plate embedded in porous medium, *Jurnal Teknologi* 2, 78, 542–554.
5. Mohamed, M. K. A., Salleh, M. Z, Hussanan, A., **Sarif, N. M.**, Noar, N. A. Z., Anuar, I., and Widodo, B., 2016. Mathematical Model of free convection boundary layer flow on solid sphere with viscous dissipation and thermal radiation, *International Journal of Computing Science and Applied Mathematics*, 2 (2), 20-25.

B Proceeding

1. **Sarif, N. M.**, Salleh, M. Z., and Nazar, R., 2013. Numerical solution of the free convection boundary layer flow over a horizontal circular cylinder with convective boundary conditions, *AIP Conference Proceedings of the 3rd International Conference on Mathematical Sciences (ICMS3) Kuala Lumpur*, 1602, 179–185.
2. **Sarif, N. M.**, Salleh, M. Z., and Nazar, R., 2012. Radiation effects on MHD flow and heat transfer over a stretching sheet with convective boundary conditions, *AIP Conference of the International Conference on Mathematical Sciences & Statistic, Kuala Lumpur Malaysia*, 1557, 200–205.

3. **Sarif, N. M.**, Salleh, M. Z., and Nazar, R., 2013. Boundary layer flow and heat transfer over a stretching sheet with convective boundary conditions, AIP Conference Proceedings of the 20th National Symposium on Mathematical Sciences (SKSM20) Putrajaya Malaysia, 1522, 420–425.
4. **Sarif, N. M.**, Salleh, M. Z., and Nazar, R., 2013. Free Convection Boundary Layer Flow of a Horizontal Circular Cylinder in a Micropolar Fluid with Convective Boundary Conditions, Malaysian Technical Universities Conference on Engineering & Technology (MUCET2013), 03-04 Dec 2013, Kuantan Pahang.
5. **Sarif, N. M.**, Salleh, M. Z., Mat Tahar, R., and Nazar, R., 2013. Forced Convection Boundary Layer Flow over a Horizontal Circular Cylinder with Convective Boundary Condition, International Conference on Applied Analysis and Mathematical Modeling (ICAAMM 2013), 2–5 June 2013, Istanbul, Turkey.
6. Yap, B. K., Hussanan, A., Mohamed, M. K. A, Ismail, Z., Salleh, M. Z., **Sarif, N. M.**, 2017. Thermal Radiation Effect on MHD Flow and Heat Transfer of Williamson Nanofluid Past Over a Stretching Sheet, IOP Conference Proceedings of International Conference on Applied Mathematics and Statistics (ICoAIMS), 8–10 June 2017, Kuantan Malaysia.
7. Alkasasbeh, H. T., **Sarif, N. M.**, Salleh, M. Z., Nazar, R. and Pop, I., 2014. Effect of radiation and magnetohydrodynamic free convection boundary layer flow on a solid sphere with Newtonian heating in a micropolar fluid, AIP Conference Proceedings 1643, 662 (2015), pp 662-669.
8. Ishak, N., Hahim, H., Mohamed, M. K. A., **Sarif, N. M.**, Salleh, M. Z., and Rosli, N., 2015. MHD flow and heat transfer for the upper-convected Maxwell fluid over a stretching/shrinking sheet with prescribed heat flux, AIP Conference Proceedings 1691 (2015)
9. Hashim, H., Mohamed, M. K. A., Hussanan, A., Ishak, N., **Sarif, N. M.**, and Salleh M. Z., 2015. The effects of slip conditions and viscous dissipation on the stagnation point flow over a stretching sheet, AIP Conference Proceedings 1691 (2015) pp 4-7.

C Exposition

1. **Sarif, N. M.**, Kasim, A. R. M., Aziz, L. A., Zokri, S. M, Arifin, N. S., Ismail, Z., Noar, N.A.Z.M., Salleh, M. Z.,,Shafie, S. 2016. Modeling on Aligned MHD Flow,

Creation, Innovation, Technology & Research Exposition (CITReX 2016), 27-28 Mac 2016, Universiti Malaysia Pahang, Malaysia.

2. **Sarif, N. M.**, Salleh, M. Z., Rosli, N. and Nazar, R., 2015. Forced Convection Boundary Layer Flow Over a Horizontal Circular Cylinder with Convective Boundary Conditions by Using Keller-Box Method, Kolokium RACE (RACE 2015), 13–14 Januari 2015, Akademi Pengajian Tinggi (AKEPT), Kuala Lumpur Malaysia.
3. **Sarif, N. M.**, Salleh, M. Z., and Nazar, R., 2013. Radiation effects on MHD flow and heat transfer over a stretching sheet with convective boundary conditions, Creation, Innovation, Technology & Research Exposition (CITReX 2013), 27–28 Mac 2013, Universiti Malaysia Pahang, Malaysia
4. **Sarif, N. M.**, Salleh, M. Z., and Nazar, R., 2012. Boundary layer flow and heat transfer over a stretching sheet with convective boundary conditions, Karnival Sains & Matematik (ez-SciMat 2012), 2–4 Nov 2012,Universiti Malaysia Pahang, Malaysia.



UMP